

KU Leuven
Biomedical Sciences Group
Faculty of Medicine
Department of Development and Regeneration
SCIL



EXPLORING STEM CELL BIOLOGY IN PITUITARY TUMORS AND DERIVED ORGANOID

Charlotte NYS

Jury:

Promoter:	Prof. Dr. Hugo Vankelecom
Chair examining committee:	Prof. Dr. Karel Talavera
Chair public defence:	Prof. Dr. Frederic Lluís Vinas
Jury members:	Prof. Dr. Frank Claessens Dr. Adrian Daly Prof. Dr. Frederik De Smet Prof. Dr. Marta Korbonits

Dissertation presented in partial fulfilment of the requirements for
the degree of Doctor in Biomedical Sciences

Leuven, March 2022

TABLE OF CONTENTS

LIST OF ABBREVIATIONS	v
SUMMARY.....	viii
SAMENVATTING	x
CHAPTER 1: GENERAL INTRODUCTION	1
1. The pituitary gland	2
1.1 Pituitary anatomy and architecture.....	2
1.2 Pituitary hormones: function and regulation	3
1.3 Pituitary embryonic development.....	4
2. Pituitary dysfunction	6
2.1 Hypopituitarism.....	6
2.2 Hyperpituitarism and pituitary tumors	7
3. Pituitary stem cells	16
3.1 Stem cells in the pituitary: identification and search for their function	16
3.2 Stem cells in pituitary tumorigenesis and search for their role.....	18
4. <i>In vitro</i> models to study pituitary biology and tumorigenesis	21
4.1 Pituitary tumor cell lines	21
4.2 Primary pituitary non-stem cell-based <i>in vitro</i> models.....	22
4.3 Primary pituitary stem cell-based <i>in vitro</i> models	23
CHAPTER 2: RESEARCH OBJECTIVES	29
CHAPTER 3: SAFETY AND EFFECTIVENESS OF TRANSNASAL TRANSSPHENOIDAL PITUITARY SURGERY IN A SINGLE CENTER, A RETROSPECTIVE STUDY.....	33
ABSTRACT.....	34
1. INTRODUCTION.....	35
2. MATERIAL AND METHODS.....	36
3. RESULTS.....	38
3.1 Demographics and tumor characteristics	38
3.2 Clinical presentation	39
3.3 Complications.....	40
3.4 Outcome	41
4. DISCUSSION	42
4.1 Demographics	42
4.2 Clinical presentation	42
4.3 Complications.....	43

4.4 Oncological outcome	44
5. CONCLUSION	45
CHAPTER 4: EXPLORING STEM CELL BIOLOGY IN PITUITARY TUMORS AND ORGANOID	47
ABSTRACT	48
1. INTRODUCTION.....	49
2. MATERIALS AND METHODS.....	51
3. RESULTS.....	56
3.1 Pituitary stem cells of the <i>Drd2</i> ^{-/-} tumorigenic gland show a proliferative and cytokine/chemokine activation phenotype	56
3.2 Organoids recapitulate the activated pituitary stem cell phenotype of the <i>Drd2</i> ^{-/-} gland.....	59
3.3 Cytokines upregulated in the tumorigenic pituitary's stem cells stimulate organoid growth	62
3.4 Stem cell phenotype in human pituitary tumors.....	66
3.5 Development and characterization of human pituitary tumor-derived organoids	69
3.6 Transcriptomic interrogation of pituitary tumors and derived organoids	72
4. DISCUSSION	77
SUPPLEMENTARY FIGURES.....	80
SUPPLEMENTARY MOVIES	89
SUPPLEMENTARY TABLES.....	90
ADDENDUM: Orthotopic <i>in vivo</i> transplantation into the mouse pituitary gland.....	103
1. INTRODUCTION.....	103
2. MATERIAL AND METHODS.....	104
3. RESULTS.....	105
4. CONCLUSION AND PERSPECTIVES.....	105
CHAPTER 5: GENERAL DISCUSSION AND FUTURE PERSPECTIVES	107
5.1 General discussion.....	108
5.2 Conclusion and future perspectives	115
REFERENCES.....	117
ADDITIONAL STATEMENTS	133
ACKNOWLEDGEMENTS	134
PERSONAL CONTRIBUTIONS.....	135
FUNDING	135
CONFLICT OF INTEREST STATEMENT	135
CURRICULUM VITAE.....	136

LIST OF ABBREVIATIONS

ACP	adamantinomatous craniopharyngioma
ACTH	adrenocorticotrophic hormone
ADH	antidiuretic hormone
AIP	aryl hydrocarbon receptor-interacting protein
AL	anterior lobe
AP	anterior pituitary
bFGF	basic fibroblast growth factor
BMP	bone-morphogenetic protein
CCL	C-C motif chemokine ligand
CD	cluster of differentiation
CDK	cyclin-dependent kinase
CDKN	cyclin-dependent kinase inhibitor
CF	cystic fibrosis
CFTR	cystic fibrosis transmembrane conductance regulator
CPHD	combined pituitary hormone deficiency
CRH	corticotropin-releasing hormone
CSF	cerebrospinal fluid
CT	cholera toxin
CXCL	chemokine (C-X-C motif) ligand
CXCR	chemokine (C-X-C motif) receptor
CYP2F2	cytochrome P450 family 2 subfamily F member 2
DI	diabetes insipidus
dpc	days post coitum
DRD2	dopamine receptor D2
E-CAD	E-cadherin
ECM	extracellular matrix
EGF	epidermal growth factor
eGFP	enhanced green fluorescent protein
ELD	external lumbar drain
EMT	epithelial-mesenchymal transition
ER α	estrogen receptor alpha

FC	fold change
FGF	fibroblast growth factor
FSH	follicle-stimulating hormone
GH	growth hormone
GHRH	growth hormone-releasing hormone
GnRH	gonadotropin-releasing hormone
H&E	haematoxylin and eosin
HER2	human epidermal growth factor receptor 2
HESX1	homeobox expressed in ES cells 1
HGF	hepatocyte growth factor
HPA	human pituitary adenoma
IGF1	insulin-like growth factor 1
IL	intermediate lobe
IL1 β	interleukin-1 beta
IL6	interleukin-6
JAK	janus kinase
KRT	keratin
LH	luteinizing hormone
LHX3	LIM-homeobox 3
MEN	multiple endocrine neoplasia
MSH	melanocyte-stimulating hormone
mTOR	mechanistic target of rapamycin kinase
MZ	marginal zone
NF κ B	nuclear factor kappa B
OptM	optimized medium
P	passage
P38-MAPK	p38 mitogen-activated protein kinases
PAX6	paired box 6
PCA	principal component analysis
PIT1	pituitary-specific positive transcription factor 1
PitNET	pituitary neuroendocrine tumor
PITX	paired-like homeodomain
PP	posterior pituitary

PRKAR1A	protein kinase cAMP-dependent type I regulatory subunit alpha
PRL	prolactin
PRLR	prolactin receptor
PROP1	prophet of PIT1
PRRX	paired-related homeobox
PTTG	pituitary tumor transforming gene
PyLT	polyoma large T antigen
RB1	RB transcriptional corepressor 1
RP	Rathke's pouch
RSPO1	R-spondin 1
SASP	senescence-associated secretory phenotype
sc	subcutaneous
scRNA-seq	single-cell RNA sequencing
SC-SP	stem cell-side population
SFDM	serum-free defined medium
SOX	sex-determining region Y-box
SP	side population
STAT	signal transducer and activator of transcription
TACSTD2	tumor associated calcium signal transducer 2
TGF	transforming growth factor
TNF α	tumor necrosis factor alpha
TRH	thyrotropin-releasing hormone
TSC	tumor stem cell
TSH	thyroid-stimulating hormone
WNT	wingless-type MMTV integration site

SUMMARY

As master orchestrator of the endocrine system, the pituitary gland steers key developmental and physiological processes such as body growth, reproduction, metabolism, stress response and immunity. Because of this primordial function, pituitary dysfunction leads to severe health problems such as infertility and osteoporosis. Pituitary tumors represent the most frequent pituitary pathology. However, the mechanisms underlying tumorigenesis in the gland remain elusive.

First, we retrospectively analysed clinical aspects of human pituitary tumor patients and the safety and effectiveness of their surgical treatment by transsphenoidal tumor resection. Patients presenting with visual problems or nerve deficits (partially) recovered following surgery. Similarly, patients with hormone-producing tumors generally regained normal (dropped) systemic hormone levels after tumor resection. Postoperative complications such as cerebrospinal fluid leakage or meningitis remained very rare, and could efficiently be treated. Despite the effectiveness and safety of surgical treatment, the majority of patients developed hypopituitarism (hormone deficiencies) after surgery, requiring lifelong hormone supplementation. Better understanding of how pituitary tumors develop and grow could improve patient clinical management in the future. To acquire more insight in pituitary tumorigenesis, we focused on the stem cells' behavior and scrutinized their phenotype and transcriptome in mouse and human pituitary tumors.

In the aged dopamine receptor D2 knockout ($Drd2^{-/-}$) mouse pituitary harboring large prolactinomas, the $SOX2^{+}$ stem cells were found to be more abundant and showed higher proliferative activity as compared to $SOX2^{+}$ stem cells of wildtype ($Drd2^{+/+}$) mice. RNA-sequencing analysis revealed an elevated cytokine/chemokine pattern in the stem cell compartment of the tumorigenic pituitary, particularly of interleukin-6 (*Il6*), *Il1b*, interferon gamma (*Ifng*) and chemokine (C-X-C motif) ligand 2 (*Cxcl2*). Organoid technology provides a cutting-edge tool to study tissue (stem cell) biology *in vitro*. Organoids develop from the tissue's stem cells which under defined culture conditions self-renew, proliferate and self-organize into 3D constructs that reliably recapitulate key characteristics of the epithelial (stem cell) compartment of the organ of origin. Starting from our group's previous achievement to grow organoids from mouse pituitary, shown to originate from the stem cells, we first refined the technique for aged pituitary, and then applied the protocol to tumorous pituitary of aged $Drd2^{-/-}$ and control $Drd2^{+/+}$ mice. Organoid cultures successfully established from both genotypes, displaying a pituitary stemness character and long-term expandability. Interestingly, the tumorous pituitary-derived organoids recapitulated the activated proliferation and cytokine/chemokine nature of its stem cell compartment. IL6, found upregulated in this compartment, stimulated organoid formation and growth, while its removal from the culture medium resulted in decreased organoid stem cell proliferation and loss of long-term expandability. Supplementation of two other cytokines that were upregulated in the activated stem cell compartment of the tumorous gland, i.e. IL1 β and IFN γ , exerted similar effects as IL6 and increased *Il6* expression, thereby suggesting that their effects are mediated by IL6. In contrast, the chemokine CXCL2, also upregulated in the activated stem cells, did not affect *Il6* expression neither organoid growth. To be able to assess tumorigenic and/or regenerative capacity of the (activated) pituitary stem cells and derived organoids, we started to design an orthotopic

transplantation protocol through transcranial stereotactic injection directly into the pituitary. Promising results were obtained but further refinements are needed. Taken together, the tumorous mouse pituitary stem cell compartment shows an activated nature in terms of proliferative and cytokine/chemokine activity, which may be involved in the tumorigenic process in the gland. IL6 appears to partake in the stem cell activation process during tumorigenesis in the gland, similar to its activity in the gland following damage.

Finally, we profiled human pituitary tumors for stem cell presence and phenotype. SOX2⁺ and SOX9⁺ stem cells were detected in the predominance of tumor samples analysed, encompassing a wide variety of types. SOX2⁺ stem cells showed a visible trend of higher abundance and increased proliferative activity in tumors as compared to healthy tissue. Interestingly, organoids very efficiently developed from the tumor biopsies, and displayed a stemness phenotype and tumor-specific expression fingerprints. However, unexpectedly, the organoids showed early expansion arrest. Transcriptomic analysis revealed fading of cytokines/chemokines in the tumor-derived organoids, but supplementation of these signals to the cultures did not improve organoid growth neither passageability.

In conclusion, this work sheds light on stem cell phenotype and behavior in pituitary tumorigenesis, which adds to the limited knowledge of this process and may eventually pave the way to clinical applications.

SAMENVATTING

Als centrale regulator van het endocrien systeem stuurt de hypofyse cruciale ontwikkelings- en fysiologische processen zoals lichaamsgroei, voortplanting, metabolisme, stress-respons en immuniteit. Omwille van deze primordiale rol leidt een verstoorde hypofysaire functie tot ernstige gezondheidsproblemen waaronder infertiliteit en osteoporose. Tumorontwikkeling is de meest voorkomende pathologie in de hypofyse. De mechanismen die aan de basis liggen van tumorigenese in de klier blijven echter weinig begrepen.

Eerst analyseerden we retrospectief klinische aspecten van hypofysetumorpatiënten, alsook de veiligheid en doeltreffendheid van hun chirurgische behandeling d.m.v. transsfenoïdale tumorresectie. Patiënten met visuele problemen of craniale zenuw-afwijkingen herstelden (minstens gedeeltelijk) na de operatie. Ook kregen patiënten met hormoonproducerende tumoren over het algemeen weer normale systemische hormoonspiegels na tumorresectie. Postoperatieve complicaties zoals lekkage van cerebrospinaalvocht of meningitis waren uitzonderlijk, en konden doeltreffend behandeld worden. Ondanks de effectiviteit en veiligheid van de chirurgische behandeling, ontwikkelde de meerderheid van de patiënten hypofyse-deficiëntie (hormonale tekorten) na de operatie waardoor levenslange hormoonsubstitutie nodig was. Een beter begrip van hoe hypofysetumoren zich ontwikkelen en groeien zou de klinische behandeling van patiënten in de toekomst kunnen verbeteren. Om meer inzicht te verwerven in hypofysaire tumorigenese hebben we ons in deze studie gefocust op het gedrag van de stamcellen, en hebben we hun fenotype en transcriptoom onderzocht in hypofysetumoren bij muizen en mensen.

In de dopaminereceptor D2 knock-out ($Drd2^{-/-}$) muishypofyse, waarin sterk-ontwikkelde prolactineproducerende tumoren gevormd zijn op oudere leeftijd, vonden we een toename in het aantal $SOX2^{+}$ stamcellen en een verhoging in hun proliferatieve activiteit t.o.v. $SOX2^{+}$ stamcellen in hypofyse zonder tumorvorming ($Drd2^{+/+}$). RNA-sequencing toonde een meer prominent cytokine/chemokinepatroon in in het stamcelcompartiment van de tumorigene hypofyse, en in het bijzonder van interleukine-6 (*Il6*), *Il1b*, interferon gamma (*Ifng*) en chemokine (C-X-C motief) ligand 2 (*Cxcl2*). Organoïde-technologie biedt een krachtige onderzoekstool om weefsel(-stamcel-)biologie te bestuderen *in vitro*. Organoïden ontwikkelen zich vanuit de weefselstamcellen die zich onder gedefinieerde cultuuromstandigheden vernieuwen, prolifereren en organiseren tot 3D constructies die op betrouwbare wijze de belangrijkste kenmerken van het epitheliale (stamcel-)compartiment van het originele orgaan reproduceren. Uitgaande van het eerdere succes van onze groep om organoïden te kweken uit muizenhypofyse, zich ontwikkelend uit de stamcellen, hebben we de techniek eerst verfijnd voor de oude muishypofyse en vervolgens dit protocol toegepast op de hypofyse van oude $Drd2^{-/-}$ en controle (normale) $Drd2^{+/+}$ muizen. De organoïden groeiden succesvol vanuit beide genotypes, en vertoonden een hypofysestamcel-natuur en langdurige expandeerbaarheid. Interessant is dat de tumorhypofyse-afkomstige organoïden de geactiveerde proliferatie- en cytokine/chemokine-aard van het stamcelcompartiment reproduceerden. IL6, wat opgereguleerd is in dit compartiment, stimuleerde de vorming en groei van de organoïden, terwijl het verwijderen van IL6 uit het medium leidde tot verminderde proliferatie van de organoïde-stamcellen en verlies van de langdurige vermenigvuldigingscapaciteit. Toevoegen van twee

andere cytokines die verhoogd waren in het geactiveerde stamcelcompartiment van de tumorale hypofyse, namelijk IL1 β and IFN γ , zorgden voor gelijkaardige effecten als IL6. Daarenboven verhoogden deze cytokines de expressie van *Il6*, wat suggereert dat hun effecten worden gemedieerd door IL6. Daarentegen beïnvloedde het chemokine CXCL2, dat ook verhoogd is in de geactiveerde stamcellen, de expressie van *Il6* en organoïde-groei niet. Om de tumorigene capaciteit en/of regeneratieve capaciteit van de (geactiveerde) hypofyse-stamcellen en afkomstige organoïden te kunnen onderzoeken, zijn we gestart met het ontwerpen van een orthotopisch transplantatieprotocol door middel van transcraniële stereotactische injectie rechtstreeks in de hypofyse. Veelbelovende resultaten werden verkregen, maar verdere verfijningen van het protocol zijn nog nodig. Samenvattend bracht onze studie naar voor dat het stamcelcompartiment van de tumor-groeiende hypofyse een activatie-status vertoont in termen van proliferatieve en cytokine/chemokine activiteit, die mogelijk betrokken is bij het tumorigene proces in de hypofyse. IL6 blijkt deel te nemen aan dit stamcelsactiveringsproces tijdens tumorvorming in de hypofyse, gelijkaardig aan de IL6 activiteit in beschadigde hypofyse.

Tot slot onderzochten we de aanwezigheid en het fenotype van stamcellen in mens-hypofysetumoren. SOX2⁺ en SOX9⁺ stamcellen werden in de meerderheid van de geanalyseerde tumoren teruggevonden en dit in de grote verscheidenheid aan klinische types. De SOX2⁺ stamcellen vertoonden een zichtbare trend van verhoging in aantal en proliferatieve activiteit in de tumoren t.o.v. gezond weefsel. Interessant is dat organoïden zich heel efficiënt ontwikkelden uit de tumorbiopten en een stamcelfenotype alsook tumor-specifieke expressiekenmerken vertoonden. Onverwacht vertoonden de organoïden echter een vroege stop in groei-expansie. Transcriptoomanalyse onthulde een sterke daling tot afwezigheid van cytokines/chemokines in de tumor-afkomstige organoïden, maar toevoeging van deze factoren aan de culturen verbeterde de organoïde-groei en -vermenigvuldiging niet.

Samenvattend geeft dit werk inzicht in het fenotype en gedrag van stamcellen bij hypofyse-tumorigenese, wat bijdraagt aan de beperkte kennis van dit proces en uiteindelijk kan leiden tot klinische vooruitgang in behandeling.

A journey of a thousand miles begins with a single step – Lao Tzu

CHAPTER 1: GENERAL INTRODUCTION

*A small part of the general introduction has been published in:

Nys, C., Vankelecom, H., 2021. Pituitary disease and recovery: how are stem cells involved? *Mol. Cell. Endocrinol.* 525(111176), 1–8. <https://doi.org/10.1016/j.mce.2021.111176>

1. The pituitary gland

1.1 Pituitary anatomy and architecture

The pituitary gland acts, together with the hypothalamus, as the master endocrine regulator, orchestrating essential physiological processes such as growth, puberty, metabolism, stress management and reproduction. The pituitary is housed in a bony structure, called the *sella turcica*, just below the brain, and is physically connected to the hypothalamus by the infundibulum (Fig. 1). In rodents, the mature gland comprises three parts, i.e. the anterior lobe (AL), the intermediate lobe (IL) and the posterior lobe (or posterior pituitary (PP)) (Cox et al., 2017). The AL and IL together constitute the adenohypophysis (or anterior pituitary (AP)), whereas the PP is referred to as the neurohypophysis.

The adenohypophysis is comprised of a large arsenal of hormone-producing cell types, secreting either prolactin (PRL), adrenocorticotrophic hormone (ACTH), growth hormone (GH), luteinizing hormone (LH), follicle-stimulating hormone (FSH), thyroid-stimulating hormone (TSH) or melanocyte-stimulating hormone (MSH) (Andoniadou et al., 2013; Cox et al., 2017; Vankelecom, 2012). In rodents, the AL and IL are clearly separated by the cleft, an embryonic rudimentary lumen. In humans, the IL structure regresses during embryonic development with its cells spreading in the AL (Cox et al., 2017) (Fig. 1). The adenohypophysis additionally contains non-hormonal cell populations including supportive mesenchymal cells, sinusoidal-capillary endothelial cells, folliculostellate cells, immune cells, and stem cells (Vankelecom, 2007a).

The neurohypophysis contains axonal projections from the hypothalamus which store and secrete the hormones oxytocin and antidiuretic hormone ((ADH), also known as vasopressin), both produced in hypothalamic neurons (Fig. 1). Furthermore, the PP contains pituicytes, a type of glial cells that have a supportive function and may assist in the storage and secretion of these hormones (Wittkowski, 1998).

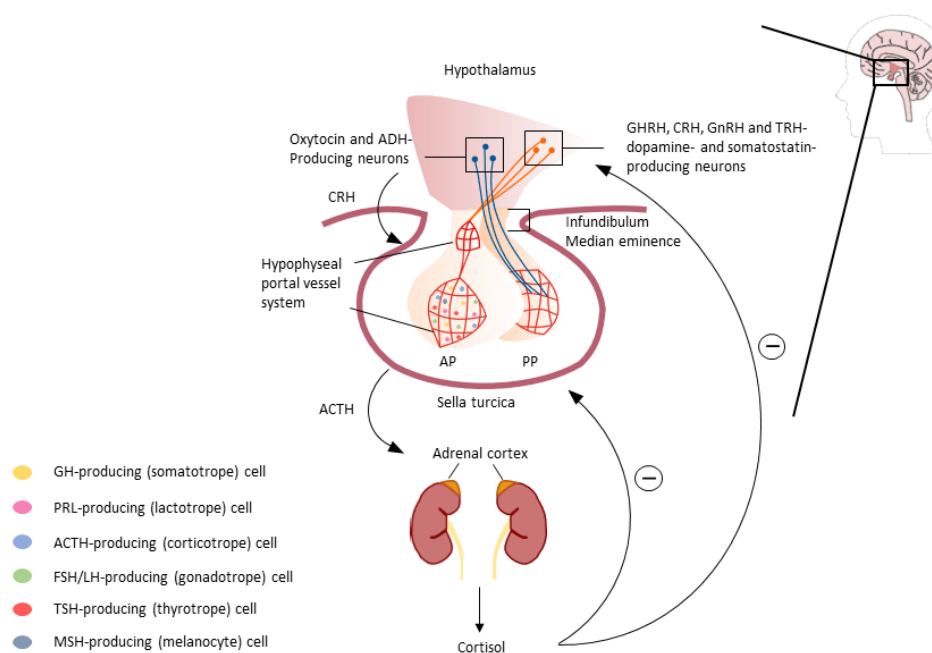


Fig. 1. Schematic representation of human pituitary and hypothalamic-pituitary-adrenal axis

The human pituitary gland consists of two lobes, the major endocrine AP and the PP. The PP is mainly composed of axonal projections descending from the hypothalamus which store and secrete the hormones oxytocin and ADH. The hypophyseal portal vessel system transports stimulatory hormones (GHRH, CRH, GnRH and TRH) and inhibitory signals (dopamine and somatostatin) from the hypothalamus to the AP to regulate synthesis and release of pituitary hormones (GH, ACTH, FSH/LH, PRL and TSH) into the circulation. The pituitary hormones affect multiple segments of the endocrine system to regulate their hormone production which in turn act as negative feedback messengers. For example, the hypothalamic-pituitary-adrenal axis is activated upon stress resulting in release of CRH from the hypothalamus that triggers ACTH secretion from the AP, which will stimulate the adrenal cortex to produce cortisol. Cortisol will negatively feed-back to the hypothalamus and pituitary to inhibit CRH and ACTH release, respectively. GHRH: growth hormone-releasing hormone; CRH: corticotropin-releasing hormone; GnRH: gonadotropin-releasing hormone; TRH: thyrotropin-releasing hormone. Figure adapted from (Vennekens and Vankelecom, 2019).

1.2 Pituitary hormones: function and regulation

Despite being a tiny, pea-sized organ in humans, the pituitary gland impressively regulates body physiology in steering the proper function of multiple distant organs by secretion of distinct hormones. The functions of pituitary hormones are diverse, affecting various segments of the endocrine system. Produced by the somatotropes, GH stimulates lipolysis in adipose tissue and generally orchestrates body and organ growth through anabolic effects in bone and muscle, mainly mediated by (peripheral) insulin-like growth factor 1 (IGF1) (Locatelli and Bianchi, 2014). GH levels increase during childhood, peak at puberty and subsequently decrease upon further aging (Laporte et al., 2021). PRL stimulates mammary gland development and regulates milk production during lactation, while exerting negative feedback on the hypothalamic-pituitary-gonadal axis and lowering serum levels of the gonadotropins LH/FSH and the associated sex hormones (estradiol, progesterone). When released following stress, ACTH activates the adrenal cortex to produce stress hormones, such as cortisol, that exert pleiotropic effects on energy supply, and fuels metabolism, immunity and cardiovascular function (Fig. 1). TSH stimulates the thyroid gland to synthesize and release triiodothyronine (T3) and thyroxine (T4) which control processes such as metabolic rate, lipolysis and cardiac output. LH and FSH regulate ovarian follicle maturation and ovulation in females, and coordinate testicular spermatogenesis in Sertoli cells and testosterone production in Leydig cells in males. Released by the IL in mice, MSH activates skin melanocytes and hair follicles

to produce melanin for pigmentation. Oxytocin and ADH are produced in the hypothalamus and transported along the hypothalamic neurons to the PP for storage and secretion. Oxytocin triggers contractile activity in uterus and mammary gland, inducing uterine contractions and cervical dilatation during parturition and milk ejection during breastfeeding, respectively. ADH coordinates blood pressure by stimulating water reabsorption in the kidney and arteriole constriction (Barkhoudarian and Kelly, 2017).

Production of pituitary hormones is profoundly regulated by central and peripheral inputs and occurs in a way (often pulsatile) according to the momentaneous physiological demands (Vankelecom, 2012). Central regulators include stimulatory and inhibitory factors from the hypothalamus. These factors are produced in distinct hypothalamic neurons, such as the paraventricular and arcuate nuclei, and are released in the median eminence into the hypothalamo-hypophyseal portal system irrigating the AP (Fig. 1). Stimulating signals include growth hormone-releasing hormone (GHRH), corticotropin-releasing hormone (CRH), thyrotropin-releasing hormone (TRH), and gonadotropin-releasing hormone (GnRH) which activate pituitary synthesis and secretion of GH, ACTH, TSH, and LH/FSH, respectively (Fig. 1). The production of LH and FSH is based on pulse frequencies of GnRH release; low pulse frequency triggers secretion of FSH, whereas high pulse frequency stimulates release of LH (Herbison, 2018). The gonadal axis is further regulated by kisspeptin, which stimulates GnRH secretion and consequentially LH/FSH production (Barkhoudarian and Kelly, 2017). Recently, an orphan G protein coupled receptor GPR101 was discovered as a potential GH (and PRL) regulator, although its physiological role is still not fully clear (Abboud et al., 2020). Pathological overexpression of GPR101 in X-linked acroigantism is associated with increased GH secretion by infant-onset GH-secreting tumors (Trivellin et al., 2014). The hypothalamus also suppresses hormone production by the pituitary through inhibitory factors. Somatostatin inhibits the release of GH, while dopamine tonically restrains the production of PRL.

Hormone production is further controlled by feedback mechanisms relayed by the hormones produced by the endocrine target glands, thus impeding the release of the corresponding hypothalamic and pituitary factors that trigger their secretion when sufficient serum levels have been reached. As an example, the hypothalamic-pituitary-adrenal axis is activated by stress. CRH is released from the hypothalamus and triggers production of ACTH by the corticotropes of the AL which then stimulates the production of cortisol in the adrenal cortex. Cortisol will feedback to the hypothalamus and pituitary to lower the synthesis and release of CRH and ACTH (Fig. 1). Other well-known peripheral feedback signals include IGF1 that inhibits the release of GHRH and GH; sex hormones (testosterone, estradiol and progesterone) that modulate the release of GnRH, LH and FSH; and T3 and T4 that impede the production of TRH and TSH (Melmed, 2017).

1.3 Pituitary embryonic development

In humans, pituitary organogenesis starts during the fourth week of embryonic development. The pituitary primordium, called Rathke's pouch (RP), develops from the oral ectoderm by thickening and invagination towards the ventral diencephalon (Larkin et al., 2017). At the same time, the eventual PP derives from the infundibulum, a downward extension of this ventral diencephalon. During weeks 6-8 of embryonic development, RP separates from the oral ectoderm and connects with the developing PP to form the pituitary gland. Cells from

RP undergo extensive proliferation to form the AL from the anterior wall and the IL from the posterior wall. Thus, the pituitary gland has a dual embryonic origin and requires precise spatial and temporal coordination between both layers to form properly, steps which have extensively been studied and unraveled in mice (Vankelecom, 2012).

Pituitary development in mice starts at 8.5 days post coitum (dpc) from the roof of the oral cavity (Fig. 2), an epithelial layer expressing homeobox expressed in ES cells 1 (HESX1) and the bicoid homeodomain factors paired-like homeodomain transcription factor (PITX) 1 and PITX2 (Vankelecom, 2012). A small part of the oral ectoderm, characterized by expression of LIM homeobox protein (LHX) 3 and LHX4 and by exclusion of sonic hedgehog (SHH) expression (in contrast to its presence in the rest of the oral ectoderm), initiates pituitary development (Zhu et al., 2007). Formation of the hypophyseal primordium (RP) requires signals from the outgrowing ventral diencephalon like bone morphogenetic protein (BMP) 2, BMP4, SHH and fibroblast growth factor (FGF) 8 and FGF10 (Kelberman et al., 2009; Vankelecom, 2012; Zhu et al., 2007). Under control of opposing gradients of these morphogens (Fig. 2), RP starts to form around 9.5 dpc by thickening and bulging of the oral ectoderm towards the ventral diencephalon. Simultaneously, a downward extension of the ventral diencephalon arises which generates the infundibulum. Around 11.5 dpc, RP separates from the underlying oral ectoderm and forms the AL and IL. During these phases of pituitary development, RP mainly consists of stem/progenitor cells, characterized by expression of sex-determining region Y-box (SOX) 2 (Kelberman et al., 2009). These cells start to transiently co-express SOX2 and prophet of PIT-1 (PROP1) as intermediate phase towards the formation of the final endocrine cells (Pérez Millàn et al., 2016). Further expansion and maturation of the RP stem/progenitor cells is controlled by several transcription factors such as *sine oculis* homeobox homolog (SIX) 1, SIX6 and paired box 6 (PAX6) (Goldsmith et al., 2016; Zhu et al., 2007). The AL further matures through proliferation of stem/progenitor cells in the marginal zone (MZ) around the cleft, and gradual differentiation of cells more ventrally located which form the distinct pituitary cell lineages. This shaping and differentiation is regulated by strict spatiotemporal expression of transcriptional regulators under influence of the opposing gradients of the morphogens (BMPs, FGFs; Fig. 2) (Vankelecom, 2012). From E13.5, specific expression patterns of transcriptional regulators are being installed that steer endocrine differentiation (Vankelecom, 2012). Expression of the transcription factor PROP1 is fundamental to activate the expression of POU domain, class 1, transcription factor 1 ((POU1F1), also known as pituitary-specific positive transcription factor 1 (PIT1)), which marks the PIT1 lineage that includes lactotropes, somatotropes and thyrotropes (Pérez Millàn et al., 2016; Vankelecom, 2012). The PIT1-negative lineage comprises corticotropes and gonadotropes that are marked by expression of T-box 19 (TBX19; also referred to as TPIT) and steroidogenic factor 1 (SF1), respectively (Andoniadou et al., 2013; Vankelecom, 2012; Zhu et al., 2007). In the end, the AL and IL have developed while the lumen of RP is maintained and persists as the pituitary cleft, separating both lobes in the mature mouse (rodent) gland (Andoniadou et al., 2013; Kelberman et al., 2009; Vankelecom, 2012; Zhu et al., 2007) (Fig. 2). Uncommitted

stem/progenitors line this cleft (MZ), whereas the parenchyma of the AL and IL is progressively populated with hormone-producing cells (Andoniadou et al., 2013).

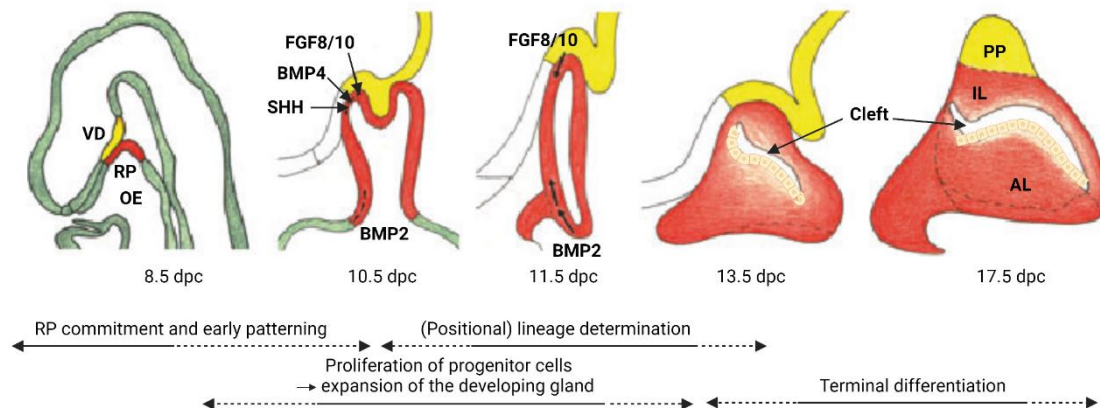


Fig. 2. Mouse pituitary embryonic development

The pituitary primordium, Rathke's pouch (RP), is formed by an invagination of the oral ectoderm (OE, red) under influence of several opposing signals from ventral diencephalon (VD, yellow) and OE. RP becomes detached, and the stem/progenitor cells located around the cleft expand and differentiate into hormonal cells, strictly regulated by gradients of signaling and transcriptional factors. Figure adapted from (Vankelecom, 2010).

2. Pituitary dysfunction

The pituitary gland strictly regulates hormone balance and has a critical impact on body development and physiology. Hence, pituitary disease and dysfunction cause multiple clinical symptoms and severe morbidity. Pituitary dysfunction can be classified into hypopituitarism, marked by insufficient hormone production, and hyperpituitarism, characterized by excess hormonal output.

2.1 Hypopituitarism

Hypopituitarism can involve one or more hormones. Panhypopituitarism or combined pituitary hormone deficiency (CPHD) refers to a shortage in all pituitary hormones. Hypopituitarism may have a congenital origin, or may be acquired during life due to pituitary-damaging processes (Nys and Vankelecom, 2021).

Congenital hypopituitarism, being sporadic or part of a hereditary syndrome, mostly involves mutations in genes encoding transcription factors crucial for pituitary embryogenesis, such as *HESX1*, *PITX2*, *PROP1*, *LHX3*, *LHX4* and *PIT1*. Mutations in *HESX1* lead to septo-optic dysplasia in humans and a comparable phenotype in mice, including the occurrence of pituitary dysplasia which may at least partly be due to aberrant hyperproliferation of the stem/progenitor cells (Dattani et al., 1998; Fang et al., 2016). *HESX1* mutant phenotypes may range from multiple misplaced glands to an absent or agenetic pituitary (Andoniadou et al., 2007; Kelberman et al., 2009). *PITX2* mutations are associated with Axenfeld-Rieger syndrome, also encompassing sporadic pituitary hypoplasia that can result in growth retardation (Tümer and Bach-Holm, 2009). *PITX2* is involved in early RP expansion, and *Pitx2*- as well as *Pitx1*-deficient mice show severe pituitary hypoplasia missing most hormonal cells except for some sporadic ACTH-expressing cells (Charles et al., 2005; Lin et al., 1999; Suh et al., 2002). Mutations in *LHX3*, which is also expressed at the RP development phase, can lead to pituitary dysfunction with GH, TSH and LH/FSH deficiency and sometimes corticotrope deficits (Gangat and Radovick, 2017; Xatzipsalti et al., 2019). *LHX4* mutations give rise to a hypoplastic pituitary gland in which all hormonal cell types are present

but at reduced numbers, in some cases leading to panhypopituitarism. Recessive mutations of *PROP1* are the most frequent cause of CPHD (Bertko et al., 2017; Xatzipsalti et al., 2019) with deficits in GH, PRL, TSH and LH/FSH. Patients with *PROP1* mutations often present with growth retardation and delayed or absent puberty, although time of onset and severity of phenotype can differ (Xatzipsalti et al., 2019). Dwarfism and infertility are similarly observed in *Prop1*-deficient Ames dwarf mice (df/df) (Sornson et al., 1996).

Acquired hypopituitarism can be caused by traumatic brain injury, such as traffic accidents, falls and acts of violence, or can result from ischemic stroke, Sheehan's syndrome (severe blood loss at birth-giving), pituitary apoplexy or infection, as well as from growth of tumors in the gland pressing on the healthy tissue, which may become (further) damaged at surgical resection of the tumor (Nys and Vankelecom, 2021; Vennekens and Vankelecom, 2019).

Currently, hypopituitarism-associated hormonal deficiencies are treated by lifelong hormonal supplementation with oral corticosteroids and L-thyroxine, oral/transdermal estrogens and testosterone to address ACTH, TSH and LH/FSH insufficiency, respectively (Schneider et al., 2007). GH is supplemented via subcutaneous (sc) administration. This supplementation provides major health benefits to all axes that are affected, and can be life-saving, in particularly in the case of corticosteroid replacement. Although hormone supplementation is clearly beneficial, there is still room for improvement in treating hypopituitarism-driven hormone deficiencies. For instance, the treatment is not always able to completely reproduce the cyclic hormonal output of the pituitary, hence requiring regular follow-up and fine-tuning of the medication scheme (Alexandraki, 2019). In addition, administered hormones may cause side effects such as development of diabetes by supplemented GH, although the overall benefit of well-adapted and titrated GH supplementation is clear (Moøller and Joørgensen, 2009). In addition to hormone supplementation, other measurements have to be taken to cope with additional complications such as osteoporosis, dyslipidemia and cardiovascular disease. Lifestyle adaptations and treatment with bisphosphonates, lipid-lowering and anti-hypertensive drugs may need to be added to the hormonal supplementation (Schneider et al., 2007).

2.2 Hyperpituitarism and pituitary tumors

Mostly, hyperpituitarism is caused by a pituitary tumor, with clinical symptoms depending on the hormone that is overproduced (summarized in Table 1). Actually, tumorigenesis is the most frequent pathology of the pituitary gland.

Pituitary tumors constitute up to 15 % of intracranial neoplasms, and are found at autopsy in up to 15 % of the general population (Kopczak et al., 2014; Melmed, 2011). Many of these tumors remain subclinical and undiagnosed, and the prevalence of symptom-associated pituitary tumors is estimated at 0.1 % (Daly and Beckers, 2020; Melmed, 2020). This prevalence is increasing over the last decades which may be due to an ageing population, more awareness and/or improved diagnostics (Daly and Beckers, 2020).

Table 1. Overview of pituitary tumors with associated clinical symptoms

Tumor type	Hormone in excess	Prevalence	Symptoms
Prolactinoma	PRL	30-60 %	Amennorhea Galactorrhoea Infertility Hypogonadism
Somatotropinoma	GH	8-15 %	Acromegaly Gigantism
Corticotropinoma	ACTH	3-6 %	Cushing's disease Hypercortisolism
Thyrotropinoma	TSH	< 1 %	Hyperthyroidism
Gonadotropinoma	LH/FSH	< 1 %	Hypergonadism
NFPA and null cell adenoma	None	14-55 %	Hypopituitarism

NFPA: non-functioning pituitary adenoma

Pituitary tumors are in general non-malignant, slow-growing lesions (adenomas), but despite their histologically benign nature, they can cause significant morbidity and increased mortality risk not only because of excess hormone-imposed clinical symptoms, but also tumor mass effects compressing healthy neighboring pituitary tissue (leading to hypopituitarism) (Table 1) as well as of adjacent neural structures such as the optic chiasm causing visual defects, and cranial nerves leading to neuropathy. These physical insults can further lead to pituitary apoplexy resulting in acute severe headache. Lastly, pituitary tumors can infiltrate into adjacent structures, such as the cavernous sinus and/or sphenoid sinus (Melmed, 2020, 2011). A considerable number (approximately 35 %) of the pituitary tumors display an invasive character as observed by lateral growth into the cavernous sinuses and/or downwards into the sphenoid sinus, and often characterized by a proliferative (Ki67) index ≥ 3 % (Hansen et al., 2014; Trouillas et al., 2020). Lateral extension is categorized by Knosp grading (ranging from 0-4), with Knosp 3 and 4 marked by extension into, or invasion of, the sinus cavernous.

Malignant pituitary tumors, i.e. which metastasize (thus referring to carcinomas), do exist but are very rare, constituting less than 0.5 % of the pituitary tumors (Melmed, 2020; Trouillas et al., 2020). However, the WHO recently described a more prevalent (7-9 %) class of 'aggressive pituitary tumors with malignant potential', being invasive tumors with a Ki67 index ≥ 10 % and immunohistochemical characteristics of other carcinomas (e.g. P53 immunopositivity and mitotic count $> 2/10$ per high-power field), but not (yet) displaying metastases (Trouillas et al., 2020).

2.2.1 Classification and treatment of pituitary tumors

Traditionally, pituitary tumors are classified according to size (microadenomas < 10 mm and macroadenomas ≥ 10 mm) and hormonal phenotype (Table 1), based on detection of (over-)production of one or more hormones in histological sections and/or circulation. Of note, pituitary tumors may also present as non-secreting lesions (comprising non-functioning pituitary adenomas (NFPA) and null cell adenomas) (Table 1). Recently, classification and nomenclature have been revised and adapted to more contemporary insights, although this

new categorization still raises some debate (Mete and Lopes, 2017; Trouillas et al., 2020). Pituitary adenomas are proposed to be referred to as pituitary neuroendocrine tumors (PitNETs) and categorized in more detail according to their cell lineage and morphological variants, based on histological and immunohistochemical features (Table 2) (Mete and Lopes, 2017; Trouillas et al., 2020). The revised classification also recognizes the importance of transcription factors and co-regulators in the tumors (such as PIT1 and estrogen receptor alpha (ER α)). For instance, a null cell adenoma is now defined by complete absence of hormonal content as well as of expression of pituitary lineage transcription factors, both still potentially observed in classical null cell adenomas. In addition, subclasses are outlined in more detail. As an example, lactotroph adenomas (prolactinomas) are histologically subdivided into sparsely granulated lactotroph tumors, densely granulated lactotroph tumors and acidophil stem cell adenomas (Table 2). All these subclasses are characterized by expression of PIT1 and ER α , but different in histological patterns. The most common subtype is the sparsely granulated lactotroph tumor, having a weak and cap-like PRL pattern and often responsive to dopamine-receptor agonists, the first line treatment of lactotroph tumors, reproducing the inhibitory dopamine activity on lactotroph function and proliferation. Densely granulated lactotroph tumors are characterized by a strong and diffuse PRL pattern. Acidophil stem cell adenomas are more rare, contain oncocytic cells with aberrant accumulation of mitochondria, and are more prone to recurrence (Larkin and Ansorge, 2017; Mete and Lopes, 2017).

Table 2. 2017 WHO pathological classification of pituitary tumors

Tumor type	Morphological variants	Pituitary hormones by IHC	Transcription factors and other co-factors by IHC
Somatotroph adenomas (= somatotropinoma)	Densely granulated somatotroph adenoma	GH, α GSU	PIT1
	Sparsely granulated somatotroph adenoma	GH	PIT1
	Mammotroph adenoma	GH + PRL (in same cells) \pm α GSU	PIT1, ER α
	Mixed somatotroph-lactotroph adenoma	GH + PRL (in different cells) \pm α GSU	PIT1, ER α
Lactotroph adenomas (= prolactinoma)	Sparsely granulated lactotroph adenoma	PRL	PIT1, ER α
	Densely granulated lactotroph adenoma	PRL	PIT1, ER α
	Acidophil stem cell adenoma	PRL, GH (focal and variable)	PIT1, ER α
Thyrotroph adenoma (= thyrotropinoma)		TSH β , α GSU	PIT1, GATA2
Corticotroph adenomas (= corticotropinoma)	Densely granulated corticotroph adenoma	ACTH	TBX19
	Sparsely granulated corticotroph adenoma	ACTH	TBX19
	Crooke's cell adenoma	ACTH	TBX19
Gonadotroph adenoma (= gonadotropinoma)		FSH β , LH β , α GSU (various combinations)	SF1, GATA2, ER α
Null cell adenoma		None	None
Plurihormonal adenomas	Pit-1-positive plurihormonal adenoma (previously termed Silent subtype 3 adenoma)	GH, PRL, TSH β \pm α GSU	PIT1
	Adenomas with unusual IHC combinations	Various combinations	

IHC, immunohistochemistry; α GSU, alpha glycoprotein hormone subunit. Table adapted from (Mete and Lopez, 2017)

Other pituitary lesions include pituicytomas, craniopharyngiomas and Rathke's cleft cysts (Mete and Lopes, 2017). Pituicytomas are very rare glial tumors originating from the pituicytes of the PP and infundibulum. Presenting symptoms vary according to tumor size and location, and consist of visual deficits, headache and hypopituitarism (Yang et al., 2016). Craniopharyngiomas and Rathke's cleft cysts are lesions that occur in the pituitary region and interfere with normal pituitary function. Craniopharyngiomas are complex epithelial tumors that can be classified as adamantinomatous craniopharyngioma (ACP) and papillary craniopharyngiomas. ACP, a mostly benign but burdening tumor that typically affects children, is hypothesized to develop from remnants of RP and is associated with activating mutations in the β -catenin (*CTNNB1*) gene, leading to constitutive activation of the wingless-type MMTV integration site (WNT) pathway (Andoniadou et al., 2012; Gaston-Massuet et al., 2011; Nielsen et al., 2011). Papillary craniopharyngiomas predominantly affect adults and are linked to B-Raf proto oncogene, serine/threonine kinase (BRAF) mutations (Larkin et al., 2014). Rathke's cleft cysts are rare, benign, fluid-filled lesions originating from epithelial remnants of RP. These cysts often remain asymptomatic (Hofmann et al., 2006).

Treatment of pituitary tumor patients aims at maximal removal of the tumor, or at least debulking, to lower the tumor mass effects, and at restoration of the hormone balance and pituitary function. PitNET-burdened patients are treated according to tumor type. Treatments include surgery, pharmacological therapy or irradiation. Prolactinomas are predominantly tackled with dopamine receptor D2 (Drd2) agonists like cabergoline and bromocriptine that inhibit PRL production and lactotrope cell proliferation (Kopczak et al., 2014; Peverelli et al., 2015). Although effective to achieve normoprolactinemia and tumor size reduction in many patients, therapy resistance is still observed in 10-30 % of them (Maiter, 2019). Underlying mechanisms remain poorly understood and may include reduction in number of (Drd2) receptors, alterations in dopamine signaling (e.g. reduced expression of the signal-involved inhibitory G protein alpha subunit) and/or reduction in transforming growth factor beta (TGF β) signaling (Li et al., 2015; Maiter, 2019). Other pituitary tumors are in first line removed through surgical (predominantly transsphenoidal) resection. First generation somatostatin analogues (e.g. octreotide) can also be used to treat GH-secreting tumors and TSH-secreting tumors, whereas second generation somatostatin analogues (e.g. pasireotide) are licensed for ACTH-secreting tumors, but one third is resistant (Kopczak et al., 2014; Peverelli et al., 2015). In general, despite a fair success rate (approximately 60 % (Fatemi et al., 2008; Melmed, 2020)), treatments remain unsatisfactory in many patients with 10-40 % recurrence and negative impact on quality of life (Daly et al., 2009; Melmed, 2020; Van der Klaauw et al., 2008). In addition, patients often need lifelong hormonal supplementation after surgery since healthy pituitary tissue may have been compressed and damaged by the expanding tumor tissue or may have been harmed during extirpation of the lesion. Hence, clinical management will certainly benefit from further improvements. A better understanding of pituitary tumorigenesis could be the first step.

2.2.2 Pituitary tumorigenesis

To date, not much is known on the initiation and development of PitNETs and the molecular pathways involved, with only 5 % of the tumors traced back to genetic mutations (Mete and Lopes, 2017; Trouillas et al., 2020). Pituitary tumors can be part of hereditary conditions, such as multiple endocrine neoplasia (MEN) syndromes (MEN1, MEN4), Carney complex, McCune-Albright syndrome and familial isolated pituitary adenoma (FIPA) caused by germline mutations in *MEN1*, *MEN4*, protein kinase cAMP-dependent type I regulatory subunit alpha (*PRKAR1A*), guanine nucleotide binding protein alpha stimulating activity polypeptide (*GNAS*) and aryl hydrocarbon receptor interacting protein (*AIP*), respectively (Daly et al., 2009; Zhou et al., 2014). Intriguingly, alterations in classical oncogenes or tumor suppressor genes are rare in pituitary tumors. Some mutations in tumor suppressor genes have been linked to (sporadic) pituitary tumors, either by gene mutations or epigenetic modifications such as promoter hypermethylation leading to downregulation of gene transcription. For instance, mutations have been identified in cell cycle and growth factor genes, such as cyclin dependent kinase inhibitor 2A (*CDKN2A*, also known as *P16*), *BMP4* and suppressor of cytokine signaling 1 (*SOCS1*) (Aflorei and Korbonits, 2014; Cano et al., 2014; Melmed, 2011; Zhou et al., 2014). In addition, recent genome sequencing studies have shown that PITNETs often display copy number alterations, mostly somatic rather than germline or hereditary (Bi et al., 2017).

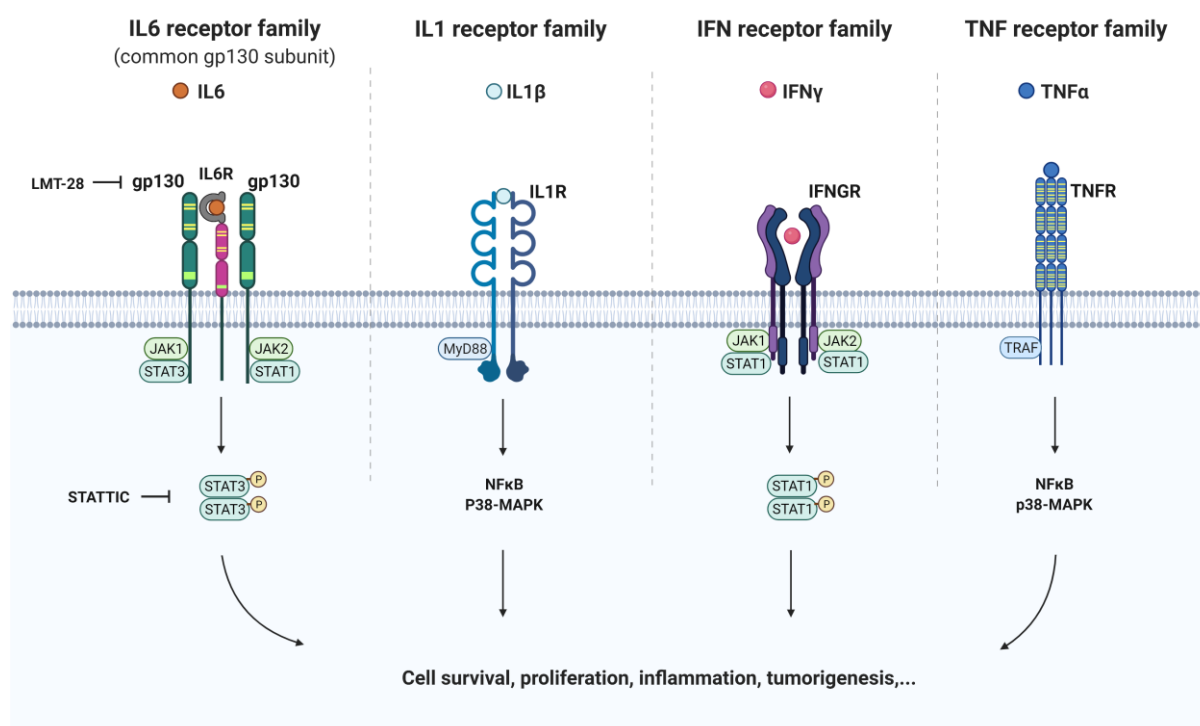


Fig. 3. Simplified overview of a selection of cytokine signaling pathways

Cytokine signaling acts *via* JAK-STATs, NFκB and p38-MAPK to stimulate transcription of target genes that are involved in various processes such as cell survival, proliferation and tumorigenesis. The inhibitors used in this study (LMT-28 and STAT3) are also indicated. Figure created with Biorender.

Further, several studies highlighted the importance of cytokine and chemokine signaling in PitNETs and their link with tumor behavior. Cytokine signaling is involved in many processes including cell proliferation and tumorigenesis. These factors can initiate a signaling cascade *via* Janus kinase (JAK)-signal transducer and

activator of transcription (STAT), nuclear factor kappa B (NFκB) and p38-mitogen-activated protein kinase (p38-MAPK) to stimulate the expression of target genes involved in cell survival, proliferation and tumorigenesis (Fig.3). For instance, the interleukin-6 (IL6) receptor family acts through binding of a ligand (e.g. IL6) to a complex consisting of the common co-signal transducer gp130 and a cytokine-specific receptor (e.g. the IL6 receptor (IL6R)). Binding of IL6 to this complex induces JAK1/2-regulated phosphorylation of STAT1/3, which will dimerize and translocate to the nucleus to stimulate transcription of target genes (Rose-John, 2018). Experimental interference with this pathway is possible through, among others, STATTIC that inhibits activation, dimerization and nuclear translocation of STAT3 or LMT-28 that directly blocks gp130 (Fig. 3). The association of cytokines and chemokines with pituitary tumors is more and more advanced. For instance, it has been shown that the cytokines IL6 and tumor necrosis factor alpha (TNFα) are upregulated in invasive pituitary tumors (Wu et al., 2016). The importance of IL6 in PitNETs was further demonstrated by impaired xenograft tumor development of the rat (GH/PRL-secreting) tumor cell line GH3 when the expression of gp130 was reduced using antisense cDNA introduced by a vector (Castro et al., 2003). Fibroblasts in the tumor microenvironment also secrete cytokines and chemokines such as IL6, IL8, C-C motif chemokine ligand 2 (CCL2), bFGF and C-X-C motif chemokine ligand 1 (CXCL1) (Marques et al., 2019a, 2019b). Also here, it was found that cytokine levels were linked to tumor behavior, as higher levels of CCL2 and IL6 were detected in more proliferative and/or invasive tumors (Marques et al., 2019a). In addition, GH3 tumor cells exposed to tumor-derived fibroblast-conditioned medium resulted in epithelial-mesenchymal transition (EMT) and increased migration and invasiveness, as compared to GH3 cells exposed to skin fibroblast-conditioned medium (Marques et al., 2019a).

Cytokine signaling in pituitary tumors may play a complex role since a number of cytokines are also involved in senescence. Senescent cells are characterized by an irreversible cell cycle arrest and the secretion of senescence-associated secretory phenotype (SASP) factors, encompassing, among others, IL6 and TNFα (McHugh and Gil, 2018). IL6 has been assigned a dual role: autocrine IL6 triggers senescence, which may contribute to the benign character of pituitary tumors, whereas paracrine IL6 fuels cell proliferation and thus tumor growth (Sapochnik et al., 2017b).

2.2.3 Mouse models to study pituitary tumor pathogenesis

Pituitary tumorigenesis has mostly been investigated using genetic mouse models. Modifications comprise overexpression of oncogenes (e.g. *Pttg*) or other regulatory factors (e.g. *Tgfa*), or inactivation of tumor suppressor genes (e.g. *Rb1*) or hormone-regulatory factors (e.g. *Drd2*). An overview of genetically modified mouse models developing pituitary tumors is presented in Table 3. Of note, mice can also spontaneously develop pituitary tumors. For instance, PRL-secreting proliferative lesions were observed in the majority (> 70 %) of aged FVB/NCr mice (Wakefield et al., 2003).

Table 3. Overview of genetically modified mouse models developing pituitary tumors

Syndrome/ disorder	Genetic change	Gene(s) modification (promoter*)	Gene description	Tumor type	Reference(s)
FIPA	Heterozygous knock-out	<i>Aip</i>	Aryl hydrocarbon receptor-interacting protein	GH-A (90 %), PRL-A	Raitila <i>et al.</i> 2010
	Tissue specific (Ins-Cre) homozygous knock-out	<i>Aip</i>	Aryl hydrocarbon receptor-interacting protein	GH-A	Barry <i>et al.</i> 2019
Acromegaly/ gigantism	Transgenic overexpression	<i>Ghrh (MT*)</i>	Growth hormone-releasing hormone	GH-A, mixed GH/PRL-A	Asa <i>et al.</i> 1992
	Homozygous knock-out	<i>p18^{Ink4c}</i>	<i>p18</i> (or cyclin-dependent kinase inhibitor 2C (<i>Cdkn2c</i>))	Acromegaly, ACTH-A in IL	Franklin <i>et al.</i> 1998
MEN1	Heterozygous knock-out	<i>Men1</i>	Multiple endocrine neoplasia type 1	PRL-A, GH-A, NFPA, mixed GH/PRL-A, ACTH-A in IL	Crebtree <i>et al.</i> 2001 Bertolino <i>et al.</i> 2003 Loffler <i>et al.</i> 2007 Harding <i>et al.</i> 2009
	Tissue-specific (Ins-Cre) homozygous knock-out	<i>Men1</i>	Multiple endocrine neoplasia type 1	PRL-A	Biondi <i>et al.</i> 2004
MEN4	Homozygous knock-out	<i>p27^{Kip1}</i>	<i>p27</i> (or cyclin-dependent kinase inhibitor 1B (<i>Cdkn1b</i>))	Tumors in IL	Nakayama <i>et al.</i> 1996
	Homozygous inactivating mutation knock-in	<i>p27^{S10A}</i> and <i>p27^{CK-}</i>	<i>p27 (Cdkn1b)</i>	Tumors in IL	Besson <i>et al.</i> 2006
Cushing's disease	Transgenic overexpression	<i>Crh</i>	Corticotropin-releasing hormone	ACTH-A	Stenzel-Poore <i>et al.</i> 1992
	Transgenic overexpression	<i>PyLT</i>	Polyoma large T antigen	ACTH-A	Helseth <i>et al.</i> 1992
Carney complex	Pituitary-specific homozygous knock-out	<i>Prkar1a (rGhrhr*)</i>	Protein kinase cAMP-dependent type I regulatory subunit alpha	GH-A, PRL-A, TSH-A	Yin <i>et al.</i> 2008
Non-syndromic	Tissue-specific (GFAP-cre) homozygous inactivation	<i>Bmi1</i>	B lymphoma Mo-MLV insertion region 1 homolog	ACTH-A in IL and AP	Westerman <i>et al.</i> 2012
	Point mutation rendering the Cdk4 protein insensitive to INK4 inhibitors (knock-in)	<i>Cdk4^{R24C/R24C}</i>	Cyclin-dependent kinase 4	PRL-A, PRL-C (15 %)	Sotillo <i>et al.</i> 2001
	Point mutation rendering the Cdk4 protein insensitive to INK4 inhibitors (knock-in) and <i>p27^{Kip1}</i> inactivation (knock-out)	Compound <i>Cdk4^{R24C/R24C} p27^{Kip1}</i> homozygous mutant mice	Cyclin-dependent kinase 4 and <i>p27 (Cdkn1b)</i>	Poorly differentiated adenomas	Sotillo <i>et al.</i> 2005

Tissue-specific knock-out (of exon 3) rendering CTNNB1 degradation resistant	<i>Cttnb1</i>	β -catenin	Craniopharyngioma	Gaston-Massuet <i>et al.</i> 2011
Tissue-specific transgenic overexpression	<i>Cyclin E (Pomc*)</i>	Cyclin E	LH-A, FSH-A, NFPA	Roussel-Gervais <i>et al.</i> 2010
Homozygous knock-out	<i>Drd2</i>	Dopamine receptor D2	PRL-A	Kelly <i>et al.</i> 1997
Transgenic overexpression	<i>Hmga1/2 (CMV*)</i>	High mobility group AT-hook 1/2	Mixed GH/PRL-A	Fedele <i>et al.</i> 2005, Fedele <i>et al.</i> 2002
Homozygous knock-out	<i>p19^{Ink4d}</i>	<i>p19</i> (or cyclin-dependent kinase 4 inhibitor D (<i>Cdkn2d</i>))	PRL-A, GH-A	Bai <i>et al.</i> 2014
Heterozygous and homozygous knock-out	<i>Prl</i>	Prolactin	PRL-A	Cruz-Soto <i>et al.</i> 2002
Homozygous knock-out	<i>Prlr</i>	Prolactin receptor	PRL-A	Schuff <i>et al.</i> 2002
Tissue-specific transgenic overexpression	<i>Prop1 (αGSU/Cga*)</i>	Prophet of Pit1	TSH-A, NFPA, GH-A, PRL-A, mixed GH/PRL-A	Egashira <i>et al.</i> 2008
Tissue-specific transgenic Pttg: <i>Rb</i> heterozygous knock-out	<i>Pttg:Rb (αGSU/Cga*)</i>	Pituitary tumor transforming gene: retinoblastoma	PRL-A, GH-A, LH-A, FSH-A, ACTH-A	Donangelo <i>et al.</i> 2006
Tissue-specific heterozygous knock-out	<i>Rb1 (Pomc*)</i>	RB transcriptional corepressor 1	MSH-A in IL	Jacks <i>et al.</i> 1992
Transgenic expression	<i>SV40 (AVP*)</i>	Large T-antigen of the simian virus 40	GH-A, ACTH-A in IL	Stefaneaunu <i>et al.</i> 1992
Transgenic expression	<i>PyLT-SV40 (Pomc*)</i>	Large T-antigen of the simian virus 40	ACTH-A	Low <i>et al.</i> 1993
Transgenic expression	<i>SV40tsTag (Fshβ*)</i>	Large T-antigen of the simian virus 40	NFPA, FSH-A, LH-A	Kumar <i>et al.</i> 1998
Tissue-specific transgenic overexpression	<i>TGFα (Prl*)</i>	Transforming growth factor alpha	PRL-A	Mcandrew <i>et al.</i> 1995

TsTag, temperature sensitive Tag; GH-A, GH-producing adenoma; PRL-A, PRL-producing adenoma; ACTH-A, ACTH-producing adenoma; NFPA, non-functioning pituitary adenoma; FSH-A, FSH-producing adenoma; LH-A, LH-producing adenoma; MSH-A, MSH-producing adenoma; TSH-A, TSH-producing adenoma; PRL-C, PRL-producing carcinoma; MT, metallothionein promoter; rGhrhr, rat GHRH receptor; CMV cytomegalovirus; α GSU/Cga., alpha glycoprotein hormone subunit/glycoprotein hormones, alpha subunit; AVP, arginine vasopressin. Table adapted and compiled from Cano *et al.* 2014; Lines *et al.* 2016; Gahete *et al.* 2019.

The *Drd2* knock-out mouse model

To study pituitary tumorigenesis, we used the *Drd2* knock-out mouse model, which we therefore describe in more detail here.

Female *Drd2* knock-out (*Drd2*^{-/-}) mice gradually develop prolactinomas in the pituitary, the most common type in humans (see above). Targeted disruption and replacement of exon 7 and the 5' half of exon 8 of the *Drd2* locus with a neomycine resistance cassette (deleting in exon 8 the sequences that encode the last two transmembrane domains, the third extracellular loop, and the intracytoplasmic carboxyl-terminal tail of the receptor) resulted in a truncated *Drd2* receptor and absence of detectable ligand binding sites (Kelly et al., 1997). Homozygous knock-out (*Drd2*^{-/-}) female mice develop chronic hyperprolactinemia from 3 months of age, evolving into progressive lactotrope hyperplasia and eventually formation of prolactinomas (from 6 to 8 months onwards), all due to the absence of the tonic negative inhibition of dopamine on lactotrope function and behavior (Asa et al., 1999; Kelly et al., 1997). Male *Drd2*^{-/-} mice have a less pronounced phenotype with hyperprolactinemia and hyperplasia only observed in aged animals (i.e. from 17 months onwards) (Kelly et al., 1997). One explanation for this sex difference may be that females have higher estrogen levels; estrogen is known to stimulate lactotrope growth and enhance PRL production, rendering the females more susceptible to prolactinoma development (Kelly et al., 1997). On the other hand, higher levels of TGFβ1 are observed in males; TGFβ signaling has been shown to inhibit lactotrope proliferation and PRL secretion (Recouvreux et al., 2013; Sarkar et al., 1992), which may explain the less pronounced impact of *Drd2* loss in males. Additionally, estrogens negatively regulate the TGFβ1 signaling system. Interaction of both pathways may thus either delay or propel prolactinoma formation according to gender (Recouvreux et al., 2013). In the clinic, 10-30 % of prolactinoma tumors show resistance to dopamine agonist therapy (Maiter, 2019). Underlying mechanisms remain poorly understood, but lower *Drd2* functionality may be one of the reasons (see above). Hence, the *Drd2* knockout model represents an interesting model to study dopamine-resistant prolactinomas.

Although genetic mouse models have improved our knowledge on pituitary tumorigenesis, causes and molecular underlying mechanisms remain poorly understood. New, original research angles are needed. Importantly, it is unclear whether and how the resident stem cells may be involved.

3. Pituitary stem cells

3.1 Stem cells in the pituitary: identification and search for their function

The first indications for the existence of stem cells in the pituitary gland dates from 1969. Pituitary chromophobe cells (i.e. lacking hormone secretory granules) were found to proliferate and give rise to hormonal cell types when transplanted under the hypothalamus of hypophysectomized rats (Yoshimura et al., 1969).

In the past 15 years, evidence has been accumulated that the adenohypophysis, like many other adult tissues, contains a population of stem cells (Vankelecom, 2012; Vankelecom and Chen, 2014) (Table 4). Our group was the first to identify a so-called side population (SP) in the mouse pituitary, based on the general property of stem cells to efflux potentially toxic compounds (Chen et al., 2009, 2006, 2005). This SP, identified by flow cytometry based on expulsion capacity for the vital dye Hoechst33342, was found to be enriched with cells exhibiting stem cell characteristics such as self-renewal and multipotent differentiation capacity. Further enrichment was achieved by depleting endothelial and hematopoietic cells from the SP, thereby yielding a small population (\pm 0.5 % of all AL cells) referred to as the stem cell-side population (SC-SP). The SC-SP showed prominent expression of multiple components of the WNT, NOTCH and SHH signaling pathways, known to be important in pituitary embryonic development and stem cell regulation of many tissues. SC-SP cells were found to express stemness markers, in particular SOX2 and SOX9, independently identified as pituitary stem cell markers by others (Fauquier et al., 2008; Garcia-Lavandeira et al., 2009). In addition, the SC-SP could give rise to clonal spheres (pituispheres), and showed multipotent differentiation capacity generating all pituitary hormonal cell types (Chen et al., 2009). Immunostaining for SOX2 and SOX9 revealed that the stem cells reside in the MZ, but that they are also present as clusters in the AL parenchyma (Andoniadou et al., 2013; Chen et al., 2009, 2005; Fauquier et al., 2008; Rizzoti et al., 2013; Vankelecom, 2007b), thereby suggesting the existence of more than one stem cell niche in the pituitary. Indeed, tissue stem cells are typically housed in niches that provide signals (soluble factors, cell surface proteins and/or extracellular matrix (ECM)) to maintain stemness and regulate differentiation of the stem cells (Yoshida et al., 2016). In the human pituitary, SOX2⁺ and SOX9⁺ stem cells were also found clustered in the parenchyma as well as in Rathke's remnant cysts showing a follicular pattern, considered to be embodiments of the MZ which is absent in the human gland (Garcia-Lavandeira et al., 2009). Meanwhile, several additional markers have been identified for pituitary stem cells like ephrin B2 (EFNB2), Coxsackie virus and adenovirus receptor (CAR) and paired-related homeobox (PRRX) 1 and PRRX2 (Chen et al., 2013; Higuchi et al., 2014; Vankelecom and Chen, 2014; Yoshida et al., 2015), recently still further complemented by, amongst others, cutting-edge single-cell RNA-sequencing (scRNA-seq) analyses such as cytochrome P450 family 2 subfamily F member 2 (CYP2F2), tumor associated calcium signal transducer 2 (TACSTD2), E-cadherin (E-CAD) and keratin 8/18 (KRT8/18) (Cheung et al., 2018; Cox et al., 2019; Vennekens et al., 2021).

Generally, the role of resident stem cells is situated in tissue homeostatic turnover, dynamic cell remodeling during physio-/pathological conditions and/or tissue repair and regeneration after damage. These roles are very clear in tissues with high turn-over such as the intestine and skin (Haegerbarth and Clevers, 2009), but more difficult to define in tissues with low turn-over such as heart and brain (Beltrami et al., 2003; Gonzalez-Perez,

2012), as well as pituitary gland (Vankelecom, 2016). Lineage tracing studies have provided support for stem cell participation in homeostatic turnover of the adult gland (Andoniadou et al., 2013; Rizzoti et al., 2013). SOX2- and SOX9-traced cells were found within all endocrine cell lineages, although at very low level while most traced cells retained their undifferentiated stem cell phenotype, thereby questioning a major role of stem cells in adult pituitary turnover. In support, substantial transgenic ablation of SOX2⁺ stem cells in the postnatal gland did not affect the presence and abundance of the different hormonal cell populations (Roose et al., 2017).

Table 4. Overview of pituitary stem cell identification

Stemness marker	Stem cell characteristics	Species	Reference
SOX2 CD133	- SP phenotype - Sphere formation - Differentiation capacity	Mouse	Chen <i>et al.</i> 2005, 2006, 2009
SOX2	- Sphere formation - Differentiation capacity	Mouse	Fauquier <i>et al.</i> 2008
GFRA2 PROP1 SOX2 SOX9	- Sphere formation - Differentiation capacity	Mouse + human	Garcia-Lavandeira <i>et al.</i> 2009
SOX2	- Sphere formation - Differentiation capacity - Self-renewal	Mouse	Andoniadou <i>et al.</i> 2013
SOX2 SOX9	- Sphere formation - Differentiation capacity - Self-renewal	Mouse	Rizzoti <i>et al.</i> 2013

The stem cells in the pituitary may rather play a role in situations of gland ‘activation’ involving dynamic tissue and cell remodeling. During the first postnatal weeks, the (mouse) pituitary undergoes an intense growth and maturation phase. The stem cell population in this neonatal gland shows an activated phenotype, characterized by higher proliferation, abundance and stemness pathway expression (Gremeaux et al., 2012). Also, sphere-forming capacity is increased and spheres show swifter differentiation capacity when compared to adult stem cells (Gremeaux et al., 2012; Laporte et al., 2021). In analogy, SOX2 and SOX9 lineage tracing revealed a more significant contribution to the endocrine cells when tracing was initiated prenatally (Andoniadou et al., 2013; Rizzoti et al., 2013). Thus, from the current knowledge it appears that the pituitary stem cells are activated and involved in the neonatal growth and maturation phase, but become dormant in the adult gland, in which their role is much less clear.

The gland is also ‘activated’ in conditions of hormonal demands to which it responds with dynamic endocrine cell remodeling, such as during pregnancy and lactation (increase in PRL-producing cells), puberty (increase in GH-producing cells), or when target glands (or their function) become absent (upsurge of specific hormonal cells according to the target organ) (Levy, 2002; Nys and Vankelecom, 2021; Rizzoti et al., 2013). It has been proposed that the resident stem cells become (re-)activated during these conditions and contribute to the hormonal cell adaptations, but support is still scarce. For instance, lineage tracing has shown that a small part ($\pm 20\%$) of the newly arising corticotropes during their transient rise following adrenalectomy originate from SOX9⁺ stem cells

(Nolan and Levy, 2006; Rizzoti et al., 2013). Similarly, SOX2⁺ stem cells display increased proliferation after gonadectomy (a condition associated with increase in gonadotropes) or upon estradiol treatment (increase in lactotropes) (Rizzoti et al., 2013).

'Activation' of the pituitary also occurs after local damage (Willems and Vankelecom, 2014). Our group has designed a mouse model to inflict local pituitary tissue damage by ablating endocrine cells, in particular somatotropes, using a transgenic mouse model (GH^{Cre/+};R26^{DTR/+}) (Fu et al., 2012). Interestingly, the resident stem cell compartment raised an immediate reaction to the injury, displaying proliferative expansion and transcriptional activation of stemness pathways (Fu et al., 2012). Moreover, the stem cells started to co-express GH, and somatotropes were found to replenish in the coming 4-5 months (Fu et al., 2012; Willems et al., 2016), thereby providing substantial supportive evidence that the stem cells are involved in the regenerative process, a competence of the pituitary not known before. Similar findings have been described in other (slowly turning-over) tissues (such as muscle and liver), in which the stem cells are also quiescent, but get activated under challenged conditions such as injury to play a role in the regenerative response (Hill et al., 2003; Huch et al., 2013b). Recently, our group showed that IL6 is upregulated upon the local pituitary damage and activates the stem cell compartment (Vennekens et al., 2021). Intriguingly, the regenerative capacity swiftly disappears at aging (from 8-10 months) (Willems et al., 2016), coinciding with increased inflammatory nature in the older gland (so-called inflammaging). Stem cells in the aging gland were found not to react anymore to the same degree, coinciding with an absence of IL6 elevation upon damage above its already high levels in the inflammatory environment, and in line with the failure of IL6 treatment to activate stem cells in the pituitary of aging mice (Vennekens et al., 2021). Importantly, when stem cells were taken out of their *in vivo* environment, they regained activatability, showing that the pituitary stem cells keep their intrinsic functionality but that the inflammatory milieu impeded their *in situ* reaction (activation). Of note, restoration was also not occurring in young mice when the injury impact was intensified (prolonged), which may be due to stem cell exhaustion after repetitive attempts to react to the continuous insult and start the regenerative response (Willems et al., 2016). Finally, the gland may be 'activated' when a disease develops in the tissue. However, not much is known on the behavior and role of the resident stem cells during pituitary pathogenesis.

3.2 Stem cells in pituitary tumorigenesis and search for their role

In several cancer types, it has been shown that tumors are driven by so-called cancer/tumor stem cells (CSCs/TSCs), i.e. cells with stemness characteristics (self-renewal, multipotency) that initiate and grow the tumor to its heterogeneous composition, and re-develop the tumor after treatment (thus, are therapy-resistant) (Clevers, 2011). The origin of TSCs is still debated and appears to differ among cancer types. TSCs may derive from the tissue's stem cells following mutations allotting growth and survival benefits (e.g. in squamous cell carcinoma (Boumadhi et al., 2014)), or by de-differentiation of mutated mature cells of the tissue to a stemness phenotype (e.g. in breast cancer (Chaffer et al., 2011)).

There have been a number of studies reporting the existence of TSCs in pituitary adenomas (Nys and Vankelecom, 2021) (Table 5). However, conclusive evidence such as *in vivo* outgrowth of pituitary tumors from

these cells remains absent. Indeed, TSCs must be capable of regrowing the tumor when transplanted into immunodeficient mice, most strictly in a clonal manner. One study identified a small population of human pituitary adenoma (HPA) cells (as investigated for one NFPA and one somatotropinoma) able to form sphere-like structures *in vitro*, expressing stemness markers like cluster of differentiation (CD) 133 and NESTIN (Xu et al., 2009). The spheres showed some, although limited, differentiation potential upon stimulation with hypothalamic hormone-releasing factors (Xu et al., 2009). CD133⁺ cells were reported by another group to represent human pituitary TSCs (as analyzed in mostly NFPA and somatotropinomas) as they showed self-renewal and proliferative capacity (i.e. sphere formation) and differentiation potential, albeit limited, upon culturing in the presence of fetal bovine serum (Würth et al., 2017). However, the isolated CD133⁺ cells were sensitive to the anti-proliferative effect of a dopamine/somatostatin chimeric agonist and thus not therapy-resistant (while resistance is a key characteristic of TSCs) (Würth et al., 2017). Another study found CD15⁺ cells in HPAs (in different tumor phenotypes, but mainly assessed in NFPA and somatotropinomas) that may represent potential TSCs (Manoranjan et al., 2016). These cells possessed higher sphere-forming capacity compared to the remaining tumor cells and showed upregulated expression of the stemness marker SOX2.

Table 5. Overview of pituitary TSC identification

Stemness marker	Functional TSC property	Limitations	Tumor subtype	Reference
CD133 NESTIN	- Sphere-like structures - (Limited) differentiation	- Low number of tumors tested - No convincing xenografting experiments	GH-A NFPA	Xu <i>et al.</i> 2009
CD133	- Self-renewal - (Limited) differentiation	- Failure to resist therapy - No xenografting experiments	GH-A NFPA	Würth <i>et al.</i> 2017
CD15 SOX2	- Sphere formation	- No xenografting experiments	Multiple types	Manoranjan <i>et al.</i> 2016
NESTIN SOX2	- SP phenotype - Sphere formation - Self-renewal	- Xenografting experiments of only AtT20 cell line	Multiple types (+ Drd2 ^{-/-} PRL-A)	Mertens <i>et al.</i> 2015

GH-A, growth hormone-secreting adenoma; PRL-A: prolactin-secreting adenoma; SP, side population

Human pituitary tumors do not show growth ability when sc engrafted (Mertens et al., 2015). This deficiency may be due to their typically benign and slow-growing nature, and/or the absence of needed growth factors in the foreign sc environment. A proper pituitary (tumor) microenvironment may be needed, including the presence of local cytokines (e.g. IL6) and chemokines (e.g. CCL5), ECM (-remodeling) components (e.g. MMP2) and angiogenic factors (such as vascular endothelial growth factor (VEGF) and hypothalamic factors (Ilie et al., 2019). Hypothalamic factors have been shown to represent more than simple secretagogues. For instance, GHRH can stimulate proliferation of somatotropes, leading to hyperplasia and neoplastic transformation (Frohman and Kineman, 2002). All of these microenvironmental factors may influence and drive pituitary tumorigenic processes, including angiogenesis, EMT and cell proliferation. Hence, to demonstrate a TSC nature, transplantation into a more natural environment (e.g. orthotopically in the pituitary region) would be valuable. Orthotopic transplantation of TSC candidate populations has not been reported. Transplantations in the neighboring brain described the emergence of tumor-like structures when starting from pituitary-adenoma

sphere cells (expressing NESTIN and CD133) (Xu et al., 2009) or CD15⁺ cells (Manoranjan et al., 2016). However, only very few tumors were analysed (one somatotropinoma and one NFPA, respectively) and the xenograft showed a different phenotype than the original tumor (e.g. no hormone expression and absence of cytokeratin, respectively). Moreover, serial transplantability of the candidate TSC population (another important hallmark of TSCs) was not shown.

Our group identified TSC candidates in HPAs using the SP approach, revealing the existence of a SC-SP in all tumors irrespective of their hormonal phenotype (Mertens et al., 2015). The SC-SP was found enriched in cells expressing TSC-associated markers (such as chemokine (C-X-C motif) receptor-4 (CXCR4) and CD44) and in stem cell-regulating signaling pathways such as WNT and EMT. In addition, the SC-SP could generate spheres, whereas the remaining bulk of the tumor cells did not display sphere-forming capacity (Mertens et al., 2015). The spheres expressed the stem cell markers SOX2 and NESTIN, showed some limited self-renewal (passaging) capacity, and were able to differentiate, although modestly, into the hormonal phenotype of the tumor (i.e. expression of GH in spheres from a somatotrope adenoma). In addition, the SP showed tumorigenic dominance upon xenografting in immunodeficient mice, although not shown using HPAs (which did not grow *in vivo*) but demonstrated with the mouse pituitary tumor AtT20 cell line (Mertens et al., 2015). Interestingly, tumor growth could be delayed when mice were treated with a CXCR4 inhibitor, injected intratumorally (Mertens et al., 2015). The same study also found that the pituitary of female *Drd2*^{-/-} mice (developing prolactinomas) harbored a larger SP than the pituitary of control mice (Mertens et al., 2015). In analogy, a rise in colony-forming and SOX2⁺ stem cells was detected, at least partially assigned to higher proliferative activity in these cells (Mertens et al., 2015).

Although TSC candidates were put forward in pituitary tumors, it has not been unequivocally demonstrated whether they represent genuine TSC driving the tumor's growth, or rather resident tissue stem cells entrapped in the tumor during the tumorigenesis process, or both. SOX2 lineage tracing revealed that *Drd2*^{-/-} tumors are not growing from the SOX2⁺ stem cells (Vankelecom and Roose, 2017), thus excluding these cells as TSCs in prolactinoma development in *Drd2*^{-/-} mice. A similar phenomenon was observed in a mouse model of ACP, in which *Ctnnb1*-mutated (constitutively active) SOX2⁺ stem cells did not directly form the tumor. Instead, they were found to release signals that transform neighboring cells to become tumorigenic (Andoniadou et al., 2013; Gonzalez-Meljem et al., 2017). Intriguingly, the tumors did not develop when the mutant β -catenin was expressed in differentiated pituitary cells such as PIT1⁺, GH⁺ or PRL⁺ cells, indicating that stem cells formed an essential part of the tumorigenic machinery (Gaston-Massuet et al., 2011). Further studies showed that the mutated stem cell clusters activate a senescence program (such as expression of *p16*, *p21* and *p53*; presence of DNA damage and activation of a DNA damage response; and expression of lysosomal β -D-galactosidase) and express SASP factors (at least at the mRNA level), among others, *IL6*, *IL1B*, *bFGF*, vascular endothelial growth factor receptor 1 (*VEGFR1*), *CXCL1* and *CXCL11*, which may lead to changes in the microenvironment and induce proliferation and transformation of nearby non-stem cells (Gonzalez-Meljem et al., 2017). In addition, a recent study showed that SOX2⁺ stem cells do not directly form tumors but that SOX2 expression is required in the pituitary stem cells to promote tumor formation of neighboring melanotropes (MSH-producing cells) as

observed in *p27^{-/-}* mice that develop IL tumors (Moncho-Amor et al., 2021). Indeed, deletion of one copy of *Sox2* reduced tumor development (Moncho-Amor et al., 2021).

Taken together, stem cells have been identified in pituitary tumors but current studies point rather to a regulatory role in tumorigenesis, being activated and acting as a paracrine signaling center (that sends out cytokines, chemokines and growth factors), than to a direct TSC role (Andoniadou et al., 2013; Mertens et al., 2015; Vankelecom and Roose, 2017).

4. *In vitro* models to study pituitary biology and tumorigenesis

Although *in vivo* studies in mice have provided multiple interesting insights into pituitary development, functioning and tumorigenesis, *in vitro* models are also considered valuable and certainly needed to explore pituitary biology and disease of humans. Here, we provide an overview of existing *in vitro* pituitary study models, all having their strengths and weaknesses (as summarized in Table 6).

4.1 Pituitary tumor cell lines

Several pituitary cell lines have been developed starting from pituitary tumors or by immortalizing specific pituitary cells. Most cell lines were established from animal (rodent) tumors or cells. Regarding the lactotrope-somatotrope lineage, the rat MMQ and GH3 (producing GH and PRL) are frequently used (Ooi et al., 2004). Various somatotrope cell lines have been developed such as GH1, GH3, GH4C1 and MtT, all from rat origin (Ooi et al., 2004; Zhu et al., 2020). The most common thyrotrope cell lines are the murine T α T-1, TtT-97 and MGH101A lines (Ooi et al., 2004). At present, only one corticotrope cell line is available (i.e. AtT20 cell line), being derived from a mouse ACTH-producing tumor. Several gonadotrope cell lines have been developed such as the mouse α T1-1 and α T3-1, and the rat L β T2 and L β T4 (Ooi et al., 2004). Only few cell lines have been derived from human pituitary tumors such as GX (from a GH-producing tumor), HP75 (a gonadotroph tumor cell line isolated from a plurihormonal NFPA), PDFS (a folliculostellate cell line obtained from a NFPA) and HPA (derived from a PRL-producing tumor although secretory capacity disappeared) (Ooi et al., 2004; Zhu et al., 2020). Pituitary cell lines have been useful to study hormone production regulation (Hashimoto et al., 2012; Ooi et al., 2004), and have revealed interesting insights into pituitary tumorigenesis (Mertens et al., 2015; Zhu et al., 2020). However, although they have the advantage to efficiently grow and expand, in contrast to primary pituitary cells (see below), and thus represent tractable models for easy and high-throughput analyses, the cell lines do not recapitulate the heterogeneous composition of pituitary tumors because of clonal selections, and suffer from loss of phenotype (e.g. loss of hormone production) in the (2D) culture conditions used. Moreover, they are mostly derived from more aggressive tumors which represent only a very small minority of pituitary tumors. On the other hand, the cell lines are amenable to *in vivo* tumor growth when transplanted into (immunodeficient) mice (in contrast to human primary tumors). For instance, AtT20 cells can form tumors when sc transplanted, thereby recapitulating Cushing's disease (Taguchi et al., 2006), and to respond to targeted drugs (i.e. slower tumor development upon treatment with a CXCR4 antagonist) (Mertens et al., 2015).

Table 6. Pros and cons of *in vitro* pituitary study models

Model	Pros	Cons
Pituitary cell lines	<ul style="list-style-type: none"> - Readily available - Easy to handle and manipulate - Cryopreservable 	<ul style="list-style-type: none"> - Tumor-derived or genetically immortalized (not representative for normal tissue cells) - Only represents a single cell type - 2D format
From primary pituitary		
Cell monolayers	<ul style="list-style-type: none"> - More pituitary cell types - Easily established 	<ul style="list-style-type: none"> - Limited expandability - Quickly lose physiological behavior - 2D format
Explants	<ul style="list-style-type: none"> - Representative (reflects tissue heterogeneity and physiological function) - Easily established - 3D format 	<ul style="list-style-type: none"> - Limited expandability - necrosis - Limited experimental possibilities for manipulations
Cell re-aggregate	<ul style="list-style-type: none"> - Representative (reflects tissue heterogeneity and physiological responses) - Easily established - Long-term culture - 3D format 	<ul style="list-style-type: none"> - Limited expandability - Difficult to enrich for FS/stem cells
From primary pituitary stem cells		
Pituispheres	<ul style="list-style-type: none"> - Self-renewal and differentiation into hormonal cells - Allows exploration of pituitary stem cell biology and activation - 3D format 	<ul style="list-style-type: none"> - Limited expandability - Limited application potential (e.g. to unravel differentiation processes)
Colonies	<ul style="list-style-type: none"> - Self-renewal and differentiation into hormonal cells - Allows exploration of pituitary stem cell biology and activation 	<ul style="list-style-type: none"> - Limited expandability - Limited application potential (e.g. to unravel differentiation processes) - 2D format
Organoids	<ul style="list-style-type: none"> - Extensive expandability of the limited number of primary (stem) cells - Self-renewal and differentiation into hormonal cells - Allows exploration of pituitary stem cell biology and activation - High application potential (e.g. mechanistic exploration, tumor/disease modeling, drug screening, ...) - Amenable to gene editing - Cryopreservable - 3D format 	<ul style="list-style-type: none"> - Cost-intensive - At present limited differentiation

Table adapted from Laporte *et al.* 2021

4.2 Primary pituitary non-stem cell-based *in vitro* models

Primary cells from dissociated pituitary tissue can be cultured as 2D monolayers in serum-free medium supplemented with insulin, transferrin and serum albumin (May and Eipper, 1986). Although easy to develop and maintain for 2-3 weeks (May and Eipper, 1986), the obtained 2D culture lacks the natural 3D configuration of essential intercellular contacts and quickly loses hormonal phenotype (hormone production and responsiveness to hypothalamic factors) (Denef, 2008). To grow human pituitary tumor-derived cells as monolayers, a thin layer of ECM was found beneficial, but such cultures have only very scarcely been used in studies (Atkin *et al.*, 1997). To grow primary tissue as 3D structures, whole pituitaries, pituitary fragments or HPAs were cultured as explants (Pereda *et al.*, 1996). Although physiologically relevant by showing hormone secretion, the explant cultures have limited lifespan because quickly becoming necrotic due to insufficient perfusion and shortage of oxygenation (Nantie *et al.*, 2014; Pereda *et al.*, 1996; SATO and MAINS, 1986). An

alternative method that has proven successful is to culture primary pituitary tissue (mostly from mouse and rat) as cell re-aggregates by incubating dissociated cells in well-defined culture medium (i.e. serum-free defined medium (SFDM) (Chen et al., 2006)) under constant gyratory movement allowing the cells to re-associate. These aggregate cultures contain all pituitary cell types (i.e. hormone-producing cells and stem cells) assembled in a histotypic configuration, are physiologically reliable (i.e. hormone production and responsiveness) and can be maintained for several months (Chen et al., 2009; Van der Schueren et al., 1982; Vankelecom and Deneff, 1997). Human pituitary tumor aggregates have also been established, and were found amenable to drug testing (Roose, 2018). Although the hormonal phenotype is improved and retained in the re-aggregate culture system as compared to 2D monolayers, these cultures are static in abundance possessing no (or only very limited) cell proliferation and expandability.

4.3 Primary pituitary stem cell-based *in vitro* models

4.3.1 3D pituispheres and 2D colonies

In 2005, Chen *et al.* developed a pituitary stem-cell based study model, referred to as pituispheres (Chen et al., 2005), in analogy with previously defined neurospheres growing from neural stem cells (Gritti et al., 1996). Culturing dispersed AP cells in suspension in SFDM supplemented with B27, bFGF and/or EGF allows the stem cells to proliferate and progressively form free-floating 3D spheres. The pituispheres are composed of SOX2⁺ stem cells and also express other stem cell markers such as NESTIN, S100 β and SOX9 (Chen et al., 2009, 2005; Fauquier et al., 2008). The spheres can be driven into differentiation toward all pituitary endocrine cell types when seeded onto ECM (Matrigel)-coated surface in medium in which the stem cell-sustaining growth factors are omitted (Chen et al., 2009; Fauquier et al., 2008). The pituispheres show self-renewal capacity, although serial re-growth (passaging) quickly declines, being limited to 3-4 passages (Chen et al., 2009, 2005; Fauquier et al., 2008; Garcia-Lavandeira et al., 2009).

To date, pituitary-derived sphere formation is mostly used as a stem cell read-out tool to test functionality and activation state of the stem cells (Fu et al., 2012; Gremeaux et al., 2012; Roose et al., 2017; Zhu et al., 2015). For instance, development of spheres from damaged pituitary (i.e. after transgenically mediated somatotrope ablation, see above) resulted in a higher number of spheres, in line with the activated phenotype of the stem cells observed upon damage (Fu et al., 2012; Willems et al., 2016). Spheres have also been derived from pituitary tumors. The number of spheres formed from IL tumors in p27^{-/-} mice was found higher than the number obtained from wildtype pituitary, suggestive of a stem cell activated phenotype in IL tumors (Moncho-Amor et al., 2021). Spheres have also been developed from human pituitary tumors, although also showing limited expandability (Manoranjan et al., 2016; Mertens et al., 2015; Würth et al., 2017). Mertens and colleagues demonstrated that only SC-SP cells (enriched in stem cells), but not non-SP tumor cells developed into spheres (Mertens et al., 2015).

Another standardly used readout of tissue or TSC activity is the 2D colony-forming assay, first described for mouse pituitary in 2005 (Lepore et al., 2005), identifying a small population (0.2 %) of agranular AL cells (belonging to the folliculostellate cell population) able to grow out into colonies in DMEM with serum. More

recent studies slightly adapted the protocol by adding cholera toxin (CT) and bFGF to the medium, resulting after 1 week in colonies mainly consisting of stem cells expressing SOX2 and NESTIN, and able to differentiate into all pituitary endocrine cell types, although at modest level (Andoniadou et al., 2013; Gleiberman et al., 2008). This technique has meanwhile been used to identify stem cells and assess their activity in both healthy and diseased pituitary (such as pituitary tumors) (Gaston-Massuet et al., 2011; Mertens et al., 2015; Pérez Millán et al., 2016).

Taken together, pituispheres and colonies represent pituitary stem cell research models showing self-renewal and multipotent differentiation capacity, although both still limited.

4.3.2 3D organoids

In 2009, the group of Hans Clevers developed a novel and revolutionary stem-cell based *in vitro* system called 'organoids' which since then has been widely applied (Dutta et al., 2017; Sato et al., 2009; Sato and Clevers, 2013; Schutgens and Clevers, 2020; Van De Wetering et al., 2015).

These so-called 'mini-organs in a dish' were first developed from mouse intestinal epithelium, in particular from the intestinal crypts or the leucine rich repeat containing G protein-coupled receptor 5 (LGR5)-expressing intestinal stem cells (Sato et al., 2009). By mimicking the *in vivo* microenvironment and stem cell niche, crypts and stem cells developed and self-organized into long-term expandable 3D organoid structures that faithfully recapitulated the functionality, structure and transcriptomic/(epi-)genetic landscape of the epithelial compartment of the primary intestine. First, tissue fragments or dissociated cells (both containing stem cells) were embedded in an ECM scaffold to mimic the basal lamina (typically Matrigel, derived from the mouse Engelbreth-Holm-Swarm tumor cell line, containing collagen IV, laminin, proteoglycans and entactin). Then, the Matrigel-organoid assemblies were cultured in a well-defined medium, containing essential niche factors that stimulate stem cells to self-renew, proliferate and maintain their stemness phenotype such as EGF, Noggin (a BMP inhibitor) and the WNT signal amplifier R-spondin 1 (RSPO1) (Barker et al., 2007; Sato et al., 2009). These culture conditions allowed the (LGR5⁺) stem cells to self-renew and proliferate, thereby developing into a 3D organ-like (organoid) structure comprising stem cells and differentiated cells (such as Paneth cells) in a specific cellular organization recapitulating the *in vivo* intestinal crypt architecture. Specifically, the organoids contained a single-layer of epithelial cells surrounding a lumen and displayed budding (i.e. crypt-like extrusions) with the stem cells primarily located at the tip of the buddings, similar to what is observed *in vivo*. Once the organoids reached a certain number and size, the structures were dissociated into small fragments and single cells which were replated in fresh Matrigel and defined medium. This passaging occurred every 7-14 days and cultures were expandable for over a year, thereby robustly retaining the tissue-recapitulating features (Sato et al., 2009).

Since this landmark study, the organoid field has boomed. Moreover, organoids have not only successfully been established from adult stem cells but also from pluripotent stem cells (PSCs) (i.e. embryonic stem cells (ESCs) and induced-pluripotent stem cells) (Clevers, 2016). The PSC-derived organoids are obtained by simulating the sequential steps of embryogenesis of the specific tissue or organ in focus. Establishment of PSC-derived organoid models is particularly valuable for complex organs that contain distinct structures or regions, such as brain (Lancaster et al., 2013), and for tissues in which adult stem cells have not (yet) conclusively been identified or are difficult to isolate, such as kidney (Xia et al., 2013).

4.3.3 Organoid applications

Nowadays, organoids have been established from multiple tissues of both mouse and human origin, such as liver (Huch et al., 2015, 2013b), endometrium (Boretto et al., 2017) and stomach (Barker et al., 2010; Bartfeld et al., 2015), enabling the profound study of tissue (stem cell) biology *in vitro*. The culture medium is typically composed of the generic organoid growth cocktail (i.e. EGF, Noggin and WNT activators) and further adapted with more tissue-specific niche factors. For instance, several gastro-intestinal organoid models (e.g. stomach-derived organoids) need gastrin (Barker et al., 2010). Some organoids contain both stem cells and specialized cells like intestinal organoids that are composed of LGR5⁺ stem cells and differentiated intestinal cells (such as Paneth cells) (Sato et al., 2009), whereas other organoids are completely composed of stem cells and need growth adjustments to generate the tissue's differentiated cell types. The differentiation protocol may require medium adaptations such as removing stem cell-sustaining factors (e.g. airway organoids (Zhou et al., 2018)), or may need *in vivo* transplantation (e.g. pancreatic organoids (Huch et al., 2013b)).

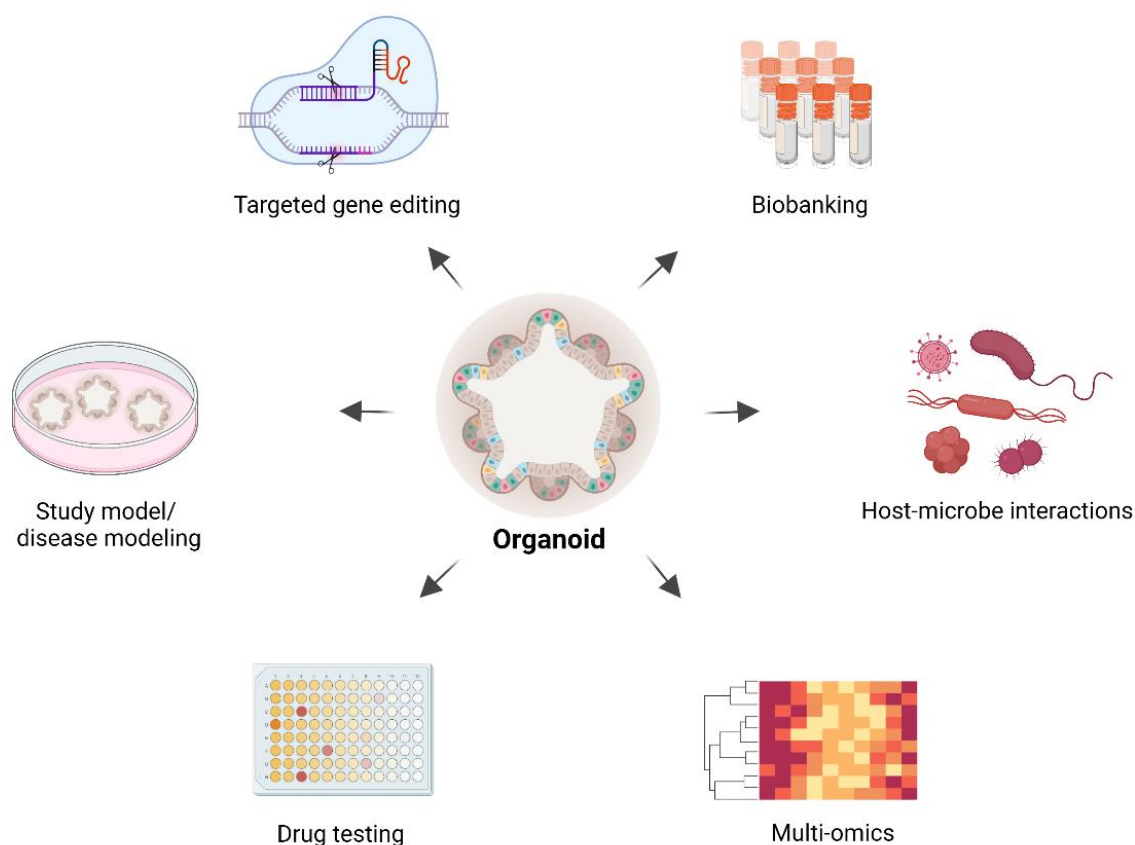


Fig. 4. Schematic overview of organoid applications

Organoids, both from healthy and diseased tissue, can be harnessed to different applications such as establishment of (patient-derived) biobanks, investigation of host-microbe interactions, multi-omics interrogations (transcriptomics, proteomics, epigenomics, metabolomics), drug-screening (even in context of personalized medicine), disease modeling and gene modifications. Figure created with Biorender.

Interestingly, organoids can also be developed from diseased tissue, thereby providing a powerful research tool to model and study human diseases (Dutta et al., 2017; Schutgens and Clevers, 2020) (Fig. 4). To date, organoids have been developed from many human disorders such as ovarian cancer (Maenhoudt et al., 2020), Barrett's syndrome (Sato et al., 2011) and endometrial cancer (Boretto et al., 2019). The organoids recapitulate and maintain the phenotypic and mutational landscape of the original disease, even after extended passaging. Currently, large patient-derived organoid biobanks are being developed for several cancer types such as colorectal cancer (Van De Wetering et al., 2015) and breast cancer (Sachs et al., 2018) (Fig. 4), also made possible by the cryopreservation ability of organoids. Because of this hallmark as well as their large and robust expandability, organoids can be efficiently harnessed to drug-screening platforms (Fig. 4). For instance, human epidermal growth factor receptor 2 (HER2)-overexpressing breast cancer organoids are sensitive to drugs targeting the HER signaling pathway (e.g. afatinib), whereas HER2-negative breast cancer organoids are resistant to these drugs (Sachs et al., 2018). Similarly, endometrial cancer-derived organoids maintain the genomic landscape of the primary tumors and show patient-specific drug responses such as higher sensitivity to everolimus (an inhibitor of mechanistic target of rapamycin kinase (mTOR)) when the tumor-derived organoids (hence, the primary tumor) house a loss-of-function mutation in *PTEN* (an inhibitor of the PI3K-AKT-mTOR pathway) (Boretto et al., 2019). Organoids can further be applied to study host-microbe interactions or infectious diseases in general (Fig. 4). *H. Pylori* infection can lead to gastric ulcers and even gastric cancer. Injection of these bacteria into the lumen of human gastric organoids initiated an inflammatory response which may be involved in gastric cancer development (Bartfeld et al., 2015). Also during the currently raging COVID-19 pandemic, organoids have been applied to study SARS-CoV2 infection and underlying mechanisms (Geurts et al., 2021; Monteil et al., 2020). Lastly, organoids are amenable to gene editing (Fig. 4) as demonstrated in cystic fibrosis (CF) patient-derived organoids. CF patients carry specific mutations in the cystic fibrosis transmembrane conductance regulator (*CFTR*) gene, disrupting normal function of this chloride channel and insufficient water transport, resulting in viscous mucus that causes severe pulmonary and digestive defects. Homologous recombination (with CRISPR/Cas9) of the *CFTR* locus in CF patient-derived rectal organoids restored the chloride channel function (Schwank et al., 2013). In addition, CF patient rectal-derived organoids are applied to test novel drugs that may restore function of *CFTR* (Dekkers et al., 2016), and are currently also used in personalized medicine, to identify drugs that target the disease in the individual patient with specific *CFTR* mutation(s).

In summary, organoids are 3D cell constructs that develop from the tissue's stem cells, are long-term expandable and retain key features of the originating organ (more in particular, of its epithelial compartment). Organoids, formed and expanded from even a small biopsy of healthy or diseased tissue, are powerful research models to study tissue (and stem cell) biology and disease in great depth (including multi-omic analyses), and can be used to establish patient-derived biobanks to search for novel and better therapeutic drugs, even in a personalized manner.

4.3.4 Pituitary organoids

Organoid models have also been developed from the pituitary gland. First, a PSC-derived model was established by recapitulating embryonic development of the gland (Suga et al., 2011). Mouse ESCs were grown as aggregates and directed to both oral and neural ectoderm lineage in adjacent layers, which *in vivo* give rise to AP and hypothalamus, respectively. It was shown that organizational and morphogenetic events, as occurring *in vivo*, were mandatory *in vitro* to obtain a RP-mimicking structure (Suga et al., 2011). Differentiation towards hormonal cells was achieved by further mimicking the embryonic development process. NOTCH inhibition resulted in corticotropes, whereas WNT pathway activation and treatment with glucocorticoids or estradiol was necessary to generate somatotropes and lactotropes, respectively. The cells that were most efficiently achieved in the tissue-like structures, i.e. the corticotropes, were found to be functional and released ACTH upon stimulation with CRH both *in vitro* and *in vivo* (Suga et al., 2011). The approach was then applied to human ESCs (Ozone et al., 2016). Initial RP-mimicking formation was similar, but differentiation towards hormone-producing cells needed different inputs, thereby highlighting the need for some caution when translating mouse developmental principles to humans. For instance, corticotropes developed spontaneously in the human ESC-derived model and gonadotropes were obtained after NOTCH inhibition (Ozone et al., 2016). Subsequently, the technique was used to model pituitary diseases such as congenital pituitary hypoplasia caused by a mutation in orthodenticle homeobox 2 (*OTX2*) (Matsumoto et al., 2020). Induced PSCs (iPSCs) from the patient (i.e. somatic cells reprogrammed to a pluripotent state (Shi et al., 2017)) were subjected to the pituitary embryogenesis-mimicking protocol. The *OTX2*-mutant derived structure showed lower *LHX3* expression, associated with elevated apoptosis of progenitor cells and impaired differentiation into endocrine cells. It was also revealed using the model that *OTX2*, expressed in the hypothalamic part of the organoid structure, was essential for progenitor cell maintenance by controlling *LHX3* expression in the oral ectoderm part (*via* hypothalamic *FGF10* expression). The phenotype could be reversed by correcting the mutation, while introduction of the *OTX2* mutation in normal control iPSCs resulted in a patient-mimicking phenotype (Matsumoto et al., 2020). Although presenting an interesting model to study pituitary embryogenesis and to model diseases *in vitro*, the protocol is lengthy and not easy to perform, and the obtained structures are not long-term expandable, nor are they highly tractable.

Recently, our group developed an organoid model starting from mouse pituitary. Dissociated AL cells were seeded in Matrigel and cultured in an optimized, well-defined medium containing generic organoid-culturing factors (see above) tuned with factors that are crucial in embryonic development of the gland, in particular *FGF8/10* and *SHH* (Cox et al., 2019). It was demonstrated that these pituitary organoids (clonally) originate from the resident *SOX2*⁺ stem cells and retain the stemness characteristics during expansive culture (Cox et al., 2019; Vennekens et al., 2021). The organoids could differentiate into specific cell types such as ACTH-expressing cells *in vitro* by exposure to retinoic acid and dexamethasone, and PRL- and GH-expressing cells *in vivo* after subrenal transplantation of the organoids in immunodeficient mice, although both at modest level (Cox et al., 2019). Importantly, (new) findings obtained in the organoids could be transposed to, and confirmed in the *in vivo* setting (such as expression of new stem cell markers), thereby indicating that this novel pituitary organoid model provides a valuable and reliable tool to study pituitary stem cell biology (Cox et al., 2019; Vennekens et al., 2021).

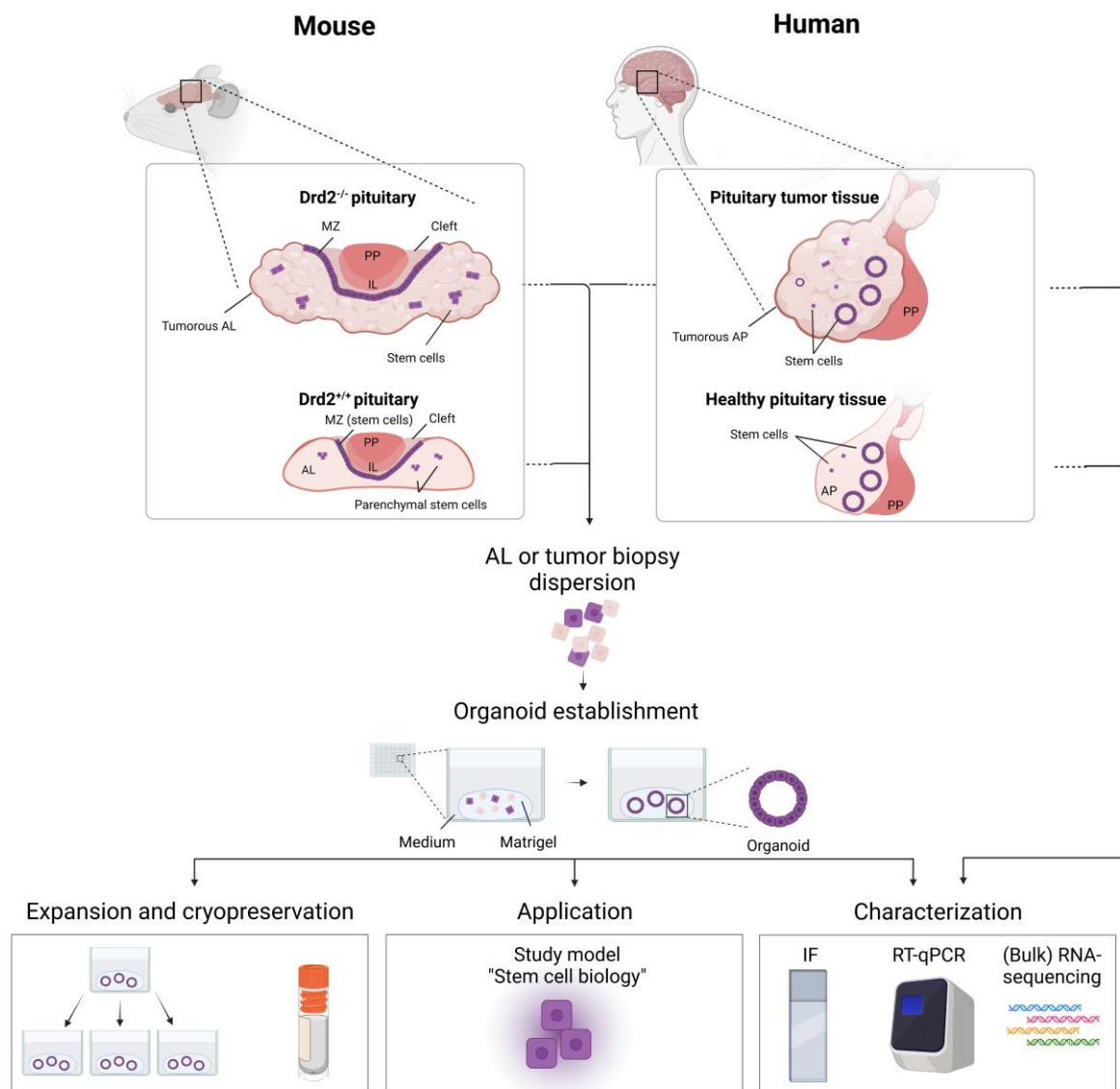
Importantly, the organoid model was found to recapitulate pituitary stem cell phenotype including activation. Among others, a higher number of organoids formed upon stem cell activation following injury inflicted in the pituitary using transgenic (GH^{Cre/+};R26^{iDTR/+}) mice (Cox et al., 2019; Vennekens et al., 2021). Transcriptome analysis of the organoids further exposed novel pituitary stem cell markers such as KRT8/18 and damage-induced upregulation of the stem cell markers *Prrx1* and *Prrx2*. Expression of *Prrx1* and *Prrx2* was also found upregulated *in vivo* upon pituitary damage, thereby further supporting the organoids' translatability (Cox et al., 2019). However, these first organoid cultures showed limited passaging capacity (Cox et al., 2019). Very recently, we identified the JAK/STAT pathway, and in particular IL6, as a pituitary stem cell-activating factor, involved in the stem cell activation process following injury (Vennekens et al., 2021). More precisely, scRNA-sequencing revealed upregulation of *Il6* in the stem cell compartment after injury, coinciding with a higher number of proliferating (SOX2⁺Ki67⁺) stem cells (Vennekens et al., 2021). Interestingly, addition of IL6 to the culture medium improved organoid outgrowth (i.e. more organoids formed) and greatly increased organoid passageability by activating the organoids' stem cells (Vennekens et al., 2021). Again, these *in vitro* organoid-based findings could be extrapolated *in vivo*. Injection of mice with IL6 provoked a pituitary stem cell-proliferative response while treating GH^{Cre/+};R26^{iDTR/+} mice with an IL6 antibody during injury induction reduced the stem cell reaction (Vennekens et al., 2021).

Taken together, mouse pituitary-derived organoids have successfully been developed, greatly recapitulating the stem cell molecular phenotype, regulation and activation. Hence, these organoids are highly valuable as a pituitary stem cell biology research model as well as read-out tool and mechanistic study model for pituitary stem cell functionality (such as activation). The organoid technique is therefore also expected to provide an interesting tool to study stem cell biology in pituitary diseases, and in particular pituitary tumorigenesis.

Science never solves a problem without creating ten more – George Bernard Shaw

CHAPTER 2: RESEARCH OBJECTIVES

RESEARCH OBJECTIVES



Graphical summary

The pituitary gland dynamically coordinates the body's endocrine system, thereby orchestrating key developmental and physiological processes. Hence, pituitary dysfunction causes major anomalies. Tumorigenesis in the gland represents the most common pituitary pathology, resulting in severe endocrine disorders. Patients are burdened with hormonal hypersecretion, or with hypopituitarism and resultant hormone deficiencies, necessitating life-long hormone supplementation.

To date, little is understood regarding mechanisms underlying pituitary tumorigenesis. Moreover, it is largely unknown how local stem cells behave during this encumbering process unfolding in their tissue. To tackle this question, we explored stem cell biology in both mouse and human pituitary tumorigenesis using transcriptomic, immunophenotyping and organoid-based approaches.

Objective 1: Gaining knowledge in the clinical pituitary tumor field (Chapter 3)

Before embarking on our detailed fundamental study, we aimed at gaining clinical background knowledge on human pituitary tumors. In this context, we performed a retrospective analysis of patients who underwent transsphenoidal tumor resection, and assessed clinical aspects including tumor type-associated patient characteristics and symptoms, peri-operative endocrine morbidity, surgical efficacy, safety and outcome, and risk factors for therapeutic success and tumor recurrence.

Objective 2: Exploring stem cell biology in pituitary tumors and derived organoids (Chapter 4)

Then, we aimed at gaining fundamental insight into local stem cells' biology in pituitary tumorigenesis in both mouse and human.

In-depth characterization of the stem cell compartment of the tumorous mouse *Drd2*^{-/-} pituitary

Using the *Drd2*^{-/-} pituitary tumorigenesis mouse model, we explored the stem cells' phenotype in the tumorous gland, and characterized the stem cell compartment in detail using immunophenotypic and transcriptomic (RNA-sequencing) interrogation. Then, we developed organoids from tumorous *Drd2*^{-/-} (and control *Drd2*^{+/+}) pituitary to generate a tractable and reliable *in vitro* research tool to study stem cells in pituitary tumorigenesis. Therefore, we investigated whether the organoids recapitulated the *in situ* stem cell phenotype of the tumorous gland, and assessed functional impact of factors/pathways found to be upregulated in the stem cells *in situ*, on stem cell-derived organoid growth characteristics.

In-depth characterization of the stem cells present in human pituitary tumors

We scrutinized human pituitary tumors, obtained after surgical resection, for stemness profile by immunostaining and gene expression analysis of stem cell markers. In addition, we set out to establish organoids from human tumors, and compared their transcriptome profile with the original lesion to investigate the organoids' stemness and tumor(-specific) phenotype. Finally, we tested several approaches to improve the observed limited expandability of these organoids.

Objective 3: Setting up an *in vivo* organoid orthotopic transplantation model (Addendum)

To eventually create the possibility to assess *in vivo* outgrowth of pituitary (tumor)-derived organoids, we designed and optimized a transcranial stereotactic injection method to deposit organoids orthotopically into the pituitary. In a proof-of-principle approach, we tested the transplantation of normal pituitary-derived organoids expressing a fluorescent reporter, and assessed their survival and growth.

Taken together, our study aimed at shedding light on the as yet highly underexposed behavior of resident stem cells during tumorigenesis in the pituitary. Further insight may eventually open up the horizon toward novel, more effective and targeted treatment strategies for pituitary tumor patients.

The important thing is not to stop questioning. Curiosity has its own reason for existing – Albert Einstein

CHAPTER 3: SAFETY AND EFFECTIVENESS OF TRANSNASAL TRANSSPHENOIDAL PITUITARY SURGERY IN A SINGLE CENTER, A RETROSPECTIVE STUDY

*This chapter has been published:

Nys C.*, Versyck G.* , Buelens E, Engelborghs K, Vankelecom H, Weyns F, Peuskens D. Transnasal transsphenoidal pituitary surgery in a large tertiary hospital, a retrospective study. Acta chirurgica Belgica, 2021, 1-9. <https://doi.org/10.1080/00015458.2021.1988231> (*contributed equally)

ABSTRACT

Objectives

Pituitary adenomas, although being small tumors, can have quite an impact on patients' lives causing hormonal and visual disturbances, for which surgery must be performed. As a large peripheral hospital with specialists in pituitary surgery, an assessment of the efficacy and safety of transnasal transsphenoidal pituitary surgery was made.

Methods

A retrospective analysis of neurosurgical reports as well as pre- and postoperative imaging was made to evaluate the presenting symptoms, tumoral variables, peri-operative morbidity, and long-term outcome.

Results

This cohort included 105 patients who were operated for pituitary adenomas over a 9-year period, with a slight male predominance. Adenomas had a mean maximum diameter of almost 25mm, with one-third of tumors presenting with a Knosp-grade 3 or 4. As expected, most patients presented with either visual (32.4 %) or hormonal (40.0%) disturbances. After surgery, 85.3 % had complete resolution of visual deficits, and 97.1 % had normalisation of hormonal hypersecretion. Postoperative hormonal insufficiency requiring substitution was observed in 43.1 % and was significantly more frequent in males and in non-functioning pituitary adenomas. Postoperative cerebrospinal fluid leakage was observed in 2.9 %, and merely one patient developed meningitis. Tumor recurrence was significantly more frequent in patients with partial resection as compared to complete resection (25.6 % vs 7.9 %).

Conclusion

This study demonstrates that transnasal transsphenoidal pituitary surgery can be performed safely and effectively in a large non-university hospital, improving visual and/or hormonal disturbances as well as providing long-term tumor control. Patients with larger adenomas are at an increased risk to develop postoperative hypopituitarism.

1. INTRODUCTION

Pituitary adenomas are mostly benign tumors originating from adenohypophyseal cells. They represent one of the most common intracranial tumors and are detected in 15-22.5 % of the population according to autopsy reports and MRI-scans for other purposes (Daly et al., 2009; Ezzat et al., 2004; Melmed, 2020). Pituitary tumors often remain small and asymptomatic, as clinically relevant tumors have a lower prevalence of approximately 0.1 % (Melmed, 2020).

Pituitary tumors can be divided regarding their size into micro- (< 10 mm) and macro-adenoma (> 10 mm), as well as secreting and non-secreting pituitary tumors (Melmed, 2020). Presenting symptoms can be due to hormonal dysregulation or mass effect on the cranial nerves surrounding the cavernous sinus, leading to visual disturbances. A less frequent presentation is pituitary apoplexy (2-12 %), where patients may present with sudden headache, visual and/or hormonal disturbances caused by an acute volume increase of a pre-existing pituitary adenomas due to a hemorrhage or necrosis (Barkhoudarian and Kelly, 2019).

In this study, a consecutive cohort of 105 patients operated for pituitary adenomas were retrospectively analysed regarding clinical presentation, surgery, complications, and outcome.

2. MATERIAL AND METHODS

Study population

This study was approved by the ethical committee of Ziekenhuis Oost Limburg (ZOL) in Genk, Belgium.

A retrospective analysis was performed on patients operated for pituitary adenomas in a single centre (ZOL) from January 1st 2010 until December 31st 2018. The year 2010 was chosen as this was the first full year of endoscopic pituitary surgeries. The patient cohort was obtained through a query in the operation logs. Cases were excluded if follow-up took place at another centre, or if pathology didn't reveal a pituitary adenoma, after which 105 individual patients remained for analysis. Patients were seen pre- and postoperatively by a neurosurgeon and an endocrinologist, as well as an ophthalmologist if visual problems were apparent during clinical examination. Imaging through MRI-scans was performed preoperatively, 3 months and 1 year postoperatively, followed by yearly scanning in most cases and more frequently in selected cases (Image 1).

Variables

Demographic variables included patient gender and age. Tumor variables covered tumor pathology, maximum tumor diameter, as well as suprasellar extension and Knosp-grading. Clinical variables were classified with presenting symptoms (apoplexy, visual deficits, hormonal imbalance, cranial neuropathy), postoperative symptoms (visual deficits, hormonal status), complications (hemorrhage, cerebrospinal fluid (CSF) leakage, meningitis) and oncological outcome. Extent of resection (partial/complete) was determined on an MRI-scan after 3 months. Recurrence was defined as tumoral regrowth in case of NFPA and renewed hormonal hypersecretion in secreting pituitary tumors. Visual deficits were evaluated with a Goldmann- or automated perimetry.

Patients presenting with hormonal imbalances were divided into hormonal hypersecretion and clinically significant hypopituitarism. A hormonal workup was performed by measuring basal hormonal production with secondary testing as needed. The hormonal status one year postoperatively was used as the final benchmark. Hypopituitarism was noted when there was a shortage of one or more hormones for which substitution therapy was required. Primary hypothyroidism was excluded as hormonal insufficiency if patients only required L-thyroxine supplementation. Panhypopituitarism was noted when supplementation of at least 4 different hormones was necessary.

Transsphenoidal surgery

A bi-nostril endoscopic endonasal approach was used to perform the transnasal transsphenoidal surgery, using a 2- or 3-handed technique. A classic procedure is performed by making a wide sphenoidotomy followed by tumor removal with a wide array of curettes until visual confirmation of a complete resection is obtained or the arachnoid membrane of the sellar diaphragm settles in. The sellar cavity is filled with either autologous adipose tissue or covered with Tisseel. In case of an apparent CSF-leak, the decision is made to place an external lumbar drain (ELD) and/or to perform a quadriceps muscle/fascia lata plasty/Tachosyl coverage or a combination depending on surgeon's preference. The ELD is left in place for 5-7 days, draining approximately 10 milliliters

CSF per hour. Postoperative nasal hemorrhages were addressed by re-look surgery to obtain hemostasis whenever nasal packing was insufficient.

Statistical analysis

Continuous data were presented as mean, median, or frequency. Frequency distribution was used for categorical variables. Study variables were analysed with a two-tailed Fisher's exact test for dichotomous variables and one-way ANOVA or Kruskal-Wallis ANOVA by ranks for dichotomous and continuous data. Results with a P-value of < 0.05 were deemed significant. Statistical analysis was performed using GraphPad Prism (version 8.4.1) and Statistica 13.

3. RESULTS

3.1 Demographics and tumor characteristics

A total of 105 patients were analysed in this retrospective series. There was slight male predominance, accounting for 56.2 % of patients. A median age of 59 years was observed (range 18-84 years) (Table 1). Patients with secreting pituitary tumors were significantly younger compared to those with a NFPA (median age 42 vs 64 years; $p < 0.0001$).

Table 1. Demographics of 105 patients with pituitary adenomas

	No. of patients (%)
Male	59 (56.2)
Female	46 (43.8)
Micro	8 (7.6)
Macro	97 (92.4)
Knosp	
	25
0	(23.8)
	12
1	(11.4)
	31
2	(29.6)
	21
3	(20.0)
	16
4	(15.2)

Table 2. Clinical presentation of 105 patients undergoing transsphenoidal resection of pituitary adenomas

Clinical presentation	No. of patients (%)
Normal	30 (28.6)
Visual field deficit	34 (32.4)
Bitemporal heteronymous hemianopia	29 (85.3)
Bilateral quadrantanopia	3 (8.8)
Central vision loss	1 (2.9)
Hemianopia	1 (2.9)
Hormonal imbalance	42 (40.0)
Hormonal shortage	8 (19.1)
Hormonal excess	34 (32.4)
PRL hypersecretion	11 (32.4)
ACTH hypersecretion	11 (32.4)
GH hypersecretion	11 (32.3)
TSH hypersecretion	1 (2.9)
Cranial neuropathy	8 (7.6)
III deficit	5 (4.8)
VI deficit	1 (0.9)
III and VI deficit	2 (1.9)
Apoplexy	17 (16.2)

While there was no difference in the distribution of micro- and macro-adenomas in both genders ($p = 0.134$), female patients did present significantly more with secreting pituitary adenomas (61.8 % vs 38.2 %; $p = 0.012$). The average size of the pituitary adenomas was 24.7 mm, and 7.6 % were micro-adenomas. There were 97 macro-adenomas (92.4 %) with 87.6 % having suprasellar extension and 35.2 % with extension into the cavernous sinus (Knosp grade 3 and 4) (Table 1 and Fig. 1).

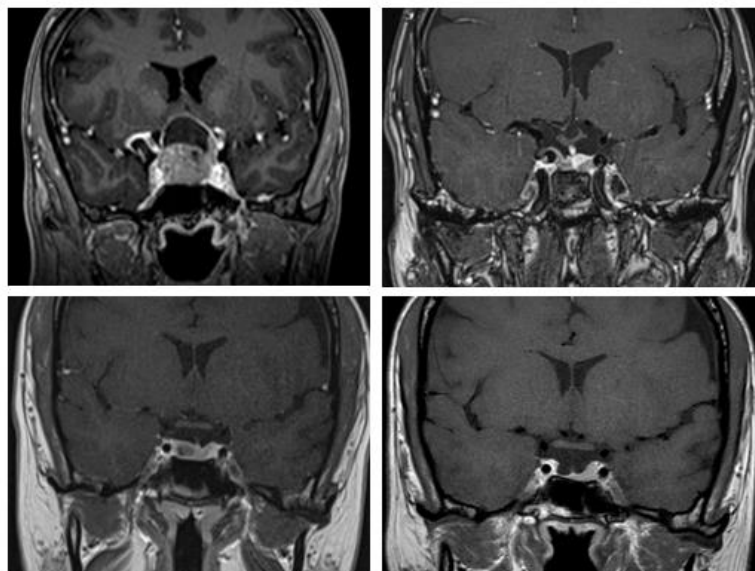


Fig. 1. MRI images before and after transsphenoidal pituitary surgery

Upper panel: Pre- (left) and postoperative (right) T1-gadolinium enhanced MRI images of a cystic pituitary macro-adenoma. Preoperatively the pituitary stalk and optic chiasm were not recognizable. The patient presented with bitemporal anopia, which resolved completely after surgery, with a visible pituitary gland and optic structures. *Lower panel:* Pre- (left) and postoperative (right) T1-gadolinium enhanced MRI images of a hypo-intense pituitary micro-adenoma in a patient with Cushing's disease.

3.2 Clinical presentation

Most presenting symptoms were visual deficits in 34 cases (32.4 % of the entire population), followed by hormonal hypersecretion in 34 cases (32.4 %), hormonal shortage in 8 cases (7.6 %), cranial nerve deficits in 8 cases (7.6 %) and 17 patients (16.2 %) with pituitary apoplexy (Table 2). Visual field deficits consisted of bitemporal heteronymous hemianopia in 85.3 %, bilateral quadrantanopia in 8.8 %, central visual loss or hemianopia in 5.8 %. Thirty-four patients had hormonal hypersecretion with an excess of PRL (32.3 %), GH (32.3 %), ACTH (32.3 %) or TSH (2.9 %). Cranial nerve deficits ($n = 8$) encompassed the oculomotor nerve (62.5 %), the abducens nerve (12.5 %), or both nerves (25.0 %) (Table 2).

All patients with a micro-adenoma ($n = 8$) underwent surgery due to hypersecretion, including 7 with Cushing's disease and one with acromegaly. All 17 patients with apoplexy had macro-adenomas, including 4 with a cranial neuropathy, 2 with a visual field deficit, 3 with hormonal imbalances, and 5 with a combination of symptoms. Three patients with apoplexy only experienced an acute headache.

3.3 Complications

Analysis of peri-operative complications revealed 3 cases (2.9 %) of postoperative nasal haemorrhage that required reoperation as nasal packing had not resolved the problem.

Intra-operative CSF-leakage was observed in 18 patients (17.1 %). Postoperative CSF-leakage was observed in 3 patients (2.9 %), including one CSF-leak that had not been detected intraoperatively. One patient developed postoperative meningitis, which was recognised early and treated with antibiotics, resulting in a rapid and complete recovery.

When comparing peri-operative CSF-leakage between different age group, no significant differences were observed (20.0 % of 18-40 years, 17.1 % of 41-60 years, and 9.1 % of > 61 years old; $p = 0.652$). Gender-analysis did reveal that women had significantly more intraoperative CSF-leaks (26.1 % vs 10.2 %; $p = 0.039$). Patients with apoplexy (5.6 % vs 19.3 %; $p = 0.294$) or cavernous sinus invasion (18.5 % vs 7.7 %; $p = 0.459$) did not have significantly more CSF-leaks. No difference was observed comparing leakage-rates between micro- and macro-adenomas (12.5 % vs 17.5 %; $p > 0.999$) or in adenomas with supra- versus infra-sellar extension (3.3 % vs 0.0 %; $p > 0.999$), individual size-analysis between pituitary tumors with diameters < 25 mm versus \geq 25 mm did reveal more CSF-leaks (9.4 % vs 25.0 %; $p = 0.041$) in the latter group.

Table 3. Total hormonal balance comparing the pre- and postoperative status of 105 patients with non-functional or secreting pituitary tumors

	No. of patients (%)	Normal - normal	Normal - impaired	Impaired - impaired	Impaired - worse	Impaired - normal	Normal - ADH insuff	ADH insuff - normal
NFPA	68 (66.7)	29 (42.6)	29 (42.6)	3 (4.0)	3 (4.0)	1 (1.5)	2 (2.9)	1 (1.5)
GH	11 (10.8)	9 (82.0)	2 (18.0)	0	0	0	0	0
PRL	11 (10.8)	5 (45.0)	4 (36.4)	0	0	0	2 (18.2)	0
ACTH	11 (10.8)	9 (82.0)	2 (18.0)	0	0	0	0	0
TSH	1 (1.0)	1 (100.0)	0	0	0	0	0	0
Total	102 (100.0)	53 (52.0)	37 (36.3)	3 (2.9)	3 (2.9)	1 (1.0)	4 (3.9)	1 (1.0)

Insuff, insufficiency

3.4 Outcome

3.4.1 Visual and other cranial nerve deficits

One patient died from non-related causes and 2 patients were lost to follow-up, 102 patients remained for the outcome analysis. Thirty-four patients experienced preoperative visual field deficits that completely resolved in 29 (85.3 %) and partially resolved in 4 (11.8 %) cases. Similar results were observed for preoperative cranial neuropathies that completely resolved in 7 patients (87.5 %) and partially resolved in one patient (12.5 %). No new cranial neuropathies or visual problems were observed postoperatively.

3.4.2 Hormonal balance

In the entire series ($n = 102$), one patient recovered from preoperative hormonal insufficiency and another patient recovered from diabetes insipidus (DI). Preoperatively, 34 patients (33.3 %) (Table 3) had hormonal hypersecretion, of which all except one (97.1 %) obtained normalization. Fifty-three patients (52.0 %) maintained a normal hormonal balance. Three patients (2.9 %) maintained their preoperative hormonal deficit. Thirty-seven patients (36.3 %) developed new hormonal insufficiencies, of which 4 patients had panhypopituitarism and 11 patients developed DI combined with other hormonal insufficiencies. Four patients (3.9 %) developed isolated DI and three patients (2.9 %) required additional hormonal supplementation after surgery.

We found that younger patients developed significantly more DI when comparing < 45 and > 65 years ($p = 0.007$). Patients with NFPA were significantly more prone to develop postoperative hypopituitarism as compared to patients with secreting tumors (51.5 % vs 23.5 %; $p = 0.010$). Furthermore, men developed significantly more postoperative hormonal insufficiency compared to women (56.1 % vs 22.2 %; $p = 0.0006$).

3.4.3 Oncological outcome

During the study period, recurrence was observed in 15 patients (14.7 %) with an average time to recurrence of 33.3 months (range 6-86 months). Seven recurrences were observed in secreting adenomas (3 ACTH-, 1 GH-, 2 PRL-, and 1 TSH-secreting). No significant difference in average time to recurrence was observed between secreting and non-secreting adenomas (26.9 months vs 39.0 months; $p = 0.280$) and invasive adenomas did not result in more recurrences ($p = 0.686$).

Postoperative MRI-scans revealed a partial resection in 39 patients (38.2 %), these patients had significantly more recurrences compared to complete resections (25.6 % vs 7.9 %; $p = 0.021$). Complete resection did not result in more hormonal imbalances as compared to incomplete resection (41.0 % vs 54.0 %; $p = 0.227$).

4. DISCUSSION

This study was performed to retrospectively evaluate the safety and efficacy of transnasal transsphenoidal surgery for different types of pituitary adenomas in a single large peripheral centre (where the technique was introduced in 2010).

4.1 Demographics

We noted a slight male predominance, which is atypical considering the female predominance in other studies on pituitary tumors. A study in another part of Belgium, as well as in Malta, demonstrated a female to male ratio of 2:1 (Daly et al., 2009; Gruppetta and Mercieca, 2013). An 8-fold higher frequency of prolactinomas was noted in females compared to males in Banbury (UK) (Fernandez et al., 2010). The rather low amount of prolactinomas included in this cohort (10.8 %) is probably due to our conservative surgical approach to prolactinomas, most of which are treated with non-surgically, which may explain our slight male predominance. However, there were significantly more secreting pituitary tumors in the female group as compared to men, in conjunction with findings in a population study in Northern Finland (Raappana et al., 2010). The median age in our cohort was 59 years, which is considerably higher than in the epidemiological studies, which registered a mean age of 32-44 years old. This is likely due to an abundance of NFPA, and the observed significant difference in median age between secreting tumors and NFPA (42 vs 64 years, $p < 0.0001$).

4.2 Clinical presentation

One-third of the population experienced preoperative visual field deficits, followed closely by presentation with hormonal hypersecretion, conform a study in New Zealand that prospectively evaluated presenting symptoms in pituitary adenomas (Ogra et al., 2014). Postoperative visual field recovery occurs in 3 stages: early fast recovery (minutes - days), early slow recovery (weeks - months), and late recovery (months - years). Most improvement is observed in the early fast phase, followed by the early slow phase, with recovery after 4 months being rather unlikely (Kerrison et al., 2000). This study reveals that 85.3% of patients experience a full visual recovery, with the remaining 14.7 % showing improved visual fields 1 year postoperatively. A meta-analysis by Thotakura et al demonstrated that care should be taken to operate in a timely fashion as patients with a shorter history of visual symptoms (< 1 year) have been shown to have significantly better visual outcomes (Thotakura et al., 2017).

Cranial nerve deficits (mostly oculomotor nerve deficits) were observed as a presenting symptom in 8 patients (7.6 %), most of which ($n = 5$, 62.5 %) had apoplexy. Postoperatively, there was normalization of cranial nerve function in 87.5 %, without any new cranial nerve deficits. New cranial nerve deficits following TS occur in 0-5.3 % of patients in recent literature (Agam et al., 2019; Cappabianca et al., 2002; Florea et al., 2019).

In this cohort, the number of patients suffering from preoperative hypopituitarism was quite low (6.9 %), in contrast to other studies mentioning an incidence as high as 39-70 % (Fatemi et al., 2008; Jahangiri et al., 2016; Magro et al., 2016). This might be due to the exclusion of primary hypothyroidism as hormonal insufficiency (patients only taking L-thyroxine preoperatively), as well as the expedient timing for surgery after a new

diagnosis of a pituitary adenoma. Because of this short interval, starting new medication for mild hormonal deficits will often be done when there is a residual deficit after surgery rather than preoperatively. Finally, the low percentage may also result from our inclusion criteria, as only clinically relevant hormonal shortages (those requiring hormonal supplementation rather than being at the lower limit of normal) were marked as an insufficiency. In this regard, another retrospective analysis found that only 50 % of patients with NFPA experience symptoms of hypopituitarism preoperatively (Jahangiri et al., 2016).

Surgery completely restored hormonal deficits in one out of 7 patients in this study. Correction of a preoperative hormonal deficit is rather rare, even after successful resection of the tumor (Buttan and Mamelak, 2019). A correction of the preoperative hormonal deficit may be obtained in 3-40 % of surgeries (Berg et al., 2010; Jahangiri et al., 2016).

All except one patient with a secreting adenoma obtained normalization of the hypersecreted hormone after surgery (n = 33, 97.1 %), indicating satisfactory results may be obtained even for secreting adenomas (often deemed as challenging cases) in large tertiary hospitals. Of note, success rates vary widely among different studies (range 32 % to 73 %) (Buttan and Mamelak, 2019; Fatemi et al., 2008).

4.3 Complications

The most frequently mentioned risks associated with pituitary tumor resection include postoperative CSF-leakage and damage to healthy pituitary tissue resulting in transient or permanent hypopituitarism and/or DI (Mehta and Lonser, 2016).

Postoperative CSF-leakage is a major cause of morbidity following endonasal transsphenoidal pituitary surgery, with the risk for developing meningitis and the need for reoperation to repair the CSF-fistula. The reported incidence of postoperative CSF-leakage varies from 1.3-13 % (Berker et al., 2012; Hannan et al., 2020; Kassam et al., 2011; Sudhakar et al., 2004). Our study reports a rate of 2.9 %, with only one patient experiencing meningitis cured by prompt treatment. Our peri-operative CSF-leakage rate was 17.1 %, and patients were usually treated with a combination of meticulous reconstruction and an ELD.

Risk factors for postoperative CSF-leakage include surgery for ACTH-producing adenomas, intra-operative CSF-leakage, and an elevated body mass index (Dlouhy et al., 2012; Hannan et al., 2020). Our study revealed a significantly increased risk for postoperative CSF-leakage in females and for adenomas ≥ 25 mm in size. Zwagerman and colleagues evaluated placement of an ELD following endoscopic endonasal skull base surgery in a randomized controlled trial and observed a significant improvement in postoperative CSF-leakage in patients with an ELD (8.2 %) as compared to a control group (21.2 %) (Zwagerman et al., 2019). Another study revealed a significantly decreased risk for postoperative CSF-leakage meningitis in patients with an ELD as compared to those without (1.4 % vs 13.6 %) (Aken et al., 2004). However, using state-of-the-art endonasal technique may not only reduce the incidence but also improve our ability to recognize and to effectively reconstruct an eventual intraoperative CSF-leak as compared to the original transseptal technique.

The incidence of postoperative hypopituitarism varies from 5.5 to 36 % among different studies (Fatemi et al., 2008; Hwang et al., 2020; Jahangiri et al., 2016; Lindholm et al., 2006; Magro et al., 2016). We observed the need for new hormonal supplementation after surgery in 43.1 % of patients. This is likely due to a lower incidence of preoperative hormonal insufficiency in this study (as explained above). A recent review revealed that the hypothalamic-pituitary-adrenal axis is more susceptible to damage with resulting low ACTH levels and a diminished stress response after surgery (Jahangiri et al., 2016). Not surprisingly, both pre- and postoperatively, hydrocortisone is the most frequently supplemented hormone in this cohort. Furthermore, gender (male) and NFPA were identified as predictors for postoperative hormonal impairment, as observed in other studies (Greenman et al., 1995). While tumor size is also believed to be a risk factor (Fatemi et al., 2008; Nelson et al., 1984), no significant difference was observed in the frequency of postoperative hormonal impairment when comparing tumors < 25 mm and \geq 25 mm.

DI is a frequent side-effect following pituitary surgery and may be transient or permanent. Permanent DI is caused by damage to hypothalamus or proximal infundibulum (Schreckinger et al., 2013) and has a variable incidence in the literature (1.9-10.1 %) (Ajlan et al., 2018; Burke et al., 2020; Magro et al., 2016), compared to 14.7 % (n = 15) in this cohort. Intra-operative CSF-leakage and younger age are inconsistently described as risk factors for development of DI (Lobatto et al., 2018). While younger age does indeed seem to be a risk factor when comparing < 45 and > 65 years old (p = 0.007). As also observed by Boling and colleagues, intra-operative CSF-leakage did not significantly correlate with an increased incidence of permanent DI (p = 0.135) in this cohort (Boling et al., 2016).

4.4 Oncological outcome

Partial resection was observed in 38.2 % of patients, in line with 33 % as reported by Lee *et al* (Lee et al., 2016). This number is quite high and may be explained by the number of large NFPA in this cohort. Extent of resection is a known risk factor for recurrence (Lee et al., 2016) as confirmed in patients with partial resection (25.6 % vs 7.9 %; p = 0.021) in this cohort.

Fifteen patients (14.7 %) had a tumor recurrence with an average time of 33 months. More precisely, 7 patients (20.6 %) with a secreting adenoma and 8 patients (11.9 %) with an NFPA recurred. Recent reports estimate the incidence of recurrence around 15-20 % (< 2 years after surgery), although this may be an underestimation, especially in NFPA, as recurrent tumors may only become symptomatic due to mass effect when they have grown quite large, taking much longer to be discovered, while emphasizing the importance of scheduled long-term follow-up (Abu Dabrh et al., 2016; Lee et al., 2016).

5. CONCLUSION

This retrospective study evaluates 105 patients who underwent transnasal transsphenoidal to remove a pituitary adenoma in a single Belgian centre. The study reveals the well-known spectrum of NFPA and secreting adenomas, with a relative shortage of (micro)prolactinomas as compared to epidemiological studies. As such, the cohort mainly consists of macro-adenomas. This analysis reveals that visual and other cranial neuropathies tend to be, at least partially, restored after tumor resection, without causing any new deficit except for hormonal insufficiency. Postoperatively, new hormonal supplementation was necessary in 39 % of patients due to inherently larger tumors of non-secreting nature and a relatively high threshold to start hormonal substitution preoperatively for hormones in the low normal range (except for cortisol). Complications were few with merely 2.9 % experiencing postoperative CSF-leakage. Not surprisingly, this study revealed a higher recurrence rate in patients with partial as compared to complete resection. While transsphenoidal surgery yields excellent results regarding visual and hormonal outcome, patients with larger adenomas should be counselled they are at an increased risk to develop postoperative hypopituitarism, while performing a more cautious partial resection comes with an increased risk of recurrence. In conclusion, transnasal transsphenoidal pituitary surgery can be considered a safe operation with good results both clinically and oncologically in a tertiary hospital with specialised surgeons.

It is impossible for a man to learn what he thinks he already knows - Epictetus

CHAPTER 4: EXPLORING STEM CELL BIOLOGY IN PITUITARY TUMORS AND ORGANOIDS

*Paper under revision (Endocrine Related Cancer):

Nys C., Lee Y.* , Roose H.* , Mertens F., De Pauw E., Kobayashi H., Sciot R., Bex M., Versyck G., De Vleeschouwer S., *et al.* Exploring stem cell biology in pituitary tumors and derived organoids. *contributed equally

ABSTRACT

Pituitary tumorigenesis is prevalent and causes major endocrine disorders. Hardly anything is known on the behavior of the local stem cells in this pathology. Here, we explored the stem cells' biology in mouse and human pituitary tumors using transcriptomic, immunophenotyping and organoid approaches. In the prolactinoma-growing pituitary of dopamine receptor D2 knock-out mice, the stem cell population displays an activated state in terms of proliferative activity and distinct cytokine/chemokine phenotype. Organoids derived from the tumorous glands' stem cells recapitulate these aspects of the stem cells' activation nature. Upregulated cytokines, in particular interleukin-6, stimulate the stem cell-derived organoid development and growth process. In human pituitary tumors, cells typified by expression of stemness markers, in particular SOX2 and SOX9, are found in a wide variety of clinical tumor types, also showing a pronounced proliferative status. Organoids efficiently develop from human tumor samples, displaying a stemness phenotype as well as tumor-specific expression fingerprints. Transcriptomic analysis revealed fading of cytokine pathways at organoid development and passaging, but their reactivation did not prove capable of rescuing early organoid expansion and passageability arrest.

Taken together, our study revealed and underscored an activated phenotype of the pituitary-resident stem cells in tumorigenic gland and tumors. Our findings pave the way to defining the functional position of the local stem cells in pituitary tumor pathogenesis, at present barely known. Deeper insight can lead to more efficient and targeted clinical management, currently still not satisfactorily.

1. INTRODUCTION

Because of its reigning position in the endocrine system, steering key developmental and physiological processes, dysfunction of the pituitary gland leads to severe health problems. Tumorigenesis in the pituitary is prevalent, being detected in 15-25 % of the general population, with serious clinical symptoms in 0.1 % (Daly et al., 2009; Ezzat et al., 2004; Melmed, 2020; Mete and Lopes, 2017). Although pituitary tumors mainly represent benign and slow-growing lesions, they cause dismal and life-threatening endocrine disturbances due to over-secretion of one or more hormones and/or mass expansion effects in the gland and brain area. Traditionally, pituitary tumors have been classified in NFPA and hormone-secreting tumors, comprising prolactinomas that produce PRL, somatotropinomas that secrete GH, corticotropinomas that release ACTH, gonadotropinomas that secrete LH and/or FSH, thyrotropinomas that produce TSH and plurihormonal tumors that express multiple hormones. Treatment typically involves transsphenoidal resection or pharmacological management (such as dopamine receptor agonists for prolactinomas). Despite fair success rates, therapies remain unsatisfactory in up to half of the patients, leading to hypopituitarism which necessitates lifelong hormone supplementation causing important adverse effects and negative impact on quality of life (Daly et al., 2009; Fatemi et al., 2008; Melmed, 2020; Van der Klaauw et al., 2008). Furthermore, a considerable number of patients (10-35 %) are therapy-resistant and/or develop tumor recurrence, in particular occurring with invasive tumors (35-50 % of all pituitary tumors) (Hansen et al., 2014; Melmed, 2020; Mete and Lopes, 2017; Peverelli et al., 2015; Trouillas et al., 2020). To date, mechanisms involved in pituitary tumorigenesis remain poorly understood. Only a minority (5-10 %) have been traced back to genetic mutations, being part of a broader syndrome (e.g. MEN1), or a familial (e.g. FIPA) or sporadic (e.g. GNAS) case (Melmed, 2020; Mete and Lopes, 2017; Trouillas et al., 2020). Rather, pituitary tumorigenesis appears to involve a coincidental growth advantage of (a) cell(s) because of yet unknown reasons (Melmed, 2011). Importantly, it is not clear yet how the local stem cells are involved or behave in pituitary tumorigenesis. From recent studies, it appears that the stem cells do not directly generate the tumor as concluded from SOX2 lineage tracing in prolactinoma-developing *Drd2^{-/-}* mice (Vankelecom and Roose, 2017), and from a mouse model of pituitary-related adenomatous craniopharyngioma; (Andoniadou et al., 2013; Gonzalez-Meljem et al., 2017)). Thus, at least in these models, the pituitary stem cells appear not to act as authentic TSCs as found in other tumor types, which by definition give rise to the lesion and directly generate and sustain the tumor's growth (Clevers, 2011). Rather, the pituitary stem cells may become activated at local tumorigenesis, and may fuel the tumors' development and growth (Andoniadou et al., 2013; Gonzalez-Meljem et al., 2017). Indeed, we before found indications that the stem cell compartment is activated at tumorigenesis in the *Drd2^{-/-}* mouse model, in which female mice develop prolactinomas in the gland from 6-8 months of age because of the absence of dopamine inhibitory tone on the lactotropes (Asa et al., 1999; Kelly et al., 1997). The stem cell compartment, as probed by SC-SP and SOX2-expressing (SOX2⁺) phenotype, was found to be expanded during the first phases of the tumorigenic process (10-14 months of age), and showed increased colony-forming capacity (a classical read-out of stem cells) (Mertens et al., 2015). In addition, we also identified a small SC-SP in human pituitary tumors, irrespective of their hormonal phenotype, showing pronounced stemness marker expression (e.g. SOX2) and sphere-forming capacity (another readout of stem cells) (Mertens et al., 2015). Aside

from these still limited findings, not much is known on the biology and behavior of pituitary stem cells in local tumorigenesis, also largely due to the absence of workable research models.

Recently, we succeeded in developing organoid models from mouse pituitary, recapitulating the gland's stem cell population and presenting as a faithful stem cell biology and activation readout tool (Cox et al., 2019; Vennekens et al., 2021). In general, organoids are 3D cell constructs that self-form and develop from the tissue's stem cells and that mimic key features of the native tissue (stem cell) epithelium biology (Schutgens and Clevers, 2020). Organoids are formed by embedding stem cell-containing tissue fragments or single-cell suspensions in an ECM-mimicking scaffold (typically Matrigel) which are then cultured in a defined cocktail of specific stem cell growth and regulatory factors. We showed that the mouse pituitary-derived organoids originated from the resident SOX2⁺ stem cells, retained their stemness character during expansive culture (passaging), and faithfully reflected the *in vivo* biology and activation phenotype of the stem cells (Cox et al., 2019; Vennekens et al., 2021). Here, we explored pituitary stem cell biology in both mouse (Drd2^{-/-}) and human pituitary tumors through transcriptomic and immunophenotyping scrutiny. Moreover, we derived organoids from the tumorous samples which were applied for transcriptomic, phenotypical and functional examination. Together, we observed an activated nature of resident stem cells in pituitary tumorigenesis, especially a prominent proliferative and cytokine/chemokine phenotype. Our study may open the way to deeper insight into pituitary tumorigenesis, in particular into the functional position of stem cells, and may eventually guide to more adequate clinical treatment modalities.

2. MATERIALS AND METHODS

Human pituitary tumors

Human pituitary tumor biopsies were collected immediately after transsphenoidal resection at the University Hospitals Leuven (UZ Leuven; Division of Neurosurgery; Belgium). Informed consent was obtained from the patients, and experiments were approved by the Ethics Committee Research UZ/KU Leuven (S59804). Tumor nature and hormonal phenotype were determined by the Department of Imaging and Pathology (UZ Leuven). Patient and tumor characteristics are summarized in Table 1. HPA numbers are listed chronologically according to surgery date.

Genetically modified mice and tamoxifen treatment

Animal experiments were approved by the KU Leuven Ethical Committee for Animal Experimentation (P218/2013 and P153/2018). Mice were bred and housed at the KU Leuven animal facility under standard conditions (constant temperature of 23 ± 1.5 °C, relative humidity 40-60 % and day/night cycle of 12/12 h), with water and food *ad libitum*.

The *Drd2*^{-/-} mouse model was purchased from The Jackson Laboratory (Bar Harbor, ME, USA). *Sox2*^{CreERT2/+} mice (kindly provided by Dr. Martinez-Barbera, UCL, London; (Andoniadou et al., 2013)), harboring a tamoxifen (TAM)-inducible *Cre* in one *Sox2* locus, were crossed with *Drd2*^{-/-} or *Drd2*^{+/+} mice and a *R26*^{YFP/YFP} conditional reporter line (containing a floxed yellow fluorescent protein (*YFP*)-coding sequence in the *Rosa26* locus; obtained from Dr. Carmeliet, KU Leuven) to generate *Sox2*^{CreERT2/+};*R26*^{YFP/+};*Drd2*^{-/-} and *Sox2*^{CreERT2/+};*R26*^{YFP/+};*Drd2*^{+/+} mice. Genotyping was executed as reported before (Andoniadou et al., 2013, 2007; Kelly et al., 1997).

To perform SOX2 lineage tracing, *Sox2*^{CreERT2/+};*R26*^{YFP/+};*Drd2*^{-/-} and *Sox2*^{CreERT2/+};*R26*^{YFP/+};*Drd2*^{+/+} mice were intraperitoneally injected for 2 days with TAM (Sigma-Aldrich, Bornem, Belgium; 0.15 mg/g bodyweight/day, dissolved in corn oil) at the age of 6 months (i.e. at the onset of tumorigenesis). At 12 months of age, mice were euthanized and pituitaries collected for FACS isolation of the YFP⁺ cells.

Sox2^{eGFP/+} reporter mice harbor an enhanced green fluorescent (*eGFP*) coding sequence in the *Sox2* open reading frame (one allele) resulting in SOX2⁺ cells expressing eGFP (Ellis et al., 2004). Offspring was genotyped by PCR for the presence of the *eGFP* transgene with 5'-TACCCCGACCACATGAAGCA-3' as forward primer and 5'-TTCAGCTCGATGCGGTTCAC-3' as reverse primer.

Organoid development and culture

Mouse pituitary was isolated from euthanized animals, and the major endocrine lobe (anterior lobe, AL) was separated from the intermediate and posterior lobes and dissociated into single cells using trypsin, all as previously described (Chen et al., 2009, 2005). Human tumor biopsies were collected and rinsed with Leibovitz's L-15 medium (Thermo Fisher Scientific, Massachusetts, USA). Samples were immediately processed for further analysis or were cryopreserved as small pieces in Leibovitz's L-15 medium with 10 % DMSO (Sigma-Aldrich) and 30 % fetal bovine serum (Thermo Fisher Scientific). Part of the sample was dissociated into single cells using

Collagenase type IV (1 mg/mL in Medium 199; Thermo Fisher Scientific), as previously reported (Mertens et al., 2015).

The obtained mouse AL or human tumor cells were embedded in 20 μ L droplets (25,000 cells/drop) consisting of basal medium (serum-free defined medium (SFDM; Thermo Fisher Scientific) or Advanced DMEM for mouse and human cells, respectively) and growth factor-reduced Matrigel (Corning, New York, USA) in a 30:70 ratio. After solidification, organoid culture medium (original or optimized organoid medium (OptM); Table S2) was added, and cultures were kept at 37 °C in an incubator with CO₂ adjusted for physiological pH buffering. Every 2-3 days, culture medium was refreshed. ROCK inhibitor (Y27632, 10 μ M; Merck, Overijse, Belgium) was supplemented to the medium at initial seeding of the primary cells (passage 0, P0). Organoids were passaged every 7-10 days following enzymatic (TrypLE Express; Thermo Fisher Scientific) and mechanical dissociation into fragments and single cells that were re-plated in Matrigel droplets, all as previously described (Cox et al., 2019; Vennekens et al., 2021; and above). Brightfield and fluorescence images were acquired using an Axiovert 40 CFL microscope (Zeiss, Jena, Germany). Quantification of organoid number and size was performed with Fiji imaging software (<https://imagej.net/Fiji> (Schindelin et al., 2019)). Organoids were enclosed in these analyses when clearly developed (from diameter \geq 50 μ m). Time-lapse recording of organoid growth was performed with the IncuCyte S3 (including Organoid QC module; Sartorius, Göttingen, Germany), acquiring brightfield images every 3 h for 6 or 9 days. Time-lapse videos were generated with IncuCyte software using 10 frames per second.

To test the effect of bone-morphogenetic protein (BMP) activation on SOX9 expression, organoids developed in OptM were exposed to BMP4 (50 ng/mL; Peprotech, London, UK) for 4 days (in SFDM with B-27, L-glutamine, N2, SHH, N-acetyl-cysteine; concentrations, see Table S2). To explore cytokine involvement in the organoid culturing, STATTIC (20 μ M; Sigma-Aldrich), LMT-28 (50 μ M; Sigma-Aldrich), IL1 β (10 ng/mL; Peprotech), IFN γ (20 ng/mL; Peprotech), TNF α (20 ng/mL; Peprotech) or CXCL2 (10 ng/mL; Peprotech) were added to the organoid medium. Also, medium was supplemented with WNT3A (200 ng/mL; R&D systems, Minneapolis, USA) or cAMP (250 μ M; Sigma-Aldrich) to assess their effect on organoid growth and passaging.

Histological and immunostaining analysis

Pituitaries, organoids and tumor biopsies were fixed with 4 % paraformaldehyde (PFA; Merck) and embedded in paraffin using the Excelsior ES Tissue Processor (Thermo Fisher Scientific). Five- μ m sections were subjected to haematoxylin and eosin (H&E) or immuno-histochemical/-fluorescence staining as described previously (Boretto et al., 2017; Cox et al., 2019; Vennekens et al., 2021). Reticulin staining, visualizing the fiber network, was performed according to the manufacturer's instructions (Reticulin silver plating kit; Merck). Antigen retrieval was done with citrate buffer (pH 6; Merck), permeabilization with Triton X-100 (0.1 % in PBS; Sigma-Aldrich) and blocking with donkey serum (Sigma-Aldrich). Following incubation with primary and secondary antibodies (see Table S5), sections were covered with Vectashield (containing 4',6-diamidino-2-phenylindole (DAPI)), or with ProLong Gold (Thermo Fisher Scientific) following nuclei labeling with Hoechst33342 (Sigma-Aldrich). Images were taken with a Leica DM5500 upright epifluorescence microscope (Leica Microsystems, Wetzlar, Germany), and converted to figure images with Fiji imaging software. Quantification of SOX2⁺, SOX9⁺ and Ki67⁺ cells was

performed in the immunostained paraffin sections by counting at least 3,000 cells per mouse pituitary and 4,000 cells per human tumor biopsy using several distinct field images.

Whole organoids were immunostained and imaged as described before (Dekkers et al., 2019). In brief, organoids were fixed with 4 % PFA, permeabilized with Triton X-100 and blocked with bovine serum albumin (Serva, Heidelberg, Germany), prior to sequential incubation with primary and secondary antibodies (see Table S5). Then, clearing was performed by incubating the organoids in a fructose-glycerol solution (Sigma-Aldrich and Thermo Fisher Scientific). The cleared organoids were mounted and images taken using a Zeiss LSM 780 – SP Mai Tai HP DS. Acquired z-stacks were imported into Fiji and 3D reconstructions were composed using the 3D viewer plugin (Pietzsch et al., 2015).

EdU labeling was executed with the Click-iT EdU Alexa Fluor 488 kit (Thermo Fisher Scientific), according to the manufacturer's protocol, involving a 3 h incubation of organoid cultures with EdU (10 μ M). Confocal imaging and quantification of EdU⁺ cells were performed in 3D whole-organoids similarly to above.

Transmission electron microscopy

Transmission electron microscopy was performed as in detail described before (Cox et al., 2019; Vennekens et al., 2021). In short, *Drd2*^{-/-} AL and corresponding organoids were fixed in glutaraldehyde, cut in blocks, and post-fixed in osmium tetroxide/potassium ferrocyanide. Blocks were mordanted using tannic acid, consecutively stained with uranyl acetate and lead aspartate, dehydrated and embedded in epoxy resin. Samples were cut in 70 nm sections and analyzed with the JEM1400 transmission electron microscope (JEOL, Tokyo, Japan) equipped with an Olympus SIS Quemesa 11 Mpxl camera (Olympus Corporation, Tokyo, Japan) or using a H-7600 transmission electron microscope (Hitachi High-Tech Corporation, Tokyo, Japan) with an AMT CCD camera system, AMT HR 1K x 1K (Advanced Microscopy Techniques Corporation, Massachusetts, USA).

Mouse magnetic resonance imaging

Drd2^{+/+} and *Drd2*^{-/-} mice (head region) were subjected to magnetic resonance imaging using a horizontal 9.4-Tesla nuclear magnetic resonance spectrometer in combination with a 40 mm diameter birdcage coil as radio frequency transmitter and receiver. Ten min before scanning, mice were intraperitoneally injected with the contrast agent gadolinium (0.50 mmol/kg body weight). During the procedure, mice were anesthetized using 1 % isoflurane in a mixture of 75 % air and 25 % oxygen. Scanning and image reconstruction was performed as previously described (Mertens et al., 2015).

SC-SP isolation by FACS

SC-SP cells were isolated by FACS from *Drd2*^{+/+} and *Drd2*^{-/-} mouse (~14 months old) AL as previously described in detail (Chen et al., 2006, 2005; Mertens et al., 2015). In short, cells were incubated with Hoechst33342, and the SC-SP (i.e. SP depleted from CD45⁺ hematopoietic and CD31⁺ endothelial cells) sorted using an Aria III (BD Biosciences, Erembodegem, Belgium). The SP phenotype was verified using the efflux blocker verapamil.

RNA-sequencing analysis

RNA was isolated from the SC-SP of *Drd2*^{-/-} and *Drd2*^{+/+} AL (*Drd2*^{-/-}: n=3 biological replicates encompassing a total of 10 mice; *Drd2*^{+/+}: n=2 encompassing a total of 6 mice; 3,000-5,000 SC-SP cells were sorted per biological

replicate) (Fig. S1B,C). In addition, RNA was extracted from FACS-isolated SOX2 lineage-traced YFP⁺ cells of *Drd2*^{-/-} and *Drd2*^{+/+} AL (see above) (n=1) (Fig. S1G). Total RNA was isolated using the RNeasy Micro Kit (Qiagen, Venlo, The Netherlands), and RNA Integrity Number (RIN) determined with Agilent Picochips on an Agilent BioAnalyzer 2100 (Agilent Technologies, Santa Clara, USA). Samples with RIN > 7.5 were sequenced (Nucleomics Core, VIB/KU Leuven). TruSeq total stranded RNA library preparation was performed, followed by sequencing on a NextSeq 500 instrument (Illumina, San Diego, USA). Raw reads generated by Illumina HiSeq2000 were subjected to quality control. Fragments Per Kilobase of gene sequence and per Million fragments of library size (FPKM) were generated by dividing the normalized counts by total number of counts (in millions), and then dividing the scaled counts by gene length (in kbp) for each gene. Sequence reads were pre-processed to remove adaptors and filter low-quality reads (i.e. FPKM < 1 values were discarded). The high-quality reads were aligned to the mouse reference genome (*Mus musculus*, GRCm3873) using Tophat (v2.0.13). Statistical analysis was performed with the edgeR 3.4.0 package of Bioconductor (<http://www.bioconductor.org>). The resulting P-values were corrected for multiple testing with Benjamini Hochberg to control the false discovery rate (FDR). Heatmaps of DEGs were created with GraphPad Prism (version 9.1.0; GraphPad Software, California, USA). Gene ontology (GO) analysis of differentially expressed genes (DEGs) ($\log_2FC > 1$ and FDR < 0.05) was executed with String (version 11.0). Enriched pathway values are presented as $-\log_{10}(FDR)$.

Regarding the human tumors, total RNA was extracted from 3 different primary tumor samples and their corresponding organoids (P0, P1 and/or P2) using the RNeasy Micro Kit. RNA libraries were prepared (TruSeq total stranded) which were sequenced on a Novaseq 6000 instrument (Illumina). Following quality control, removal of adaptors and filtering of low-quality reads by Trim Galore! (version 0.6.6) set on paired mode, remaining sequencing reads were mapped to the human reference genome (hg19, GRCh38.93) using STAR 2.7.8a and annotated using the GENCODE 38 annotation file. Uniquely aligned reads were quantified and assigned to genomic features using the featureCounts function from the R Bioconductor package Rsubread (version 2.0.1). DEG analysis was done using the DESeq2 package (version 1.30.1) as previously reported (Love et al., 2014). PCA analysis was performed using the plotPCA function from the DESeq2 package after rlog transformation. Differences in gene expression were presented as \log_2 values after size-factor normalization (using DESeq2). Results are presented as log fold change (FC), or log transcript per million (TPM)+1 (to enable visualization of TPM values of 0), visualized in heatmaps using GraphPad Prism and edgeR (version 4.0.3). GO analysis of DEGs was performed with STRING (version 11.0). Enriched pathway values are presented as $-\log_{10}(FDR)$.

Gene expression analysis by reverse transcription-quantitative PCR

RNA was isolated using the RNeasy Micro kit, and cDNA prepared by reverse transcription (RT) with the Superscript III First-Strand Synthesis Supermix (Thermo Fisher Scientific) according to the manufacturer's protocol. Gene expression levels were determined by quantitative (real-time) PCR (qPCR) with Platinum SYBR green SuperMix-UDG mastermix (Thermo Fisher Scientific) using the StepOnePlus Real-Time PCR System (AB Applied Biosystems, Massachusetts, USA) according to the manufacturer's instructions. Forward and reverse primers (IDT Technologies, Haasrode, Belgium; Table S6) were designed using PrimerBank

(<https://pga.mgh.harvard.edu/primerbank/>) and PrimerBLAST (<https://www.ncbi.nlm.nih.gov/tools/primer-blast/>). Glyceraldehyde-3-phosphate dehydrogenase (*GAPDH*) and β -actin (*Actb*) served as housekeeping genes. Relative gene expression levels were presented as bar graphs of delta(Δ)CT values ($Ct^{\text{target}} - Ct^{\text{housekeeping gene}}$). Furthermore, gene expression levels were compared between sample and reference as relative expression ratio (fold change), calculated using the formula $2^{-(\Delta Ct \text{ sample} - \Delta Ct \text{ reference})}$.

Statistical analysis

GraphPad Prism was used to perform statistical analysis (for $n \geq 3$ biological replicates). To compare two and multiple groups, unpaired two-tailed t-Student test and one- or two-way ANOVA were employed, respectively. Results were defined statistically significant if $P < 0.05$.

3. RESULTS

3.1 Pituitary stem cells of the *Drd2*^{-/-} tumorigenic gland show a proliferative and cytokine/chemokine activation phenotype

Female mice with homozygous knockout of the *Drd2*^{-/-} gradually develop prolactinomas in the AL from 6-8 months of age (Kelly et al, 1997; Cristina *et al.* 2006; Mertens et al, 2015). Our previous study provided indications of an activated stem cell compartment in the *Drd2*^{-/-} AL early in the tumorigenic process (10-14 months of age), including the presence of an enlarged SC-SP and more abundant SOX2⁺ stem cells, all as compared to *Drd2* wildtype (*Drd2*^{+/+}) mice (Mertens et al., 2015). Here, we observed that, at later full-blown development of the tumors (18-21 months of age; Fig. 1A), the absolute SOX2⁺ cell number in the *Drd2*^{-/-} AL remains significantly higher than in wildtype AL (Fig. 1A; ~8-fold; as compared to 2.5-fold at the earlier ~1-year age, see (Mertens et al., 2015)). The rise in number coincides with an increase in proliferating (Ki67⁺) SOX2⁺ cells when compared to *Drd2*^{+/+} pituitary (Fig. 1A), gradually rising from the onset of tumorigenesis (Fig. S1A) (Mertens et al., 2015).

To delve deeper into the phenotype of the stem cells in the tumorigenic pituitary, we performed RNA-seq analysis of FACS-isolated SC-SP from *Drd2*^{-/-} and control *Drd2*^{+/+} AL (Fig. S1B,C). Principal component analysis (PCA) revealed clear separation between the *Drd2*^{-/-} and *Drd2*^{+/+} SC-SP (Fig. S1D). Differentially expressed gene (DEG) analysis exposed 940 genes that were upregulated and 1047 downregulated (≥ 2 -fold) in the *Drd2*^{-/-} pituitary SC-SP *versus* *Drd2*^{+/+} SC-SP, yielding a total of 932 upregulated and 550 downregulated corresponding mouse ENSEMBL IDs (Fig. S1E; Table S1, listing the top 100 up- and downregulated genes). In analogy with the findings above, expression of *Mki67* (encoding Ki67) was found increased within the SC-SP, as well as of several recently identified pituitary stem cell markers (such as *Tacstd2* (*alias Trop2*), *Lgr6*, *Cd44* and *S100a6* (Cox et al., 2019; Mertens et al., 2015; Vennekens et al., 2021)) (Fig. S1F). In line with the (proliferative) activation, Gene Ontology (GO) analysis using the upregulated DEGs revealed enrichment of 'regulation of cell population proliferation', 'cell division' and '(regulation of) cell activation' processes (Fig. 1B). Remarkably, also immune/inflammatory, and chemokine- and cytokine-related terms (such as interleukins, NFκB and interferon gamma (IFNγ) signaling) were significantly enriched in the stem cell compartment of the tumorigenic *versus* wildtype pituitary (Fig. 1B), epitomized by the upregulation of several key pathway genes (Fig. 1C). Of note, we recently discovered that the IL6/JAK-STAT pathway is an activator of pituitary stem cells as emerging following local damage in the gland (Vennekens et al., 2021). 'Positive regulation of interleukin 6 production' is enriched in the *Drd2*^{-/-} AL stem cell compartment (Fig. 1B) and *Il6* expression is upregulated (Fig. 1C). Together, transcriptome analysis further indicates that the pituitary stem cell compartment is activated when tumors develop in the gland, both regarding proliferation and cytokine/chemokine phenotype.

SOX2 expression, although present within the PRL⁺-rich tumor areas of the *Drd2*^{-/-} pituitary, does not overlap with PRL⁺ cells (Fig. 1A; (Mertens et al., 2015)). Moreover, our earlier SOX2 lineage tracing analysis provided evidence that the SOX2⁺ stem cells do not lineally lead to the development and growth of the prolactinoma tumors in the *Drd2*^{-/-} pituitary (Vankelecom and Roose, 2017). YFP-labeled PRL⁺ cells were scarce in tamoxifen

(TAM)-treated $SOX2^{CreERT2/+};R26^{YFP/+};Drd2^{-/-}$ mice, moreover not different from control $SOX2^{CreERT2/+};R26^{YFP/+};Drd2^{+/+}$ animals (Vankelecom and Roose, 2017). The abundance of the YFP-labeled cells (encompassing $SOX2^+$ stem cells and potential progeny) increased during the tracing in the progressively tumorous gland (Vankelecom and Roose, 2017), in line with the expansion of $SOX2^+$ cells (see above and (Mertens et al., 2015)). To further complement the analysis of the stem cells' molecular phenotype in the tumorous pituitary (as done above), we performed RNA-seq examination of the YFP-labeled cells as isolated by FACS 6 months after TAM injection of $SOX2^{CreERT2/+};R26^{YFP/+};Drd2^{-/-}$ and control $SOX2^{CreERT2/+};R26^{YFP/+};Drd2^{+/+}$ mice (Fig. S1G). Stemness markers (such as *Sox2*, *Sox9*, *Nestin (Nes)*, *Cd44*) were found highly expressed, corroborating the largely retained stem cell nature of the YFP⁺ ($SOX2$ lineage-traced) cells (which is in line with $SOX2$ lineage-tracing findings of others; (Andoniadou et al., 2013; Rizzoti et al., 2013)), and were found upregulated in the cells of the tumorous gland (Fig. S1H). Again, *Mki67* expression was higher (Fig. S1H), as well as the expression of several cytokines (including *Il6*) and chemokines (Fig. S1I), and GO analysis identified ILs, JAK/STAT, $IFN\gamma$, NF κ B and chemokine signaling pathways as significantly enriched (Fig. S1J). In particular, 'regulation of cell population proliferation', 'cell activation' and 'positive regulation of IL6 production' were again revealed as upregulated biological processes. Overall, biological pathways and terms of activation and cytokine/chemokine phenotype as identified were similar to the processes in the SC-SP compartment of the $Drd2^{-/-}$ pituitary (see above).

Taken together, the pituitary stem cell compartment shows an activated phenotype regarding proliferation and cytokine/chemokine nature during tumor development and growth in the gland, suggesting that local tumorigenesis imposes an activated imprint on the local pituitary stem cells.

Fig. 1

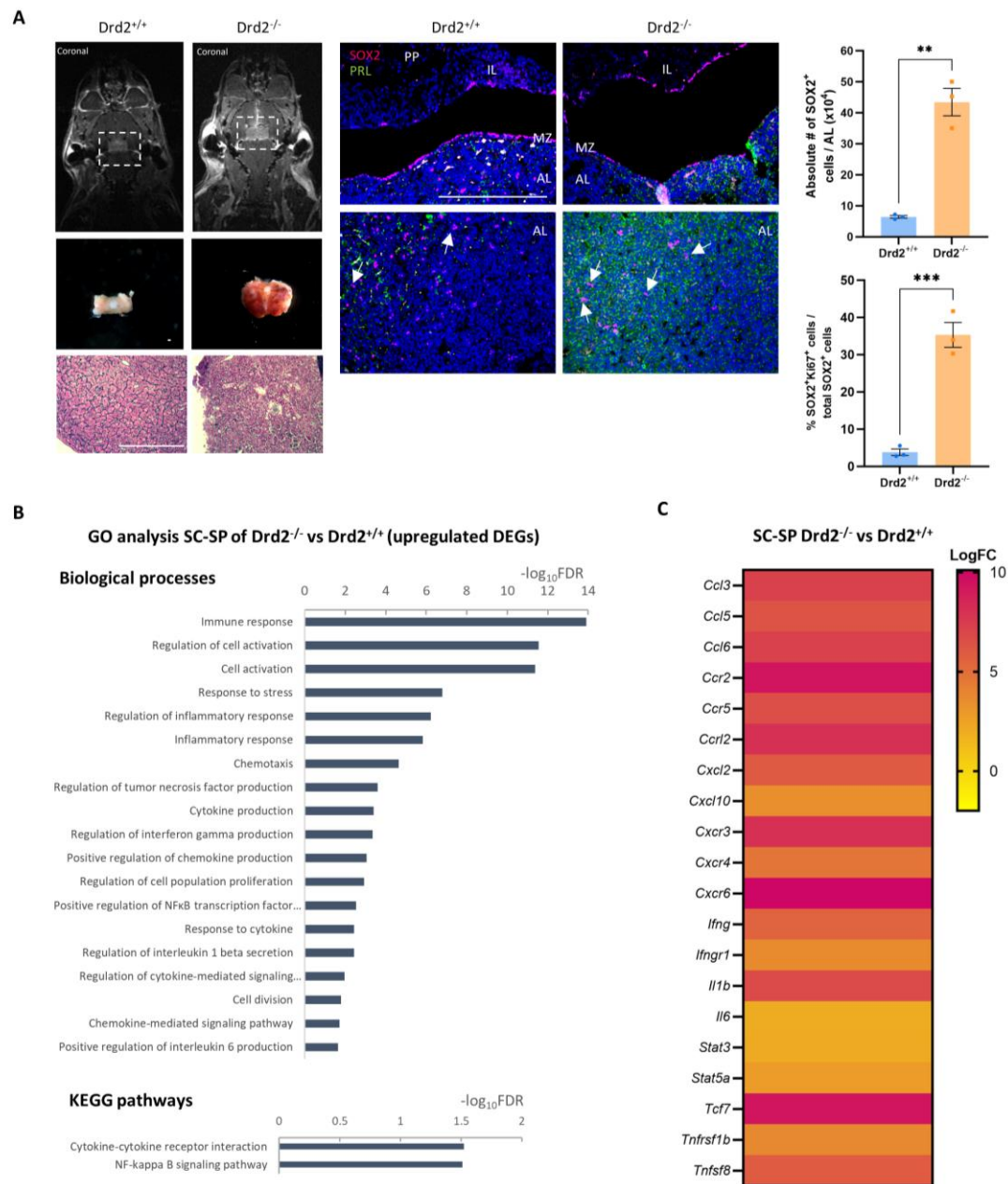


Fig. 1. Activated stem cell compartment in the tumorous Drd2^{-/-} pituitary

A Left: coronal MRI image of aged (18 months-old) Drd2^{+/+} and Drd2^{-/-} mouse exposing the pituitary gland region (dotted box) (top); microscopic capture of isolated pituitaries (middle); reticulin staining showing tumor nature (interrupted fiber network) in the Drd2^{-/-} pituitary (bottom). **Middle:** immunofluorescence staining of Drd2^{+/+} and Drd2^{-/-} pituitary for SOX2 (magenta) and PRL (green). Nuclei are labeled with Hoechst 33342 (blue). Arrows indicate parenchymal SOX2⁺ stem cell clusters, also found in the PRL⁺ tumor region (Drd2^{-/-} pituitary). AL, anterior lobe; IL, intermediate lobe; PP: posterior pituitary; MZ: marginal zone. Scalebar: 250 μ m. **Right:** absolute number of SOX2⁺ cells per AL of 18-21 months-old Drd2^{+/+} and Drd2^{-/-} female mice (top); proportion of double SOX2⁺Ki67⁺ cells in the SOX2⁺ cell population of Drd2^{+/+} and Drd2^{-/-} female mice (bottom). Bars represent mean \pm SEM. Data points indicate biological replicates. **P < 0.01, ***P < 0.001. **B** GO analysis (biological processes and KEGG pathways) of the 940 upregulated DEGs in the SC-SP of Drd2^{-/-} versus (vs) control Drd2^{+/+} pituitary with STRING represented as $-\log_{10}FDR$. **C** Heatmap showing chemokine- and cytokine-related gene expression (presented as log fold change (FC)) in the SC-SP of Drd2^{-/-} vs control Drd2^{+/+} pituitary.

3.2 Organoids recapitulate the activated pituitary stem cell phenotype of the *Drd2*^{-/-} gland

We recently achieved the establishment of organoid cultures from mouse AL, developing from the resident (SOX2⁺) stem cells (Cox et al., 2019; Vennekens et al., 2021). Moreover, we authenticated this organoid model as a valuable and effective readout tool of pituitary stem cell biology and activation (Cox et al., 2019; Vennekens et al., 2021).

Here, we first optimized the culture medium to establish organoids from AL of aged (18-21 months old) mice. Before, omission of nicotinamide and WNT3A from the originally defined medium (Cox et al., 2019), together with addition of IL6, already proved beneficial to grow organoids from middle-aged (~1-year old) pituitary (Vennekens et al., 2021). We first confirmed that EGF and CT were essential also for aged AL-initiated organoid development, and further found that adding hepatocyte growth factor (HGF), which is supplemented to organoid culture medium for multiple tissues (Fujii and Sato, 2021), and lowering the concentration of the p38 inhibitor SB202190 (SB; from 10 μ M to 100 nM), made organoid outgrowth more efficient (as assessed by organoid size; Fig. S2A). Reducing the concentrations of the TGF β signaling inhibitor A83-01 (from 0.5 μ M to 0.25 μ M) and of IGF1 (from 100 ng/mL to 40 ng/mL) did not negatively affect organoid formation (Fig. S2A). Eventually, we reached an optimized medium (OptM) to efficiently grow organoids from aged mouse AL (Table S2), resulting in significantly larger structures and higher split ratios at passaging (Fig. 2A) than the original medium (Cox et al., 2019; Vennekens et al., 2021). Then, we validated whether organoids from the pituitary of old animals also originate from the SOX2⁺ stem cells as before demonstrated for young and middle-aged mice (Cox et al., 2019; Vennekens et al., 2021). Organoids from the AL of old (18 months) SOX2^{eGFP/+} reporter mice (expressing enhanced green fluorescent protein (eGFP) in SOX2⁺ cells) were all fluorescent (eGFP⁺; Fig S2B), and mixed SOX2^{eGFP/+}/wildtype (WT) AL cells gave rise to either eGFP⁺ or non-fluorescent organoids (Fig. S2B), thereby pointing to a clonal origin.

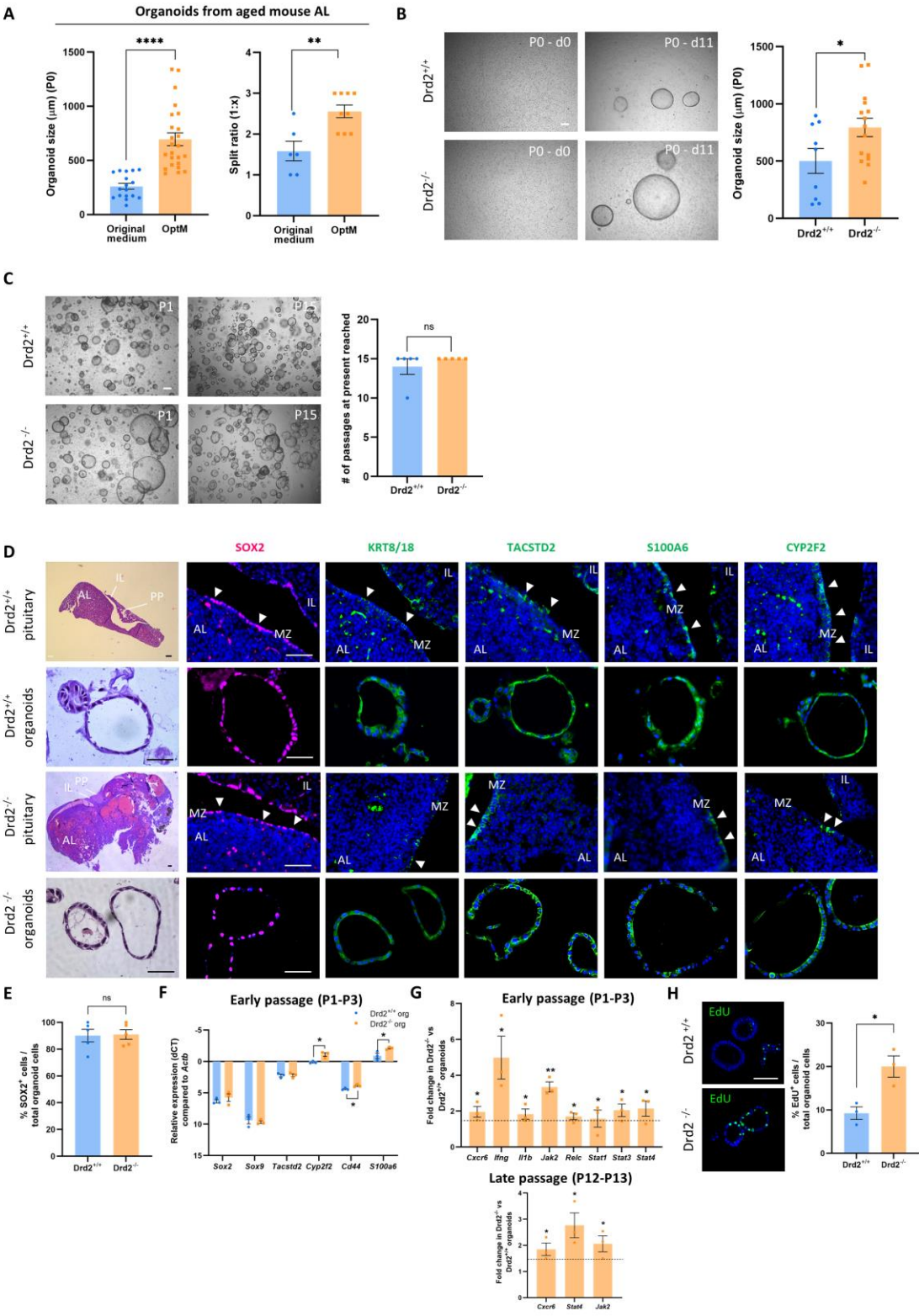
We then established organoid cultures from the (aged) pituitary of *Drd2*^{-/-} and *Drd2*^{+/+} mice using the refined OptM, and found that organoid development from *Drd2*^{-/-} AL was more efficient in that structures grew faster and to larger size than from control *Drd2*^{+/+} pituitary (Fig. 2B; Fig. S2C), in line with the activated stem cell phenotype as observed in the *Drd2*^{-/-} AL. Although only a small number of organoids (3 to 12 per well) developed after AL cell seeding (passage 0 (P0); Fig. 2B) (as also true for organoid initiation from young-adult and middle-aged AL; (Cox et al., 2019; Vennekens et al., 2021)), the organoids started to substantially expand after the first passaging (Fig. 2C). Size differences between *Drd2*^{-/-} and *Drd2*^{+/+} origin remained visible at P1, but faded at further culture (Fig. 2C). Eventually, organoids could be serially expanded (Movie 1) for more than 4 months (15 passages), not different between *Drd2*^{-/-} and *Drd2*^{+/+} AL (Fig. 2C). The organoids obtained displayed a cystic morphology with a single layer of columnar-type cells surrounding a central lumen (Fig. 2B-D), and showed polarization with apical microvilli, as also found in the marginal-zone (MZ) stem cell niche in the primary pituitary tissue (Fig. S2D).

The organoids from both *Drd2*^{-/-} and *Drd2*^{+/+} AL expressed pituitary stem cell markers (SOX2, KRT8/18, TACSTD2, S100A6, CYP2F2 and E-CAD (Cox et al., 2019; Vennekens et al., 2021)), corresponding to expression in the primary tissue's MZ (and parenchymal) stem cell niches (Fig. 2D; Movie 2 and 3), while not expressing hormones

(Fig. S2E). SOX2⁺ cells in the organoids were highly abundant which was not different between *Drd2*^{-/-} and *Drd2*^{+/+} background (Fig. 2E). Similarly, gene expression levels of *Sox2*, as well as of *Sox9* and *Tacstd2*, were not distinct, while expression of other pituitary stem cell markers (*Cyp2f2*, *Cd44* and *S100a6*) were higher in the *Drd2*^{-/-} AL-derived organoids (Fig. 2F). The stemness expression phenotype was maintained after long-term passaging although differences between *Drd2*^{-/-} and *Drd2*^{+/+} background disappeared (Fig. S2F). Intriguingly, while *Sox9* was detected at the transcriptional level, SOX9 protein was not observed in the organoids (Fig. S2G). In other tissues, SOX9 expression is stimulated by activating the BMP pathway (Kishi et al., 2011). In line, we observed that exposure to BMP4 induced SOX9 protein expression in both *Drd2*^{+/+} and *Drd2*^{-/-} AL-derived organoids (Fig. S2G), corresponding to the presence of SOX9 in the pituitary MZ stem cell niche (Fig. S2G). Next, we assessed the cytokine/chemokine phenotype of *Drd2*^{-/-} versus *Drd2*^{+/+} AL-derived organoids. Expression of several chemokines (*Cxcr6*), cytokines (*Ifng*, *Il1b*) and associated JAK/STAT and NFκB signaling components (*Stat1/3/4*, *Jak2*, *Relc*) were found significantly increased (≥ 1.5 -fold, $P < 0.05$; Fig. 2G), while additional components showed a clear trend (≥ 1.5 -fold; Fig. S2H). Some specific significant differences were maintained after multiple weeks of passaging (Fig. 2G). Finally, proliferative activity (as analyzed by EdU incorporation) was found substantially higher in *Drd2*^{-/-} versus *Drd2*^{+/+} AL organoids (Fig. 2H), thus mirroring the *in vivo* proliferative stem cell phenotype. Intriguingly, this elevated proliferative activation status is retained during long-term culturing with persistent higher split-ratios (Fig. S2I,J).

Taken together, organoids can be developed from the AL of aged mouse pituitary, and recapitulate and confirm the activated phenotype of the stem cell compartment as present in the adenomatous *Drd2*^{-/-} pituitary *in vivo*, with retention of particular distinctions with wildtype AL organoids at proceeding culture.

Fig. 2



(Legend on the next page)

Fig. 2. Organoids from tumorous $Drd2^{-/-}$ and control $Drd2^{+/+}$ pituitary

A Medium optimization for deriving organoids from AL of aged (18-21 months-old) mice. *Left*: organoid size in passage 0 (P0) at day 11 after culture initiation in original pituitary organoid medium and optimized medium (OptM). Data points represent individual organoids from 4 biological replicates. *Right*: split ratio of organoid cultures in original medium and OptM (P1-P3). Bars represent mean \pm SEM. Data points indicate biological replicates. $**P < 0.01$, $****P < 0.0001$. **B** Organoid development (P0) from aged (18-21 months-old) $Drd2^{+/+}$ and $Drd2^{-/-}$ AL. *Left*: representative light-microscopic pictures of organoid culture at day 0 (d0) and d11 after seeding. *Right*: organoid size at d11 after seeding (P0) (mean \pm SEM). Data points represent the average organoid size per well from 4 ($Drd2^{+/+}$) and 5 ($Drd2^{-/-}$) biological replicates. $*P < 0.05$. Scalebar: 200 μ m. **C** Organoid growth at passaging. *Left*: representative light-microscopic pictures of organoid cultures at P1 and P15. *Right*: the at present (i.e. at end of study) number of passages reached for $Drd2^{+/+}$ and $Drd2^{-/-}$ AL-derived organoids (after which the organoid lines were cryopreserved). Bars represent mean \pm SEM. Data points indicate biological replicates. ns, non-significant. **D** H&E staining and immunofluorescence analysis of SOX2 (magenta), KRT8/18, TACSTD2, S100A6 and CYP2F2 (all green) in $Drd2^{+/+}$ and $Drd2^{-/-}$ pituitary and corresponding organoids. Nuclei are stained with Hoechst 33342 (blue). Arrowheads indicate some selected immunopositive cells in the MZ stem cell niche. AL, anterior lobe; IL, intermediate lobe; MZ, marginal zone. Scalebar: 100 μ m. **E** Proportion of SOX2⁺ cells in $Drd2^{+/+}$ and $Drd2^{-/-}$ AL-derived organoids. Bars represent mean \pm SEM. Data points indicate biological replicates. ns: non-significant. **F** RT-qPCR gene expression analysis of pituitary stem cell markers in $Drd2^{+/+}$ and $Drd2^{-/-}$ AL-derived organoids at early passage (P1-P3). Bars represent mean \pm SEM. Data points indicate biological replicates. $*P < 0.05$. **G** RT-qPCR gene expression analysis of several cytokines/chemokines and related genes in $Drd2^{+/+}$ and $Drd2^{-/-}$ AL-derived organoids of early (P1-P3) and late (P12-P13) passage. Bars represent mean \pm SEM. Data points indicate biological replicates. $*P < 0.05$, $**P < 0.01$. **H** Proliferative activity in $Drd2^{+/+}$ and $Drd2^{-/-}$ AL-derived organoids. *Left*: representative immunofluorescence images of EdU⁺ cells (green) in the organoids. Nuclei are stained with Hoechst33342 (blue). *Right*: percentage of EdU⁺ cells in the indicated AL-derived organoids. Bars represent mean \pm SEM. Data points indicate biological replicates. $*P < 0.05$.

3.3 Cytokines upregulated in the tumorigenic pituitary's stem cells stimulate organoid growth

We tested whether some specific cytokines/chemokines, upregulated in the activated stem cell compartment of the tumorigenic $Drd2^{-/-}$ pituitary, influenced the stem cell-derived organoid development and growth process. First, we assessed the significance and impact of IL6 which we recently identified as stem cell-activating factor in the pituitary of young-adult mice (Vennekens et al., 2021), and which was added to the organoid medium during optimization (OptM; Table S2). Omission of IL6 from OptM reduced organoid formation efficiency at P0, significantly from both $Drd2^{-/-}$ AL and $Drd2^{+/+}$ AL, but interestingly more pronounced from $Drd2^{-/-}$ AL (2.1-fold *versus* 1.4-fold from $Drd2^{+/+}$ AL; $P < 0.05$). Moreover, removal of IL6 led to a decrease in organoid re-formation at subsequent passaging, resulting in early arrest of organoid passageability, both from $Drd2^{+/+}$ and $Drd2^{-/-}$ pituitary (Fig. 3A). In accordance to their reduced number and expandability, proliferation is significantly decreased in organoids grown in the absence of IL6 (Fig. 3B). Reduction of proliferative activity is again more pronounced in $Drd2^{-/-}$ AL-derived organoids (15-fold *versus* 5-fold in $Drd2^{+/+}$ AL organoids, $P < 0.05$). Endogenous *IL6* expression was found to rapidly decrease in organoid cultures (Fig. 3C), indicating that the stem cells *ex vivo* need (exogenous) IL6 to remain activated toward sustainable organoid growth. The reduction is more prominent in $Drd2^{-/-}$ AL organoids (P2 *versus* primary: 2.4-fold in $Drd2^{-/-}$ and 1.6-fold in $Drd2^{+/+}$ background, $P < 0.001$) with eventually significantly lower expression levels than in $Drd2^{+/+}$ AL organoids at P2 (Fig. 3C). Blocking the gp130 co-receptor of the IL6 receptor complex with LMT-28 in cultures without IL6, or inhibiting the JAK/STAT pathway (through which IL6 typically operates; (Rose-John, 2018)) with STATTIC, completely abrogated organoid initiation (P0; Fig. S3), supporting the importance of endogenous IL6(gp130)/JAK-STAT signaling for organoid development (thus, for stem cell functionality) from the AL of aged $Drd2^{+/+}$ and $Drd2^{-/-}$ mice (as also found before for young pituitary; (Vennekens et al., 2021)).

Then, we assessed the effect of IFN γ and IL1 β on organoid culturing, two other cytokines found upregulated in the activated stem cell compartment of the $Drd2^{-/-}$ pituitary (see above). Both factors increased the number of

organoids formed in P0 and drastically increased organoid passageability (in the absence of IL6) of both *Drd2*^{+/+} and *Drd2*^{-/-} AL (Fig. 3D), all similar to the effect of IL6 suggesting that IL1 β and IFN γ may act through this cytokine since they are known stimulators of IL6 production (e.g. in the immune system; (Stark et al., 2018)). Indeed, IL1 β and IFN γ were found to increase *Il6* expression in the organoids (Fig. 3E). Finally, we examined the effect of a chemokine found upregulated in the stem cells, i.e. CXCL2 (see above). The chemokine did not affect the number of organoids formed at P0, neither did it enable prolonged growth (Fig. 3D). In the same context, CXCL2 did not stimulate *Il6* expression (Fig. 3E). Taken together, the cytokines IFN γ and IL1 β , both upregulated in the activated stem cell compartment during tumorigenesis, also activate the pituitary stem cells as read-out by organoid growth, likely through IL6.

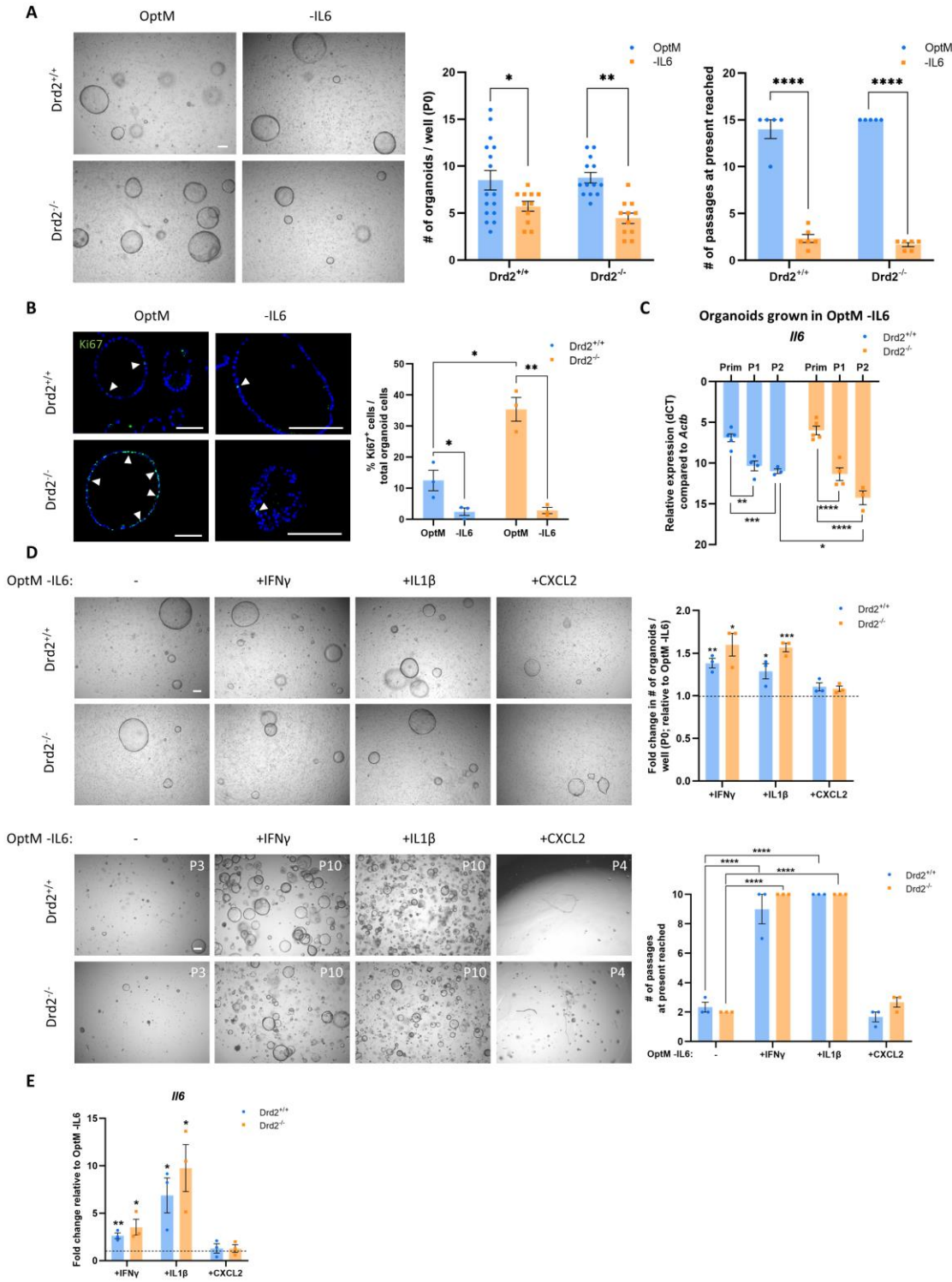
Table 1. Overview of human pituitary tumors including stemness profile and organoid formation outcome

Pituitary tumor pathology	Patient ^a	Age	Gender	Max. tumor diameter (mm)	Relapse	Invasive	Knosp degree	SOX2 ⁺	SOX9 ⁺	SOX2 ⁺ /SOX9 ⁺	Topography ^b	Organoid development (P0)
GH-secreting with co-expression of other hormones	HPA-1	38	F	10.2	-	-	0	38.24%	7.27%	7.27%	D	-
GH-secreting	HPA-6	64	M	20.3	-	-	1	0.08%	0.05%	0.05%	C	+
GH-secreting	HPA-8	59	F	20.2	-	-	1	0.31%	0.06%	0.03%	D + F	+
GH-secreting with co-expression of other hormones	HPA-14	48	F	20.6	-	-	1	6.35%	0.21%	0.05%	C + D + F	+
GH-secreting	HPA-17	55	F	8	-	-	0	3.30%	1.70%	1.02%	C + D	nd
GH-secreting	HPA-18	52	M	13.7	-	-	0	nd	nd	nd	nd	+
GH-secreting	HPA-19	38	F	16.5	+	-	1	nd	nd	nd	nd	+
GH-secreting	HPA-25	23	M	35	+	+	4	0.05%	0.07%	0.05%	C + D	nd
LH-secreting	HPA-2	78	M	25.3	-	-	1	2.73%	1.72%	1.40%	C + D	+
Limited LH-secreting	HPA-7	50	M	24.6	-	+	3	1.20%	0.09%	0.07%	C + D	+
Strongly LH- poorly FSH-secreting	HPA-11	66	M	33.3	-	+	2	12.15%	3.89%	3.66%	D + F	+
LH-secreting	HPA-12	46	F	20.1	-	-	1	0.27%	0.00%	0.00%	C + D	+
LH-secreting	HPA-15	42	M	21.8	-	-	1	nd	nd	nd	nd	+
ACTH-secreting	HPA-16	42	M	6	-	-	0	1.72%	0.03%	0.03%	C + D	nd
ACTH-secreting	HPA-21	49	F	11	-	-	0	0.11%	0.05%	0.05%	D	nd
FSH- and TSH-secreting	HPA-3	68	M	20.4	-	-	1	0.90%	0.14%	0.10%	C + D	+
GH- and PRL-secreting	HPA-10	29	M	36	-	+	2	nd	nd	nd	nd	+
NFPA	HPA-4	58	M	37.8	-	-	2	nd	nd	nd	nd	+
NFPA	HPA-5	36	F	13.9	-	-	0	14.07%	2.68%	2.01%	D	nd
NFPA	HPA-9	65	F	31.6	-	-	2	4.35%	3.17%	2.97%	C + D	nd
NFPA	HPA-13	64	M	28.6	-	-	1	1.02%	0.56%	0.47%	D	+
NFPA	HPA-20	53	M	15.2	+	+	0	4.28%	0.00%	0.00%	C + D + F	+
NFPA	HPA-22	71	M	26	-	-	2	0.39%	0.39%	0.05%	D	+
NFPA	HPA-24	69	F	33	-	+	3	1.11%	0.00%	0.00%	F	nd
NFPA	HPA-26	35	M	15.3	+	-	0	nd	nd	nd	nd	+
NFPA; potential carcinoma	HPA-27	70	M	50	-	+	4	0.05%	0.07%	0.05%	D	+
NFPA	HPA-28	62	M	25	-	+	3	0.35%	0.27%	0.27%	D	+
Craniopharygioma	HPA-23	72	M	58	-	+	4	nd	nd	nd	nd	+
Healthy pituitary tissue	Healthy-1	31	F	-	-	-	-	1.07%	0.00%	0.00%	C + D	nd
Healthy pituitary tissue	Healthy-2	67	F	-	-	-	-	0.04%	0.00%	0.00%	C + D	nd
Healthy pituitary tissue	Healthy-3	50	F	-	-	-	-	1.15%	0.00%	0.00%	D	nd

^a HPA numbers, assigned chronologically according to surgery date

^b C, clustered; D, dispersed; F, follicular; nd, not determined

Fig. 3



(Legend on the next page)

Fig. 3. Effect of cytokines/chemokines on organoid growth from tumorous *Drd2*^{-/-} and control *Drd2*^{+/+} pituitary.

A Effect of IL6 on organoid growth from *Drd2*^{+/+} and *Drd2*^{-/-} AL. *Left*: representative light-microscopic pictures of organoid culture (P0) in medium with IL6 (OptM) and in OptM without IL6 (-IL6). Scalebar: 200 μ m. *Middle*: number of organoids formed in P0 from *Drd2*^{+/+} and *Drd2*^{-/-} AL in OptM (i.e. with IL6) and in absence of IL6 (-IL6). Data points represent the number of organoids per well for 4 biological replicates. *Right*: number of passages at present (i.e. at end of study) reached (after which the organoid lines were cryopreserved) in OptM (i.e. with IL6) and in absence of IL6 (-IL6). Bars represent mean \pm SEM. Data points indicate biological replicates. *P < 0.05, **P < 0.01, ****P < 0.0001. **B** Proliferative activity in *Drd2*^{+/+} and *Drd2*^{-/-} AL-derived organoids established in OptM (i.e. with IL6) and in absence of IL6 (-IL6). *Left*: representative pictures of immunofluorescence analysis for Ki67 (green). Nuclei are stained with Hoechst33342 (blue). Arrowheads indicate some selected Ki67⁺ cells. Scalebar: 100 μ m. *Right*: proportion of Ki67⁺ cells in *Drd2*^{+/+} and *Drd2*^{-/-} AL-derived organoids cultured as indicated. Bars represent mean \pm SEM. Data points indicate biological replicates. *P < 0.05. **C** RT-qPCR gene expression analysis of *Il6* in *Drd2*^{+/+} and *Drd2*^{-/-} primary AL tissue (Prim) and corresponding organoids at indicated passages (P1, P2). Bars represent mean \pm SEM. Data points indicate biological replicates. *P < 0.05, **P < 0.01, ***P < 0.001, ****P < 0.0001. **D** Organoid development from *Drd2*^{+/+} and *Drd2*^{-/-} AL, and their passaging, in absence of IL6 (-) but presence of the indicated cytokines/chemokines (added to OptM -IL6). *Upper left*: representative brightfield images of organoid cultures as indicated. Scalebar: 200 μ m. *Upper right*: number of organoids formed in P0 at d11 in the indicated conditions relative to organoids formed in OptM -IL6. Bars represent mean \pm SEM. Data points indicate biological replicates. P < 0.05, **P < 0.01, ***P < 0.001. *Lower left*: representative brightfield images of organoid passaging as indicated. Scalebar: 200 μ m. *Lower right*: the at present (i.e. at end of study) number of passages reached (after which the organoid lines were cryopreserved) in the indicated conditions. Bars represent mean \pm SEM. Data points indicate biological replicates. ****P < 0.0001. **E** RT-qPCR gene expression analysis of *Il6* in *Drd2*^{+/+} and *Drd2*^{-/-} AL-derived organoids grown in the absence of IL6 but supplemented with the indicated cytokines. Bars represent mean \pm SEM. Data points indicate biological replicates. *P < 0.05, **P < 0.01.

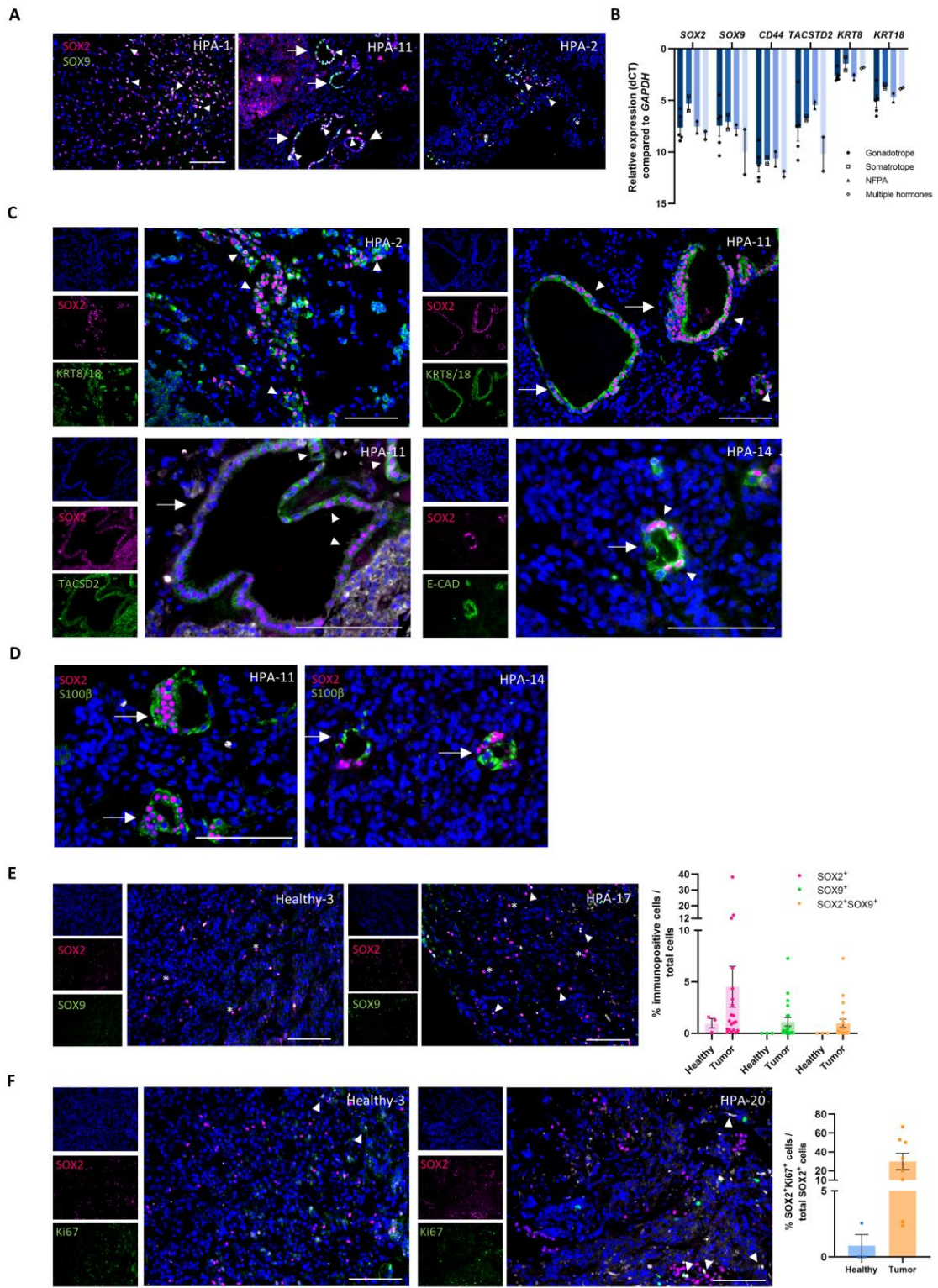
3.4 Stem cell phenotype in human pituitary tumors

Previously, we also identified a stemness population (SC-SP) in pituitary adenomas acquired from human patients, irrespective of their clinical phenotype (Mertens et al., 2015). Here, we more deeply explored the stem cell presence and phenotype in human pituitary tumors. First, we analyzed the *in situ* expression of the key pituitary stem cell markers SOX2 and SOX9 in multiple patient tumors (n=21), encompassing different types including invasive adenomas (e.g. HPA-11) as well as an aggressive potential carcinoma (HPA-27) (Table 1). All biopsies were verified to represent tumor tissue, as examined by H&E staining (revealing large dark (hyperchromatic) nuclei with different sizes and interstitial tumor fibrosis), reticulin staining (disrupted fiber network), and immunostaining for the neuroendocrine markers synaptophysin (SYP) and chromogranin A (CHGA), and for the specific hormone produced in excess by the patient tumor (see example in Fig. S4A). Analyzing the SOX2⁺/SOX9⁺ stem cell topography in the tumors revealed three patterns. Most stem cells appeared scattered throughout the tumor (e.g. HPA-1, Fig. 4A), or were housed in a follicular arrangement (e.g. HPA-11, Fig. 4A). A minority of the stem cells were found in small clusters of 2 to 5 cells (e.g. HPA-2, Fig. 4A). The different patterns were observed in distinct tumors, but could also be discerned in one and the same tumor (all topographical phenotypes summarized in Table 1). Gene transcription analysis validated the expression of SOX2 and SOX9, and also revealed the presence of markers recently identified in mouse pituitary stem cells (TACSTD2, KRT8 and KRT18; (Cox et al., 2019; Mertens et al., 2015; Vennekens et al., 2021)), irrespective of pituitary tumor phenotype (Fig. 4B), hence presenting potential novel markers for the stem cells of the human pituitary. KRT8/18 and TACSTD2 proteins were indeed found co-expressed with SOX2 in manifold cells (Fig. 4C). Co-expression was also observed of SOX2 and the known pituitary stem cell marker E-CAD (Fig. 4C), as well as of SOX2 and S100 β (Fig. 4D), a marker of folliculostellate cells which represent a heterogeneous cell population in the pituitary, also comprising stem cells (Chen et al., 2009, 2005; Fauquier et al., 2008; Garcia-Lavandeira et al., 2009; Vennekens et al., 2021).

Expression of SOX2 was detected in all tumors analyzed (21/21), and of SOX9 in the majority of them (18/21), but both markers at divergent abundance and topography per patient tumor (Fig. 4A,C,D; Fig. S4B; Table 1). Interestingly, SOX9⁺ cells were only detected in the tumors, not in healthy pituitary tissue analyzed (n=3; Table 1), while the abundance of SOX2⁺ cells appeared higher in the tumors than healthy tissue, although not reaching statistical significance (P=0.53) because of high variation between the distinct patient tumors (Fig. 4E; Table 1). Overall, SOX2⁺ cells were more abundant (ranging between 0.05 % and 38.24 %) than SOX9⁺ cells (between 0 % and 7.27 %; Fig. 4E; Fig. S4B and Table 1) in the tumors. Double SOX2⁺SOX9⁺ cells ranged from 0 % to 7.27 %, also showing distinct abundance across the patient tumors (Table 1). Most of the SOX9⁺ cells co-expressed SOX2, but not the other way around (Fig. 4A,E; Fig. S4B; Table 1). Overall, the fraction of proliferating cells within the SOX2⁺ cell population appeared higher in tumor than healthy pituitary tissue, although variation between patient tumors is also high (P=0.08; Fig. 4F). Of note, the number of healthy samples analyzed remained limited (n=3 *versus* n=8 tumors) due to restricted availability, but the observation of only scarce proliferating stem cells corresponds to (very) low proliferative activity in healthy, steady-state human pituitary as reported by others (Filippella et al., 2006; Fusco et al., 2008).

Taken together, cells expressing pituitary stemness markers are present in human pituitary tumors, and our data suggest that their proliferative activity is upregulated. Not much is known on their biology and phenotype in the tumors, in the first place because of lacking study models. Therefore, we embarked on the development of organoids from human pituitary tumors.

Fig. 4



(Legend on the next page)

Fig. 4. Stem cells in human pituitary tumors.

A Immunofluorescence analysis of human pituitary tumors for *SOX2* (magenta) and *SOX9* (green). Nuclei are stained with Hoechst 33342 (blue). Arrowheads indicate double *SOX2*⁺*SOX9*⁺ cells, arrows point to follicles and asterisks mark stem cell clusters. Scalebar: 100 μ m. **B** RT-qPCR gene expression analysis of pituitary stem cell markers in different human pituitary tumor types. Gonadotrope tumors include HPA-2, HPA-7, HPA-11, HPA-12 and HPA-15; somatotrope tumors HPA-6 and HPA-8; and NFPA HPA-20 and HPA-27. Multiple hormone-secreting tumors include HPA-10 and HPA-14. Bars represent mean \pm SEM. Data points indicate biological replicates. **C** Immunofluorescence analysis of *SOX2* (magenta), *KRT8/18*, *TACSTD2* and *E-CAD* (all in green) in human pituitary tumors. Nuclei are stained with Hoechst 33342 (blue). Arrowheads indicate double-immunopositive cells and arrows mark stem cell follicles. Scalebar: 100 μ m. **D** Immunofluorescence staining of *SOX2* (magenta) and *S100b* (green) in pituitary tumors, tagging stem cell follicles (arrows). Nuclei are stained with Hoechst33342 (blue). Scalebar: 100 μ m. **E Left:** immunofluorescence analysis of *SOX2* (magenta) and *SOX9* (green) in control (healthy) human pituitary and tumor. Arrowheads indicate double *SOX2*⁺*SOX9*⁺ cells and asterisks mark *SOX2*⁺ cells. Nuclei are stained with Hoechst 33342 (blue). Scalebar: 100 μ m. **Right:** percentage of *SOX2*⁺ and/or *SOX9*⁺ cells in pituitary tumors and healthy pituitary. Bars represent mean \pm SEM. Data points indicate biological replicates. **F Proliferative activity of stem cells in human pituitary and tumor. Left:** immunofluorescence analysis of *SOX2* (magenta) and *Ki67* (green) in healthy pituitary and tumor. Arrowheads indicate double *SOX2*⁺*Ki67*⁺ cells. Nuclei are stained with Hoechst 33342 (blue). Scalebar: 100 μ m. **Right:** proportion of double *SOX2*⁺*Ki67*⁺ cells in the *SOX2*⁺ cell population of healthy tissue and pituitary tumors. Bars represent mean \pm SEM. Data points indicate biological replicates.

3.5 Development and characterization of human pituitary tumor-derived organoids

Using the medium optimized to generate organoid cultures from tumorous mouse pituitary (OptM), organoids very efficiently developed from (dissociated) HPA samples (20 of 21 tested, i.e. 95 % efficiency; Fig. 5A; Table 1), even when starting from cryopreserved tissue (Movie 4). SFDM was eventually substituted for Advanced DMEM (Adv. DMEM; Table S2) which enabled still more efficient organoid outgrowth (Fig. S5A). The cultures were made up of dense and/or cystic organoids, of which the relative abundance varied with patient tumor (Fig. 5A,B; Fig. S5A). Both organoid types showed expression of pituitary stem cell markers (*SOX2*, *SOX9*, *TACSTD2*, *KRT8/18*, *CD44* and *E-CAD*) while lacking hormones (Fig. 5C; Fig. S5B,C), thus indicating their stemness phenotype. The organoids showed some histological features (such as differently sized and shaped nuclei) as present in the original tumor tissue (e.g. HPA-11 and HPA14; Fig. 5D). The aggressive HPA-27-derived organoids displayed a squamous cell pattern (at the border), and a reticular network with inflated cells (toward the center), strikingly resembling typical features of craniopharyngioma (*viz.* squamous cell groups, stellate reticulum, vacuolization of cells; Fig. S5D) which might provide some hints to HPA-27's origin (also from Rathke's pouch remnants?; (Andoniadou et al., 2013; Gonzalez-Meljem et al., 2017)) and to its aggressiveness. Of note, we could also develop organoids from clinical craniopharyngioma (HPA-23) (Fig. S5D).

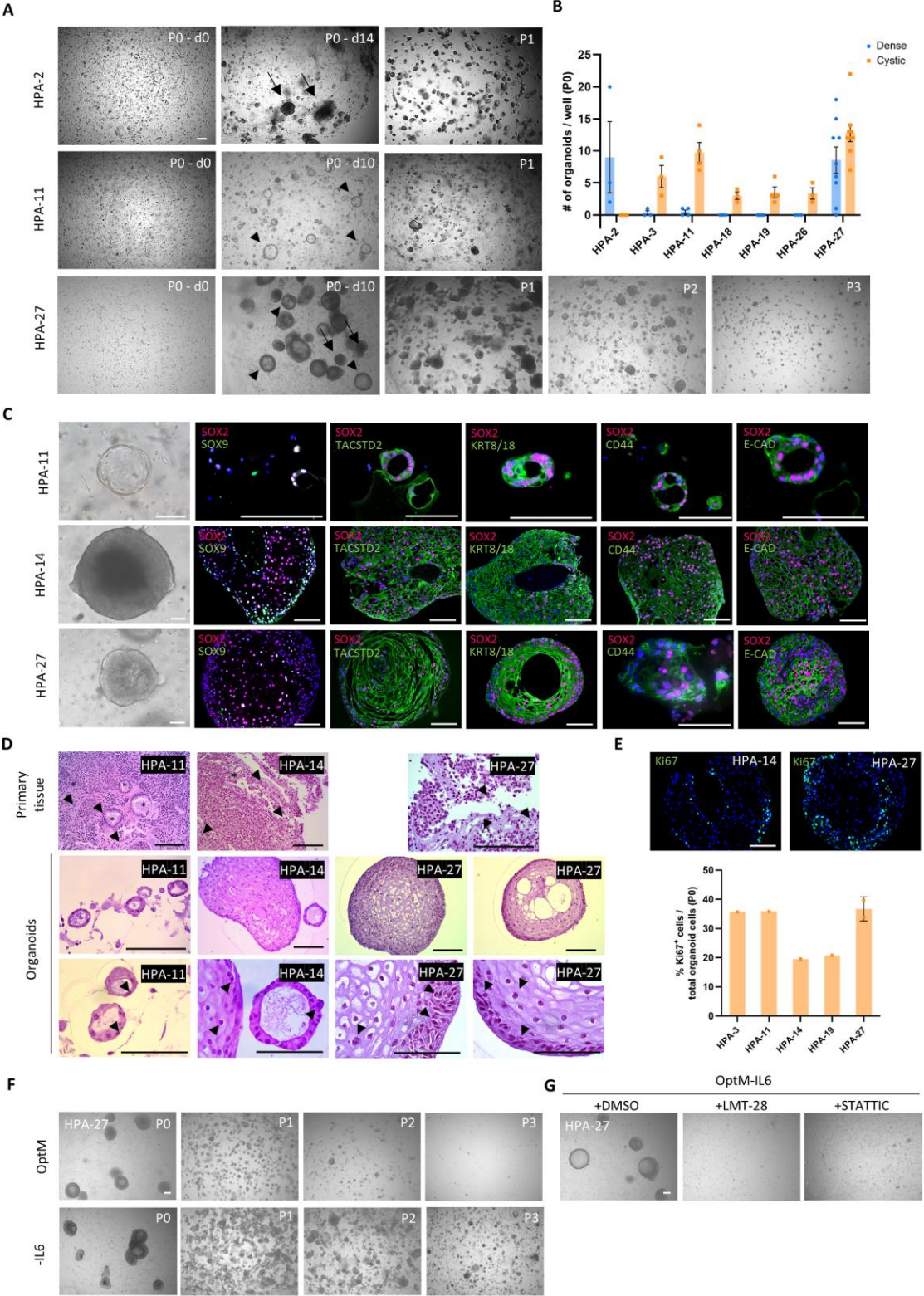
Unexpectedly, the tumor-derived organoids failed to efficiently regrow at passaging and stopped expanding already in P1 (Fig. 5A), although proliferation was substantially high in P0 (Fig. 5E). Of note, the cultures derived from the aggressive HPA-27 tumor could be passaged to P2 coinciding with high and sustained proliferative (*Ki67*⁺) activity at P0 and P1 (Fig. 5A,E; Fig. S5E). Since passageable (although still limited), we used this organoid line to assess the effect of the IL6 pathway, shown beneficial for tumorous mouse pituitary-derived organoid growth (see above). Surprisingly, although omission of IL6 from the culture medium did not affect initial organoid formation (P0; Fig. 5F; Fig. S5F), also not from other tumors (Fig. S5F), cultures became more packed at passaging indicative of more abundant and larger organoids (Fig. 5F). Since IL6 is a component of senescence-associated secretory phenotype (SASP), we hypothesized that IL6 may be part of, and contribute to, a senescence program unfolding in the organoids, and that adding IL6 may thus be detrimental. In line, other senescence markers (such as *IL8*, *P16* and *P21*) were clearly detected in the organoids (Fig. S5G, with a trend of upregulation at passaging) as well as in the primary tumors irrespective of clinical phenotype (Fig. S5G,H). Notwithstanding, removal of IL6

did eventually not extend the passageability, and organoids stopped growing after P2, similar to organoids cultured in the presence of IL6 (Fig. 5A,F). Blocking gp130-mediated signaling with LMT-28 or JAK-STAT activity with STATTIC both abrogated organoid initiation (P0, without IL6; Fig. 5G), thus indicating the importance of endogenous IL6(gp130)/JAK-STAT pathway for organoid outgrowth as found above for tumorous mouse AL-derived organoids. In line, *IL6* is highly expressed in the tumor at seeding, but immediately drops at P0 (Fig. S5G), as found for mouse AL-derived organoids in culture (see above; (Vennekens et al., 2021)). Together, IL6 might exert a dual effect, with the endogenous IL6 pathway needed for organoid development (thus, stem cell activity) and exogenous IL6 acting within a senescence program during organoid growth.

Finally, we tested whether addition (1:1) of early-passage organoid conditioned medium ((CM); both from human and *Drd2*^{-/-} mouse origin) could prolong human tumor organoid expandability, but regrowth of organoids at P1 was not enhanced and growth still stopped at P2 (Fig. S5I).

Taken together, organoids could be efficiently developed from divergent types of pituitary tumors, but did not highly expand in all culture conditions tested.

Fig. 5



(Legend on the next page)

Fig. 5. Organoids from human pituitary tumors.

A Light-microscopic images of human pituitary tumor-derived organoid cultures at d0 and d10/d14 after seeding, and at P1, P2 and P3. Arrows indicate dense organoids and arrowheads cystic organoids. Scalebar: 100 μ m. **B** Number of dense and cystic organoids formed in P0 from different pituitary tumors (HPA). Bars represent mean \pm SEM. Data points indicate technical replicates per biological HPA sample. **C** Representative brightfield pictures of individual tumor (HPA)-derived organoids and immunofluorescence analysis of SOX2 (magenta), SOX9, TACSTD2, KRT8/18, CD44 and E-CAD (all in green). Nuclei are stained with Hoechst 33342 (blue). Scalebar: 100 μ m. **D** H&E staining analysis of primary HPA tissue and derived organoids. Asterisks indicate stem cell follicles and arrowheads point to differently sized and shaped nuclei. Scalebar: 100 μ m. **E** Proliferative activity in human pituitary tumor-derived organoids. *Top*: representative pictures of immunofluorescence analysis for Ki67 (green). Nuclei are stained with Hoechst33342 (blue). Scalebar: 100 μ m. *Bottom*: proportion of Ki67⁺ cells in different HPA-derived organoids (P0). Bars represent mean \pm SD. Data points indicate technical replicates per biological HPA sample. **F** Representative light-microscopic pictures of HPA-27-derived organoid culture at the indicated passages in medium with IL6 (OptM) and in OptM without IL6 (-IL6). Scalebar: 100 μ m. **G** Representative brightfield pictures of organoid development from HPA-27 (P0) in the presence of LMT-28, STATTIC or vehicle (DMSO). Scalebar: 100 μ m.

3.6 Transcriptomic interrogation of pituitary tumors and derived organoids

To more in detail search for factors still missing in the culture medium that would be essential for efficient organoid expansion, and at the same time provide a broader view on tumor and organoid transcriptome and (stem cell) signaling pathways, we performed RNA-seq analysis of 3 divergent tumors (i.e. HPA-11, HPA-18 and HPA-27), together with their organoids at the reachable passages (Table 1). PCA positioned the primary tumors at comparable PC1, but at distinct PC2 for the aggressive potential carcinoma HPA-27 on the one hand, and the two more benign adenomas on the other hand (Fig. 6A). The organoids were located at distinct position from their primary tumors (predominantly at PC1), not illogical since the organoids only enrich and grow the stem cells from the heterogeneous tumor. The different-passage organoids from HPA-27, largely clustering together, clearly separated from the benign adenomas-derived (P0) organoids which also grouped together. DEG analysis of the whole-genome expression data of all P0 organoids taken together *versus* all primary tumor samples together exposed 3306 downregulated and 2086 upregulated genes in the organoids ($\log_{2}FC > 1$, $P < 0.05$). A first focused analysis revealed enriched expression of multiple pituitary stem cell markers (such as *SOX2*, *CDH1* (encoding E-CAD), *CD44*, *KRT8/18* and *S100A6*) in all organoids (Fig. 6B), thus corroborating their stemness phenotype and confirming the findings above. The distinct PCA clustering of the aggressive (HPA-27) and benign (HPA-11, HPA-18) tumor organoids and the more distinctive correspondence of the organoids with their primary tumor at PC2 (Fig. 6A) suggests that the organoids reflect some specific transcriptomic features of the original patient tumor. This idea is supported by gene expression patterns (Fig. S6A). First, genes commonly upregulated in both benign *versus* the aggressive tumor (e.g. *HP*, *ACSS3*, *ANKRD1*) remained highly expressed in the benign tumor-derived organoids, thereby retaining the distinct pattern with the aggressive tumor organoids. Some genes even became enriched in one or both of the benign tumor organoids (e.g. *AGT*, *CH3L1*, *ALDH1A2*, *CHST1*). The individual primary tumor-organoid pairs also showed distinct expression prints, such as *POU1F1* and *DLK1* for HPA-18, *BPIFB4* for HPA-11, and *FOXG1* and *NRG1* for HPA-27 (Fig. S6A). While retained expression in the benign tumor-derived organoids might still be assigned to some residual presence of tumor's non-stem/endocrine cells at P0 (e.g. *POU1F1*, prominent in the GH-secreting tumor HPA-18 and detected in the derived P0 organoids), the persistent expression of genes across multiple passages as found in HPA-27-derived organoids strongly support that such gene expressions are definitely not all due to contaminating cells. Second, expression of certain other genes (e.g. *SPTBN1*, *DUSP6*, *ATF1*) is not very different among the three primary tumors, and this pattern is also retained in the organoids (Fig. S6A). Third, and further interestingly, the recently

reported pituitary tumor-related genes *AMIGO2*, *ZFP36*, *BTG1* and *DLG5* (Cui et al., 2021) are not only highly expressed in the tumors, but also in the derived stemness organoids (Fig. S6A). Moreover, expression of *DLG5*, as opposed to the other genes, is increased (enriched) in the organoids, which may advance *DLG5* as a pituitary tumor-related stem cell marker. Interestingly, the cytokine LIF (leukemia-inhibitory factor) shows a resembling picture. Taken together, there are clearly tumor-specific expression features which are recapitulated in the derived stem-cell organoids.

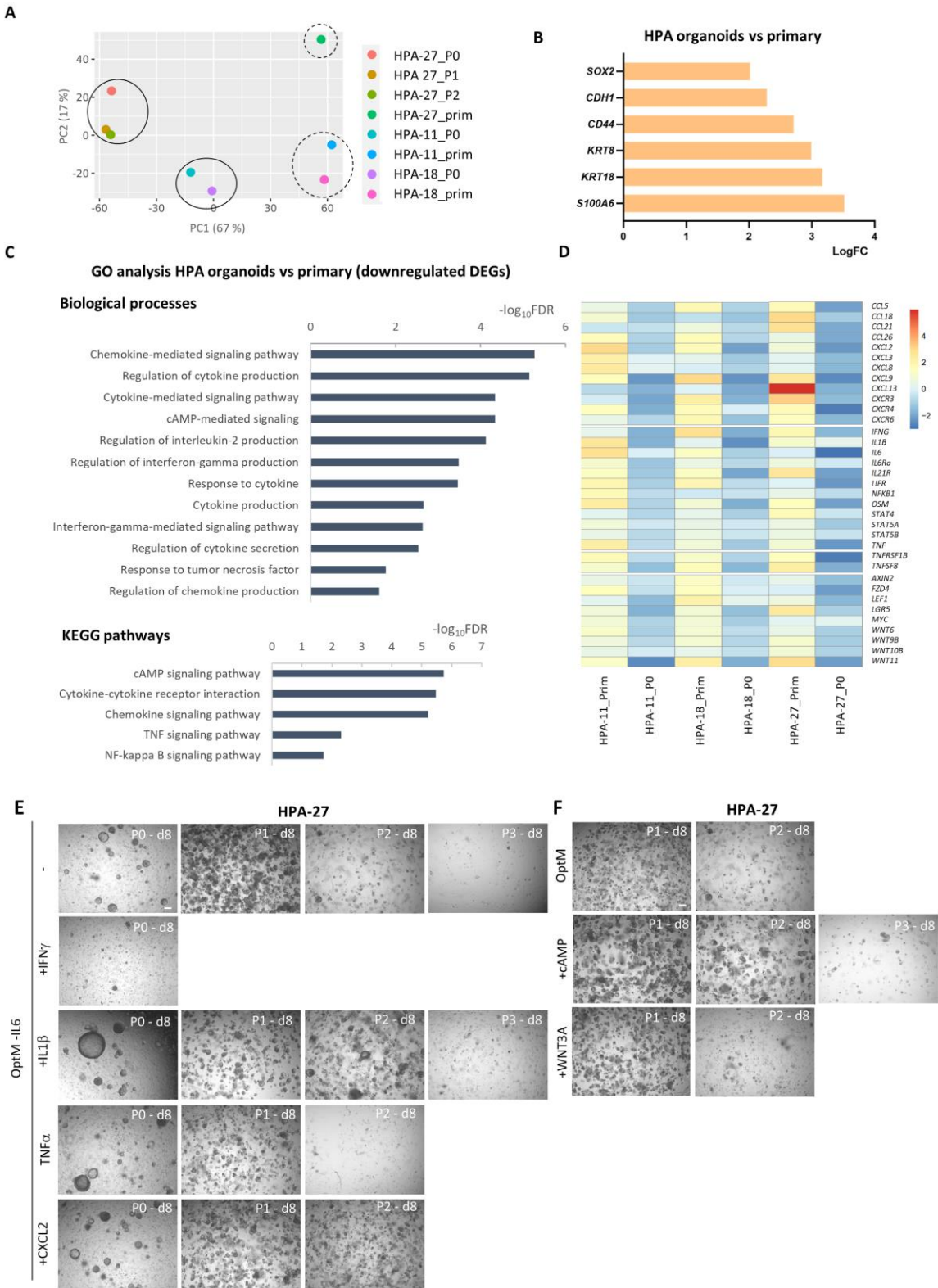
We then applied the RNA-seq data to search for underlying molecular causes of the organoids' limited expandability. We hypothesized that, in addition to potential senescence (see above), certain stem cell-driving/-activating factors which are present *in vivo* may disappear when the tumor is seeded in organoid culture (e.g. because they are produced by non-stem cells which do not grow in the organoid conditions, or because they are not upregulated anymore in the stem cells when the cells are isolated from their 'stimulatory' microenvironment). To search for these factors, we performed an extensive comparison of the top ~2000 DEGs (i.e. with $\log_{2}FC > 3.2$, $P < 0.05$) of all P0 organoids together *versus* all primary tumors. Of these exactly 1994 DEGs, 1484 genes were downregulated and 510 upregulated in the organoids (Table S3), resulting in 1108 downregulated and 393 upregulated corresponding human ENSEMBL IDs. To search for factors/pathways disappearing in organoid culture, we performed GO analysis on the downregulated genes. Interestingly, cytokine/chemokine biological processes and KEGG pathways were identified as downregulated in the organoids, as well as 'cAMP-mediated signaling' (Fig. 6C). In accordance, individual gene assessment within these pathways showed downregulation of key cytokines/chemokines and related genes such as *IL6* (as found above; Fig. S5E) and *OSM* (IL6 family member), *IL1B*, *CXCL2*, *CXCR4*, *IFNG*, *TNFA*, *NFKB1* and *STAT4* (Fig. 6D), further validated by RT-qPCR (Fig. S6B), as well as of certain WNT pathway components (such as *LGR5*, *AXIN2*, *LEF1*, *FZD4*, *WNT11*) (Fig. 6D). Together, these data suggest that the cytokine/chemokine system is also high in human pituitary tumors (and their stem cells), as found in mouse, and that vanishing of this system may be responsible for declined stem cell activation in organoid culture, and hence early termination of organoid growth and expansion. Therefore, we tested the effect of several of these cytokines/chemokines (IFN γ , IL1 β , TNF α , CXCL2) on organoid culturing of different tumors (HPA-27 and HPA-28) in the absence of IL6 (Fig. 6E; Fig. S6C). IFN γ abrogated organoid formation, thus not representing the missing element in organoid culture, while the other factors did not have an effect on the expandability (Fig. 6E; Fig. S6C). Moreover, their supplementation on top of IL6 did also not result in better expansion (Fig. S6D). Interestingly, counteracting the fading cAMP and WNT signaling visibly fortified organoid regrowth as assessed at P1, although passageability was also not extended (Fig. 6F).

Since the aggressive HPA-27 tumor was culturable to P2 (but stopped then; Fig. 5A), we compared the P2 to the P0 organoid transcriptomes to search for declining factors or pathways at serial culturing which may be involved in the halted organoid expansion. We identified 326 downregulated ($\log_{2}FC < -1$) and 231 upregulated genes ($\log_{2}FC > 1$) in P2 *versus* P0 organoids (Table S4). GO analysis of the downregulated genes again revealed cytokine/chemokine and cAMP biological processes that disappeared at passaging (Fig. S6E), but also HIF1 and insulin signaling (Fig. S6E).

Finally, we compared the expression levels of selected interesting genes (i.e. genes with high counts/TPM and different in primary tumors and corresponding organoids) in all samples (primary tumors, P0, P1 and P2 organoids) to search for factors or pathways (using GSEA-based gene collections) that may underlie the limited passageability of the HPA-derived organoids (Fig. S6F). Within the apoptosis pathway, expression of several proteolytic enzymes (such as *CASP2*, *CASP6*) and pro-apoptotic genes (such as *BAX*, *FAS*, *BCL10*) is increased in the organoids, while expression of the anti-apoptotic gene *BCL2* (see 'hypoxia' cluster) as well as of cytokines that promote cell-survival (such as *IL6*, *TNF*) is decreased (Fig. S6F), pointing to cells entering apoptosis which may explain, or contribute to, the early cessation of the organoid culture. Other potentially important pathways such as IFN γ , NOTCH, WNT and PIK3-AKT-mTOR signaling may also be involved. Expression of *IFNG* has completely faded in the organoid cultures, whereas levels of IFNG receptors are upregulated (Fig. S6F). However, addition of IFN γ did not counteract the organoids' limited expandability (Fig. 6E; Fig. S6C). Expression of the NOTCH signal modifiers *DTX2* and *DTX4* increased while the NOTCH ligand *DLL1* and target genes *HES1* and *HEYL* declined in the organoid cultures (Fig. S6F). In contrast, PIK3-AKT-mTOR signaling may be elevated in the HPA-derived organoids as suggested by increased expression of *AKT1*, *CDK1/4*, *RAF1* and *MAP1K* (Fig. S6F). Regarding the WNT pathway, expression of the WNT inhibitors *DKK1*, *DKK4* and *DVL2* is increased whereas expression of WNT ligands (*WNT1*, *WNT6*) is completely lost in the organoids, both corresponding with a decreased expression of the WNT target gene *AXIN2* (Fig. S6F). Addition of WNT3A indeed appeared beneficial for organoid regrowth after passaging, although it did not prolong expandability (Fig. 6F). Lastly, organoids showed increased expression of hypoxia-induced genes (such as *ANXA2*, *ENO1*, *SDC4*) and decreased expression of hypoxia-induced cell survival genes (such as *ADM*, *BCL2*) (Fig. S6F), which may suggest that organoid cells may experience hypoxic stress which could cause them to die.

Taken together, transcriptomic interrogation revealed that several tumor-specific fingerprints are retained in the organoids, thus indicating that the organoids are patient tumor-specific, but also that signaling factors/pathways are faded, or other processes upregulated (e.g. apoptosis), which may underlie the deteriorating organoid culturing, although thus far functional examination did not yet identify the crucial player(s). Alternatively, human pituitary (tumor) stem cells may be inherently not capable of sustaining prolonged organoid growth.

Fig. 6



(Legend on the next page)

Fig. 6. Transcriptomic analysis of human pituitary tumors and derived organoids and resulting cytokine/chemokine functional testing.

A PCA plot of all human pituitary tumors and corresponding organoids subjected to RNA-seq analysis (variance per component as indicated). **B** Expression levels of stem cell markers, extracted from the RNA-seq analysis and presented as log fold change (FC). **C** GO analysis (biological processes and KEGG pathways) with STRING of the 1484 downregulated DEGs in all P0 HPA-derived organoids *versus* (vs) all primary tumors represented as $-\log_{10}\text{FDR}$. **D** Heatmap showing chemokine-, cytokine- and WNT-related gene expression (presented as normalized counts) in the primary HPA samples and corresponding organoids at P0. **E** Brightfield images of organoid cultures at the indicated passages in medium without IL6 (OptM -IL6; '-') and supplemented with the indicated cytokines/chemokine. Scalebar: 100 μm . **F** Brightfield images of organoid cultures in P1, P2 and P3, grown in OptM, and supplemented (from P1 onwards) with cAMP or WNT3A as indicated. Scalebar: 100 μm .

4. DISCUSSION

Our study explored the biology of local stem cells in pituitary tumorigenesis in both mouse and human, and revealed an activated proliferation and cytokine/chemokine nature, as supported by transcriptomic, protein expression and organoid findings. In a recent study, we identified IL6 as a pituitary stem cell-activating factor, being majorly involved in the stem cells' stimulation following local injury (Vennekens et al., 2021). IL6 may thus also play a role in stem cell activation at pituitary tumorigenesis, potentially being part of an assortment of activating impacts during this perturbing and burdening *in situ* process. In other tumor types, stemness cells (particularly TSCs) have been described to secrete interleukins and other cytokines for their maintenance (Andrés et al., 2020), and IL6 has been shown to activate TSC in tumors (Zheng et al., 2019). Regarding pituitary tumors, studies have shown that cytokines, in particular IL6 and TNF α , are higher expressed in invasive than non-invasive human adenomas (Wu et al., 2016), and that chemokine (CXCR4) signaling may play a role in human (*in vitro*) and rodent (xenograft) pituitary tumor growth (Barbieri et al., 2008; Kim et al., 2011; Mertens et al., 2015). In addition, IL6, as part of SASP, has been proposed to act in an autocrine manner to induce pituitary tumor senescence as a tumor suppressor mechanism (Sapochnik et al., 2017a, 2017b), while others have shown a paracrine tumor-fueling role of SASP (encompassing IL6 and IL1 β) when released by WNT/ β -catenin-mutated senescing stem cells in a mouse model of craniopharyngioma (Andoniadou et al., 2013; Gonzalez-Meljem et al., 2017). Together, our study reports on an original observation of activation of tissue stem cells in tumorigenic conditions which has, apart from findings on (authentic) TSCs, barely been found to our knowledge.

Of note, the (Drd2^{-/-} AL-derived) organoid model recapitulated the activated phenotype of the stem cell compartment, as before also shown in a pituitary damage model (Cox et al., 2019; Vennekens et al., 2021), thus further underscoring organoid (out-)growth as valuable and interesting read-out tool for pituitary stem biology and activation, in both healthy and diseased conditions.

Before, stem cell populations have been described in human pituitary tumors (Garcia-Lavandeira et al., 2009; Manoranjan et al., 2016; Mertens et al., 2015; Shirian et al., 2021; Würth et al., 2017). However, detailed *in situ* analysis was not reported. Here, we identified SOX2⁺ and SOX9⁺ stem cells in a wide variety of pituitary tumor types, presenting in different topographical patterns. Recently, a similar SOX2⁺ cell topography was reported but limited to somatotropinomas (Soukup et al., 2020). Intriguingly, we did not detect SOX9 expression in normal human pituitary tissue (which is largely similar to (Shirian et al. (2021), but different from (Garcia-Lavandeira et al. (2009))), thus suggesting its induction (upregulation) at tumorigenesis. Similarly, SOX2⁺ cells appeared more abundant in the tumors. However, definite conclusions await the analysis of many more healthy (and age-matched) pituitary samples, which are obviously not highly available. Of note, we did not find indications that invasive tumors may contain more SOX2⁺/SOX9⁺ stem cells (also not the potential carcinoma HPA-27), in agreement with the lack of prognostic significance of SOX2⁺ cells in the study by Soukup et al. (2020).

The organoids derived from human pituitary tumors showed a stemness phenotype comparable to the *in situ* stem cells. Interestingly, the organoids displayed distinct morphological and transcriptional features (epitomized by different PCA clustering) according to tumor type, with transcriptomic fingerprints similar to the original patient tumor (thus, being tumor-specific), which is reminiscent of cancer-derived organoid models

('tumoroids') as established from other tumor types (Boj et al., 2015; Boretto et al., 2019; Broutier et al., 2017; Van De Wetering et al., 2015). At present, it remains unclear whether the human pituitary tumor-derived organoids are developing from genuine TSCs present in the pituitary tumor, or from the pituitary tissue stem cells becoming enclosed in the tumor during its development and growth. Thus far, no convincing proof has been provided for the existence of TSC in pituitary tumors (which is considered difficult since the benign pituitary tumor cells do not grow in xenograft conditions (Mertens et al., 2015), a prerequisite to show TSC nature (Clevers, 2011)). Alternatively, enclosed tissue stem cells may suffer from the patient germline (epi-)genetic aberrations that have led to the tumor formation or from non-germline mutations leading to fueling of tumorigenesis in neighboring cells, or may be specifically impacted (activated) by the surrounding tumorigenic process burden, all potential explanations of patient tumor specificity of the organoids. Whole (epi-)genome sequencing is now needed to disentangle these possibilities by searching for (non-)germline aberrations (mutations, copy number variations) in the tumor (see e.g. (Bi et al., 2017; Cui et al., 2021; Ronchi et al., 2016)) and their recapitulation in derived organoids. A recent study reported on the development of a 'cell aggregate' ('tumoroid') from ACTH-secreting corticotropinomas, surprisingly using serum, triiodothyronine (T3), thyrotropin-releasing hormone (TRH) and bovine hypothalamus extract in the culture medium, and recapitulating ACTH secretion in some but not all of the established cultures (Zhang et al., 2021). However, these cell constructs were not analyzed for (clonal) stem cell origin neither for passageability, and did not use WNT/RSPO activation signals, all hallmarks of current-concept organoid/tumoroid models (Schutgens and Clevers, 2020). Interestingly, the study performed scRNA-seq analysis and revealed the presence of pituitary stem cells in the corticotropinoma biopsies. Another recent scRNA-seq study also showed the presence of pituitary stem cells within the normal (non-tumoral) cell fraction as present in multiple tumor type samples, analyzed all together as one group (Cui et al., 2021). Clearly, further studies are needed to untangle all these puzzles, as well as the role of cytokines/chemokines in the *in situ* stem cell role during the tumorigenic process. Unexpectedly, although initial formation was highly efficient (95 % success rate), the human pituitary tumor-derived organoids did not serially expand and showed early arrest. Several attempts were undertaken to extend the organoids' passageability (such as addition of specific cytokines that faded at organoid culturing, cAMP and WNT activation, supplementation of plain CM), however unsuccessful so far. It is concluded that either culture conditions are not competent yet and still miss essential cues to maintain organoid growth (thus, stem cell activity), or that human pituitary stem cells inherently lack the capacity for long-term self-renewal and proliferative growth, hence becoming rapidly exhausted. Similarly, stem cells of human hippocampus and forebrain have been shown to undergo fast exhaustion, certainly after high proliferative stress (Kippin et al., 2005; Sierra et al., 2015). Alternatively, the tumor-enclosed stem cells may be rendered sensitive to senescence which occurs in the tumor. Several studies have indeed reported senescence in pituitary tumors (Gonzalez-Meljem et al., 2017; Sabatino et al., 2015). Moreover, SASP factors such as IL6 have been proposed to play a dual role in pituitary tumorigenesis. Cell-autonomously, IL6 may induce senescence and inhibit tumor growth (Sapochnik et al., 2017a, 2017b), whereas non-cell autonomously, it may stimulate tumor growth (Andoniadou et al., 2013; Gonzalez-Meljem et al., 2017). Additional detailed scrutiny of the acquired RNA-seq datasets may further guide us to missing factors (to enable substantial organoid expansion, which would be instrumental to

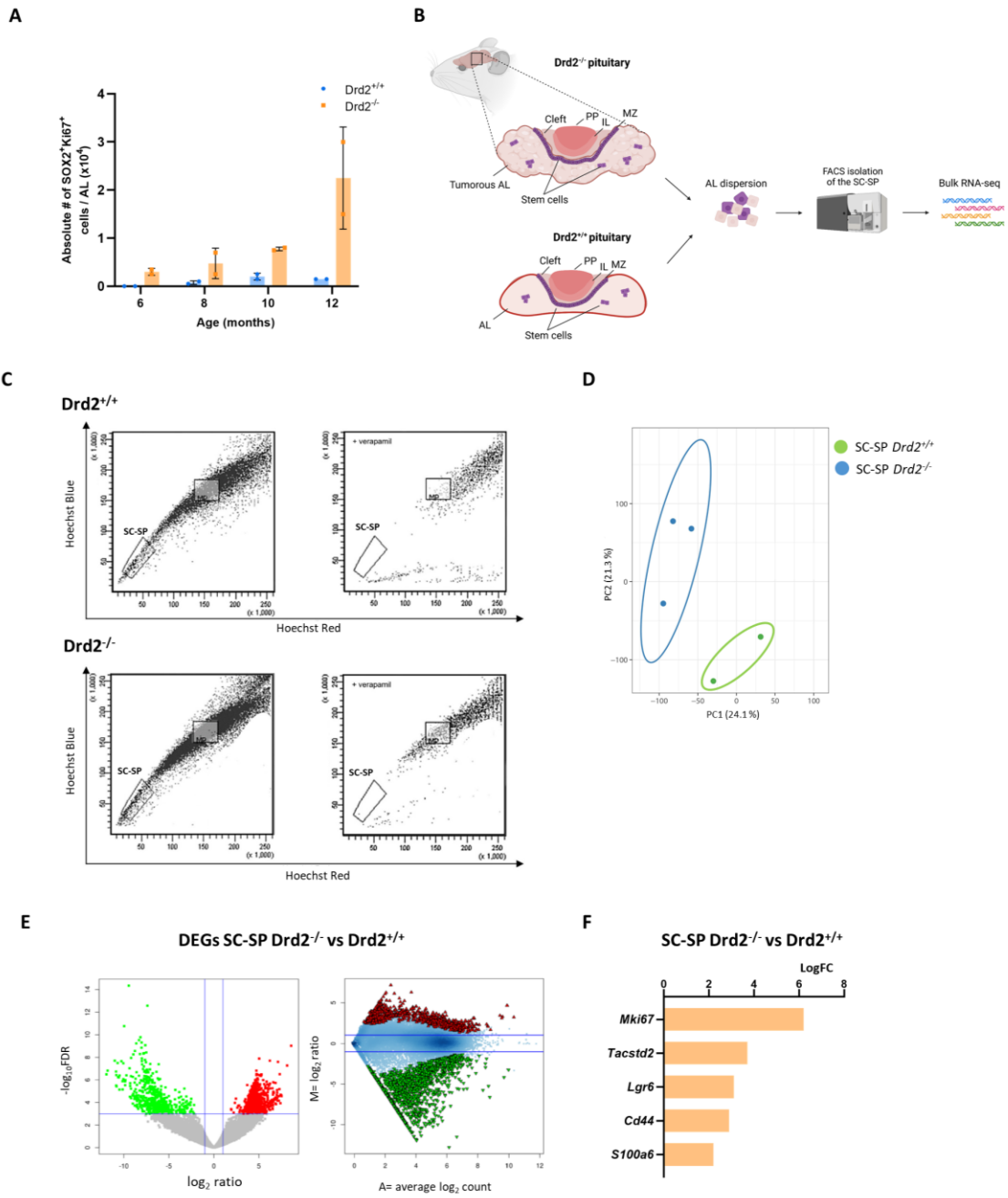
extensive downstream analysis), and simultaneously to the identification of molecular mechanisms of human pituitary tumorigenesis.

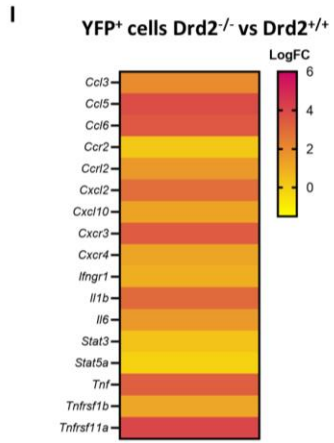
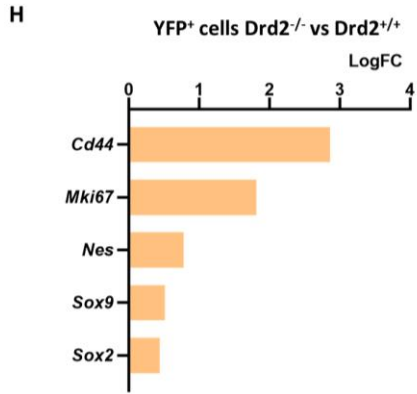
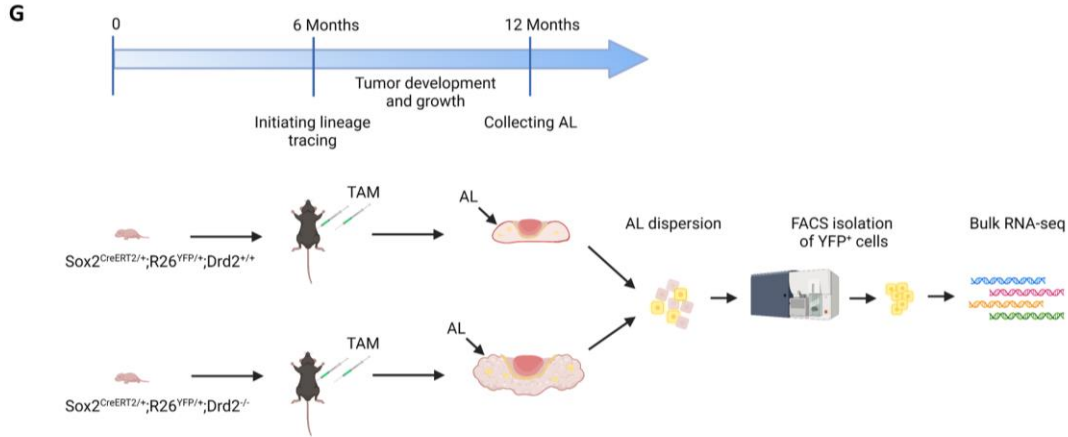
Overall, we found that local stem cells show an activated phenotype in pituitary tumorigenesis, suggesting that the local pathologic process imposes an activated imprint on the cells. Why the stem cells become stimulated remains speculative. They may get activated because of the threatening event occurring in their home tissue so that they unfold a defense reaction (which may paradoxically feed the tumor?). Activation may occur by an inflammatory/immune reaction during tumorigenesis or by paracrine (feedback-ward) signaling from the tumor to the stem cells. More research is needed to unravel these ideas. Eventually, the activated stem cell activation may fuel the tumorigenic process as found in the mouse craniopharyngioma model in which activated (mutated) SOX2⁺ stem cells incite neighboring cells to ‘transform’ into tumor cells by sending SASP factors (encompassing IL6 and IL1 β) that further stimulate tumor cell proliferation (Andoniadou et al., 2013; Gonzalez-Meljem et al., 2017). Finally, it should be noted that, to have a still broader view on the behavior and role of stem cells in pituitary tumorigenesis, more additional mouse models should be scrutinized by, for instance, stem cell lineage tracing, although appropriate models for tumor development specifically in the AL (where most clinical tumors are found) are scarce (Cano et al., 2014), mainly due to the absence of knowledge on the underlying (genetic) drivers.

Taken all together, we identified stem cell activation in pituitary tumorigenesis, being recapitulated in derived organoid models, which may be involved in the pathogenetic process, at present far from understood. Our findings can help to understand pituitary tumorigenesis, and eventually lead to new clinical treatment options.

SUPPLEMENTARY FIGURES

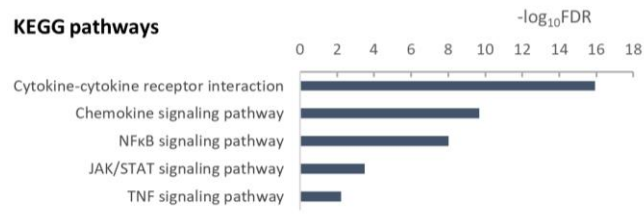
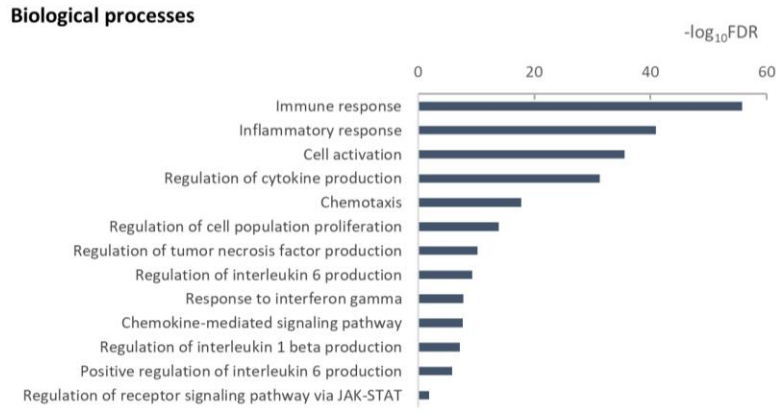
Fig. S1





J

GO analysis YFP+ cells of *Drd2*^{-/-} vs *Drd2*^{+/+} (upregulated DEGs)

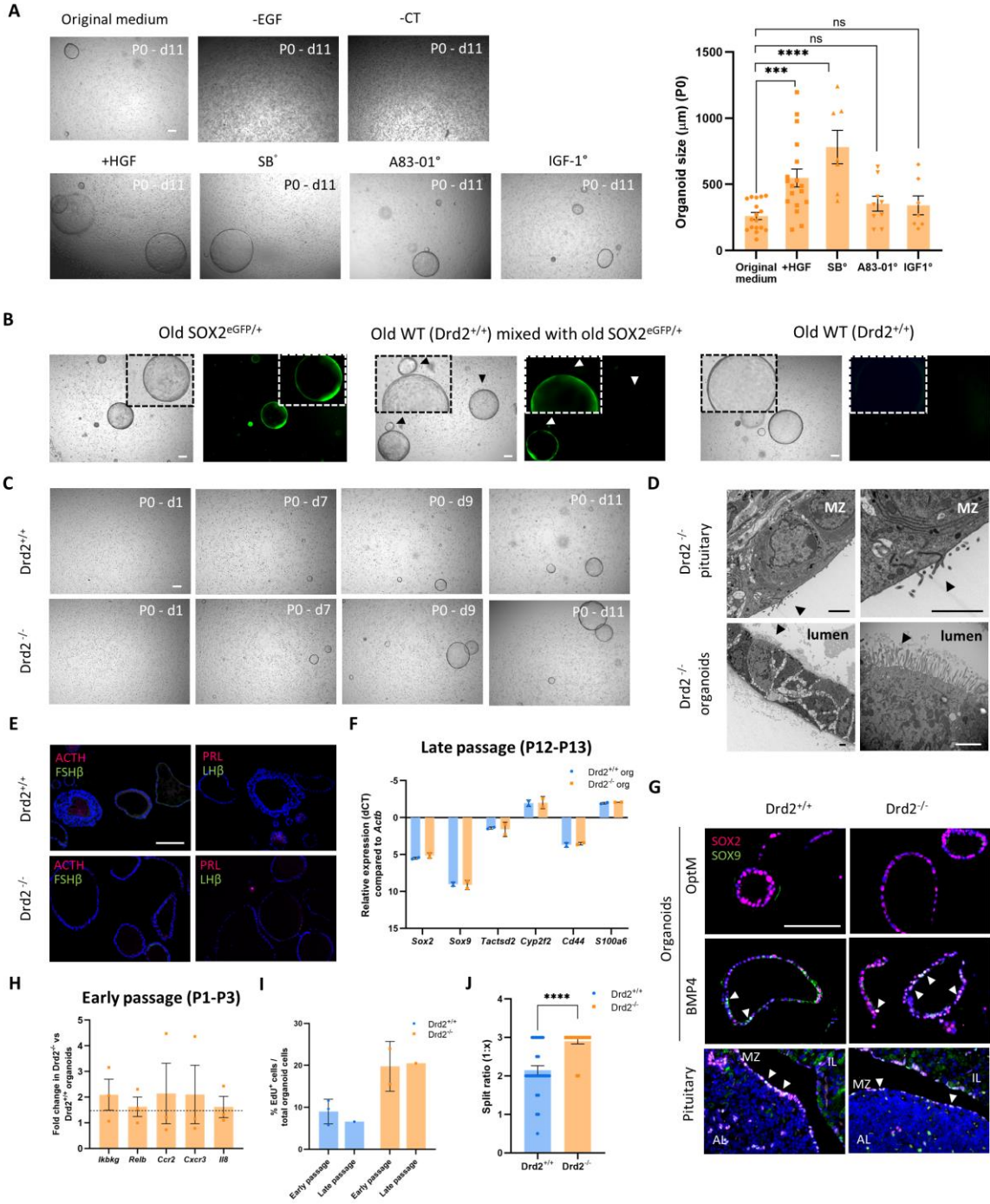


(Legend on the next page)

Fig. S1. Transcriptomic analysis of the stem cell compartment from tumorous *Drd2*^{-/-} and control *Drd2*^{+/+} pituitary

A Absolute number of SOX2⁺Ki67⁺ cells per AL of *Drd2*^{+/+} and *Drd2*^{-/-} female mice at indicated age. Bars represent mean ± SD. Data points indicate biological replicates. **B** Experimental schematic of FACS isolation of SC-SP from *Drd2*^{-/-} and *Drd2*^{+/+} AL for bulk RNA-seq analysis. Illustration created with Biorender. **C** Flow-cytometric analysis of SC-SP. *Upper panel*: dot plots of dual-wavelength FACS analysis of *Drd2*^{+/+} AL cells after incubation with Hoechst33342 alone (left) or together with verapamil (right). *Lower panel*: dot plots of dual-wavelength FACS analysis of *Drd2*^{-/-} AL cells after incubation with Hoechst33342 alone (left) or together with verapamil (right). The SC-SP and main population (MP; (Mertens et al., 2015)) are indicated. Representative examples are shown. **D** PCA plot of SC-SP samples subjected to RNA-seq analysis (variance per component as indicated). Prediction ellipses are such that a new observation from the same group will fall inside the ellipse with a probability of 0.95. **E** *Left*: Volcano plot (\log_2 ratio versus $-\log_{10}$ FDR value) of whole-genome expression data from the SC-SP of *Drd2*^{-/-} and *Drd2*^{+/+} AL. Statistically upregulated genes (in *Drd2*^{-/-} AL) are indicated in red, downregulated genes in green (cut-off: genes with a \log_2 -ratio < -1 and > 1 and FDR < 0.05. *Right*: MA plot (average intensity versus \log_2 ratio) of whole-genome expression data from the SC-SP of *Drd2*^{-/-} and *Drd2*^{+/+} AL. The points are colored green (downregulated) and red (upregulated) based on the FDR and \log_2 ratio (i.e. cut-off: genes with \log_2 -ratio < -1 and > 1 and FDR < 0.05). **F** Expression levels of stem cell markers and proliferation marker *Mki67*, extracted from the RNA-seq analysis and presented as log fold change (FC). **G** Schematic overview of SOX2 lineage tracing in *Drd2*^{+/+} and *Drd2*^{-/-} mice. At 6 months of age, *Sox2*^{CreERT2/+;R26^{YFP/+};Drd2^{+/+} and *Sox2*^{CreERT2/+;R26^{YFP/+};Drd2^{-/-} mice were injected twice with tamoxifen (TAM) to initiate lineage tracing. At 12 months of age the AL was collected and the (lineage-traced) YFP⁺ cells isolated by FACS for subsequent RNA-seq analysis. AL, anterior pituitary. Illustration created with Biorender. **H** Expression levels of stem cell markers and proliferation marker *Mki67*, extracted from the RNA-seq analysis and presented as logFC (n=1). **I** Heatmap showing chemokine- and cytokine-related gene expression (presented as logFC) in the SOX2 lineage-traced YFP⁺ cells of *Drd2*^{-/-} versus (vs) control *Drd2*^{+/+} pituitary (n=1). **J** GO analysis (biological processes and KEGG pathways) of the 1052 upregulated DEGs in the SOX2 lineage-traced YFP⁺ stem cells of *Drd2*^{-/-} vs control *Drd2*^{+/+} pituitary with STRING represented as $-\log_{10}$ FDR.}}

Fig. S2



(Legend on the next page)

Fig. S2. Organoids from aged pituitary and tumorous *Drd2*^{-/-} and control *Drd2*^{+/+} gland

A Medium optimization for deriving organoids from AL of aged (18-21 months-old) mice. *Left*: representative light-microscopic pictures of organoid culture at d11 after seeding. *Right*: organoid size at d11 after seeding (P0). ° means reduced concentration (see Table S2). Data points represent individual organoids from 3 biological replicates. ***P < 0.001, ****P < 0.0001. Scalebar: 200 μm. **B** Organoid development from AL cells of aged (18-21 months-old) *SOX2*^{eGFP/+} or wildtype (WT) mice, or from a 1:1 mixture of aged *SOX2*^{eGFP/+} and WT AL cells (P0). Representative brightfield and epifluorescence (eGFP) pictures are shown. Arrowheads indicate WT (thus eGFP^{neg}) organoids. Boxes show magnifications. Scalebar: 200 μm. **C** Organoid development from aged (18-21 months-old) *Drd2*^{+/+} and *Drd2*^{-/-} AL at indicated timepoints following seeding (P0). Scalebar: 200 μm. **D** Transmission electron-microscopical images of *Drd2*^{-/-} pituitary and *Drd2*^{-/-} AL-derived organoids. Arrowheads indicate microvilli. Scalebar: 2 μm. MZ, marginal zone. **E** Immunofluorescence analysis of ACTH and PRL (both magenta), and of FSHβ and LHβ (both green). Nuclei are stained with Hoechst 33342 (blue). Scalebar: 100 μm. **F** RT-qPCR gene expression analysis of pituitary stem cell markers in *Drd2*^{+/+} and *Drd2*^{-/-} AL-derived organoids at late passage (P12-P13). Bars represent mean ± SD. Data points indicate biological replicates. **G** Immunofluorescence analysis of SOX2 (magenta) and SOX9 (green) in *Drd2*^{+/+} and *Drd2*^{-/-} pituitary and AL-derived organoids. Nuclei are stained with Hoechst 33342 (blue). Arrowheads mark SOX9⁺ (i.e. double SOX2⁺SOX9⁺) cells. Scalebar: 100 μm. **H** RT-qPCR gene expression analysis of several cytokines/chemokines and related genes in *Drd2*^{+/+} and *Drd2*^{-/-} AL-derived organoids of early passage (P1-P3). Bars represent mean ± SEM. Data points indicate biological replicates. **I** Percentage of EdU⁺ cells in early (P3-P4) and late (P12-P13) passage *Drd2*^{+/+} and *Drd2*^{-/-} AL-derived organoids. Bars represent mean ± SD. Data points indicate biological replicates. **J** Split ratio of *Drd2*^{+/+} and *Drd2*^{-/-} AL-derived organoid cultures (P3-P15). Bars represent mean ± SEM. Data points indicate biological replicates. ****p < 0.0001.

Fig. S3

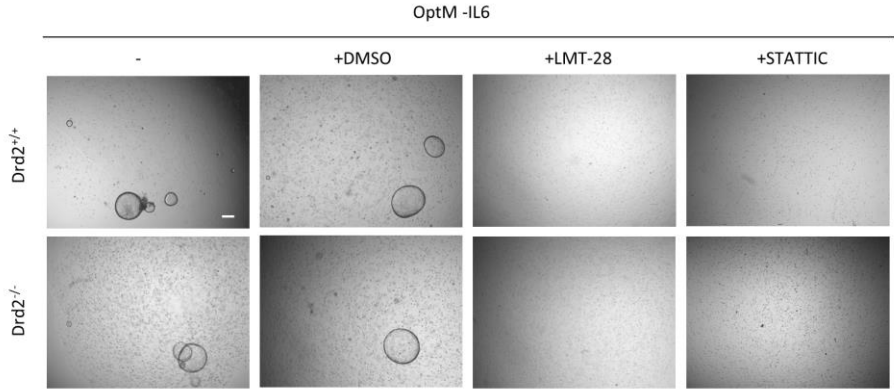


Fig. S3. IL6 signaling and organoids from tumorous Drd2^{-/-} and control Drd2^{+/+} pituitary
Organoid development from Drd2^{+/+} and Drd2^{-/-} AL in absence of IL6 (Optm -IL6; '-') but supplemented with vehicle (DMSO), LMT-28 or STATTC. Scalebar: 200 μ m.

Fig. S4

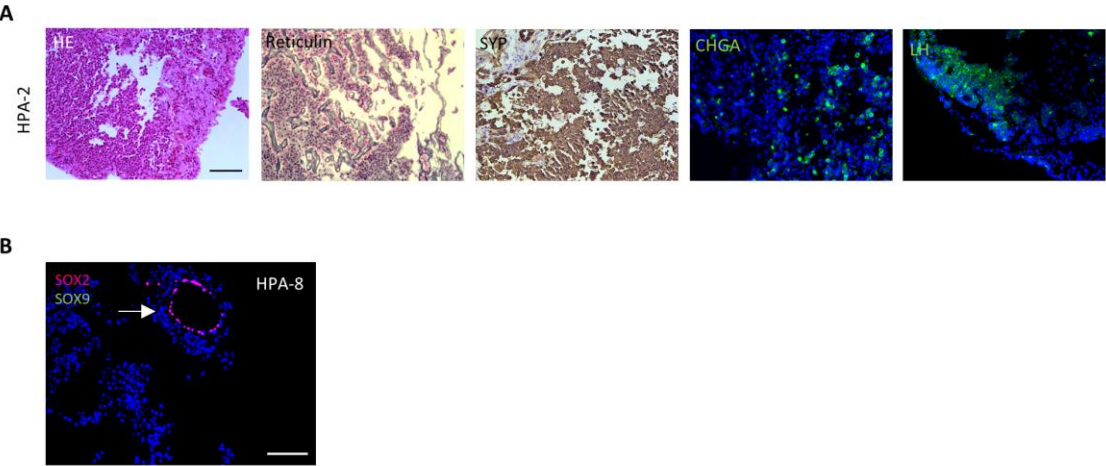
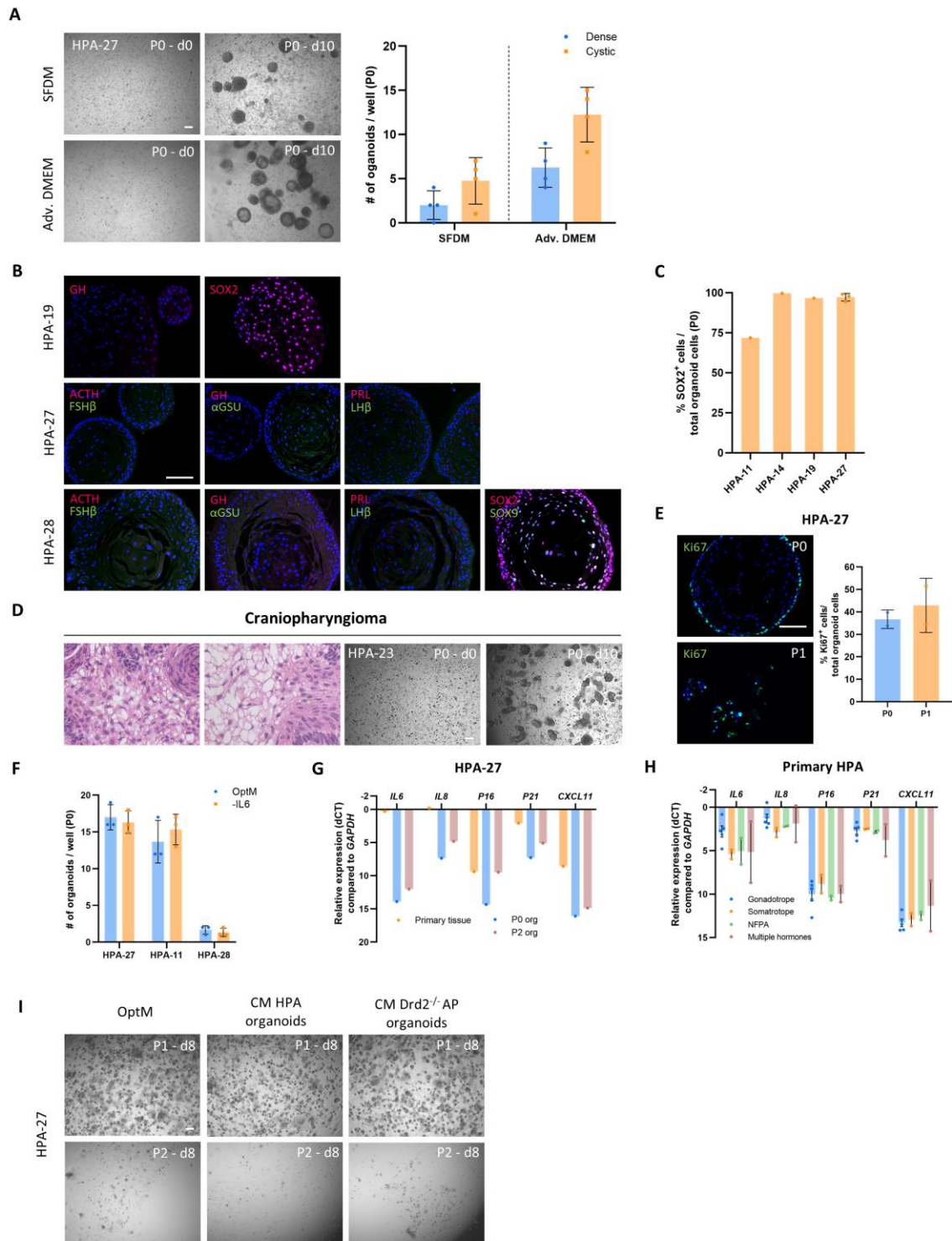


Fig. S4. Pathological characterization of human pituitary tumor
A Representative pictures of pituitary tumor characterization, shown for HPA-2. H&E staining reveals tumor cells with large nuclei and tumorous connective tissue. Reticulin staining exposes tumor nature by interrupted fiber network. Immunostaining analysis shows expression of neuro-endocrine tumor markers (synaptophysin (SYP), brown; and chromogranin A (CHGA), green) and of the tumor type-specific hormone (LH, green). Nuclei are stained with Hoechst 33342 (blue). Scalebar: 100 μ m. **B** Immunofluorescence analysis of SOX2 (magenta) and SOX9 (green; not expressed). Nuclei are stained with Hoechst 33342 (blue). Arrow indicates a stem cell follicular pattern. Scalebar: 100 μ m.

Fig. S5



(Legend on the next page)

Fig. S5. Organoids from human pituitary tumors

A *Left*: representative light-microscopic pictures of organoid formation at d0 and d10 after pituitary tumor cell seeding (P0) in SFDM or Advanced DMEM (Adv. DMEM) as basal medium, supplemented with growth factors (see Table S2). Scalebar: 200 μ m. *Right*: number of organoids developed per well in P0 in indicated conditions. Bars represent mean \pm SD. Data points represent technical replicates of 2 biological replicates. **B** Immunofluorescence analysis of ACTH, GH, PRL, SOX2 (all magenta), and of FSH β , α GSU, LH β and SOX9 (all green). Nuclei are stained with Hoechst 33342 (blue). Scalebar: 100 μ m. **C** Proportion of SOX2⁺ cells in HPA-derived organoids. Bars represent mean \pm SD. Data points indicate technical replicates per biological sample. **D** *Left*: H&E staining of a craniopharyngioma section showing typical histological features. *Middle and right*: organoid development at d0 and d10 after seeding (P0) a craniopharyngioma biopsy. Scalebar: 200 μ m. **E** Proliferative activity of HPA-27-derived organoids in P0 and P1. *Left*: immunofluorescence analysis of Ki67 (green). Nuclei are stained with Hoechst 33342 (blue). Scalebar: 100 μ m. *Right*: proportion of Ki67⁺ cells. Bars represent mean \pm SD. Data points represent technical replicates. **F** Number of organoids formed in presence (OptM) or absence (-IL6) of IL6. Bars represent mean \pm SD. Data points indicate technical replicates. **G** RT-qPCR expression analysis of cytokine and senescence-associated genes in primary tumor tissue and corresponding organoids (at P0 and P2). **H** RT-qPCR expression analysis of cytokine and senescence-associated genes in different pituitary tumor subtypes. Gonadotrope tumors include HPA-2, HPA-7, HPA-11, HPA-12 and HPA-15; somatotrope tumors HPA-6 and HPA-8; NFPA HPA-20 and HPA-27; and multiple hormone-secreting tumors HPA-10 and HPA-14. Bars represent mean \pm SEM. Data points indicate biological replicates. **I** Organoid re-growth at passaging (P1) in OptM, with or without supplementation of conditioned medium (CM) (1:1) of *Drd2*^{-/-} AL-derived organoids or HPA-27-derived organoids (collected in P0). Representative light-microscopic images are shown at indicated timepoints. Scalebar: 100 μ m.

Fig. S6

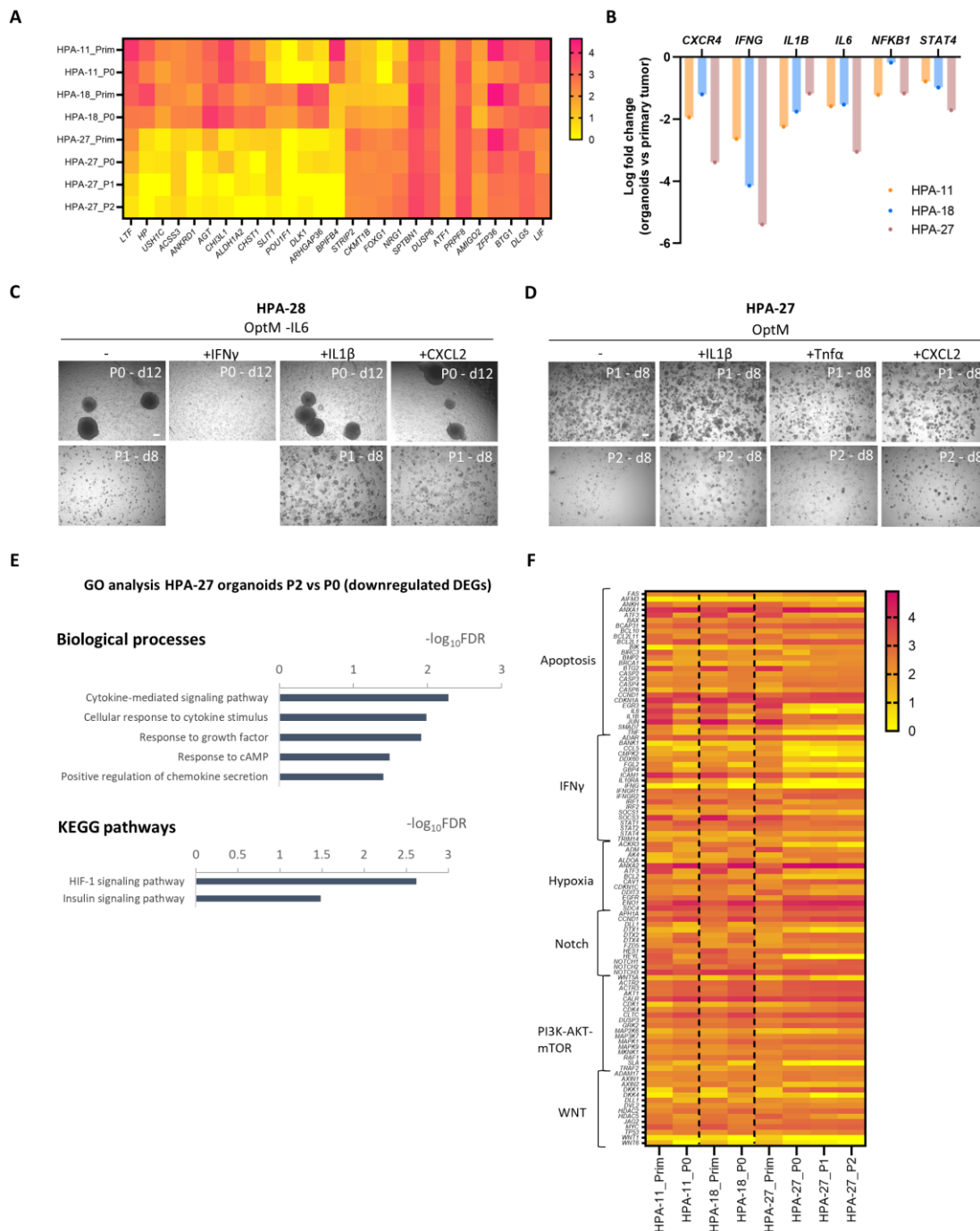


Fig. S6. Transcriptomic analysis of human pituitary tumors and derived organoids and resulting cytokine/chemokine functional testing
A Heatmap showing expression levels of a selection of genes (represented as $\log(\text{TPM}+1)$) specific for one or more of the HPA samples sequenced. **B** RT-qPCR expression analysis of cytokine- and chemokine-related genes in organoids (P0) of 3 biological replicates (i.e. 3 HPAs), presented as log fold change *versus* primary tumor. **C** Brightfield images of organoid cultures derived from HPA-28 at the indicated passages in medium without IL6 (OptM -IL6; '-') and supplemented with the indicated cytokines/chemokine. Scalebar: 100 μm . **D** Brightfield images of organoid cultures derived from HPA-27 at the indicated passages in medium with IL6 (OptM; '-') and supplemented with the indicated cytokines/chemokine. Scalebar: 100 μm . **E** GO analysis (biological processes and KEGG pathways) with STRING of the 326 downregulated DEGs in P2 organoids compared to P0 organoids derived from HPA-27, represented as $-\log_{10}\text{FDR}$ ($n=1$). **F** Heatmap showing expression levels of a selection of pathway genes (represented as $\log(\text{TPM}+1)$) for all HPA samples sequenced.

SUPPLEMENTARY MOVIES

Movie 1. Aged mouse AP-derived organoid regrowth after passaging (soon available at Figshare)

Time-lapse video of aged ($Drd2^{-/-}$) AP organoid re-development and re-growth at passaging. Video reconstruction of live time-lapse brightfield images captured by IncuCyte S3 after dissociation of P3 organoids and re-seeding organoid fragments and single cells to regrow into P4. Cultures were scanned automatically every 3 h for 6 days.

Movie 2. Whole 3D mouse AP-derived organoid immunostained for SOX2 (soon available at Figshare)

Movie of z-stacks taken through a whole 3D $Drd2^{-/-}$ AP organoid immunofluorescently stained for SOX2 (magenta). Nuclei were labeled with Hoechst33342 (blue).

Movie 3. Whole 3D mouse AP-derived organoid immunostained for E-cadherin (soon available at Figshare)

Movie of z-stacks taken through a whole 3D $Drd2^{-/-}$ AP organoid immunofluorescently stained for E-cadherin (green). Nuclei were labeled with Hoechst33342 (blue).

Movie 4. Organoid development from cryopreserved human pituitary tumor tissue (P0) (soon available at Figshare)

Time-lapse video of organoid development in P0 from a cryopreserved human pituitary tumor (HPA-11). Video reconstruction of live time-lapse brightfield images captured by IncuCyte S3 of organoid development after HPA fragment/cell seeding. Cultures were scanned automatically every 3 h for 9 days.

SUPPLEMENTARY TABLES

Table S1. Differentially expressed genes in SC-SP of *Drd2*^{-/-} versus *Drd2*^{+/+} pituitary (top 100 up- and downregulated genes)

UP			DOWN		
Gene	Log FC	FDR	Gene	Log FC	FDR
<i>Cd53</i>	11.93	0.00	<i>Crhbp</i>	-8.54	0.00
<i>Plek</i>	11.80	0.00	<i>Edn1</i>	-8.09	0.00
<i>Ano1</i>	11.01	0.00	<i>Ptgdr</i>	-7.46	0.00
<i>Itgal</i>	10.87	0.00	<i>Mmp10</i>	-7.43	0.00
<i>Coro1a</i>	10.85	0.00	<i>Plch1</i>	-7.41	0.00
<i>Il18rap</i>	10.84	0.00	<i>Abcc12</i>	-7.36	0.00
<i>Ms4a6b</i>	10.81	0.00	<i>Grk1</i>	-7.36	0.00
<i>Casq2</i>	10.68	0.00	<i>Cacna1e</i>	-7.35	0.00
<i>Cytip</i>	10.63	0.00	<i>Hhat1</i>	-7.27	0.00
<i>Itga7</i>	10.56	0.00	<i>Ano5</i>	-7.24	0.00
<i>Cd6</i>	10.49	0.00	<i>Kcns2</i>	-7.17	0.00
<i>Atp2a3</i>	10.48	0.00	<i>Ptchd4</i>	-7.15	0.00
<i>Selplg</i>	10.27	0.00	<i>Ccbp2</i>	-7.15	0.00
<i>Dock10</i>	10.14	0.00	<i>AL844859.1</i>	-7.10	0.00
<i>Cxcr6</i>	10.13	0.00	<i>Rxfp1</i>	-7.07	0.00
<i>Myh11</i>	10.05	0.00	<i>Alx4</i>	-7.03	0.00
<i>Ikzf3</i>	10.05	0.00	<i>Ugt2b34</i>	-6.99	0.00
<i>Prf1</i>	9.96	0.00	<i>Ryr3</i>	-6.98	0.00
<i>Cd2</i>	9.86	0.00	<i>4930452B06Rik</i>	-6.97	0.00
<i>Cyth4</i>	9.86	0.00	<i>Cdh3</i>	-6.94	0.00
<i>Nckap1l</i>	9.84	0.00	<i>Fcer2a</i>	-6.86	0.00
<i>Myo1g</i>	9.72	0.00	<i>Sp7</i>	-6.81	0.00
<i>Rpa1</i>	9.44	0.00	<i>Il17f</i>	-6.80	0.00
<i>Pde3b</i>	9.37	0.00	<i>Aspg</i>	-6.80	0.00
<i>Gfi1</i>	9.33	0.00	<i>Lrrtm4</i>	-6.79	0.00
<i>Ccr2</i>	9.29	0.00	<i>C1qtnf3</i>	-6.78	0.00
<i>Tcf7</i>	9.29	0.00	<i>Fev</i>	-6.63	0.00
<i>Sidt1</i>	9.20	0.00	<i>4930452L02Rik</i>	-6.61	0.00
<i>Txx</i>	9.20	0.00	<i>Pcdhb18</i>	-6.59	0.00
<i>Dok2</i>	9.19	0.00	<i>AL671873.1</i>	-6.55	0.00
<i>Gsap</i>	9.18	0.00	<i>Nanog</i>	-6.54	0.00
<i>Klrb1c</i>	9.05	0.00	<i>2010002M12Rik</i>	-6.54	0.00
<i>Cd36</i>	9.00	0.00	<i>Gm5698</i>	-6.53	0.00
<i>Lat</i>	9.00	0.00	<i>Mapk15</i>	-6.52	0.00
<i>Col6a3</i>	8.96	0.00	<i>Zfp385b</i>	-6.51	0.01
<i>Aim1</i>	8.94	0.00	<i>Slc17a8</i>	-6.49	0.01
<i>Klrg1</i>	8.83	0.00	<i>Lingo2</i>	-6.47	0.01
<i>Myo1f</i>	8.82	0.00	<i>Slc8a2</i>	-6.46	0.00
<i>Sash3</i>	8.82	0.00	<i>AC137902.1</i>	-6.46	0.00
<i>Btbd11</i>	8.79	0.00	<i>Mael</i>	-6.43	0.00
<i>Traf3ip3</i>	8.78	0.01	<i>Mdfi</i>	-6.40	0.00
<i>Vav1</i>	8.77	0.00	<i>Klh131</i>	-6.33	0.00

<i>Prss28</i>	8.76	0.00
<i>Lef1</i>	8.76	0.00
<i>Sytl2</i>	8.70	0.00
<i>Cables1</i>	8.70	0.00
<i>Kcnn4</i>	8.68	0.00
<i>Itgam</i>	8.62	0.00
<i>Ikzf1</i>	8.62	0.00
<i>Pptc7</i>	8.61	0.00
<i>Ptpn7</i>	8.61	0.00
<i>Sell</i>	8.61	0.00
<i>AI467606</i>	8.60	0.00
<i>Pik3r5</i>	8.59	0.01
<i>Ltb</i>	8.57	0.00
<i>Rasal3</i>	8.56	0.00
<i>Cd48</i>	8.56	0.00
<i>Higd1b</i>	8.55	0.00
<i>Ly6c2</i>	8.54	0.00
<i>Ccdc88b</i>	8.53	0.00
<i>Pdcd1</i>	8.50	0.01
<i>Adcyap1r1</i>	8.47	0.00
<i>Il18r1</i>	8.42	0.00
<i>Gatm</i>	8.40	0.01
<i>Rnf157</i>	8.35	0.00
<i>Emid1</i>	8.32	0.00
<i>Rbbp5</i>	8.32	0.00
<i>Arhgap9</i>	8.29	0.00
<i>Galnt6</i>	8.26	0.00
<i>Ap1g2</i>	8.25	0.00
<i>Bcl11b</i>	8.24	0.00
<i>Slc19a1</i>	8.23	0.00
<i>Aacs</i>	8.21	0.00
<i>Il1rn</i>	8.19	0.01
<i>Dennd1c</i>	8.18	0.00
<i>Gpr68</i>	8.16	0.00
<i>Aar2</i>	8.16	0.00
<i>Cd84</i>	8.15	0.00
<i>Haus4</i>	8.09	0.00
<i>Irf5</i>	8.08	0.00
<i>Syk</i>	8.08	0.00
<i>Itgax</i>	8.05	0.00
<i>Slc35b4</i>	8.04	0.00
<i>Adcy3</i>	8.03	0.00
<i>Kifc2</i>	8.03	0.00
<i>Cxcr3</i>	8.02	0.01
<i>Tmem192</i>	8.00	0.00
<i>Thap4</i>	8.00	0.00
<i>Pkp3</i>	7.99	0.00

<i>Ptgfr</i>	-6.33	0.01
<i>Tnfsf18</i>	-6.31	0.00
<i>Car3</i>	-6.26	0.01
<i>Dusp15</i>	-6.23	0.00
<i>P2rx2</i>	-6.21	0.01
<i>Wfikkn2</i>	-6.19	0.00
<i>Lhb</i>	-6.19	0.01
<i>Arsj</i>	-6.19	0.00
<i>Reln</i>	-6.18	0.00
<i>Ccdc151</i>	-6.18	0.00
<i>Sstr3</i>	-6.18	0.01
<i>Cga</i>	-6.17	0.00
<i>Gm6276</i>	-6.12	0.00
<i>Nlrp6</i>	-6.09	0.01
<i>AL669855.1</i>	-6.06	0.00
<i>Csta</i>	-6.06	0.01
<i>Cyp2d11</i>	-6.05	0.00
<i>D330022K07Rik</i>	-5.98	0.00
<i>Prr9</i>	-5.98	0.00
<i>Znrf4</i>	-5.95	0.01
<i>Gm8221</i>	-5.94	0.01
<i>Olfr91</i>	-5.94	0.00
<i>Gm766</i>	-5.94	0.00
<i>Gm15383</i>	-5.93	0.00
<i>Gm13449</i>	-5.92	0.00
<i>Grxcr1</i>	-5.92	0.00
<i>4930551L18Rik</i>	-5.92	0.00
<i>Spink4</i>	-5.91	0.00
<i>Crtac1</i>	-5.91	0.01
<i>Ccdc85c</i>	-5.90	0.00
<i>Glp2r</i>	-5.88	0.00
<i>Dlgap1</i>	-5.85	0.00
<i>Gm6268</i>	-5.82	0.00
<i>Tal1</i>	-5.82	0.02
<i>Mroh4</i>	-5.81	0.01
<i>Atp8a2</i>	-5.81	0.02
<i>Nrk</i>	-5.80	0.01
<i>4933407L21Rik</i>	-5.80	0.00
<i>Fabp12</i>	-5.80	0.00
<i>Tubb1</i>	-5.76	0.01
<i>Mmp19</i>	-5.76	0.01
<i>A530084C06Rik</i>	-5.76	0.00
<i>Tmprss12</i>	-5.73	0.01
<i>Hist1h1b</i>	-5.72	0.01
<i>5330413P13Rik</i>	-5.70	0.00
<i>Gap43</i>	-5.68	0.01
<i>Mlph</i>	-5.68	0.01

<i>Ccrl2</i>	7.96	0.00
<i>Cd3g</i>	7.95	0.00
<i>Slc7a11</i>	7.95	0.00
<i>Gzmk</i>	7.93	0.01
<i>Panx1</i>	7.93	0.00
<i>Serpinb9b</i>	7.92	0.00
<i>Pik3cg</i>	7.91	0.01
<i>Lfng</i>	7.90	0.00
<i>Card11</i>	7.88	0.00
<i>Bri3bp</i>	7.87	0.00
<i>Sncg</i>	7.85	0.01

<i>Cyp2s1</i>	-5.67	0.01
<i>Olfrl160</i>	-5.66	0.00
<i>Tnni2</i>	-5.65	0.00
<i>Sema4g</i>	-5.65	0.00
<i>Rnf144b</i>	-5.64	0.00
<i>Bean1</i>	-5.64	0.03
<i>Neil3</i>	-5.64	0.01
<i>Hist1h2ad</i>	-5.61	0.00
<i>Slc13a5</i>	-5.60	0.01
<i>Fgf17</i>	-5.59	0.01
<i>Lypd2</i>	-5.58	0.01

Table S2. Medium composition for organoid development and growth (OptM)

Component	Concentration	Catalogue #	Company
SFDM*			
B27	2 %	12587010	Thermo Fisher Scientific, Massachusetts, USA
L-glutamine**	2 mM	25030081	Thermo Fisher Scientific
bFGF (FGF2)	20 ng/mL	234-FSE	R&D systems, Minneapolis, USA
IGF1	40 ng/mL	100-11	Peprtech, London, UK
N2	1 %	17502048	Thermo Fisher Scientific
N-acetyl-cysteine	1.25 mM	A7250	Sigma-Aldrich, Missouri, USA
FGF8	200 ng/mL	100-25	Peprtech
FGF10	100 ng/mL	100-26	Peprtech
A83-01	0.25 μ M	SML0788	Sigma-Aldrich
SHH	100 ng/mL	464-SH	R&D systems
EGF	50 ng/mL	236-EG	R&D systems
SB202190	100 nM	S7067	Sigma-Aldrich
Noggin	100 ng/mL	120-10C	R&D systems
Cholera Toxin	100 ng/mL	C8052	Sigma-Aldrich
RSPO1	200 ng/mL	120-38	Peprtech
HGF	20 ng/mL	100-39	Peprtech
IL6	20 ng/mL	AF-200-06	Peprtech

bFGF, basic fibroblast growth factor; IGF1, insulin-like growth factor 1; FGF8/10, fibroblast growth factor 8/10; SHH, sonic hedgehog; EGF, epidermal growth factor; RSPO1, R-spondin 1; HGF, hepatocyte growth factor; IL6, interleukin-6.

*SFDM for mouse pituitary organoids, Advanced DMEM (supplemented with 1% Glutamax) for human pituitary tumor organoids

**Not added for human pituitary tumor organoid cultures since Glutamax is added to Advanced DMEM

Table S3. Differentially expressed genes in HPA-derived organoids versus primary tumors (top 100 up- and downregulated genes)

UP			DOWN		
Gene ID	logFC	FDR	Gene ID	LogFC	FDR
<i>TMPRSS11B</i>	23.54	0.00	<i>IGHV3-13</i>	-21.07	0.00
<i>FOXP1</i>	22.26	0.00	<i>OLR1</i>	-12.70	0.00
<i>LEP</i>	22.06	0.00	<i>NPAS4</i>	-11.56	0.00
<i>KLK7</i>	10.79	0.00	<i>IGKV4-1</i>	-10.89	0.03
<i>SPRR1B</i>	10.62	0.00	<i>FOSB</i>	-10.79	0.00
<i>SPRR2D</i>	10.62	0.00	<i>JCHAIN</i>	-10.71	0.02
<i>PADI3</i>	10.26	0.00	<i>HBB</i>	-10.65	0.03
<i>MMP3</i>	10.14	0.00	<i>IGLV3-21</i>	-10.60	0.03
<i>FGFBP1</i>	10.10	0.00	<i>RGS1</i>	-10.47	0.00
<i>TMPRSS11E</i>	9.94	0.00	<i>TPSAB1</i>	-10.34	0.04
<i>KRT6A</i>	9.74	0.00	<i>IGHV5-51</i>	-10.05	0.04
<i>PGLYRP3</i>	9.13	0.00	<i>IGHA2</i>	-9.98	0.00
<i>LINC01940</i>	9.10	0.00	<i>AC022217.1</i>	-9.88	0.00
<i>CLCA2</i>	9.06	0.00	<i>IGHG2</i>	-9.86	0.00
<i>TMPRSS11A</i>	8.94	0.00	<i>ICOS</i>	-9.68	0.00
<i>CD177</i>	8.88	0.00	<i>CXCL13</i>	-9.65	0.05
<i>NLRP10</i>	8.83	0.00	<i>IGKV3-20</i>	-9.64	0.01
<i>KRT16P5</i>	8.81	0.08	<i>SELE</i>	-9.58	0.00
<i>RPSAP52</i>	8.71	0.00	<i>AC011511.5</i>	-9.56	0.00
<i>AL590644.1</i>	8.71	0.00	<i>IGHA1</i>	-9.47	0.00
<i>LINC02582</i>	8.64	0.09	<i>CXCL9</i>	-9.44	0.00
<i>KLK5</i>	8.62	0.00	<i>AC022217.2</i>	-9.33	0.00
<i>TMPRSS11F</i>	8.61	0.00	<i>IGLV6-57</i>	-9.30	0.04
<i>KRT6C</i>	8.56	0.00	<i>IGLC2</i>	-9.30	0.00
<i>S100A14</i>	8.51	0.00	<i>ARC</i>	-9.26	0.00
<i>CPA4</i>	8.51	0.00	<i>MRO</i>	-9.17	0.00
<i>TMPRSS11BNL</i>	8.44	0.00	<i>IGHV1-18</i>	-9.10	0.07
<i>PNLIPRP3</i>	8.37	0.00	<i>IGLC3</i>	-9.08	0.00
<i>ADGRF1</i>	8.31	0.00	<i>FAM69C</i>	-9.02	0.00
<i>KRT24</i>	8.29	0.10	<i>HBA2</i>	-8.97	0.08
<i>HMGA2</i>	8.28	0.00	<i>IGHV3-21</i>	-8.88	0.08
<i>SPRR2A</i>	8.04	0.00	<i>CCL19</i>	-8.85	0.07
<i>SLURP1</i>	7.94	0.01	<i>IGHD</i>	-8.80	0.08
<i>AC078923.1</i>	7.92	0.00	<i>ASPN</i>	-8.78	0.00
<i>SERPINB13</i>	7.89	0.00	<i>VWC2L</i>	-8.75	0.00
<i>UPK1B</i>	7.89	0.00	<i>CD300LB</i>	-8.73	0.00
<i>ADGRF4</i>	7.86	0.00	<i>CPA3</i>	-8.72	0.02
<i>KLK10</i>	7.82	0.00	<i>OR2B11</i>	-8.67	0.00
<i>ANXA8L1</i>	7.69	0.00	<i>IGHV1-2</i>	-8.65	0.09
<i>FAM83A-AS1</i>	7.68	0.00	<i>OR51A8P</i>	-8.65	0.09
<i>AL049555.1</i>	7.68	0.00	<i>CCR4</i>	-8.63	0.09
<i>SCEL</i>	7.66	0.00	<i>IGLV3-1</i>	-8.63	0.09
<i>SERPINB7</i>	7.65	0.00	<i>IGLV2-14</i>	-8.62	0.08

<i>B3GNT3</i>	7.65	0.00
<i>SERPINB4</i>	7.61	0.00
<i>FETUB</i>	7.50	0.00
<i>PCSK9</i>	7.48	0.00
<i>SERPINB3</i>	7.46	0.00
<i>GPX2</i>	7.43	0.00
<i>C2orf54</i>	7.37	0.00
<i>SLCO1B3</i>	7.30	0.00
<i>LINC02178</i>	7.24	0.00
<i>WNT7A</i>	7.14	0.00
<i>MIR205</i>	7.09	0.00
<i>GJB3</i>	7.08	0.00
<i>ALDH3A1</i>	7.05	0.00
<i>MUC21</i>	7.03	0.00
<i>TMEM45B</i>	7.01	0.00
<i>SFN</i>	6.98	0.00
<i>AL365356.3</i>	6.91	0.11
<i>MIR205HG</i>	6.88	0.00
<i>GPR78</i>	6.88	0.00
<i>AL138789.1</i>	6.87	0.00
<i>MUC6</i>	6.85	0.00
<i>KRT16P1</i>	6.83	0.03
<i>AC005256.1</i>	6.82	0.00
<i>DQX1</i>	6.77	0.00
<i>AC004990.1</i>	6.76	0.00
<i>AC068633.1</i>	6.75	0.01
<i>CBLC</i>	6.74	0.00
<i>CEACAM6</i>	6.72	0.00
<i>LINC00887</i>	6.68	0.00
<i>GJB5</i>	6.67	0.00
<i>ABCB11</i>	6.67	0.01
<i>AC093904.3</i>	6.66	0.10
<i>MUCL1</i>	6.66	0.04
<i>AC005392.2</i>	6.63	0.04
<i>OTOP3</i>	6.63	0.02
<i>DUSP9</i>	6.63	0.01
<i>SDC1</i>	6.60	0.00
<i>FER1L6</i>	6.60	0.00
<i>FERMT1</i>	6.58	0.00
<i>AL121761.2</i>	6.55	0.00
<i>AC007207.2</i>	6.54	0.02
<i>GRHL3</i>	6.54	0.00
<i>FAM83C</i>	6.50	0.00
<i>CRYBG2</i>	6.50	0.00
<i>KRT31</i>	6.49	0.08
<i>AL356867.1</i>	6.44	0.00
<i>CHRNA9</i>	6.43	0.00

<i>IGKV3-15</i>	-8.56	0.00
<i>IGHG3</i>	-8.51	0.01
<i>LCN10</i>	-8.49	0.10
<i>ART4</i>	-8.45	0.00
<i>IFNG</i>	-8.42	0.00
<i>IGHV3-15</i>	-8.41	0.00
<i>OR2W5</i>	-8.39	0.04
<i>TULP2</i>	-8.35	0.00
<i>CYP4F24P</i>	-8.33	0.10
<i>RPL7P19</i>	-8.30	0.00
<i>IGKV1-16</i>	-8.29	0.03
<i>IGLV3-10</i>	-8.26	0.02
<i>AL133163.1</i>	-8.25	0.00
<i>AC010976.2</i>	-8.25	0.00
<i>RAMP3</i>	-8.25	0.02
<i>GCSAML</i>	-8.22	0.02
<i>CLEC4F</i>	-8.22	0.00
<i>FCER1A</i>	-8.21	0.00
<i>MYH6</i>	-8.20	0.00
<i>IRF4</i>	-8.18	0.00
<i>HSPA6</i>	-8.18	0.00
<i>IGLV2-23</i>	-8.17	0.00
<i>IGHV3-33</i>	-8.16	0.00
<i>EGR2</i>	-8.11	0.00
<i>CLEC3B</i>	-8.09	0.00
<i>CCKBR</i>	-8.09	0.00
<i>IGKC</i>	-8.06	0.02
<i>AC020728.1</i>	-8.05	0.00
<i>IGLV3-19</i>	-8.00	0.00
<i>AP003354.2</i>	-8.00	0.00
<i>AC004687.1</i>	-7.90	0.00
<i>KIAA1210</i>	-7.89	0.00
<i>SCN1A</i>	-7.84	0.03
<i>GUCA1C</i>	-7.82	0.00
<i>TRAT1</i>	-7.81	0.00
<i>IGLV2-8</i>	-7.81	0.00
<i>LCN6</i>	-7.80	0.00
<i>PLA2G5</i>	-7.78	0.05
<i>ATP1A2</i>	-7.77	0.00
<i>WNT11</i>	-7.75	0.00
<i>PLD4</i>	-7.73	0.00
<i>IGLV1-40</i>	-7.71	0.00
<i>BTNL9</i>	-7.66	0.00
<i>AP001107.5</i>	-7.64	0.00
<i>CD1C</i>	-7.62	0.00
<i>SCN4A</i>	-7.61	0.00
<i>MS4A14</i>	-7.61	0.00

<i>COL17A1</i>	6.41	0.00
<i>LAD1</i>	6.40	0.00
<i>NDP</i>	6.38	0.00
<i>LINC00973</i>	6.36	0.00
<i>CLCA3P</i>	6.36	0.00
<i>ANXA8</i>	6.35	0.00
<i>GSDMC</i>	6.34	0.00
<i>KRT34</i>	6.33	0.00
<i>DUOXA2</i>	6.33	0.00
<i>RPL10P13</i>	6.30	0.00

<i>IGHV1-3</i>	-7.60	0.00
<i>HRH3</i>	-7.59	0.00
<i>XCL2</i>	-7.58	0.00
<i>CXCR3</i>	-7.57	0.00
<i>TBX21</i>	-7.55	0.00
<i>COX6A2</i>	-7.55	0.05
<i>MS4A2</i>	-7.55	0.00
<i>CD207</i>	-7.54	0.00
<i>GPR17</i>	-7.53	0.00
<i>GPR183</i>	-7.53	0.00

Table S4. Differentially expressed genes in HPA-27-derived organoids at P2 versus P0 (top 100 up- and downregulated genes)

UP		DOWN	
Gene ID	logFC	Gene ID	logFC
<i>AL662797.1</i>	inf	<i>SPINK7</i>	inf
<i>AC006064.4</i>	inf	<i>MAL</i>	inf
<i>AC125611.3</i>	inf	<i>TGM3</i>	-10.20
<i>RPL3P4</i>	inf	<i>CRNN</i>	-8.41
<i>AC026403.1</i>	inf	<i>VGF</i>	-8.33
<i>AC011603.2</i>	9.53	<i>CRCT1</i>	-7.70
<i>AP002990.1</i>	7.06	<i>EGLN3</i>	-6.90
<i>PIGR</i>	4.76	<i>HOPX</i>	-6.26
<i>C3</i>	4.31	<i>CAPN14</i>	-5.96
<i>MUC5AC</i>	4.23	<i>LGALS7B</i>	-5.93
<i>SAA1</i>	4.10	<i>ECM1</i>	-5.43
<i>CFB</i>	3.96	<i>SPRR3</i>	-5.40
<i>BPIFB1</i>	3.59	<i>KRT16</i>	-5.25
<i>BPIFA1</i>	3.58	<i>KRT16P6</i>	-4.92
<i>LCN2</i>	3.52	<i>SPINK5</i>	-4.86
<i>SLC12A2</i>	3.34	<i>NDRG1</i>	-4.77
<i>CXCL8</i>	2.79	<i>RHCG</i>	-4.60
<i>CCNB1</i>	2.69	<i>KLK12</i>	-4.59
<i>RRM2</i>	2.65	<i>S100P</i>	-4.50
<i>PXDN</i>	2.62	<i>SPRR1A</i>	-4.46
<i>MUC16</i>	2.57	<i>UPK3BL1</i>	-4.45
<i>PTGES</i>	2.50	<i>TGM1</i>	-4.25
<i>HSPH1</i>	2.47	<i>A2ML1</i>	-4.08
<i>ANLN</i>	2.42	<i>CEACAM5</i>	-3.87
<i>WFDC2</i>	2.42	<i>PI3</i>	-3.84
<i>CXCL1</i>	2.37	<i>IL1RN</i>	-3.75
<i>VMO1</i>	2.32	<i>ALOX15B</i>	-3.74
<i>TUBB3</i>	2.31	<i>CLCA4</i>	-3.71
<i>THBS1</i>	2.23	<i>KLK13</i>	-3.67
<i>TOMM40</i>	2.20	<i>IFITM1</i>	-3.40
<i>MKI67</i>	2.18	<i>CEACAM1</i>	-3.38
<i>DHX9</i>	2.17	<i>TMPRSS11D</i>	-3.36
<i>EMC10</i>	2.16	<i>CLIC3</i>	-3.35
<i>SLC4A2</i>	2.15	<i>ADAMTSL4</i>	-3.29
<i>HNRNPM</i>	2.13	<i>PADI1</i>	-3.29
<i>SRSF1</i>	2.12	<i>SDCBP2</i>	-3.26
<i>PRSS23</i>	2.11	<i>GABRE</i>	-3.25
<i>HMG2</i>	2.07	<i>CSTA</i>	-3.20
<i>CDC20</i>	2.06	<i>RHOF</i>	-3.12
<i>TUBA1B</i>	2.02	<i>JMJD7-PLA2G4B</i>	-3.03
<i>DNMT1</i>	2.02	<i>CD68</i>	-2.98
<i>EPCAM</i>	2.02	<i>MALL</i>	-2.97
<i>CYCS</i>	2.01	<i>AQP5</i>	-2.96

<i>KPNA2</i>	2.00
<i>NOP56</i>	1.98
<i>MCM4</i>	1.96
<i>DNAJC10</i>	1.94
<i>HMGCS1</i>	1.92
<i>GOLM1</i>	1.91
<i>SLC44A4</i>	1.90
<i>CCT2</i>	1.87
<i>ACAT2</i>	1.86
<i>NOL6</i>	1.86
<i>ELOVL6</i>	1.85
<i>HSP90AA1</i>	1.85
<i>MCM7</i>	1.83
<i>PARP1</i>	1.81
<i>SRSF3</i>	1.78
<i>UBE2S</i>	1.77
<i>OAT</i>	1.76
<i>SLC20A1</i>	1.71
<i>TUBB</i>	1.71
<i>FST</i>	1.70
<i>DHX30</i>	1.69
<i>LMNB2</i>	1.65
<i>TOP2A</i>	1.65
<i>TXNRD1</i>	1.65
<i>HNRNPAB</i>	1.63
<i>PHB</i>	1.61
<i>MLEC</i>	1.61
<i>CTSC</i>	1.60
<i>CCT5</i>	1.60
<i>NCL</i>	1.60
<i>CCT3</i>	1.59
<i>CSE1L</i>	1.59
<i>GDF15</i>	1.58
<i>TFDP1</i>	1.58
<i>HSPA8</i>	1.57
<i>PRMT1</i>	1.56
<i>HSPD1</i>	1.56
<i>XBP1</i>	1.56
<i>EI24</i>	1.56
<i>TM7SF3</i>	1.55
<i>BCLAF1</i>	1.55
<i>PSME3</i>	1.53
<i>ABCE1</i>	1.50
<i>TCOF1</i>	1.50
<i>RPS6KA4</i>	1.49
<i>AGR2</i>	1.49
<i>PSME4</i>	1.48

<i>SLC6A8</i>	-2.92
<i>SLC5A3</i>	-2.90
<i>LYPD3</i>	-2.86
<i>GLTP</i>	-2.83
<i>CES2</i>	-2.82
<i>P4HA1</i>	-2.74
<i>IL33</i>	-2.72
<i>MXD1</i>	-2.71
<i>PLEKHG5</i>	-2.69
<i>SULT2B1</i>	-2.67
<i>TMEM184A</i>	-2.65
<i>SPRR1B</i>	-2.64
<i>KRT6B</i>	-2.63
<i>WSB1</i>	-2.60
<i>SERPINE1</i>	-2.59
<i>ALS2CL</i>	-2.58
<i>DUOXA1</i>	-2.56
<i>ZNF750</i>	-2.54
<i>PEG10</i>	-2.53
<i>SLC37A2</i>	-2.50
<i>DUSP5</i>	-2.47
<i>PPL</i>	-2.47
<i>EPS8L1</i>	-2.42
<i>TMEM40</i>	-2.41
<i>CSTB</i>	-2.41
<i>LY6D</i>	-2.38
<i>TXNIP</i>	-2.36
<i>THBD</i>	-2.35
<i>S100A14</i>	-2.35
<i>JUNB</i>	-2.35
<i>NCCRP1</i>	-2.34
<i>CD55</i>	-2.31
<i>GRHL3</i>	-2.26
<i>BHLHE40</i>	-2.26
<i>KRT4</i>	-2.26
<i>MAPK3</i>	-2.25
<i>SCEL</i>	-2.25
<i>RASSF5</i>	-2.23
<i>PRSS3</i>	-2.22
<i>NT5E</i>	-2.21
<i>TIMP1</i>	-2.13
<i>TMEM45B</i>	-2.13
<i>TRIP10</i>	-2.12
<i>ALDH3B2</i>	-2.12
<i>PTK6</i>	-2.11
<i>KLK11</i>	-2.10
<i>SNX33</i>	-2.09

<i>FUS</i>	1.47
<i>C1QBP</i>	1.46
<i>ASCC3</i>	1.46
<i>CCT6A</i>	1.46
<i>ILF2</i>	1.45
<i>RANBP1</i>	1.45
<i>TGFBR2</i>	1.45
<i>CCND1</i>	1.45
<i>DNAJA1</i>	1.44
<i>TCP1</i>	1.44

<i>POLR2J3</i>	-2.09
<i>EGR1</i>	-2.08
<i>ADIRF</i>	-2.07
<i>VEGFA</i>	-2.06
<i>IL20RB</i>	-2.03
<i>DSG3</i>	-2.03
<i>ZNF185</i>	-2.03
<i>DSP</i>	-2.01
<i>ANO9</i>	-2.00
<i>EVPL</i>	-2.00

Table S5. Overview of primary and secondary antibodies used for immunostaining analyses

Primary antibodies				
Antigen	Host	Catalogue#	Company	Dilution
CD44	Mouse	MA5-15462	Thermo Fisher Scientific	1:1,000
CHGA	Mouse	MA5-13093	Thermo Fisher Scientific	1:800
CYP2F2	Mouse	SC-374470	Santa Cruz Biotechnology	1:100
KRT8/18	Guinea-pig	GP11	Progen	1:500
E-CAD	Rabbit	24E10	Cell Signaling Technology	1:400
Ki67	Mouse	RM-9106-S	Thermo Fisher Scientific	1:50
LH β	Guinea-pig		Dr. A.F Parlow, NHPP, Harbor-UCLA Medical Center, Torrance, CA	1:10,000
PRL	Rabbit		Dr. A.F Parlow, NHPP, Harbor-UCLA Medical Center, Torrance, CA	1:10,000
S100A6	Rabbit	10245-1-AP	Proteintech	1:100
SOX2	Goat	GT15098	Immune systems	1:750
SOX2	Rabbit	AB92494	Abcam	1:2,000
SOX9	Goat	AF3075	R&D systems	1:500
S100 β	Mouse	S2532	Sigma-Aldrich	1:1,000
SYP	Mouse	IR660	Dako	Ready-to-use
TACSTD2	Goat	AF1122	R&D systems	1:50

Secondary antibodies				
Antigen (fluorophore)	Host	Catalogue#	Company	Dilution
Goat IgG (Alexa 555)	Donkey	A-21432	Thermo Fisher Scientific	1:1,000
Rabbit IgG (Alexa 488)	Donkey	A-21206	Thermo Fisher Scientific	1:1,000
Rabbit IgG (Alexa 555)	Donkey	A-31572	Thermo Fisher Scientific	1:1,000
Mouse IgG (Alexa 488)	Donkey	A-21202	Thermo Fisher Scientific	1:1,000
Mouse IgG (Alexa 555)	Donkey	A-31570	Thermo Fisher Scientific	1:1,000
Guinea pig IgG (FITC)	Donkey	706-545-148	Jackson Immuno Research	1:1,000

Table S6. Overview of primer sequences used for RT-qPCR

Mouse		
Target	Primer forward (5' -> 3')	Primer backward (5' -> 3')
<i>Actb</i>	GCTGAGAGGGAAATCGTGCGTG	CCAGGGAGGAAGAGGATGCGG
<i>Ccr2</i>	ACAGCTCAGGATTAACAGGGACTTG	ACCACTTGCATGCACACATGAC
<i>Cxcr3</i>	CTGCTGCCAGTGGGTTT	GTTGATGTTGAACAGGGCACC
<i>Cxcr6</i>	GGTTCTTCTGCCATTGCTCAC	GCAGGAACACAGCCACTACAAG
<i>Cyp2f2</i>	AGGAGGCTCTTGTTGGACAAAGG	CCGAGGATTTGGACAGAGAA
<i>Ifng</i>	GCCACGGCACAGTCATTG	TGCTGATGGCCTGATTGTCTT
<i>Ikbkg</i>	TCTTCGGAGTCAGAGGGAACAG	TCCTGGAGTTCTCCGAGCAATG
<i>Il1b</i>	TGGACCTTCCAGGATGAGGACA	GTTTCATCTCGGAGCCTGTAGTG
<i>Il6</i>	TCTGCAAGAGACTTCCATCC	CGACTTGTGAAGTGGTATAGAC
<i>Il8</i>	CAAGGCTGGTCCATGCTCC	TGCTATCACTTCTTTCTGTTC
<i>Jak2</i>	AGAAAGGGCGGAATAAGGGC	CTGCTCCAACCTCACGAATCCT
<i>Relb</i>	GTTCTTGACCCTTCCATGCTCC	TAGGCAAAGCCATCGTCCAGGA
<i>Relc</i>	GAAGACTGCGACCTCAATGTGG	TCTTGTTCACACGGCAGATCCTT
<i>S100a6</i>	GCAAGGAAGGTGACAAGCACAC	CCTGATCCTTGTACGGTCCAG
<i>Sox2</i>	AAAGTATCAGGAGTTGTCAAGG	CTCTTCTTTCTCCAGCCC
<i>Sox9</i>	CGGAACAGACTCACATCTCTCC	GCTTGACGTCGGTTTTGG
<i>Stat1</i>	GCTGCCTATGATGTCTCGTTT	TGCTTTCCGTATGTTGTGCT
<i>Stat3</i>	CACCTTGGATTGAGAGTCAAGAC	AGGAATCGGCTATATTGCTGGT
<i>Stat4</i>	TCAGTGAGAGCCATCTTGAGG	TGTAGTCTCGCAGGATGTCAGC
<i>Tacstd2</i>	GTCTGCCAATGTCGGGCAA	GTTGTCCAGTATCGCGTGCT

Human		
Target	Primer forward (5' -> 3')	Primer backward (5' -> 3')
<i>CXCL11</i>	AAGGACAACGATGCCTAAATCCC	CAGATGCCCTTTCCAGGACTTC
<i>CD44</i>	CCAGAAGGAACAGTGGTTTGCC	ACTGTCTCTGGGCTTGGTGTT
<i>GAPDH</i>	GGTATCGTGGAAGGACTCATGAC	ATGCCAGTGAGCTTCCCGTTCCAG
<i>IL1B</i>	CCACAGACCTTCCAGGAGAATG	GTGCAGTTCAGTGATCGTACAGG
<i>IL6</i>	GGCACTGGCAGAAAACAACC	GCAAGTCTCCTCATTGAATCC
<i>IL8</i>	ATGACTTCCAAGCTGGCCGT	TCCTTGGCAAACTGCACCT
<i>KRT8</i>	ACAAGGTAGAGCTGGAGTCTCG	AGCACACAGATGTGTCCGAGA
<i>KRT18</i>	AAAGGCCTACAAGCCAGAT	CACTGTGGTCTCTCCTCAA
<i>P16</i>	GAGCAGCATGGAGCCTTC	CCTCCGACCGTAACATTCG
<i>P21</i>	AAGACCATGTGGACCTGTCA	GGCTTCTCTTGGAGAAGAT
<i>SOX2</i>	GCTACAGCATGATGCAGGACCA	TCTGCGAGCTGGTCATGGAGTT
<i>SOX9</i>	GAGCTGAGCAGCGACGTCATCT	GGCGGCGCCTGCTGCTGGACA
<i>TACTSD2</i>	CGGCAGAACACGTCTCAGAAG	CCTTGATGTCCCTCTCGAAGTAG

ADDENDUM: Orthotopic *in vivo* transplantation into the mouse pituitary gland

1. INTRODUCTION

Several candidate TSC populations have been proposed to exist in human pituitary tumors (Nys and Vankelecom, 2021). However, conclusive proof, i.e. *in vivo* tumorigenic capacity after xenografting with regrowth of the original tumor composition (Clevers, 2011), is still lacking. When transplanted under the skin or the kidney capsule of immunodeficient mice, human pituitary tumor fragments or dissociated cells did not generate a developing and growing tumor (Mertens et al., 2015; Würth et al., 2017). Human pituitary tumors may be too benign and too low in proliferative activity to result in *in vivo* tumor growth. Alternatively, they may need a more natural (micro-)environment to grow out. Following transplantation into the neighboring brain region, it was reported that human pituitary tumors (re-)grew (Manoranjan et al., 2016; Xu et al., 2009). However, real expansion and proliferation was not shown, and tumors/cells may merely have survived. Moreover, only very few tumors were assessed (one or two per study), and serial regrowth was not analysed, being another important hallmark of TSCs (Clevers, 2011). In addition, some tumor characteristics (such as cytokeratin expression) disappeared in the graft (Manoranjan et al., 2016).

Hence, real orthotopic transplantation into the pituitary gland may be needed to evaluate the tumorigenic capacity of candidate TSCs. So far, stereotactic injections into animals' pituitaries have mainly been performed to deliver viral vectors for exploring gene therapy. For instance, viral vectors harboring a β -galactosidase reporter gene were successfully injected directly into rat and ovine pituitary gland resulting in high expression of β -galactosidase around the site of injection (Bolognani et al., 2001; Davis et al., 2001; Lee et al., 2000). Later, focal delivery of fluorescent dextran and subsequent *in vivo* imaging was described in the mouse pituitary to monitor GH output (Lafont et al., 2010). This technique was recently further finetuned for imaging and manipulation of the pituitary gland in awake mice (i.e. injection of viral vectors to render somatotropes sensitive to laser-light pulses (i.e. optogenetics) for releasing GH) to study the relationship between hypothalamic signals and pituitary hormonal output (Hoa et al., 2019). However, coordinates of the viral vector injection were only poorly described, and success rate was not mentioned. Therefore, we here set out to design a defined and reproducible method to orthotopically graft pituitary (stem) cells directly into the pituitary gland.

2. MATERIAL AND METHODS

Mice

Animal experiments were approved by the KU Leuven Ethical Committee for Animal Experimentation (P218/2013, P153/2018). Mice were bred and housed in the KU Leuven animal facility under standard conditions (constant temperature of 23 ± 1.5 °C, relative humidity 40-60 % and day/night cycle of 12/12 h), with water and food *ad libitum*.

The R26^{mT/mG} reporter mouse expresses, in the absence of Cre-mediated recombination, cell membrane-localized fluorescent tdTomato (tdT) in all cells (Muzumdar et al., 2007).

Immunodeficient NOD-SCID mice were provided by Prof. C. Mathieu and Jos Laureys (Department of Chronic Diseases, Metabolism and Ageing, Clinical and Experimental Endocrinology, KU Leuven).

Organoid development and passaging

The AL was isolated from R26^{mT/mG} mice and enzymatically and mechanically dissociated into single cells. Cells were embedded in a Matrigel drop (25,000 cells/well) and cultured in optimized medium (OptM; Table S2) to develop into organoids. For passaging, organoids were dissociated by a combination of enzymatic and mechanical dissociation, and small organoid fragments were again reseeded. Experiments were performed with organoids of P2-P6.

In vivo transplantation

To stereotactically inject trypan blue (0.04 %; Sigma-Aldrich) or graft a mixture of organoid fragments and dissociated cells in the pituitary gland, acceptor NOD-SCID mice were anaesthetized by intraperitoneal injection of a mixture of ketamine (100 mg/kg) and xylazine (10 mg/kg). Then, the mouse's eyes were protected with an ocular lubricant (Duratears), and xylocaine gel (2 %) was applied on the upper side of the head for 10 min. Subsequently, the mice were placed in a stereotactic apparatus and the head was fixed. The skin on top of the cranium was opened up with a sterile blade and the stereotactic needle positioned at the starting point (Lambda) to mark the sites for injection by setting the coordinates. Two small burr holes were carefully made with a drill head of 0.7 mm at the locations where the needle had to enter (Hamilton syringe (HAMICAL80430) with a long (51 mm) small (0.11 mm) needle (HAMI7762-05; type 3 Gauge 33)). Finally, each mouse was injected with a volume of 2-6 μ L suspension at both left and right side of the midline with the following coordinates: +0.1 anteroposterior and +0.5 lateral, and +0.3 anteroposterior and -0.6 lateral, starting from Lambda. Depth of injection was \sim -6.0 mm, exactly determined for each mouse individually by inserting the needle till the base of the skull (indicated by a little bending) and then retracting the needle for 0.3 mm upwards. Mice received analgesia at 12 h and 24 h after surgery *via* sc injection of buprenorphine (0.05-0.1 mg/kg). The mice were euthanized using CO₂ asphyxiation immediately, 12h or 4 weeks after surgery as specified.

3. RESULTS

To graft directly into the pituitary gland, we first optimized the transcranial stereotactic protocol. Once the head of the mouse was fixed in a stereotactic apparatus (Fig. 1A), the needle was positioned at the starting point and the coordinates were set. Several coordinates were tested by injecting mice with trypan blue until both injection imprints were found localized in the pituitary gland in the post-surgery euthanized mouse (Fig. 1B).

Next, we developed fluorescently (tdT⁺) labeled pituitary organoids from the AL of R26^{mT/mG} mice and expanded the organoids extensively (Fig. 1C). A mixture of organoid fragments and single cells was transplanted. Four weeks after their stereotactic injection, tdT⁺ grafts could not be detected (anymore) (Fig. 1D), despite the presence of clear intra-pituitary needle entry points (Fig. 1E). These findings suggest that the transplanted organoid structures and cells did not survive, at least not for 4 weeks. To test whether organoid fragments were highly and irreversibly damaged because of the shear stress in the small needle, we reseeded organoid fragments *in vitro* after passing them through the needle. Organoids were found to regrow (Fig. 1F), indicating that they were not fatally damaged but may lack essential growth/survival factors immediately after their transplantation. Therefore, we transplanted organoid fragments and cells in the presence of 50 % Matrigel and EGF (250 ng/mL). Twelve hours after transplantation, tdT⁺ grafts could be detected at the injection sites of the pituitary (Fig. 1G).

4. CONCLUSION AND PERSPECTIVES

Taken together, we designed a method to stereotactically graft organoid fragments and cells into the living mouse pituitary. Further evaluation is still needed, such as survival and behavior of the organoid fragments and cells injected in Matrigel and EGF after longer time periods (from 3 days to 4 weeks). If long-term survival is achieved, tumor-derived organoid fragments and single cells can be transplanted to investigate whether they represent authentic TSCs and are able to regrow the tumor. In addition to applying human pituitary tumor organoid fragments/cells, organoids can also be established from SOX2^{eGFP/+};Drd2^{-/-} and SOX2^{eGFP/+};Drd2^{+/+} pituitary. Finally, the designed protocol will not only allow to evaluate the tumorigenic capacity of pituitary tumor TCS candidates, but also to explore the restorative and regenerative capacity of (normal) pituitary stem cells to repair local tissue upon injury, and hence restore (physiological) hormone production.

Fig. 1

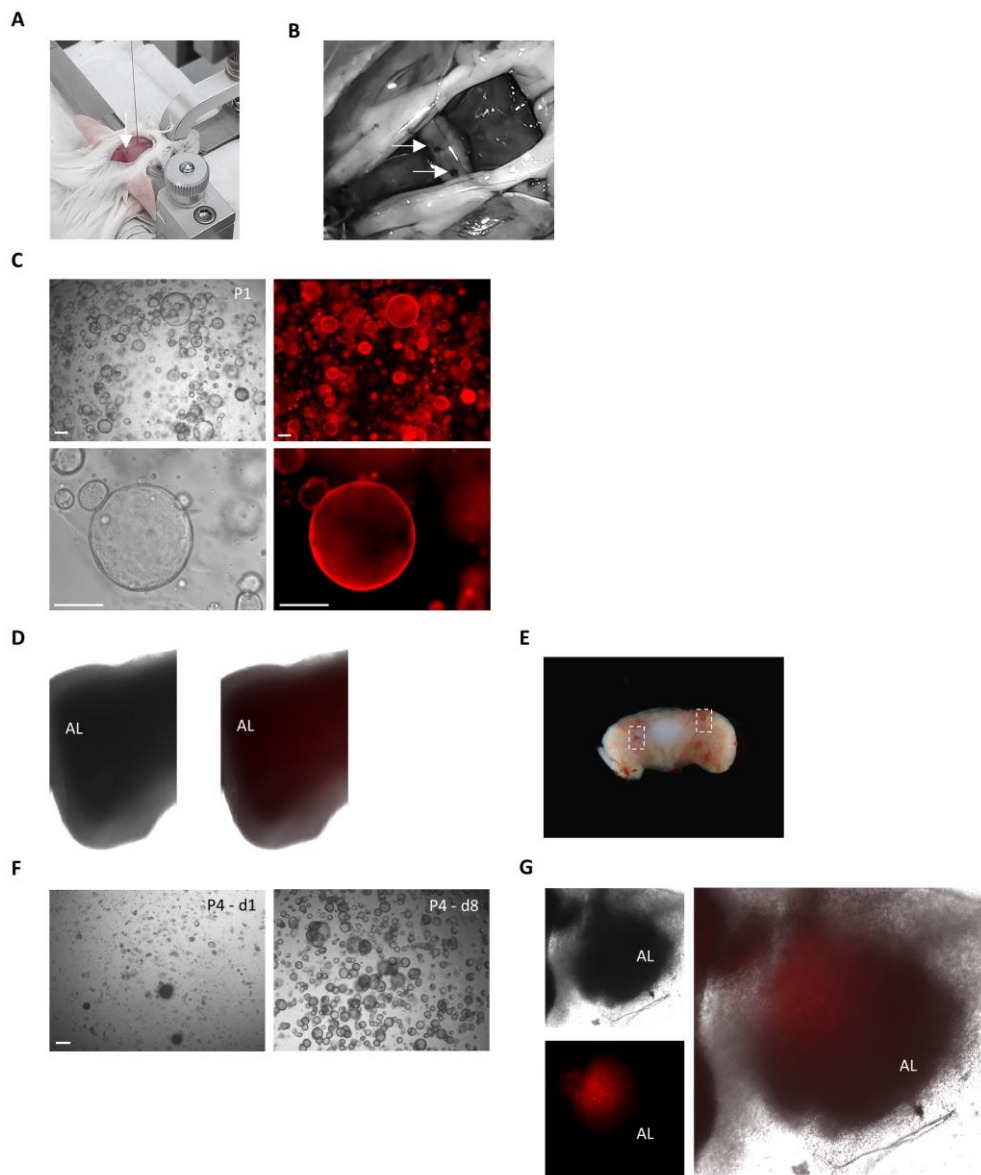


Fig. 1. Designing a method for *in vivo* orthotopic transplantation in mouse pituitary

A Mouse head fixed in a stereotactic apparatus. The arrow indicates the starting point (Lambda) to set the coordinates. **B** Microscopic picture of mouse pituitary stereotactically injected at two spots with trypan blue, to determine the coordinates for the protocol. Arrows show the injection sites. **C** Organoid growth from R26^{mT/mG} reporter mouse pituitary (shown at P1). Representative brightfield and epifluorescence (tdT) pictures are presented. Scale bar: 200 μ m. **D** Brightfield (*left*) and epifluorescence (tdT, *right*) pictures of a part of the isolated pituitary 4 weeks after transplantation. **E** Microscopic picture of the isolated pituitary 4 weeks after tdT⁺ organoid fragment transplantation. Dotted boxes mark the injection sites. **F** Organoid regrowth after passing the organoid fragments through the 0.11 mm Hamilton needle. Scale bar: 200 μ m. **G** Brightfield and epifluorescence (tdT) pictures, and their overlay, of a part of the isolated pituitary 12 h after transplantation of tdT⁺ organoid fragments.

The science of today is the technology of tomorrow – Edward Teller

CHAPTER 5: GENERAL DISCUSSION AND FUTURE PERSPECTIVES

CHAPTER 5: GENERAL DISCUSSION AND FUTURE PERSPECTIVES

5.1 General discussion

Pituitary tumors are present in a considerable number of people and the prevalence is still increasing, likely due to progressing ageing of the population, more awareness and improved diagnostics (Daly and Beckers, 2020). Overall, surgical resection is the standard treatment, apart from certain types such as prolactinomas, which are in first line treated with dopamine-agonist like cabergoline and bromocriptine, and somatotropinomas, which can be treated with somatostatin analogues such as octreotide and lanreotide (Melmed, 2020).

In our study, we first assessed safety and effectiveness of transnasal transsphenoidal pituitary surgery (Chapter 3) and then investigated pituitary tumors in more detail (Chapter 4) to better understand their pathogenesis, and more in particular, to decode the phenotype and behavior of stem cells in pituitary tumorigenesis.

5.1.1 Pituitary tumor surgery

Over the last decades, pituitary tumor surgery has substantially evolved. In the very beginning, pituitary tumors were resected *via* an invasive transcranial approach. In 1907, Hermann Schloffer performed the first transnasal transsphenoidal surgery circumventing the need for craniotomy and thus lowering infection risks. The transsphenoidal approach was further modified by Harvey Cushing, who performed his first transsphenoidal surgery in 1909, in a patient with acromegaly (Schmidt et al., 2012). This ground-breaking achievement laid the foundation for further refinement of the transsphenoidal approach, which became the mainstay treatment for pituitary tumors with the introduction of the operation microscope by Jules Hardy in the 1960s (Hardy, 1969; Schmidt et al., 2012). In the 1990s, the microsurgical procedure was progressively replaced by an endoscopic procedure to minimize surgical invasiveness, which is now standard procedure for pituitary surgery (Cappabianca et al., 1999). The endoscopic transnasal procedure has shown beneficial resulting in shorter duration time of the surgery, reduced postsurgical hospitalisation and overall less postoperative hypopituitarism (Cappabianca et al., 1999; Moller et al., 2020).

In the first part of our study, we retrospectively analysed presentation, outcome and complications of pituitary tumor patients undergoing endoscopic transsphenoidal surgery in a single peripheral clinical centre. Almost all patients presented with symptoms, consisting of hormonal abnormalities, visual disturbances, cranial nerve deficits or apoplexy (with headache). Surgical resection of the tumor at least partially restored visual and cranial nerve deficits in almost all patients. Similarly, serum hormone normalisation was obtained for almost all secreting-adenoma patients. In contrast, preoperative hypopituitarism was only restored in one out of seven patients. Restoration of hypopituitarism is generally rather rare, even after successful surgery (Berg et al., 2010; Buttan and Mamelak, 2019; Jahangiri et al., 2016). In our retrospective analysis, the majority of the patients regained partial to normal vision. It has been shown that time between onset of symptoms and surgery is determinative for restoration of visual deficits. Shorter time of visual symptoms (< 1 year) is associated with better visual restoration outcome (Thotakura et al., 2017). In our analysis, not many surgical complications were observed postoperatively. Among others, CSF-leakage was present in < 3 % of the patients and only one patient

developed meningitis, that, once treated, resolved in rapid and complete recovery, all together showing the safety of the pituitary tumor operation procedure.

In conclusion, transsphenoidal surgery was assessed effective and safe. Nonetheless, many of the patients suffered from hypopituitarism, with half of them developing this deficiency postoperatively, thus requiring lifelong hormone substitution. Therefore, clinical management can still significantly benefit from further improvements. To work toward this goal, a much better understanding of the mechanisms underlying pituitary tumorigenesis is needed which we investigated in our study.

5.1.2 Stem cells in pituitary tumors

In general, tumors are characterized by a heterogeneous composition, harboring distinct cell types (Dagogo-Jack and Shaw, 2018). In addition to the bulk of cells, tumors also appear to contain a small population of TSCs that can initiate and grow the tumor and are therapy-resistant, thereby regrowing the tumor after treatment (Clevers, 2011). TSCs have been identified in multiple types of cancers, such as colon (O'Brien et al., 2007), breast (Ponti et al., 2005) and ovarian cancer (Zhang et al., 2008). Experimental approaches to identify and characterize TSCs have been based on expression of stemness surface markers (e.g. CD133, CD44), SP phenotype and/or ability to form 3D spheres/organoids *in vitro* (Andrés et al., 2020). The origin of TSCs is still debated and may be different among tumor types. TSCs may originate from the tissue's stem/progenitor cells following gene mutations allotting growth and survival benefits to the cells (as for instance observed in squamous cell carcinoma with SOX2⁺ stem cells (Boumadhi et al., 2014)), or from mutated mature cells that undergo de-differentiation and regain stemness characteristics (as for example described in mammary gland (Chaffer et al., 2011)).

Several studies have reported the presence of candidate TSCs in pituitary adenomas (Nys and Vankelecom, 2021), although conclusive evidence, such as *in vivo* tumorigenic capacity after xenografting, remains absent, thereby still questioning whether these cells represent authentic TSCs. The purported TSCs may as well represent tissue stem cells that became entrapped in the growing tumor. In our study, we identified cells expressing the principal pituitary stem cell markers SOX2 and SOX9 in a wide variety of human pituitary tumors. These cells were arranged in distinct topographical patterns, either spread throughout the tumor, housed in small clusters or organized in a follicular pattern, the latter also recently described in GH-secreting tumors (Soukup et al., 2020). Using the *Drd2*^{-/-} mouse model of pituitary tumorigenesis (Asa et al., 1999; Kelly et al., 1997), we here also found SOX2⁺ stem cells in the pituitary tumor region, besides their localization in the normal MZ stem cell niche. Interestingly, we observed an increase in SOX2⁺ stem cells in the tumorigenic pituitary, which was also a visible trend in human pituitary tumors. The tumors that develop in the *Drd2*^{-/-} pituitary do not originate from SOX2⁺ stem cells as supported by lineage tracing experiments (Vankelecom and Roose, 2017). Hence, the (expanded) SOX2⁺ stem cell population may rather be indirectly involved in the tumorigenic process. In support of this idea, SOX2⁺ pituitary stem cells were recently reported to act as a paracrine signaling hub providing proliferation-stimulatory signals to neighboring cells during early-postnatal gland development (Russell et al., 2021). Similarly, WNT/ β -catenin-mutated SOX2⁺ stem cells were found to fuel tumor growth in a paracrine

fashion in a mouse craniopharyngioma model (Gonzalez-Meljem et al., 2017). Along the same line, stem cell SOX2 expression was found to contribute to the transformation of neighboring melanotropes towards developing IL tumors as observed in *p27^{-/-}* mice (Moncho-Amor et al., 2021). SOX2⁺ stem cells did not directly form the IL tumors, but *Sox2* haploinsufficiency impaired tumor development (Moncho-Amor et al., 2021).

In tumorigenesis in various organs, SOX2 appears to be a major player in the development, maintenance and clinical phenotype of the tumors (Wuebben and Rizzino, 2017). For instance, an increase in SOX2⁺ cells was found to correlate with higher grades in prostate cancer (Kregel et al., 2013), ovarian cancer (Ye et al., 2011) and glioma (Schmitz et al., 2007). Also, SOX2, while absent in normal skin epidermis, becomes expressed during hyperplastic and tumorigenic events (Boumadhi et al., 2014). Conditional SOX2⁺ cell lineage ablation in the primary skin tumors resulted in complete regression of benign tumors and strong regression of invasive squamous cell carcinomas (Boumadhi et al., 2014). Moreover, SOX2⁺ cells isolated from primary tumors showed greater ability to form tumors upon xenografting than the remainder non-SOX2⁺ cells (e.g. from squamous cell carcinoma (Boumadhi et al., 2014) and medulloblastoma (Vanner et al., 2014)). The SOX2⁺ cells showed therapy resistance as they repopulated the medulloblastoma following drug withdrawal (Vanner et al., 2014). The SOX2 transcription factor directly interacts with multiple target genes involved in stemness but also tumor growth, progression and invasion (malignancy) as found in many tumor types (such as esophageal, ovarian and pancreatic cancer (Wuebben and Rizzino, 2017)). Mostly, involvement of SOX2 in tumorigenesis includes SOX2 gene amplification and/or overexpression (Wuebben and Rizzino, 2017). Elevated SOX2 levels were reported in esophageal and colorectal cancer and in glioblastoma, and were found to correlate with tumor progression and poor prognosis. SOX2 overexpression has not only been associated with resistance and recurrence, but also with infiltrative and metastatic capacity of tumors (such as in colorectal (Han et al., 2012) and prostate cancer (Jia et al., 2011)). In this regard, SOX2 has been linked to EMT driving migration, invasion and metastasis as for instance revealed by knocking-down SOX2 in colorectal tumor cells leading to less plasticity (Han et al., 2012).

Of note, caution must be taken when interpreting SOX2 levels. Changes may cause different outcomes according to tumor type. Although SOX2 overexpression has been reported in many tumors, sudden elevation has been shown to result in inhibition of tumor growth (e.g. in a pancreatic cancer cell line both *in vitro* and *in vivo* (Wuebben et al., 2016)), while low levels of SOX2 have been linked to poor prognosis in squamous cell lung (Wilbertz et al., 2011) and gastric cancer (Chen et al., 2016). In gastric cancer, SOX2 seems to operate as a tumor suppressor, in contrast to its function as oncogene in other tumor types (Carrasco-Garcia et al., 2016). Progressive reduction of SOX2 expression was observed from healthy gastric mucosa towards invasive gastric cancer cells (Otsubo et al., 2008; Wang et al., 2015).

The other SOX stem cell marker, SOX9, has also been linked to tumorigenesis in different tissues (e.g. breast and pancreatic cancer, hepatocellular carcinoma,) where it is often overexpressed and related to poor prognosis (Aguilar-Medina et al., 2019). Several oncogenic SOX2 functions (e.g. bypassing senescence) are (at least partially) regulated in crosstalk with SOX9, as for instance shown in glioblastoma (de la Rocha et al., 2014; Garros-Regulez et al., 2016). Intriguingly, we did not detect SOX9 expression in normal human pituitary tissue (which is comparable to another study (Shirian et al., 2021), but different from a previous report (Garcia-Lavandeira et al., 2009)), but observed SOX9⁺ stem cells in pituitary tumors which may suggest its induction during pituitary

tumorigenesis. However, since the number of healthy pituitary samples was low, definite conclusions await analysis of more samples, which are not straightforward to obtain.

Finally, we did not observe indications of a prognostic value of SOX2 and/or SOX9 expression in pituitary tumors, as invasive tumors did not contain more SOX2⁺/SOX9⁺ stem cells than non-invasive tumors, in agreement with another recent study (Soukup et al., 2020).

5.1.3 Stem cell activation in pituitary tumorigenesis

Previously, our group found indications of stem cell activation in the prolactinoma-bearing *Drd2*^{-/-} pituitary in the early stage of the tumorigenic process (10-14 months of age), including an enlarged SC-SP and more abundant SOX2⁺ stem cells (Mertens et al., 2015). In our study here, we analysed the pituitary at later stages when full-blown tumors are present (18-21 months old). The SOX2⁺ stem cell compartment remained activated, including higher cell number and proliferative activity, which was also a visible trend in human pituitary tumors when compared to healthy tissue. Similarly, higher stem cell proliferative activity was also supported in *p27*^{-/-} mice that develop IL tumors, shown by higher sphere-forming capacity from the IL (Moncho-Amor et al., 2021). Pituitary stem cell activation has also been observed upon transgenically inflicted injury in the gland, as start of the ensuing regenerative process (Fu et al., 2012; Willems et al., 2016). Together, stem cells seem to react and become proliferatively activated when damage, of different cause, occurs in their tissue. To further decipher the activated phenotype and search for signaling factors and pathways involved in this process, we explored the stem cell compartments' transcriptome. RNA-seq analysis revealed enrichment of cytokine/chemokine signaling pathways, and in particular, upregulated expression of *Il6*, *Il1b*, *Ifng* and *Cxcl2*. Interestingly, IL6 was recently identified as pituitary stem cell-activating factor being part of the stem cell activation reaction upon local damage (Vennekens et al., 2021). IL6 may thus also be involved in stem cell activation during tumorigenesis in the gland. In other tumor types, (tumor) stem cells have been shown to secrete interleukins and other cytokines for stemness maintenance (Andrés et al., 2020; Prager et al., 2019), and IL6 in particular has been demonstrated to activate TSCs in thyroid tumors (Zheng et al., 2019).

Regarding pituitary tumors, a number of studies have highlighted the involvement of cytokines and chemokines in the tumorigenic process. Among others, these factors contribute to the immune response, which may exert both pro- and anti-tumorigenic effects. Chemokines, released by tumor cells, can attract and modulate immune cells, regulate angiogenesis and steer tumor invasion. To date, not much is known on the immune landscape of pituitary tumors. Macrophages appear to be the most abundant in PitNETs (Marques et al., 2019b). A recent study reported that pituitary tumor-derived factors can induce macrophage migration and activation as examined using GH3 cells (Marques et al., 2019b). More precisely, tumor-derived factors initiated morphological changes in macrophages, resulting in activated and migrating cells. Interestingly, signaling was found to be bidirectional since macrophage-derived factors increased tumor invasiveness by inducing EMT and influenced the cytokine secretome (e.g. upregulated secretion of IL1 β), suggesting that tumor cells can hijack immune cells for their benefit (Marques et al., 2019b). The importance of cytokine (IL6) signaling is further shown by impaired GH3 tumor growth *in vivo* in immunodeficient mice following suppression of gp130 (i.e. antisense cDNA) in the cells (Castro et al., 2003; Rose-John, 2018). Also, IL6 and TNF α were found to be expressed more in invasive than

non-invasive pituitary tumors (Marques et al., 2019a; Wu et al., 2016). Inhibition of chemokine (CXCR4) signaling led to impaired growth of human (*in vitro*) and mouse AtT20 (*in vivo*) pituitary tumors (Barbieri et al., 2008; Kim et al., 2011; Mertens et al., 2015). Intriguingly, IL6 is also part of SASP, and has been proposed to play a dual role. Autocrine IL6 may induce senescence in pituitary tumors and thus act as tumor suppressor, which may explain the benign character of pituitary adenomas (Sapochnik et al., 2017a, 2017b). In contrast, paracrine IL6 (and other SASP factors like IL1 β) has been shown to be part of the SASP of WNT/ β -catenin-mutated senescing stem cells, suggested to fuel craniopharyngioma development and growth (Andoniadou et al., 2013; Gonzalez-Meljem et al., 2017).

Taken together, stem cells in tumorigenic pituitary and its tumors show an activated phenotype in terms of proliferation and cytokine/chemokine status. The activated stem cell secretome may interact with other cell types in the neighborhood that may play a role in the tumorigenic process, not only the epithelial (tumor) cells but also immune, endothelial and mesenchymal cells (e.g. tumor-associated fibroblasts), together constituting the tumor microenvironment (Plaks et al., 2015; Prager et al., 2019). Along this line, it is well known that TSCs secrete cytokines and chemokines to engineer a growth-permissive and protected microenvironment (Andrés et al., 2020).

5.1.4 Mouse and human pituitary tumor-derived organoids

To validate and further elaborate our stem cell findings of the tumorigenic pituitary, we employed cutting-edge organoid technology. Organoids develop *in vitro* from (tissue) stem cells that self-renew, proliferate and self-organize into 3D structures which recapitulate key characteristic of the tissue's stem cells and epithelium, thus providing a highly useful and faithful model to study tissue (stem cell) biology (Schutgens and Clevers, 2020). Importantly, organoids can be long-term expanded while remaining phenotypically and genomically stable. Organoids have been established from various tissues of both mouse and human origin (e.g. liver (Huch et al., 2015, 2013a), endometrium (Boretto et al., 2017)). Interestingly, organoids can also be applied to model diseases, in particular cancer (Dutta et al., 2017). Tumor-derived organoids (tumoroids) have been developed from many cancer types, including endometrial (Boretto et al., 2019), colorectal (Van De Wetering et al., 2015) and breast cancer (Sachs et al., 2018). Tumoroids recapitulate key pathophysiological and mutational features of the original tumor, even after long-term culturing, and can be applied for drug screening. For instance, endometrial cancer organoids from patients harboring a loss-of-function mutation in *PTEN* (an inhibitor of the PI3K-AKT-mTOR pathway) housed the same gene alteration and were found sensitive to everolimus (an mTOR inhibitor) (Boretto et al., 2019). Similarly, tumoroids established from patients with breast cancer characterized by HER2 overexpression recapitulated this expression phenotype and were sensitive to drugs targeting the HER signaling pathway like afatinib, while HER2-negative tumoroids were resistant (Sachs et al., 2018).

Recently, our group established organoids from young-adult (8-12 weeks) and middle-aged (10-14 months) mouse pituitary (Cox et al., 2019; Vennekens et al., 2021). The organoids were shown to originate from the SOX2⁺ stem cells, and maintained their stemness phenotype during expansive culture (Cox et al., 2019; Vennekens et al., 2021). In our study, we set up a protocol to develop organoids from the pituitary of aged (18-21 months old) mice, to then apply this optimized method to aged *Drd2*^{-/-} mouse pituitary, when full-blown

tumor development has occurred. Among others, addition of HGF, shown to stimulate proliferation of epithelial cells in many tissues (such as liver and endometrium) and supplemented in multiple other organoid culture types (Fujii and Sato, 2021; Kato, 2017), was found beneficial. Using the optimized medium, organoids were successfully obtained from both *Drd2^{+/+}* and *Drd2^{-/-}* pituitary. The activated phenotype of the *Drd2^{-/-}* pituitary stem cell compartment was recapitulated in the organoid culture, including higher proliferative activity with larger organoid size after seeding, and more pronounced cytokine/chemokine expression profile. Omission of IL6 from the organoid medium reduced organoid formation as well as proliferation and passageability, found to be more pronounced in the *Drd2^{-/-}* pituitary-derived organoids, suggesting that the stem cells of the tumorigenic gland show (have developed) higher dependency for IL6. In addition, the (rapid) drop of endogenous *Il6* expression in the organoid cultures was also more prominent in the tumorous pituitary-derived organoids. Together, these findings indicate the importance of IL6 to render the stem cells activated and keep them in such state towards sustainable organoid growth. Blocking the endogenous gp130/JAK-STAT signaling through which IL6 typically acts (Rose-John, 2018), completely abrogated organoid formation (in other words, blocked stem cell activity/functionality). Taken together, these findings support that IL6 plays an important role in the stem cells' activation during tumorigenesis in the gland, similarly to the finding that IL6 acts as a pituitary stem cell activator following injury (Vennekens et al., 2021). Also in other tumor types, IL6 stimulates stem cell proliferation, as for instance found in thyroid cancer cell lines by sphere formation readout (Zheng et al., 2019). Two other cytokines upregulated in the activated stem cell compartment of the *Drd2^{-/-}* pituitary, i.e. IFN γ and IL1 β , exerted similar effects on organoid growth, and stimulated *Il6* expression in the organoids, suggesting that these cytokines may exert their stem cell-activating effect *via* IL6. In contrast to the upregulated cytokines, the chemokine CXCL2, also found elevated in the tumorous stem cell compartment, did not stimulate organoid development, neither did it prolong organoid growth. Interestingly, CXCL2 did not increase *Il6* expression, again indirectly pointing to the importance of IL6 in the stem cell activation. Of note, the organoid findings here again underscore the utility and relevance of this new model to document and study stem cell biology and activation, both in healthy and diseased conditions such as following injury (Cox et al., 2019; Vennekens et al., 2021) and tumorigenesis (this study).

Organoids established from human pituitary tumor biopsies showed a stemness phenotype similar to the tumor's *in situ* stem cells, and presented transcriptomic fingerprints of the original tumor (e.g. expression of *POU1F1* and *DLK1* replicating the original GH-secreting tumor), thereby advancing that they are patient tumor-specific. Moreover, the tumor-derived organoids expressed the recently identified pituitary tumor-related genes *AMIGO2*, *BTG1*, *ZFP36* and *DLG5* (Cui et al., 2021). Notwithstanding these observations, it remains at present unclear whether these organoids are established from authentic TSCs (tumoroids), or from tumor-entrapped and -activated tissue stem cells which are (epi-)genetically and transcriptomically impacted by the patient or pituitary tumorigenic constitution. Knowledge on the genomic landscape of pituitary tumors is still limited. Whole-exome sequencing of PitNETs revealed genomic disruptions including mutations, deletions/insertions and distinct copy number profiles among different tumor subtypes, but prevalent, recurrent mutations were not detected (Bi et al., 2017). Similarly, a recent scRNA-seq study revealed high prevalence (up to 60 %) of copy number variations (mostly somatic rather than germline or hereditary), but no mechanistic link has so far been

found between this copy number variation and tumorigenesis (Cui et al., 2021). Finally, functional pituitary tumors (and atypical adenomas) seem to display more genomic disruptions than NFPAs, and frequently harbored loss of chromosome 1p or 11 (Bi et al., 2017). *MEN1* and *AIP*, two genes found mutated in hereditary PitNETs, are located on chromosome 11q and have extensively been studied (Daly et al., 2009).

As described above, authentic TSCs are able to regrow the original tumor when transplanted in immunodeficient mice (Clevers, 2011). Future studies should address this conundrum by, in particular, assessing the *in vivo* tumorigenic capacity of the tumor biopsy-derived stem cells (as such or expanded as organoids). Since human pituitary tumor fragments and cells did not show tumor-growth capacity when transplanted under the skin (sc) or kidney capsule (Mertens et al., 2015), it is hypothesized that a more natural environment, meaning orthotopic transplantation, may be needed. In our study, we set up a method to stereotactically inject into the pituitary gland of (immunodeficient) mice. We concluded that only very small volumes are amenable for injection directly into the pituitary, and that addition of Matrigel and EGF are beneficial, although the new protocol still needs further refinements.

Unexpectedly, despite high formation efficiency of the organoids (i.e. from virtually all tumor biopsies tested), they showed early growth arrest. Transcriptomic analysis revealed high expression of cytokines/chemokines in the primary tumors, which rapidly faded in the organoid cultures. However, supplementation of these cytokines did not prolong organoids' passageability, neither did activating the cAMP or WNT pathway which were also found downregulated in the organoid cultures. Several hypotheses are proposed. First, the medium may still lack essential factors which are present in the *in vivo* microenvironment to fuel stem cell activity but which disappear in culture and are thus lacking for optimal organoid expansion. These factors may be produced by non-stem cells that do not survive in the organoid culture conditions, or may fade in the stem cells themselves when taken out of their 'stimulatory' microenvironment. Along this line, it is well established that the tumor microenvironment plays a key role in maintaining TSC characteristics (Plaks et al., 2015). Second, human pituitary stem cells may inherently lack the potential for long-term self-renewal and proliferation, and thus become quickly exhausted when too much 'pushed' to do so. Stem cell exhaustion has been described in other tissues such as the hippocampus and forebrain, in particular following impacts leading to high proliferative stress (Kippin et al., 2005; Sierra et al., 2015). Thirdly, the stem cells may experience senescence as occurring in the tumor. Indeed, senescence has been described in pituitary tumors (Gonzalez-Meljem et al., 2017; Sabatino et al., 2015) and SASP factors, in particular IL6, have been proposed to play a dual role in pituitary tumorigenesis as described earlier (i.e. cell-autonomous IL6 may induce senescence (Sapochnik et al., 2017a, 2017b), whereas non-cell autonomous IL6 may promote tumor growth (Andoniadou et al., 2013; Gonzalez-Meljem et al., 2017)).

Overall, our study showed similar observations in mouse and human pituitary tumors, i.e. that stem cells are present and display an activated phenotype. Further studies are now needed to compare different subtypes of pituitary tumors. In particular, human prolactinomas, representing the most prevalent pituitary tumors, are still absent in our analysis. This deficiency is due to the fact that prolactinomas are primarily treated with dopamine agonists, meaning that surgical resection is very rare. A recent analysis from the University Hospital of Leuven (which provided the tumor biopsies) showed that from all 322 pituitary tumors removed by transsphenoidal surgery over a time period of 10 years, only 14 lesions were prolactinomas (4.3 %) (Van Gerven et al., 2021).

During the 3-year collection period of our study, only 2 prolactinomas were surgically removed, but biopsy collection was impossible due to small tumor size (i.e. micro-prolactinomas) and prioritization of pathological examination for appropriate patient care. The choice for a prolactinoma-developing mouse model may then appear less appropriate. However, although multiple mouse models have been described (see Table 3, section 2.2.3), the *Drd2*^{-/-} mouse model has been selected as the best choice for several reasons. First, as mentioned, prolactinomas are the most common pituitary tumors, having a major public health importance. Second, the preponderance of pituitary tumor mouse models develop lesions in the IL, which is less relevant since this lobe is absent in the human pituitary and the high majority of human pituitary tumors originate, and are located, in the AL. Thirdly, tumor development starts around 6-8 months in the *Drd2*^{-/-} mice, which is comparable to prolactinoma development in humans with patients averaging 20-50 years of age when presenting with prolactinomas (Ciccarelli et al., 2005). Finally, these tumors gradually develop and are not due to mutations in tumor-suppressor genes or oncogenes, which is very rare in human pituitary tumorigenesis.

5.2 Conclusion and future perspectives

Although transsphenoidal surgery of pituitary tumors is safe and effective, patients often require lifelong hormonal supplementation. Better understanding of pituitary tumorigenesis is expected to further advance clinical management. Our study unveiled an activated proliferation and cytokine/chemokine profile of the stem cells in pituitary tumorigenesis, as exposed by protein and transcriptomic features and organoid readouts. Gaining further insight into this stem cell activation process in pituitary tumors may pave the way toward a better understanding of tumor development and growth in the gland, including the involvement of immune/inflammatory processes, and may thereby project new clinical opportunities.

Stem cell activation in the tumorigenic process of the gland seems driven by IL6. To further elucidate this involvement, the IL6 knock-out (*IL6*^{-/-}) mouse can be used. Crossbreeding with *Drd2*^{-/-} mouse will allow to investigate the effect of IL6 absence on tumorigenesis in the gland (including tumor formation and burden, and stem cell activation). Furthermore, to validate an indirect (i.e. tumor-fueling) role of the SOX2⁺ cells, SOX2⁺ cell ablation can be performed in *Drd2*^{-/-} mice and the effect on tumor development and growth assessed. Ablation of SOX2⁺ cells was previously optimised (Roose et al., 2017), and can be applied in a *SOX2*^{CreERT2/+};*R26*^{iDTR/+};*Drd2*^{-/-} crossbreed background.

Regarding the early growth arrest of human pituitary tumor-derived organoids, further detailed scrutiny of the RNA-seq data may expose still other potential factors or pathways needed for retained stem cell activation and organoid growth. The organoids show signs of patient tumor-specificity. However, to conclusively demonstrate this relationship, whole (epi-)genome sequencing should be performed to investigate whether (non-)germline abnormalities (such as genomic mutations or copy number variations) in the primary tumors are recapitulated in the derived organoids. Simultaneously, these sequencing efforts can lead to identification of (new) genetic aberrations in pituitary tumorigenesis. Recent studies already touched upon this (e.g. (Bi et al., 2017; Cui et al., 2021); see above). A further objective would be to increase the number of healthy pituitary biopsies to reach

still better supported conclusions. One path may be to obtain pituitary biopsies at autopsy of people deceased by other-than-pituitary reasons.

Our observations of cytokines and chemokines being important for (tumor) stem cells, together with recent findings concerning these factors in the pituitary tumor microenvironment, are interesting starting points for further research. Among others, the impact of conditioned medium of immune cells and fibroblasts on stem-cell organoid cultures could be tested. In addition, co-cultures of pituitary (tumor) organoids and other cell types (e.g. macrophages) may further expose the importance of cellular crosstalk. Finally, being able to orthotopically transplant into the pituitary gland may have significant implications in the field, not only for exploring the tumorigenic capacity of tumor-derived organoids, but also for assessing the regenerative capacity of stem cell organoids (or purified stem cells) in injured pituitary. For instance, fluorescent SOX2⁺ stem cells could be isolated from SOX2^{eGFP/+};Drd2^{-/-} mice by FACS, which could then be orthotopically transplanted, or organoids could first be grown to substantially expand the number of stem cells prior to their transplantation. Similarly, human pituitary tumor-derived organoids can be injected into the pituitary of immunodeficient mice and tumorigenic capacity monitored, which will address the question on stem cell or TSC nature.

REFERENCES

REFERENCES

- Abboud, D., Daly, A.F., Dupuis, N., Bahri, M.A., Inoue, A., Chevigné, A., Ectors, F., Plenevaux, A., Pirotte, B., Beckers, A., *et al.*, 2020. GPR101 drives growth hormone hypersecretion and gigantism in mice via constitutive activation of Gs and Gq/11. *Nat. Commun.* 11(4752), 1–16. <https://doi.org/10.1038/s41467-020-18500-x>
- Abu Dabrh, A.M., Ospina, N.M.S., Al Nofal, A., Farah, W.H., Benkhadra, K., Carranza Leon, B.G., Al, E., 2016. Predictors of biochemical remission and recurrence after surgical and radiation treatments of cushing disease: a systematic review and meta-analysis. *Endocr. Pract.* 22(4), 466–476. <https://doi.org/10.4158/EP15922.RA>
- Aflorei, E.D., Korbonits, M., 2014. Epidemiology and etiopathogenesis of pituitary adenomas. *J. Neurooncol.* 117(3), 379–394. <https://doi.org/10.1007/s11060-013-1354-5>
- Agam, M.S., Wedemeyer, M.A., Wrobel, B., Weiss, M.H., Carmichael, J.D., Zada, G., 2019. Complications associated with microscopic and endoscopic transsphenoidal pituitary surgery: experience of 1153 consecutive cases treated at a single tertiary care pituitary center. *J. Neurosurg.* 130, 1576–1583. <https://doi.org/10.3171/2017.12.JNS172318.J>
- Aguilar-Medina, M., Avendaño-Félix, M., Lizárraga-Verdugo, E., Bermúdez, M., Romero-Quintana, J.G., Ramos-Payan, R., Ruíz-García, E., López-Camarillo, C., 2019. SOX9 stem-cell factor: clinical and functional relevance in cancer. *J. Oncol.* 1–19. <https://doi.org/10.1155/2019/6754040>
- Ajlan, A.M., Bin, S., Achal, A., Feroze, A.H., Katznelson, L., Harsh, R., 2018. Diabetes insipidus following endoscopic transsphenoidal surgery for pituitary adenoma. *J. Neurol. Surg. B. Skull Base* 79(2), 117–122.
- Alexandraki, K.I., 2019. Management of hypopituitarism. *J. Clin. Med.* 8(2153), 1–23. <https://doi.org/10.3390/jcm8122153>
- Andoniadou, C.L., Matsushima, D., Mousavy Gharavy, S.N., Signore, M., Mackintosh, A.I., Schaeffer, M., Gaston-Massuet, C., Mollard, P., Jacques, T.S., Le Tissier, P., *et al.*, 2013. Sox2+ stem/progenitor cells in the adult mouse pituitary support organ homeostasis and have tumor-inducing potential. *Cell Stem Cell* 13(4), 433–445. <https://doi.org/10.1016/j.stem.2013.07.004>
- Andoniadou, C.L., Gaston-Massuet, C., Reddy, R., Schneider, R.P., Blasco, M.A., Le Tissier, P., Jacques, T.S., Pevny, L.H., Dattani, M.T., Martinez-Barbera, J.P., 2012. Identification of novel pathways involved in the pathogenesis of human adamantinomatous craniopharyngioma. *Acta Neuropathol.* 124(2), 259–271. <https://doi.org/10.1007/s00401-012-0957-9>
- Andoniadou, C.L., Signore, M., Sajedi, E., Gaston-Massuet, C., Kelberman, D., Burns, A.J., Itasaki, N., Dattani, M., Martinez-Barbera, J.P., 2007. Lack of the murine homeobox gene *Hesx1* leads to a posterior transformation of the anterior forebrain. *Development* 134(8), 1499–1508. <https://doi.org/10.1242/dev.02829>
- Andrés, L. De, Oncol, J.H., Andrés, J.L. De, Lisón, C.G., Jiménez, G., Marchal, J.A., 2020. Cancer stem cell secretome in the tumor microenvironment: a key point for an effective personalized cancer treatment. *J. Hematol. Oncol.* 13(136), 1–22. <https://doi.org/10.1186/s13045-020-00966-3>
- Asa, S.L., Kelly, M.A., Grandy, D.K., Low, M.J., 1999. Pituitary lactotroph adenomas develop after prolonged lactotroph hyperplasia in dopamine D2 receptor-deficient mice. *Endocrinology* 140(11), 5348–5355. <https://doi.org/10.1210/endo.140.11.7118>
- Atkin, S., Hipkin, L., Jeffreys, R., Foy, P., White, M., 1997. Human anterior pituitary adenoma cell attachment in vitro. *Vitr. Cell. Dev. Biol. Anim.* 33(3), 158–160. <https://doi.org/10.1080/13518040701205365>
- Barbieri, F., Bajetto, A., Stumm, R., Pattarozzi, A., Porcile, C., Zona, G., Dorcaratto, A., Ravetti, J.L., Minuto, F., Spaziante, R., *et al.*, 2008. Overexpression of stromal cell-derived factor 1 and its receptor CXCR4 induces autocrine/paracrine cell proliferation in human pituitary adenomas. *Clin. Cancer Res.* 14(16), 5022–5032. <https://doi.org/10.1158/1078-0432.CCR-07-4717>
- Barker, N., Huch, M., Kujala, P., Wetering, M. Van De Snippert, H.J., Van Es, J.H., Sato, T., Stange, D.E., Begthel, H., Van Den Born, M., *et al.*, 2010. Lgr5+ve stem cells drive self-renewal in the stomach and build long-lived gastric units in vitro. *Stem Cell* 6(1), 25–36. <https://doi.org/10.1016/j.stem.2009.11.013>
- Barker, N., van Es, J.H., Kuipers, J., Kujala, P., van den Born, M., Cozijnsen, M., Haegerbarth, A., Korving, J., Begthel, H., Peters, P.J., *et al.*, 2007. Identification of stem cells in small intestine and colon by marker gene *Lgr5*. *Nature* 449(7165), 1003–1007. <https://doi.org/10.1038/nature06196>
- Barkhoudarian, G., Kelly, D.F., 2019. Pituitary apoplexy. *Neurosurg. Clin. N. Am.* 30(4), 457–463. <https://doi.org/10.1016/j.nec.2019.06.001>

- Barkhoudarian, G., Kelly, D.F., 2017. The pituitary gland: anatomy, physiology, and its function as the master gland. <https://doi.org/10.1016/B978-0-12-804340-0/00001-2>. (accessed 02/10/2021)
- Bartfeld, S., Bayram, T., Van De Wetering, M., Huch, M., Begthel, H., 2015. In vitro expansion of human gastric epithelial stem cells and their responses to bacterial infection. *Gastroenterology* 148(1), 126–136. <https://doi.org/10.1053/j.gastro.2014.09.042>.In
- Beltrami, A.P., Barlucchi, L., Torella, D., Baker, M., Limana, F., Chimenti, S., Kasahara, H., Rota, M., Musso, E., Urbanek, K., *et al.*, 2003. Adult cardiac stem cells are multipotent and support myocardial regeneration. *Cell* 114(6), 763–776. [https://doi.org/10.1016/S0092-8674\(03\)00687-1](https://doi.org/10.1016/S0092-8674(03)00687-1)
- Berg, C., Meinel, T., Lahner, H., Mann, K., Petersenn, S., 2010. Recovery of pituitary function in the late-postoperative phase after pituitary surgery: results of dynamic testing in patients with pituitary disease by insulin tolerance test 3 and 12 months after surgery. *Eur. J. Endocrinol.* 162(5), 853–859. <https://doi.org/10.1530/EJE-09-0997>
- Berker, M., Hazer, D.B., Yü cel, T., Gürlek, A., Cila, A., Aldur, M., Önerci, M., 2012. Complications of endoscopic surgery of the pituitary adenomas: analysis of 570 patients and review of the literature. *Pituitary* 15(3), 288–300. <https://doi.org/10.1007/s11102-011-0368-2>
- Bertko, E., Klammt, J., Dusatkova, P., Bahceci, M., Gonc, N., Ten Have, L., Kandemir, N., Mansmann, G., Obermannova, B., Oostdijk, W., *et al.*, 2017. Combined pituitary hormone deficiency due to gross deletions in the POU1F1 (PIT1) and PROP1 genes. *J. Hum. Genet.* 62(8), 755–762. <https://doi.org/10.1038/jhg.2017.34>
- Bi, W.L., Horowitz, P., Greenwald, N.F., Abedalthagafi, M., Agarwalla, P.K., Gibson, W.J., Mei, Y., Schumacher, S.E., Ben-David, U., Chevalier, A., *et al.*, 2017. Landscape of genomic alterations in pituitary adenomas. *Clin. Cancer Res.* 23(7), 1841–1851. <https://doi.org/10.1158/1078-0432.CCR-16-0790>
- Boj, S.F., Hwang, C.I., Baker, L.A., Chio, I.I.C., Engle, D.D., Corbo, V., Jager, M., Ponz-sarvise, M., Tiriác, H., Spector, M.S., *et al.*, 2015. Organoid model of human and mouse pancreatic ductal adenocarcinoma. *Cell* 160(0), 324–338. <https://doi.org/10.1016/j.cell.2014.12.021>.Organoid
- Boling, C.C., Karnezis, T.T., Baker, A.B., A, L.L., Soler, Z.M., Vandergrift, W.A., Wise, S.K., Al, E., 2016. Multi-institutional study of risk factors for perioperative morbidity following transnasal endoscopic pituitary adenoma surgery. *Int. Forum Allergy Rhinol.* 6(1), 101–107. <https://doi.org/10.1002/alr.21622>
- Bolognani, F., Albariño, C., Romanowski, V., Carri, N.G., Goya, R.G., 2001. In vitro and in vivo herpetic vector-mediated gene transfer in the pituitary gland: impact on hormone secretion. *Eur. J. Endocrinol.* 145(4), 497–503. <https://doi.org/10.1530/eje.0.1450497>
- Boretto, M., Maenhoudt, N., Luo, X., Hennes, A., Boeckx, B., Bui, B., Heremans, R., Perneel, L., Kobayashi, H., Van Zundert, I., *et al.*, 2019. Patient-derived organoids from endometrial disease capture clinical heterogeneity and are amenable to drug screening. *Nat. Cell Biol.* 21, 1041–1051. <https://doi.org/10.1038/s41556-019-0360-z>
- Boretto, M., Cox, B., Noben, M., Hendriks, N., Fassbender, A., Roose, H., Amant, F., Timmerman, D., Tomassetti, C., Vanhie, A., *et al.*, 2017. Development of organoids from mouse and human endometrium showing endometrial epithelium physiology and long-term expandability. *Development* 144(10), 1775–1786. <https://doi.org/10.1242/dev.148478>
- Boumadhi, S., Driessens, G., Lapouge, G., Rorive, S., Nassar, D., Le mercier, M., Delatte, B., Caauwe, A., Lenglez, S., Nkusi, E., *et al.*, 2014. SOX2 controls tumour initiation and cancer stem-cell functions in squamous-cell carcinoma. *Nature* 511, 246–250. <https://doi.org/10.1038/nature13305>
- Broutier, L., Mastrogiovanni, G., Versteegen, M.M., Francies, H.E., Gavarró, L.M., Bradshaw, C.R., Allen, G.E., Arnes-Benito, R., Sidorova, O., Gaspersz, M.P., *et al.*, 2017. Human primary liver cancer-derived organoid cultures for disease modeling and drug screening. *Nat. Med.* 23(12), 1424–1435. <https://doi.org/10.1038/nm.4438>
- Burke, W.T., Cote, D.J., Penn, D.L., Iuliano, S., Mcmillen, K., Laws, E.R., 2020. Diabetes insipidus after endoscopic transsphenoidal surgery. *Neurosurgery* 87(5), 949–955. <https://doi.org/10.1093/neuros/nyaa148>
- Buttan, A., Mamelak, A.N., 2019. Endocrine outcomes after pituitary surgery. *Neurosurg. Clin. N. Am.* 30(4), 491–498. <https://doi.org/10.1016/j.nec.2019.05.009>
- Cano, D.A., Soto-moreno, A., Leal-cerro, A., 2014. Genetically engineered mouse models of pituitary tumors. *Front. Oncol.* 4(203), 1–10. <https://doi.org/10.3389/fonc.2014.00203>
- Cappabianca, P., Cavallo, L.M., Colao, A.M., De Divitiis, E., 2002. Surgical complications associated with the endoscopic endonasal transsphenoidal approach for pituitary adenomas. *J. Neurosurg.* 97(2), 293–298. <https://doi.org/10.3171/jns.2002.97.2.0293>

- Cappabianca, P., Alfieri, A., Colao, A., Ferone, D., Lombardi, G., Divitiis, E., 1999. Endoscopic endonasal transsphenoidal approach: an additional reason in support of surgery in the management of pituitary lesions. *Skull Base Surg.* 9(2), 109–117. <https://doi.org/10.1055/s-2008-1058157>
- Carrasco-Garcia, E., Santos, J.C., Garcia, I., Brianti, M., García-Puga, M., Pedrazzoli, J., Matheu, A., Ribeiro, M.L., 2016. Paradoxical role of SOX2 in gastric cancer. *Am. J. Cancer Res.* 6(4), 701–713.
- Castro, C.P., Giacomini, D., Nagashima, A.C., Onofri, C., Graciarena, M., Kobayashi, K.E.N., Pa, M., Renner, U., Stalla, G.U.N.K., Arzt, E., 2003. Reduced expression of the cytokine transducer gp130 inhibits hormone secretion, cell growth, and tumor development of pituitary lactosomatotrophic GH3 cells. *Endocrinology* 144(2), 693–700. <https://doi.org/10.1210/en.2002-220891>
- Chaffer, C.L., Brueckmann, I., Scheel, C., Kaestli, A.J., Wiggins, P.A., Rodrigues, L.O., Brooks, M., Reinhardt, F., Suc, Y., Polyak, K., *et al.*, 2011. Normal and neoplastic nonstem cells can spontaneously convert to a stem-like state. *PNAS* 108(19), 7950–7955. <https://doi.org/10.1073/pnas.1102454108>
- Charles, M.A., Suh, H., Hjalt, T.A., Drouin, J., Camper, S.A., Gage, P.J., 2005. PITX genes are required for cell survival and *Lhx3* activation. *Mol. Endocrinol.* 19(7), 1893–1903. <https://doi.org/10.1210/me.2005-0052>
- Chen, J., Gremeaux, L., Fu, Q., Liekens, D., Van Laere, S., Vankelecom, H., 2009. Pituitary progenitor cells tracked down by side population dissection. *Stem Cells* 27(5), 1182–1195. <https://doi.org/10.1002/stem.51>
- Chen, J., Crabbe, A., Van Duppen, V., Vankelecom, H., 2006. The Notch signaling system is present in the postnatal pituitary: marked expression and regulatory activity in the newly discovered side population. *Mol. Endocrinol.* 20(12), 3293–3307. <https://doi.org/10.1210/me.2006-0293>
- Chen, J., Hersmus, N., Van Duppen, V., Caesens, P., Deneff, C., Vankelecom, H., 2005. The adult pituitary contains a cell population displaying stem/progenitor cell and early-embryonic characteristics. *Endocrinology* 146(9), 3985–3998. <https://doi.org/10.1210/en.2005-0185>
- Chen, M., Kato, T., Higuchi, M., Yoshida, S., Yako, H., Kanno, N., Kato, Y., 2013. Coxsackievirus and adenovirus receptor-positive cells compose the putative stem/progenitor cell niches in the marginal cell layer and parenchyma of the rat anterior pituitary. *Cell Tissue Res.* 354(3), 823–836. <https://doi.org/10.1007/s00441-013-1713-8>
- Chen, Y., Huang, Y., Zhu, L., Chen, M., Huang, Y., Zhang, J., He, S., Li, A., Chen, R., Zhou, J., 2016. SOX2 inhibits metastasis in gastric cancer. *J. Cancer Res. Clin. Oncol.* 142(6), 1221–1230. <https://doi.org/10.1007/s00432-016-2125-4>
- Cheung, L.Y.M., George, A.S., McGee, S.R., Daly, A.Z., Brinkmeier, M.L., Ellsworth, B.S., Camper, S.A., 2018. Single-Cell RNA sequencing reveals novel markers of male pituitary stem cells and hormone-producing cell types. *Endocrinology* 159(12), 3910–3924. <https://doi.org/10.1210/en.2018-00750>
- Ciccarelli, A., Daly, A.F., Beckers, A., 2005. The epidemiology of prolactinomas. *Pituitary* 8(1), 3–6. <https://doi.org/10.1007/s11102-005-5079-0>
- Clevers, H., 2016. Modeling development and disease with organoids. *Cell* 165(7), 1586–1597. <https://doi.org/10.1016/j.cell.2016.05.082>
- Clevers, H., 2011. The cancer stem cell: premises, promises and challenges. *Nat. Med.* 17(3), 313–319. <https://doi.org/10.1038/nm.2304>
- Cox, B., Laporte, E., Vennekens, A., Kobayashi, H., Nys, C., Van Zundert, I., Ujii, H., Drubbel, A.V., Beck, B., Roose, H., *et al.*, 2019. Organoids from pituitary as a novel research model toward pituitary stem cell exploration. *J. Endocrinol.* 240(2), 287–308. <https://doi.org/10.1530/JOE-18-0462>
- Cox, B., Roose, H., Vennekens, A., Vankelecom, H., 2017. Pituitary stem cell regulation: who is pulling the strings? *J. Endocrinol.* 243(3), 135–158. <https://doi.org/10.1530/JOE-17-0083>
- Cui, Y., Li, C., Jiang, Z., Zhang, S., Li, Q., Liu, X., Zhou, Y., Li, R., Wei, L., Li, L., *et al.*, 2021. Single-cell transcriptome and genome analyses of pituitary neuroendocrine tumors. *Neuro. Oncol.* 23(11), 1859–1871. <https://doi.org/10.1093/neuonc/noab102>
- Dagogo-Jack, I., Shaw, A.T., 2018. Tumour heterogeneity and resistance to cancer therapies. *Nat. Rev. Clin. Oncol.* 15(2), 81–94. <https://doi.org/10.1038/nrclinonc.2017.166>
- Daly, A.F., Beckers, A., 2020. The epidemiology of pituitary adenomas. *Endocrinol. Metab. Clin. N. Am.* 49(3), 347–355. <https://doi.org/10.1016/j.ecl.2020.04.002>

- Daly, A.F., Tichomirowa, M.A., Beckers, A., 2009. The epidemiology and genetics of pituitary adenomas. *Best Pract. Res. Clin. Endocrinol. Metab.* 23(5), 543–554. <https://doi.org/10.1016/j.beem.2009.05.008>
- Dattani, M.T., Martinez-Barbera, J.P., Thomas, P.Q., Brickman, J.M., Gupta, R., Mårtensson, I.L., Toresson, H., Fox, M., Wales, J.K.H., Hindmarsh, P.C., *et al.*, 1998. Mutations in the homeobox gene HESX1/Hesx1 associated with septo-optic dysplasia in human and mouse. *Nat. Genet.* 19(2), 125–133. <https://doi.org/10.1038/477>
- Davis, J.R.E., McVerry, J., Lincoln, G.A., Windeatt, S., Lowenstein, P.R., Castro, M.G., McNeilly, A.S., 2001. Cell type-specific adenoviral transgene expression in the intact ovine pituitary gland after stereotaxic delivery: an in vivo system for long-term multiple parameter evaluation of human pituitary gene therapy. *Endocrinology* 142(2), 795–801. <https://doi.org/10.1210/endo.142.2.7963>
- de la Rocha, A.M.A., Sampron, N., Alonso, M.M., Matheu, A., 2014. Role of SOX family of transcription factors in central nervous system tumors. *Am. J. Cancer Res.* 4(4), 312–324.
- Dekkers, J.F., Alieva, M., Wellens, L.M., Ariese, H.C.R., Jamieson, P.R., Vonk, A.M., Amatngalim, G.D., Hu, H., Oost, K.C., Snippert, H.J.G., *et al.*, 2019. High-resolution 3D imaging of fixed and cleared organoids. *Nat. Protoc.* 14, 1756–1771. <https://doi.org/10.1038/s41596-019-0160-8>
- Dekkers, J.F., Berkers, G., Kruisselbrink, E., Vonk, A., 2016. Characterizing responses to CFTR-modulating drugs using rectal organoids derived from subjects with cystic fibrosis. *Sci. Transl. Med.* 8(344), 1–12. <https://doi.org/10.1126/scitranslmed.aad8278>
- Denef, C., 2008. Paracrinicity: The story of 30 years of cellular pituitary crosstalk. *J. Neuroendocrinol.* 20(1), 1–70. <https://doi.org/10.1111/j.1365-2826.2007.01616.x>
- Dlouhy, B.J., Madhavan, K., Clinger, J.D., Reddy A., Dawson, J.D., O'Brien, E.K., Chang, E., Graham, S.M., Greenlee, J.D.W., 2012. Elevated body mass index and risk of postoperative CSF leak following transsphenoidal surgery. *J. Neurosurg.* 116(6), 1311–1217. <https://doi.org/10.3171/2012.2.JNS111837>
- Dutta, D., Heo, I., Clevers, H., 2017. Disease modeling in stem cell-derived 3D organoid systems. *Trends Mol. Med.* 23(5), 393–410. <https://doi.org/10.1016/j.molmed.2017.02.007>
- Ellis, P., Fagan, B.M., Magness, S.T., Hutton, S., Taranova, O., Hayashi, S., McMahon, A., Rao, M., Pevny, L., 2004. SOX2, a persistent marker for multipotential neural stem cells derived from embryonic stem cells, the embryo or the adult. *Dev. Neurosci.* 26, 148–165. <https://doi.org/10.1159/000082134>
- Ezzat, S., Asa, S.L., Couldwell, W.T., Barr, C.E., Dodge, W.E., Vance, M.L., McCutcheon, I.E., 2004. The prevalence of pituitary adenomas: a systematic review. *Cancer* 101(3), 613–619. <https://doi.org/10.1002/cncr.20412>
- Fang, Q., Benedetti, A.F.F., Ma, Q., Gregory, L., Li, J.Z., Dattani, M., Sadeghi-Nejad, A., Arnhold, I.J.P., Bilharinho, B., Camper, S.A., *et al.*, 2016. HESX1 mutations in patients with congenital hypopituitarism: variable phenotypes with the same genotype. *Physiol. Behav.* 176(1), 139–148. <https://doi.org/10.1111/cen.13067.HESX1>
- Fatemi, N., Dusick, J.R., Mattozo, C., McArthur, D.L., Cohan, P., Boscardin, J., Wang, C., Swerdloff, R.S., Kelly, D.F., 2008. Pituitary hormonal loss and recovery after transsphenoidal adenoma removal. *Neurosurgery* 63(4), 709–718. <https://doi.org/10.1227/01.NEU.0000325725.77132.90>
- Fauquier, T., Rizzoti, K., Dattani, M., Lovell-Badge, R., Robinson, I.C.A.F., 2008. SOX2-expressing progenitor cells generate all of the major cell types in the adult mouse pituitary gland. *Proc. Natl. Acad. Sci. U. S. A.* 105(8), 2907–12. <https://doi.org/10.1073/pnas.0707886105>
- Fernandez, A., Karavitaki, N., Wass, J.A.H., 2010. Prevalence of pituitary adenomas: a community-based, cross-sectional study in Banbury (Oxfordshire, UK). *Clin. Endocrinol.* 72, 377–382. <https://doi.org/10.1111/j.1365-2265.2009.03667.x>
- Filippella, M., Galland, F., Kujas, M., Young, J., Faggiano, A., Lombardi, G., Colao, A., Meduri, G., Chanson, P., 2006. Pituitary tumour transforming gene (PTTG) expression correlates with the proliferative activity and recurrence status of pituitary adenomas: a clinical and immunohistochemical study. *Clin. Endocrinol.* 65(4), 536–543. <https://doi.org/10.1111/j.1365-2265.2006.02630.x>
- Florea, S.M., Graillon, T., Cuny, T., Gras, R., Brue, T., Dufour, H., 2019. Ophthalmoplegic complications in transsphenoidal pituitary surgery. *J. Neurosurg.* 1–9. <https://doi.org/10.3171/2019.5.JNS19782>
- Frohman, L.A., Kineman, R.D., 2002. Growth hormone-releasing hormone and pituitary development, hyperplasia and tumorigenesis. *Trends Endocrinol. Metab.* 13(7), 299–303. [https://doi.org/10.1016/S1043-2760\(02\)00613-6](https://doi.org/10.1016/S1043-2760(02)00613-6)

- Fu, Q., Gremeaux, L., Luque, R.M., Liekens, D., Chen, J., Buch, T., Waisman, A., Kineman, R., Vankelecom, H., 2012. The adult pituitary shows stem/progenitor cell activation in response to injury and is capable of regeneration. *Endocrinology* 153(7), 3224–3235. <https://doi.org/10.1210/en.2012-1152>
- Fujii, M., Sato, T., 2021. Somatic cell-derived organoids as prototypes of human epithelial tissues and diseases. *Nat. Mater.* 20(2), 156–169. <https://doi.org/10.1038/s41563-020-0754-0>
- Fusco, A., Zatelli, M.C., Bianchi, A., Cimino, V., Tilaro, L., Veltri, F., Angelini, F., Lauriola, L., Vellone, V., Doglietto, F., *et al.*, 2008. Prognostic significance of the Ki67 labeling index in growth hormone-secreting pituitary adenomas. *J. Clin. Endocrinol. Metab.* 93(7), 2746–2750. <https://doi.org/10.1210/jc.2008-0126>
- Gangat, M., Radovick, S., 2017. Pituitary hypoplasia. *Endocrinol. Metab. Clin. N. Am.* 46(2), 247–257. <https://doi.org/10.1016/j.ecl.2017.01.003>
- Garcia-Lavandeira, M., Quereda, V., Flores, I., Saez, C., Diaz-rodriguez, E., Japon, M.A., Ryan, A.K., Blasco, M.A., Dieguez, C., Malumbres, M., *et al.*, 2009. A GRFa2/Prop1/stem (GPS) cell niche in the pituitary. *PLoS ONE* 4(3), 1–16. <https://doi.org/10.1371/journal.pone.0004815>
- Garros-Regulez, L., Aldaz, P., Arrizabalaga, O., Moncho-Amor, V., Carrasco-Garcia, E., Manterola, L., Moreno-Cugnon, L., Barrera, C., Villanua, J., Ruiz, I., *et al.*, 2016. MTOR inhibition decreases SOX2-SOX9 mediated glioma stem cell activity and temozolomide resistance. *Expert Opin. Ther. Targets* 20(4), 393–405. <https://doi.org/10.1517/14728222.2016.1151002>
- Gaston-Massuet, C., Andoniadou, C.L., Signore, M., Jayakody, S.A., Charolidi, N., Kyeyune, R., Vernay, B., Jacques, T.S., Taketo, M.M., Le Tissier, P., *et al.*, 2011. Increased Wnt signaling in pituitary progenitor/stem cells gives rise to pituitary tumors in mice and humans. *Proc. Natl. Acad. Sci. U. S. A.* 108(28), 11482–11487. <https://doi.org/10.1073/pnas.1101553108>
- Geurts, M.H., van der Vaart, J., Beumer, J., Clevers, H., 2021. The organoid platform: promises and challenges as tools in the fight against COVID-19. *Stem Cell Reports* 16(3), 412–418. <https://doi.org/10.1016/j.stemcr.2020.11.009>
- Gleiberman, A.S., Michurina, T., Encinas, J.M., Roig, J.L., Krasnov, P., Balordi, F., Fishell, G., Rosenfeld, M.G., Enikolopov, G., 2008. Genetic approaches identify adult pituitary stem cells. *Proc. Natl. Acad. Sci. U. S. A.* 105(7), 6332–6337. <https://doi.org/10.1073/pnas.0801644105>
- Goldsmith, S., Lovell-badge, R., Rizzoti, K., 2016. SOX2 is sequentially required for progenitor proliferation and lineage specification in the developing pituitary. *Development* 143, 2376–2388. <https://doi.org/10.1242/dev.137984>
- Gonzalez-Meljem, J.M., Haston, S., Carreno, G., Apps, J.R., Pozzi, S., Stache, C., Kaushal, G., Virasami, A., Panousopoulos, L., Neda Mousavy-Gharavy, S., *et al.*, 2017. Stem cell senescence drives age-attenuated induction of pituitary tumours in mouse models of paediatric craniopharyngioma. *Nat. Commun.* 8(1), 1–14. <https://doi.org/10.1038/s41467-017-01992-5>
- Gonzalez-Perez, O., 2012. Neural stem cells in the adult human brain. *Biol. Biomed. Rep.* 2(1), 59–69.
- Greenman, Y., Tordjman, K., Kisch, E., Razon, N., Ouaknine, G., Stern, N., 1995. Relative sparing of anterior pituitary function in patients with growth hormone-secreting macroadenomas: comparison with nonfunctioning macroadenomas. *J. Clin. Endocrinol. Metab.* 80(5), 1577–1583. <https://doi.org/10.1210/jcem.80.5.7745003>
- Gremeaux, L., Fu, Q., Chen, J., Vankelecom, H., 2012. Activated phenotype of the pituitary stem/progenitor cell compartment during the early-postnatal maturation phase of the gland. *Stem Cells Dev.* 21(5), 801–813. <https://doi.org/10.1089/scd.2011.0496>
- Gritti, A., Parati, E.A., Cova, L., Frolichsthal, P., Galli, R., Wanke, E., Faravelli, L., Morassutti, D.J., Roisen, F., Nickel, D.D., *et al.*, 1996. Multipotential stem cells from the adult mouse brain proliferate and self-renew in response to basic fibroblast growth factor. *J. Neurosci.* 16(3), 1091–1100.
- Gruppetta, M., Mercieca, C., 2013. Prevalence and incidence of pituitary adenomas: a population based study in Malta. *Pituitary* 16, 545–553. <https://doi.org/10.1007/s11102-012-0454-0>
- Haegebarth, A., Clevers, H., 2009. Wnt signaling, Lgr5, and stem cells in the intestine and skin. *Am. J. Pathol.* 174(3), 715–721. <https://doi.org/10.2353/ajpath.2009.080758>
- Han, X., Fang, X., Lou, X., Hua, D., Ding, W., Foltz, G., Hood, L., Yuan, Y., Lin, B., 2012. Silencing SOX2 induced mesenchymal-epithelial transition and its expression predicts liver and lymph node metastasis of CRC patients. *PLoS One* 7(8), 1–9. <https://doi.org/10.1371/journal.pone.0041335>

- Hannan, C.J., Almhanedi, H., Al-Mahfoudh, R., Bhojak, M., Looby, S., Javadvpour, M., 2020. Predicting post-operative cerebrospinal fluid (CSF) leak following endoscopic transnasal pituitary and anterior skull base surgery: a multivariate analysis. *Acta Neurochir.* 162(6), 1309–1315. <https://doi.org/10.1007/s00701-020-04334-5>
- Hansen, T.M., Batra, S., Lim, M., Gallia, G.L., Burger, P.C., Salvatori, R., Wand, G., Quinones-Hinojosa, A., Kleinberg, L., Redmond, K.J., 2014. Invasive adenoma and pituitary carcinoma: a SEER database analysis. *Neurosurg. Rev.* 37(2), 279–286. <https://doi.org/10.1007/s10143-014-0525-y>
- Hardy, J., 1969. Transphenoidal microsurgery of the normal and pathological pituitary. *Clin. Neurosurg.* 16(10), 185–217. https://doi.org/10.1093/neurosurgery/16.cn_suppl_1.185
- Hashimoto, S., Yoshimura, H., Okada, K., Uramaru, N., Sugihara, K., Kitamura, S., Imaoka, S., 2012. Effects of polybrominated diphenyl ethers (PBDEs) and their derivatives on protein disulfide isomerase activity and growth hormone release of GH3 cells. *Chem. Res. Toxicol.* 25, 656–663.
- Herbison, A.E., 2018. The gonadotropin-releasing hormone pulse generator. *Endocrinology* 159(11), 3723–3736. <https://doi.org/10.1210/en.2018-00653>
- Higuchi, M., Yoshida, S., Ueharu, H., Chen, M., Kato, T., Kato, Y., 2014. PRRX1 and PRRX2 distinctively participate in pituitary organogenesis and a cell-supply system. *Cell Tissue Res.* 357(1), 323–335. <https://doi.org/10.1007/s00441-014-1861-5>
- Hill, M., Wernig, A., Goldspink, G., 2003. Muscle satellite (stem) cell activation during local tissue injury and repair. *J. Anat.* 203(1), 89–99. <https://doi.org/10.1046/j.1469-7580.2003.00195.x>
- Ho, O., Lafont, C., Fontanaud, P., Guillou, A., Kemkem, Y., Kineman, R.D., Luque, R.M., Fiordelisio Coll, T., Le Tissier, P., Mollard, P., 2019. Imaging and manipulating pituitary function in the awake mouse. *Endocrinology* 160(10), 2271–2281. <https://doi.org/10.1210/en.2019-00297>
- Hofmann, B.M., Kreutzer, J., Saeger, W., Buchfelder, M., Blümcke, I., Fahlbusch, R., Buslei, R., 2006. Nuclear (beta)-catenin accumulation as reliable marker for the differentiation between cystic craniopharyngiomas and Rathke cleft cysts: a clinico-pathologic approach. *Am. J. Surg. Pathol.* 30(12), 1595–1603. <https://doi.org/10.1097/01.pas.0000213328.64121.12>
- Huch, M., Gehart, H., Van Boxtel, R., Hamer, K., Blokzijl, F., Versteegen, M.M.A., Ellis, E., Van Wenum, M., Fuchs, S.A., De Ligt, J., *et al.*, 2015. Long-term culture of genome-stable bipotent stem cells from adult human liver. *Cell* 160, 299–312. <https://doi.org/10.1016/j.cell.2014.11.050>
- Huch, M., Bonfanti, P., Boj, S.F., Sato, T., Loomans, C.J.M., van de Wetering, M., Sojoodi, M., Li, V.S.W., Schuijers, J., Gracanin, A., *et al.*, 2013a. Unlimited in vitro expansion of adult bi-potent pancreas progenitors through the Lgr5/R-spondin axis. *EMBO J.* 32(20), 2708–2721. <https://doi.org/10.1038/emboj.2013.204>
- Huch, M., Dorrell, C., Boj, S.F., Es, J.H., van de Wetering, M., Li, V.S.W., Hamer, K., Sasaki, N., Finegold, M.J., Haft, A., *et al.*, 2013b. In vitro expansion of single Lgr5+ liver stem cells induced by Wnt-driven regeneration. *Nature* 494(7436), 247–250. <https://doi.org/10.1038/nature11826>
- Hwang, J.Y., Aum, D.J., Chicoine, M.R., Dacey, R.G., Osburn, J.W., Rich, K.M., Zipfel, G.J., Klatt-Cromwell, C.N., McJunkin, J.L., Pipkorn, P., *et al.*, 2020. Axis-specific analysis and predictors of endocrine recovery and deficits for non-functioning pituitary adenomas undergoing endoscopic transsphenoidal surgery. *Pituitary* 23(4), 389–399. <https://doi.org/10.1007/s11102-020-01045-z>
- Jahangiri, A., Wagner, J.R., Han, S.W., Tran, M.T., Miller, L.M., Chen, R., Tom, M.W., Ostling, L.R., Kunwar, S., Blevins, L., *et al.*, 2016. Improved versus worsened endocrine function after transsphenoidal surgery for nonfunctional pituitary adenomas: rate, time course, and radiological analysis. *J. Neurosurg.* 124(3), 589–595. <https://doi.org/10.3171/2015.1.JNS141543>
- Jia, X., Li, X., Xu, Y., Zhang, S., Mou, W., Liu, Y., Liu, Y., Lv, D., Liu, C.H., Tan, X., *et al.*, 2011. SOX2 promotes tumorigenesis and increases the anti-apoptotic property of human prostate cancer cell. *J. Mol. Cell Biol.* 3(4), 230–238. <https://doi.org/10.1093/jmcb/mjr002>
- Kassam, A.B., Prevedello, D.M., Carrau, R.L., Snyderman, C.H., Thomas, A., Gardner, P., Zanation, A., Duz, B., Stefko, S.T., Byers, *et al.*, 2011. Endoscopic endonasal skull base surgery: analysis of complications in the authors' initial 800 patients. *J. Neurosurg.* 114(6), 1544–1568. <https://doi.org/10.3171/2010.10.JNS09406>
- Kato, T., 2017. Biological roles of hepatocyte growth factor-Met signaling from genetically modified animals. *Biomed. reports* 7, 495–503. <https://doi.org/10.3892/br.2017.1001>

- Kelberman, D., Rizzoti, K., Lovell-badge, R., Robinson, I.C.A.F., Dattani, M.T., 2009. Genetic regulation of pituitary gland development in human and mouse. *Endocr. Rev.* 30(7), 790–829. <https://doi.org/10.1210/er.2009-0008>
- Kelly, M.A., Rubinstein, M., Asa, S.L., Zhang, G., Saez, C., Bunzow, J.R., Allen, R.G., Hnasko, R., Ben-Jonathan, N., Grandy, D.K., *et al.*, 1997. Pituitary lactotroph hyperplasia and chronic hyperprolactinemia in dopamine D2 receptor-deficient mice. *Neuron* 19(1), 103–113. [https://doi.org/10.1016/S0896-6273\(00\)80351-7](https://doi.org/10.1016/S0896-6273(00)80351-7)
- Kerrison, J.B., Lynn, M.J., Baer, C.A., Newman, S.A., Blousse, V., Newman, N.J., 2000. Stages of improvement in visual fields after pituitary tumor resection. *Am. J. Ophthalmol.* 130(6) 813–820. [https://doi.org/10.1016/s0002-9394\(00\)00539-0](https://doi.org/10.1016/s0002-9394(00)00539-0)
- Kim, J.M., Lee, Y.H., Ku, C.R., Lee, E.J., 2011. The cyclic pentapeptide d-arg3FC131, a CXCR4 antagonist, induces apoptosis of somatotrope tumor and inhibits tumor growth in nude mice. *Endocrinology* 152(2), 536–544. <https://doi.org/10.1210/en.2010-0642>
- Kippin, T.E., Martens, D.J., Kooy, D. Van Der, 2005. p21 loss compromises the relative quiescence of forebrain stem cell proliferation leading to exhaustion of their proliferation capacity. *Genes Dev.* 19, 756–767. <https://doi.org/10.1101/gad.1272305.all>
- Kishi, F., Abe, H., Akiyama, H., Tominaga, T., Taichi, M., Mima, A., Nagai, K., Kishi, F., Matsuura, M., Matsubara, T., *et al.*, 2011. SOX9 protein induces a chondrogenic phenotype of mesangial cells and contributes to advanced diabetic nephropathy. *J. Biol. Chem.* 286(37), 32162–32169. <https://doi.org/10.1074/jbc.M111.244541>
- Kopczak, A., Renner, U., Stalla, G.K., 2014. Advances in understanding pituitary tumors. *F1000Prime Rep.* 6(5), 4–9. <https://doi.org/10.12703/P6-5>
- Kregel, S., Kiriluk, K.J., Rosen, A.M., Cai, Y., Reyes, E.E., Otto, K.B., Tom, W., Paner, G.P., Szmulewitz, R.Z., Vander Griend, D.J., 2013. Sox2 is an androgen receptor-repressed gene that promotes castration-resistant prostate cancer. *PLoS One* 8(1), 1–14. <https://doi.org/10.1371/journal.pone.0053701>
- Lafont, C., Desarménien, M.G., Cassou, M., Molino, F., Lecoq, J., Hodson, D., Lacampagne, A., Mennessier, G., El Yandouzi, T., Carmignac, D., *et al.*, 2010. Cellular in vivo imaging reveals coordinated regulation of pituitary microcirculation and GH cell network function. *Proc. Natl. Acad. Sci. U. S. A.* 107(9), 4465–4470. <https://doi.org/10.1073/pnas.0902599107>
- Lancaster, M.A., Renner, M., Martin, C.A., Wenzel, D., Bicknell, L.S., Hurler, M.E., Homfray, T., Penninger, J.M., Jackson, A.P., Knoblich, J.A., 2013. Cerebral organoids model human brain development and microcephaly. *Nature* 501(7467), 373–379. <https://doi.org/10.1038/nature12517>
- Laporte, E., Vennekens, A., Vankelecom, H., 2021. Pituitary remodeling throughout life: are resident stem cells involved? *Front. Endocrinol.* 11, 1–18. <https://doi.org/10.3389/fendo.2020.604519>
- Larkin, S., Ansorge, O., 2017. Development and microscopic anatomy of the pituitary gland. [Updated 2017 Feb 15]. In: Feingold KR, Anawalt B, Boyce A, *et al.*, editors. *Endotext* [Internet]. South Dartmouth (MA): MDTText.com, Inc.; 2000. Available from: <https://www.ncbi.nlm.nih.gov/books/NBK425703/>
- Larkin, S.J., Preda, V., Karavitaki, N., Grossman, A., Ansorge, O., 2014. BRAF V600E mutations are characteristic for papillary craniopharyngioma and may coexist with CTNNB1-mutated adamantinomatous craniopharyngioma. *Acta Neuropathol.* 127(6), 927–929. <https://doi.org/10.1007/s00401-014-1270-6>
- Lee, E.J., Thimmapaya, B., Jameson, J.L., 2000. Stereotactic injection of adenoviral vectors that target gene expression to specific pituitary cell types: implications for gene therapy. *Neurosurgery* 46(6), 1461–1469. <https://doi.org/10.1097/00006123-200006000-00029>
- Lee, M.H., Lee, J.H., Seol, H.J., Lee, J.-I., Kim, J.H., Kong, D.-S., Nam, D.-H., 2016. Clinical concerns about recurrence of non-functioning pituitary adenoma. *Brain Tumor Res. Treat.* 4(1), 1–7. <https://doi.org/10.14791/btrt.2016.4.1.1>
- Lepore, D.A., Roeszler, K., Wagner, J., Ross, S.A., Bauer, K., Thomas, P.Q., 2005. Identification and enrichment of colony-forming cells from the adult murine pituitary. *Exp. Cell Res.* 308, 166–176. <https://doi.org/10.1016/j.yexcr.2005.04.023>
- Levy, A., 2002. Physiological implications of pituitary trophic activity. *J. Endocrinol.* 174, 147–155. <https://doi.org/10.1677/joe.0.1740147>
- Li, Z., Liu, Q., Li, C., Zong, X., Bai, J., Wu, Y., Lan, X., Yu, G., Zhang, Y., 2015. The role of TGF- β / Smad signaling in dopamine agonist-resistant prolactinomas. *Mol. Cell. Endocrinol.* 402, 64–71. <https://doi.org/10.1016/j.mce.2014.12.024>
- Lin, C.R., Kloussi, C., O'Connell, S., Briata, P., Szeto, D., Liu, F., Izpisua-Belmonte, J.C., Rosenfeld, M.G., 1999. Pitx2 regulates lung asymmetry, cardiac positioning and pituitary and tooth morphogenesis. *Nature* 401(6750), 279–282. <https://doi.org/10.1038/45803>

- Lindholm, J., Nielsen, E.H., Bjerre, P., Christiansen, J.S., Hagen, C., Juul, S., Jørgensen, J., Kruse, A., Laurberg, P., Stochholm, K., 2006. Hypopituitarism and mortality in pituitary adenoma. *Clin. Endocrinol.* 65(1), 51–58. <https://doi.org/10.1111/j.1365-2265.2006.02545.x>
- Lobatto, D.J., de Vries, F., Najafabadi, A.H.Z., Pereira, A.M., Peul, W.C., Vliet Vlieland, T.P.M., Biermasz, N.R., Van Furth, W.R., 2018. Preoperative risk factors for postoperative complications in endoscopic pituitary surgery: a systematic review. *Pituitary* 21, 84–97. <https://doi.org/10.1007/s11102-017-0839-1>
- Locatelli, V., Bianchi, V.E., 2014. Effect of GH/IGF-1 on bone metabolism and osteoporosis. *Int. J. Endocrinol.* 1–25. <https://doi.org/10.1155/2014/235060>
- Love, M.I., Huber, W., Anders, S., 2014. Moderated estimation of fold change and dispersion for RNA-seq data with DESeq2. *Genome Biol.* 15(550), 1–21. <https://doi.org/10.1186/s13059-014-0550-8>
- Maenhoudt, N., Defraye, C., Boretto, M., Jan, Z., Heremans, R., Boeckx, B., Hermans, F., Arijs, I., Cox, B., Van Nieuwenhuysen, E., *et al.*, 2020. Developing organoids from ovarian cancer as experimental and preclinical models. *Stem Cell Reports* 14(4), 717–729. <https://doi.org/10.1016/j.stemcr.2020.03.004>
- Magro, E., Graillon, T., Lassave, J., Castinetti, F., Boissonneau, S., Tabouret, E., Fuentes, S., Velly, L., Gras, R., Dufour, H., 2016. Complications related to the endoscopic endonasal transsphenoidal approach for nonfunctioning pituitary macroadenomas in 300 consecutive patients. *World Neurosurg.* 89, 442–453. <https://doi.org/10.1016/j.wneu.2016.02.059>
- Maiter, D., 2019. Management of dopamine agonist-resistant prolactinoma. *Neuroendocrinology* 109, 42–50. <https://doi.org/10.1159/000495775>
- Manoranjan, B., Mahendram, S., Almenawer, S.A., Venugopal, C., Mcfarlane, N., Hallett, R., Vijayakumar, T., Algird, A., Murty, N.K., Sommer, D.D., *et al.*, 2016. The identification of human pituitary adenoma-initiating cells. *Acta Neuropathol. Commun.* 4(125), 1–13. <https://doi.org/10.1186/s40478-016-0394-4>
- Marques, P., Barry, S., Carlsen, E., Collier, D., Ronaldson, A., Awad, S., Dorward, N., 2019a. Pituitary tumour fibroblast-derived cytokines influence tumour aggressiveness. *Endocr. Relat. Cancer* 26(12), 853–865.
- Marques, P., Barry, S., Carlsen, E., Collier, D., Ronaldson, A., Awad, S., Dorward, N., Grieve, J., Mendoza, N., Muquit, S., Grossman, A.B., Balkwill, F., Korbonits, M., 2019b. Chemokines modulate the tumour microenvironment in pituitary neuroendocrine tumours. *Acta Neuropathol. Commun.* 7(172), 1–21.
- Matsumoto, R., Suga, H., Aoi, T., Bando, H., Fukuoka, H., Iguchi, G., Narumi, S., Hasegawa, T., Muguruma, K., Ogawa, W., *et al.*, 2020. Congenital pituitary hypoplasia model demonstrates hypothalamic OTX2 regulation of pituitary progenitor cells. *J. Clin. Invest.* 130(2), 641–654. <https://doi.org/10.1172/JCI127378>
- May, V., Eipper, B.A., 1986. Long term culture of primary rat pituitary adrenocorticotropin/endorphin-producing cells in serum-free medium. *Endocrinology* 118(4), 1284–1295.
- Mchugh, D., Gil, J., 2018. Senescence and aging: causes, consequences, and therapeutic avenues. *J. Cell Biol.* 217(1), 65–77. <https://doi.org/10.1083/jcb.201708092>
- Mehta, G.U., Lonser, R.R., 2016. Management of hormone-secreting pituitary adenomas. *Neuro. Oncol.* 19(6), 762–773. <https://doi.org/10.1093/neuonc/now130>
- Melmed, S., 2020. Pituitary-tumor endocrinopathies. *N. Engl. J. Med.* 382(10), 937–950. <https://doi.org/10.1056/nejmra1810772>
- Melmed, S., 2017. Chapter 15 - hypothalamic–pituitary regulation. Editor(s): P. Michael Conn, *Conn's Translational Neuroscience*, Academic Press, 2017, Pages 317-331, ISBN 9780128023815, <https://doi.org/10.1016/B978-0-12-802381-5.00025-7>. (<https://www.sciencedirect.com/science/article/pii/B9780128023815000257>)
- Melmed, S., 2011. Pathogenesis of pituitary tumors. *Nat. Rev. Endocrinol.* 7(5), 257–266. <https://doi.org/10.1038/nrendo.2011.40>
- Mertens, F., Gremeaux, L., Chen, J., Fu, Q., Willems, C., Roose, H., Govaere, O., Roskams, T., Cristina, C., Becú-Villalobos, D., *et al.*, 2015. Pituitary tumors contain a side population with tumor stem cell-associated characteristics. *Endocr. Relat. Cancer* 22(4), 481–504. <https://doi.org/10.1530/ERC-14-0546>
- Mete, O., Lopes, M.B., 2017. Overview of the 2017 WHO classification of pituitary tumors. *Endocr. Pathol.* 28(3), 228–243. <https://doi.org/10.1007/s12022-017-9498-z>

- Moller, M.W., Andersen, M.S., Glintborg, D., Pedersen, C.B., Halle, B., Kristensen, B.W., Poulsen, F.R., 2020. Endoscopic vs. microscopic transsphenoidal pituitary surgery: a single centre study. *Sci. Rep.* 10(1), 1–8. <https://doi.org/10.1038/s41598-020-78823-z>
- Moncho-amor, V., Chakravarty, P., Galichet, C., Matheu, A., Lovell-badge, R., 2021. SOX2 is required independently in both stem and differentiated cells for pituitary tumorigenesis in p27-null mice. *Proc. Natl. Acad. Sci. U. S. A.* 118(7), 1–12. <https://doi.org/10.1073/pnas.2017115118>
- Monteil, V., Kwon, H., Prado, P., Hagelkrüys, A., Wimmer, R.A., Stahl, M., Leopoldi, A., Garreta, E., Hurtado del Pozo, C., Prosper, F., *et al.*, 2020. Inhibition of SARS-CoV-2 infections in engineered human tissues using clinical-grade soluble human ACE2. *Cell* 181(4), 905–913. <https://doi.org/10.1016/j.cell.2020.04.004>
- Moøller, N., Joørgensen, J.O.L., 2009. Effects of growth hormone on glucose, lipid, and protein metabolism in human subjects. *Endocr. Rev.* 30(2), 152–177. <https://doi.org/10.1210/er.2008-0027>
- Muzumdar, M.D., Tasic, B., Miyamichi, K., Li, L., Luo, L., 2007. A global double-fluorescent Cre reporter mouse. *genesis* 45(9), 593–605. <https://doi.org/10.1002/dvg.20335>
- Nantie, L.B., Himes, A.D., Getz, D.R., Raetzman, L.T., 2014. Notch signaling in postnatal pituitary expansion: proliferation, progenitors, and cell specification. *Mol. Endocrinol.* 28(5), 731–744. <https://doi.org/10.1210/me.2013-1425>
- Nelson, A.T., Tucker, H.G., Becker, D.P., 1984. Residual anterior pituitary function following transsphenoidal resection of pituitary macroadenomas. *J. Neurosurg.* 61(3), 577–580. <https://doi.org/10.3171/jns.1984.61.3.0577>
- Nielsen, E.H., Poulsgaard, L., Astrup, J., Bjerre, P., Andersen, M., Andersen, C., Lindholm, J., Laurberg, P., 2011. Incidence of craniopharyngioma in Denmark (n=189) and estimated world incidence of craniopharyngioma in children and adults. *J. Neurooncol.* 104, 755–763. <https://doi.org/10.1007/s11060-011-0540-6>
- Nolan, L.A., Levy, A., 2006. A population of non-luteinising hormone/non-adrenocorticotrophic hormone-positive cells in the male rat anterior pituitary responds mitotically to both gonadectomy and adrenalectomy. *J. Neuroendocrinol.* 18(9), 655–661. <https://doi.org/10.1111/j.1365-2826.2006.01459.x>
- Nys, C., Vankelecom, H., 2021. Pituitary disease and recovery: how are stem cells involved? *Mol. Cell. Endocrinol.* 525(111176), 1–8. <https://doi.org/10.1016/j.mce.2021.111176>
- O'Brien, C.A., Pollett, A., Gallinger, S., Dick, J.E., 2007. A human colon cancer cell capable of initiating tumour growth in immunodeficient mice. *Nature* 445(7123), 106–110. <https://doi.org/10.1038/nature05372>
- Ogra, S., Nichols, A.D., Stylli, S., Kaye, A.H., Savino, P.J., Danesh-meyer, H. V., 2014. Visual acuity and pattern of visual field loss at presentation in pituitary adenoma. *J. Clin. Neurosci.* 21(5), 735–740. <https://doi.org/10.1016/j.jocn.2014.01.005>
- Ooi, G.T., Tawadros, N., Escalona, R.M., 2004. Pituitary cell lines and their endocrine applications. *Mol. Cell. Endocrinol.* 228, 1–21. <https://doi.org/10.1016/j.mce.2004.07.018>
- Otsubo, T., Akiyama, Y., Yanagihara, K., Yuasa, Y., 2008. SOX2 is frequently downregulated in gastric cancers and inhibits cell growth through cell-cycle arrest and apoptosis. *Br. J. Cancer* 98(4), 824–831. <https://doi.org/10.1038/sj.bjc.6604193>
- Ozone, C., Suga, H., Eiraku, M., Kadoshima, T., Yonemura, S., Takata, N., Oiso, Y., Tsuji, T., Sasai, Y., 2016. Functional anterior pituitary generated in self-organizing culture of human embryonic stem cells. *Nat. Commun.* 7(10351), 1–10. <https://doi.org/10.1038/ncomms10351>
- Paez Pereda, M., Goldberg, V., Chervirf, A., Carrizo, G., Molinad, A., Rennef, U., Sauer, J., 1996. Interleukin-2 (IL-2) and IL-6 regulate c-fos protooncogene in human pituitary adenoma explants expression. *Mol. Cell. Endocrinol.* 124, 33–42. [https://doi.org/10.1016/S0303-7207\(96\)03924-X](https://doi.org/10.1016/S0303-7207(96)03924-X)
- Pérez Millán, M.I., Brinkmeier, M.L., Mortensen, A.H., Camper, S.A., 2016. PROP1 triggers epithelial-mesenchymal transition-like process in pituitary stem cells. *Elife* 5, 1–24. <https://doi.org/10.7554/eLife.14470.001>
- Peverelli, E., Treppiedi, D., Giardino, E., Vitali, E., Lania, A.G., Mantovani, G., 2015. Dopamine and somatostatin analogues resistance of pituitary tumors: focus on cytoskeleton involvement. *Front. Endocrinol.* 6(187), 1–10. <https://doi.org/10.3389/fendo.2015.00187>
- Pietzsch, T., Saalfeld, S., Preibisch, S., Tomancak, P., 2015. BigDataViewer: visualization and processing for large image data sets. *Nat. Methods* 12(6), 481–483. <https://doi.org/10.1038/nmeth.3392>
- Plaks, V., Kong, N., Werb, Z., 2015. The cancer stem cell niche: how essential is the niche in regulating stemness of tumor cells? *Cell Stem Cell* 16(3), 225–238. <https://doi.org/10.1016/j.stem.2015.02.015>

- Ponti, D., Costa, A., Zaffaroni, N., Pratesi, G., Petrangolini, G., Coradini, D., Pilotti, S., Pierotti, M.A., Daidone, M.G., 2005. Isolation and in vitro propagation of tumorigenic breast cancer cells with stem/progenitor cell properties. *Cancer Res.* 65(13), 5506–5511. <https://doi.org/10.1158/0008-5472.CAN-05-0626>
- Prager, B.C., Xie, Q., Bao, S., Rich, J.N., 2019. Cancer stem cells: the architects of the tumor ecosystem. *Cell Stem Cell* 24(1), 41–53. <https://doi.org/10.1016/j.stem.2018.12.009>
- Raappana, A., Koivukangas, J., Ebeling, T., Pirila, T., 2010. Incidence of pituitary adenomas in Northern Finland in 1992–2007. *J Clin Endocrinol Metab* 95(9), 4268–4275. <https://doi.org/10.1210/jc.2010-0537>
- Recouvreux, M.V., Lapyckyj, L., Camilletti, M.A., Guida, M.C., Ornstein, A., Rifkin, D.B., Becu-villalobos, D., Díaz-torga, G., 2013. Sex differences in the pituitary transforming growth factor- β 1 system: studies in a model of resistant prolactinomas. *Endocrinology* 154(11), 4192–4205. <https://doi.org/10.1210/en.2013-1433>
- Rizzoti, K., Akiyama, H., Lovell-badge, R., 2013. Mobilized adult pituitary stem cells contribute to endocrine regeneration in response to physiological demand. *Cell Stem Cell* 13(4), 419–432. <https://doi.org/10.1016/j.stem.2013.07.006>
- Ronchi, C.L., Peverelli, E., Herterich, S., Weigand, I., Mantovani, G., Schwarzmayr, T., Sbiera, S., Allolio, B., Honegger, J., Appenzeller, S., Lania, A.G., *et al.*, 2016. Landscape of somatic mutations in sporadic GH-secreting pituitary adenomas. *Eur. J. Endocrinol.* 174(3), 363–372. <https://doi.org/10.1530/EJE-15-1064>
- Roose, H., 2018. The role of pituitary stem cells in homeostasis and tumorigenesis of the pituitary gland.
- Roose, H., Cox, B., Boretto, M., Gysemans, C., Vennekens, A., Vankelecom, H., 2017. Major depletion of SOX2+stem cells in the adult pituitary is not restored which does not affect hormonal cell homeostasis and remodelling. *Sci. Rep.* 7(1), 1–11. <https://doi.org/10.1038/s41598-017-16796-2>
- Rose-John, S., 2018. Interleukin-6 family cytokines. *Cold Spring Harb. Perspect. Biol.* 10(2), 1–17. <https://doi.org/10.1101/cshperspect.a028415>
- Russell, J.P., Lim, X., Santambrogio, A., Yianni, V., Kemkem, Y., Wang, B., Fish, M., Haston, S., Grabek, A., Hallang, S., *et al.*, 2021. Pituitary stem cells produce paracrine WNT signals to control the expansion of their descendant progenitor cells. *Elife* 10, 1–23. <https://doi.org/10.7554/ELIFE.59142>
- Sabatino, M.E., Petiti, J.P., Del Valle Sosa, L., Pérez, P.A., Gutiérrez, S., Leimgruber, C., Latini, A., Torres, A.I., De Paul, A.L., 2015. Evidence of cellular senescence during the development of estrogen-induced pituitary tumors. *Endocr. Relat. Cancer* 22(3), 299–317. <https://doi.org/10.1530/ERC-14-0333>
- Sachs, N., de Ligt, J., Kopper, O., Gogola, E., Bounova, G., Weeber, F., Vanita Balgobind, A., Wind, K., Gracanin, A., Begthel, H., *et al.*, 2018. A living biobank of breast cancer organoids captures disease heterogeneity. *Cell* 172, 373–382. <https://doi.org/10.1016/j.cell.2017.11.010>
- Sapochnik, M., Fuertes, M., Arzt, E., 2017a. Programmed cell senescence: role of IL-6 in the pituitary. *J. Mol. Endocrinol.* 58(4), R241–R253. <https://doi.org/10.1530/JME-17-0026>
- Sapochnik, M., Haedo, M.R., Fuertes, M., Ajler, P., Carrizo, G., Cervio, A., Sevlever, G., Stalla, G.K., Arzt, E., 2017b. Autocrine IL-6 mediates pituitary tumor senescence. *Oncotarget* 8(3), 4690–4702. <https://doi.org/10.18632/oncotarget.13577>
- Sarkar, K., Kim, H., Biology, C., 1992. Transforming growth factor- β 1 messenger RNA and protein expression in the pituitary gland: its action on prolactin secretion and lactotropic growth. *Mol. Endocrinol.* 6(11), 1825–1833.
- Sato, S.M., Mains, R.E., 1986. Regulation of adrenocorticotropin/endorphin-related peptide secretion in neonatal rat pituitary cultures. *Endocrinology* 119(2), 793–801. <https://doi.org/10.1210/endo-119-2-793>
- Sato, T., Clevers, H., 2013. Growing self-organizing mini-guts from a single intestinal stem cell: mechanism and applications. *Science* 340(6137), 1190–1194. <https://doi.org/10.1126/science.1234852>
- Sato, T., Stange, D.E., Ferrante, M., Vries, R.G.J., Van Es, J.H., Van Den Brink, S., Van Houdt, W.J., Pronk, A., Van Gorp, J., Siersema, P.D., *et al.*, 2011. Long-term expansion of epithelial organoids from human colon, adenoma, adenocarcinoma, and Barrett's epithelium. *Gastroenterology* 141(5), 1762–1772. <https://doi.org/10.1053/j.gastro.2011.07.050>
- Sato, T., Vries, R.G., Snippert, H.J., Van De Wetering, M., Barker, N., Stange, D.E., Van Es, J.H., Abo, A., Kujala, P., Peters, P.J., *et al.*, 2009. Single Lgr5 stem cells build crypt-villus structures in vitro without a mesenchymal niche. *Nature* 459, 262–266. <https://doi.org/10.1038/nature07935>

- Schindelin, J., Arganda-carreras, I., Frise, E., Kaynig, V., Pietzsch, T., Preibisch, S., Rueden, C., Saalfeld, S., Schmid, B., Tinevez, J., *et al.*, 2019. Fiji - an open source platform for biological image analysis. *Nat. Methods* 9(7), 1–15. <https://doi.org/10.1038/nmeth.2019.Fiji>
- Schmidt, R.F., Choudhry, O.J., Takkellapati, R., Eloy, J.A., Couldwell, W.T., Liu, J.K., 2012. Hermann Schloffer and the origin of transsphenoidal pituitary surgery. *Neurosurg. Focus* 33(2), 1–10. <https://doi.org/https://doi.org/10.3171/2012.5.FOCUS12129>
- Schmitz, M., Temme, A., Senner, V., Ebner, R., Schwind, S., Stevanovic, S., Wehner, R., Schackert, G., Schackert, H.K., Füssel, M., *et al.*, 2007. Identification of SOX2 as a novel glioma-associated antigen and potential target for T cell-based immunotherapy. *Br. J. Cancer* 96(8), 1293–1301. <https://doi.org/10.1038/sj.bjc.6603696>
- Schneider, H.J., Aimaretti, G., Kreitschmann-Andermahr, I., Stalla, G.-K., Ghigo, E., 2007. Hypopituitarism. *Lancet* 369(9571), 1461–1470. [https://doi.org/10.1016/S0140-6736\(07\)60673-4](https://doi.org/10.1016/S0140-6736(07)60673-4)
- Schreckinger, M., Szerlip, N., Mittal, S., 2013. Diabetes insipidus following resection of pituitary tumors. *Clin. Neurol. Neurosurg.* 115(2), 121–126. <https://doi.org/10.1016/j.clineuro.2012.08.009>
- Schutgens, F., Clevers, H., 2020. Human organoids: tools for understanding biology and treating diseases. *Annu. Rev. Pathol. Mech. Dis.* 15, 211–234. <https://doi.org/10.1146/annurev-pathmechdis-012419-032611>
- Schwank, G., Koo, B., Sasselli, V., Dekkers, J.F., Heo, I., Demircan, T., Sasaki, N., Boymans, S., Cuppen, E., Van Der Ent, C.K., *et al.*, 2013. Functional repair of CFTR by CRISPR/ Cas9 in intestinal stem cell organoids of cystic fibrosis patients. *Stem Cell* 13(6), 653–658. <https://doi.org/10.1016/j.stem.2013.11.002>
- Shi, Y., Inoue, H., Wu, J.C., Yamanaka, S., 2017. Induced pluripotent stem cell technology: a decade of progress. *Nat. Rev. Drug Discov.* 16(2), 115–130. <https://doi.org/10.1038/nrd.2016.245>
- Shirian, F.I., Ghorbani, M., Khamseh, M.E., Imani, M., Panahi, M., Alimohammadi, A., Nourbakhsh, M., Salimi, V., Tavakoli-Yaraki, M., 2021. Up-regulation of sex-determining region Y-box 9 (SOX9) in growth hormone-secreting pituitary adenomas. *BMC Endocr. Disord.* 21(1), 50. <https://doi.org/10.1186/s12902-021-00720-x>
- Sierra, A., Martín-suárez, S., Valcárcel-martín, R., Pascual, J., Anderson, A.E., Baekelandt, V., Maletić-savatić, M., Juan, M., 2015. Neuronal hyperactivity accelerates depletion of neural stem cells and impairs hippocampal neurogenesis. *Cell Stem Cell* 16(5), 488–503. <https://doi.org/10.1016/j.stem.2015.04.003>
- Sornson, M.W., Wu, W., Dasen, J.S., Flynn, S.E., Norman, D.J., O’Connell, S.M., Gukovsky, L., Carrière, C., Ryan, A.K., Miller, A.P., *et al.*, 1996. Pituitary lineage determination by the Prophet of Pit1 homeodomain factor defective in Ames dwarfism. *Nature* 384(6607), 327–333. <https://doi.org/10.1038/384327a0>
- Soukup, J., Česák, T., Hornychová, H., Michalová, K., Michnová, L., Netuka, D., Čáp, J., Gabalec, F., 2020. Stem cell transcription factor sox2 is expressed in a subset of folliculo-stellate cells of growth hormone-producing pituitary neuroendocrine tumours and its expression shows no association with tumour size or IGF1 levels: a clinicopathological study of 1. *Endocr. Pathol.* 31(4), 337–347. <https://doi.org/10.1007/s12022-020-09634-1>
- Stark, G.R., Cheon, H., Wang, Y., 2018. Responses to cytokines and interferons that depend upon JAKs and STATs. *Cold Spring Harb. Perspect. Biol.* 10(1), 1–16. <https://doi.org/10.1101/cshperspect.a028555>
- Sudhakar, N., Ray, A., Vafidis, J.A., 2004. Complications after trans-sphenoidal surgery: our experience and a review of the literature. *Br. J. Neurosurg.* 18(5), 507–512. <https://doi.org/10.1080/02688690400012459>
- Suga, H., Kadoshima, T., Minaguchi, M., Ohgushi, M., Soen, M., Nakano, T., Takata, N., 2011. Self-formation of functional adeno-hypophysis in three-dimensional culture. *Nature* 480(7375), 57–62. <https://doi.org/10.1038/nature10637>
- Suh, H., Gage, P.J., Drouin, J., Camper, S.A., 2002. Pitx2 is required at multiple stages of pituitary organogenesis: Pituitary primordium formation and cell specification. *Development* 129(2), 329–337. <https://doi.org/10.1242/dev.129.2.329>
- Taguchi, T., Takao, T., Iwasaki, Y., Nishiyama, M., Asaba, K., Hashimoto, K., 2006. Suppressive effects of dehydroepiandrosterone and the nuclear factor- κ B inhibitor parthenolide on corticotroph tumor cell growth and function in vitro and in vivo. *J. Endocrinol.* 188(2), 321–331. <https://doi.org/10.1677/joe.1.06418>
- Thotakura, A., Patibandla, M., Panigrahi, M., Addagada, G., 2017. Predictors of visual outcome with transsphenoidal excision of pituitary adenomas having suprasellar extension: a prospective series of 100 cases and brief review of the literature. *Asian J. Neurosurg.* 12(1), 1–5. <https://doi.org/10.4103/1793-5482.149995>
- Trivellin, G., Daly, A.F., Faucz, F.R., Yuan, B., Rostomyan, L., Larco, D.O., Scherthaner-Reiter, M.H., Szarek, E., Leal, L.F., Caberg, J.-H., *et al.*, 2014. Gigantism and acromegaly due to Xq26 microduplications and GPR101 mutation. *N. Engl. J. Med.* 371(25), 2363–2374. <https://doi.org/10.1056/nejmoa1408028>

- Trouillas, J., Vasiljevic, A., Dekkers, O., Popovic, V., 2020. Are aggressive pituitary tumors and carcinomas two sides of the same coin? Pathologists reply to clinician's questions. *Rev. Endocr. Metab. Disord.* 21(2), 243–251. <https://doi.org/10.1007/s11154-020-09562-9>
- Tümer, Z., Bach-Holm, D., 2009. Axenfeld-Rieger syndrome and spectrum of PITX2 and FOXC1 mutations. *Eur. J. Hum. Genet.* 17(12), 1527–1539. <https://doi.org/10.1038/ejhg.2009.93>
- Van Aken, M.O., Feelders, R.A., Marie, S. De, Delwel, E.J., Romijn, J.A., Lely, A.J. Van Der, De Herder, W.W., 2004. Cerebrospinal fluid leakage during transsphenoidal surgery: postoperative external lumbar drainage reduces the risk for meningitis. *Pituitary* 7(2), 89–93.
- Van De Wetering, M., Francies, H.E., Francis, J.M., Bounova, G., Iorio, F., Pronk, A., Van Houdt, W., Van Gorp, J., Taylor-Weiner, A., Kester, L., *et al.*, 2015. Prospective derivation of a living organoid biobank of colorectal cancer patients. *Cell* 161(4), 933–945. <https://doi.org/10.1016/j.cell.2015.03.053>
- Van der Klaauw, A., Kars, M., Biermasz, N.R., Roelfsema, F., Dekkers, O.M., Corssmit, E.P., Van Aken, M.O., Havekes, B., Pereira, A.M., Pijl, H., *et al.*, 2008. Disease-specific impairments in quality of life during long-term follow-up of patients with different pituitary adenomas. *Clin. Endocrinol.* 69(5), 775–784. <https://doi.org/10.1111/j.1365-2265.2008.03288.x>
- Van der Schueren, B., Deneff, C., Cassiman, J.-J., 1982. Ultrastructural and Functional Characteristics of Rat Pituitary Cell Aggregates*. *Endocrinology* 110, 513–523. <https://doi.org/10.1210/endo-110-2-513>
- Van Gerven, L., Qian, Z., Starovoyt, A., Jorissen, M., Meulemans, J., van Loon, J., De Vleeschouwer, S., Lambert, J., Bex, M., Vander Poorten, V., 2021. Endoscopic, endonasal transsphenoidal surgery for tumors of the sellar and suprasellar region: a monocentric historical cohort study of 369 patients. *Front. Oncol.* 11, 1–11. <https://doi.org/10.3389/fonc.2021.643550>
- Vankelecom, H., 2016. Pituitary stem cells: quest for hidden functions. *Stem Cells Neuroendocr.* 81–101. https://doi.org/10.1007/978-3-319-41603-8_7
- Vankelecom, H., 2012. Pituitary stem cells drop their mask. *Curr. Stem Cell Res. Ther.* 7(1), 36–71. <https://doi.org/10.2174/157488812798483467>
- Vankelecom, H., 2010. Pituitary stem/progenitor cells: embryonic players in the adult gland? *Eur. J. Neurosci.* 32(12), 2063–2081. <https://doi.org/10.1111/j.1460-9568.2010.07523.x>
- Vankelecom, H., 2007a. Non-hormonal cell types in the pituitary candidating for stem cell. *Semin. Cell Dev. Biol.* 18(4), 559–570. <https://doi.org/10.1016/j.semcdb.2007.04.006>
- Vankelecom, H., 2007b. Stem cells in the postnatal pituitary? *Neuroendocrinology* 85(2), 110–130. <https://doi.org/10.1159/000100278>
- Vankelecom, H., Chen, J., 2014. Pituitary stem cells: where do we stand? *Mol. Cell. Endocrinol.* 385(1-2), 2–17. <https://doi.org/10.1016/j.mce.2013.08.018>
- Vankelecom, H., Deneff, C., 1997. Paracrine communication in the anterior pituitary as studied in reaggregate cell cultures. *Microsc. Res. Tech.* 39(2), 150–156. [https://doi.org/10.1002/\(SICI\)1097-0029\(19971015\)39:2<150::AID-JEMT6>3.0.CO;2-P](https://doi.org/10.1002/(SICI)1097-0029(19971015)39:2<150::AID-JEMT6>3.0.CO;2-P)
- Vankelecom, H., Roose, H., 2017. The stem cell connection of pituitary tumors. *Front. Endocrinol.* 8(339), 6–8. <https://doi.org/10.3389/fendo.2017.00339>
- Vanner, R.J., Remke, M., Gallo, M., Selvadurai, H.J., Coutinho, F., Lee, L., Kushida, M., Head, R., Morrissy, S., Zhu, X., *et al.*, 2014. Quiescent Sox2+ cells drive hierarchical growth and relapse in sonic hedgehog subgroup medulloblastoma. *Cancer Cell* 26(1), 33–47. <https://doi.org/10.1016/j.ccr.2014.05.005>
- Vennekens, A., Laporte, E., Hermans, F., Cox, B., Modave, E., Janiszewski, A., Nys, C., Kobayashi, H., Malengier-Devlies, B., Chappell, J., *et al.*, 2021. Interleukin-6 is an activator of pituitary stem cells upon local damage, a competence quenched in the aging gland. *Proc. Natl. Acad. Sci. U. S. A.* 118(25), 1–11. <https://doi.org/10.1073/pnas.2100052118>
- Vennekens, A., Vankelecom, H., 2019. Traumatic brain injury and resultant pituitary dysfunction: insights from experimental animal models. *Pituitary* 22(3), 212–219. <https://doi.org/10.1007/s11102-019-00961-z>
- Wakefield, L.M., Thordarson, G., Nieto, A.I., Shyamala, G., Galvez, J.J., Anver, M.R., Cardiff, R.D., 2003. Spontaneous pituitary abnormalities and mammary hyperplasia in FVB/NCr mice: implications for mouse modeling. *Comp. Med.* 53(4), 424–432.

- Wang, S., Tie, J., Wang, R., Hu, F., Gao, L., Wang, W., Wang, L., Li, Z., Hu, S., Tang, S., *et al.*, 2015. SOX2, a predictor of survival in gastric cancer, inhibits cell proliferation and metastasis by regulating PTEN. *Cancer Lett.* 358(2), 210–219. <https://doi.org/10.1016/j.canlet.2014.12.045>
- Wilbertz, T., Wagner, P., Petersen, K., Stiedl, A.C., Scheble, V.J., Maier, S., Reischl, M., Mikut, R., Altorki, N.K., Moch, H., *et al.*, 2011. SOX2 gene amplification and protein overexpression are associated with better outcome in squamous cell lung cancer. *Mod. Pathol.* 24(7), 944–953. <https://doi.org/10.1038/modpathol.2011.49>
- Willems, C., Fu, Q., Roose, H., Mertens, F., Cox, B., Chen, J., Vankelecom, H., 2016. Regeneration in the pituitary after cell- ablation injury: time-related aspects and molecular analysis. *Endocrinology* 157(2), 705–721. <https://doi.org/10.1210/en.2015-1741>
- Willems, C., Vankelecom, H., 2014. Pituitary cell differentiation from stem cells and other cells: toward restorative therapy for hypopituitarism? *Regen. Med.* 9(4), 513–34. <https://doi.org/10.2217/rme.14.19>
- Wittkowski, W., 1998. Tanycytes and pituicytes: morphological and functional aspects of neuroglial interaction. *Microsc. Res. Tech.* 41(1), 29–42. [https://doi.org/10.1002/\(SICI\)1097-0029\(19980401\)41:1<29::AID-JEMT4>3.0.CO;2-P](https://doi.org/10.1002/(SICI)1097-0029(19980401)41:1<29::AID-JEMT4>3.0.CO;2-P)
- Wu, J.L., Qiao, J.Y., Duan, Q.H., 2016. Significance of TNF- α and IL-6 expression in invasive pituitary adenomas. *Genet. Mol. Res.* 15(1), 1–9. <https://doi.org/10.4238/gmr.15017502>
- Wuebben, E.L., Rizzino, A., 2017. The dark side of SOX2: cancer-a comprehensive overview. *Oncotarget* 8(27), 44917–44943. <https://doi.org/10.18632/oncotarget.16570>
- Wuebben, E.L., Wilder, P.J., Cox, J.L., Grunkemeyer, J.A., Caffrey, T., Hollingsworth, M.A., Rizzino, A., 2016. SOX2 functions as a molecular rheostat to control the growth, tumorigenicity and drug responses of pancreatic ductal adenocarcinoma cells. *Oncotarget* 7(23), 34890–34906. <https://doi.org/10.18632/oncotarget.8994>
- Würth, R., Barbieri, F., Pattarozzi, A., Gaudenzi, G., Gatto, F., Fiaschi, P., Ravetti, J., Zona, G., Daga, A., Persani, L., *et al.*, 2017. Phenotypical and pharmacological characterization of stem-like cells in human pituitary adenomas. *Mol. Neurobiol.* 54(7), 4879–4895. <https://doi.org/10.1007/s12035-016-0025-x>
- Xatzipsalti, M., Voutetakis, A., Stamoyannou, L., Chrousos, G.P., Kanaka-gantenbein, C., 2019. Congenital hypopituitarism: various genes, various phenotypes. *Horm. Metab. Res.* 51(2), 81–90. <https://doi.org/10.1055/a-0822-3637>
- Xia, Y., Nivet, E., Sancho-Martinez, I., Gallegos, T., Suzuki, K., Okamura, D., Wu, M.Z., Dubova, I., Esteban, C.R., Montserrat, N., *et al.*, 2013. Directed differentiation of human pluripotent cells to ureteric bud kidney progenitor-like cells. *Nat. Cell Biol.* 15(12), 1507–1515. <https://doi.org/10.1038/ncb2872>
- Xu, Q., Yuan, X., Tunici, P., Liu, G., Fan, X., Xu, M., Hu, J., Hwang, J.Y., Farkas, D.L., Black, K.L., *et al.*, 2009. Isolation of tumour stem-like cells from benign tumours. *Br. J. Cancer* 101(2), 303–311. <https://doi.org/10.1038/sj.bjc.6605142>
- Yang, X., Liu, X., Li, W., Chen, D., 2016. Pituicytoma: a report of three cases and literature review. *Oncol. Lett.* 12(5), 3417–3422. <https://doi.org/10.3892/ol.2016.5119>
- Ye, F., Li, Y., Hu, Ying, Zhou, C., Hu, Yuting, Chen, H., 2011. Expression of Sox2 in human ovarian epithelial carcinoma. *J. Cancer Res. Clin. Oncol.* 137(1), 131–137. <https://doi.org/10.1007/s00432-010-0867-y>
- Yoshida, S., Kato, T., Higuchi, M., Chen, M., Ueharu, H., Nishimura, N., Kato, Y., 2015. Localization of juxtacrine factor ephrin-B2 in pituitary stem/progenitor cell niches throughout life. *Cell Tissue Res.* 359(3), 755–766. <https://doi.org/10.1007/s00441-014-2054-y>
- Yoshida, S., Kato, T., Kato, Y., 2016. Regulatory system for stem/progenitor cell niches in the adult rodent pituitary. *Int. J. Mol. Sci.* 17(1), 1–16. <https://doi.org/10.3390/ijms17010075>
- Yoshimura, F., Harumiya, K., Ishikawa, H., Ohtsuka, Y., 1969. Differentiation of isolated chromophobes into acidophils or basophils when transplanted into the hypophysiotrophic area of hypothalamus. *Endocrinol. Jpn.* 16(5), 531–540. <https://doi.org/10.1507/endocrj1954.16.531>
- Zhang, D., Hugo, W., Redublo, P., Miao, H., Bergsneider, M., Wang, M.B., Kim, W., Yong, W.H., Heaney, A.P., 2021. A human ACTH-secreting corticotroph tumoroid model. Novel human ACTH-secreting tumor cell in vitro model. *EBioMedicine* 66(103294), 1–12. <https://doi.org/10.1016/j.ebiom.2021.103294>
- Zhang, S., Balch, C., Chan, M.W., Lai, H., Matei, D., Schilder, J.M., Yan, P.S., Huang, T.H., Nephew, K.P., 2008. Identification and characterization of ovarian cancer-initiating cells from primary human tumors. *Cancer Res.* 68(11), 4311–4320. <https://doi.org/10.1158/0008-5472.CAN-08-0364>

- Zheng, R., Chen, G., Li, X., Wei, X., Liu, C., Derwahl, M., 2019. Effect of IL-6 on proliferation of human thyroid anaplastic cancer stem cells. *Int. J. Clin. Exp. Pathol.* 12(11), 3992–4001.
- Zhou, J., Li, C., Sachs, N., Chun, M., Wong, B.H., Chu, H., 2018. Differentiated human airway organoids to assess infectivity of emerging influenza virus. *Proc. Natl. Acad. Sci. U. S. A.* 115(26), 6822–6827. <https://doi.org/10.1073/pnas.1806308115>
- Zhou, Y., Zhang, X., Klibanski, A., 2014. Genetic and epigenetic mutations of tumor suppressive genes in sporadic pituitary adenoma. *Mol Cell Endocrinol.* 386(0), 16–33. <https://doi.org/10.1016/j.mce.2013.09.006>.Genetic
- Zhu, X., Gleiberman, A.S., Rosenfeld, M.G., 2007. Molecular physiology of pituitary development: signaling and transcriptional networks. *Physiol. Rev.* 87(3), 933–963. <https://doi.org/10.1152/physrev.00006.2006>
- Zhu, X., Tollkuhn, J., Taylor, H., Rosenfeld, M.G., 2015. Notch-dependent pituitary SOX2+ stem cells exhibit a timed functional extinction in regulation of the postnatal gland. *Stem Cell Reports* 5(6), 1196–1209. <https://doi.org/10.1016/j.stemcr.2015.11.001>
- Zhu, Z., Cui, W., Zhu, D., Gao, N., Zhu, Y., 2020. Common tools for pituitary adenomas research: cell lines and primary cells. *Pituitary* 23(2), 182–188. <https://doi.org/10.1007/s11102-019-01003-4>
- Zwagerman, N.T., Wang, E.W., Shin, S.S., Chang, Y., Fernandez-miranda, J.C., Snyderman, C.H., Gardner, P.A., 2019. Does lumbar drainage reduce postoperative cerebrospinal fluid leak after endoscopic endonasal skull base surgery? A prospective, randomized controlled trial. *J. Neurosurg.* 131, 1172–1178. <https://doi.org/10.3171/2018.4.JNS172447.J>

It always seems impossible, until it's done – Nelson Mandela

ADDITIONAL STATEMENTS

ACKNOWLEDGEMENTS

PERSONAL CONTRIBUTIONS

The PhD candidate, Charlotte Nys, designed the concepts and experiments, collected and processed biopsies, performed the experiments and the data analysis, interpreted the results and wrote this PhD thesis. The promoter, Prof. Dr. Hugo Vankelecom, supervised all processes and revised and corrected this PhD thesis. The PhD candidate had support from co-authors (chapter 2, 3 and 4), and other people and facilities as acknowledged per chapter.

All figures and tables of the general introduction were generated by the PhD candidate or adapted from papers under appropriate citation. All tables and figures provided in the 'Objectives' (chapter 2) and 'Results' sections (chapter 3, chapter 4 and addendum) were generated by the PhD candidate, some of them with Biorender as indicated. The mouse transcriptomic dataset used in chapter 3 was generated by Dr. Roose.

FUNDING

This work was supported by grants from the KU Leuven Research Fund and from the Fund for Scientific Research (FWO) - Flanders (Belgium). Charlotte Nys was supported by a PhD Fellowship from the FWO (1S14218N).

CONFLICT OF INTEREST STATEMENT

Charlotte Nys and all other co-authors declare no conflicts of interest.

CURRICULUM VITAE

CHARLOTTE NYS



charlotte.nys@kuleuven.be



+32484/96.27.49



Leuven, Belgium



27-10-1994



Let's connect!

WORK EXPERIENCE

- 10/2017 – current **PhD researcher in the laboratory of Tissue Plasticity in Health and Disease (SCIL, KU Leuven)**
Exploring stem cell biology in pituitary tumors and derived organoids
Promoter: Hugo Vankelecom
Grant: Strategic basic research grant – FWO
- 09/2016 – 05/2017 **Internship at pharmacy Masschelin (Heffen)**
Supervisor: Annelies Masschelin
- 02/2016 – 06/2016 **Senior internship in the laboratory of Tissue Plasticity in Health and Disease (SCIL, KU Leuven)**
Pituitary organoids: characterization of growth conditions and phenotype
Promoter: Hugo Vankelecom
- 09/2015 **Student researcher (4 weeks) in the laboratory of Clinical and Experimental Endocrinology (CEE, KU Leuven)**

EDUCATION

- 2015 – 2017 **Master in drug development (KU Leuven)**
- 2012 – 2015 **Bachelor in pharmaceutical sciences (KU Leuven)**

ADDITIONAL EDUCATION

- 2016 FELASA B
- 2017 Introduction to confocal microscopy
- 2018-2019 Presentation skills
- 2018-2019 French classes
- 2019 Essentials of Image Editing
- 2021 Biorender visualization

TEACHING ACTIVITIES

- 2018 Training of PhD student from Argentina (6 months)
- 2018 'Dag van de Wetenschap' KU Leuven
- 2019-2020 Supervision of master student
- 2020 Teaching assistant in Track Hormonology (Hot Topics) for Master students in Biomedical Sciences
- 2020-2021 Supervision of master student

PUBLICATIONS

Nys C., Lee Y.*, Roose H.*, Mertens F., De Pauw E., Kobayashi H., Sciot R., Bex M., Versyck G., De Vleeschouwer S., *et al.* Exploring stem cell biology in pituitary tumors and derived organoids. (paper under revision – Endocrine-Related Cancer) *contributed equally

Laporte E., Hermans F., De Vriendt S., Vennekens A., Lambrechts D., **Nys C.**, Cox B., Vankelecom H. Decoding the activated stem cell phenotype of the vividly maturing neonatal pituitary. (paper under revision – eLife)

Laporte E.*, **Nys C.***, Vankelecom H. Development of organoids from mouse pituitary as powerful model to explore pituitary stem cell biology. (paper under revision – JoVE) *contributed equally

Nys C.*, Versyck G.*, Buelens E, Engelborghs K, Vankelecom H, Weyns F, Peuskens D. Transnasal transsphenoidal pituitary surgery in a large tertiary hospital, a retrospective study. *Acta chirurgica Belgica*, 2021, 1-9. <https://doi.org/10.1080/00015458.2021.1988231> (*contributed equally)

Nys, C., Vankelecom, H., 2021. Pituitary disease and recovery: How are stem cells involved? *Mol. Cell. Endocrinol.* 525(111176), 1–8. <https://doi.org/10.1016/j.mce.2021.111176>

Vennekens, A.*, Laporte, E*., Hermans, F., Cox, B., Modave, E., Janiszewski, A., **Nys, C.**, Kobayashi, H., Malengier-Devlies, B., Chappell, J., *et al.*, 2021. Interleukin-6 is an activator of pituitary stem cells upon local damage, a competence quenched in the aging gland. *Proc. Natl. Acad. Sci. U. S. A.* 118(25), 1–11. <https://doi.org/10.1073/pnas.2100052118> (*contributed equally)

Cox, B., Laporte, E., Vennekens, A., Kobayashi, H., **Nys, C.**, Van Zundert, I., Ujii, H., Drubbel, A.V., Beck, B., Roose, H., *et al.*, 2019. Organoids from pituitary as a novel research model toward pituitary stem cell exploration. *J. Endocrinol.* 240(2), 287–308. <https://doi.org/10.1530/JOE-18-0462>

CONFERENCE CONTRIBUTIONS

21-26/06/2021 Virtual conference	ISSCR 2021 The global stem cell event Oral presentation: Stem cell biology in pituitary tumors and derived organoids
11/02/2021 Virtual conference	Departmental day Oral presentation: Stem cell biology in pituitary tumors and derived organoids
19/02/2020 Leuven, Belgium	Departmental day Poster presentation: Unraveling the role of pituitary stem cells during pituitary tumorigenesis and regeneration
13/09/2019 Brussels, Belgium	6th Belgian Society for Stem Cell Researchers (BeSSCR) Meeting Poster presentation: Unraveling the role of pituitary stem cells in pituitary tumorigenesis
28/02/2019 Leuven, Belgium	Departmental Day Poster presentation: Unraveling the role of pituitary stem cells during pituitary tumorigenesis and regeneration
26/10/2018 Brussels, Belgium	5th Belgian Society for Stem Cell Researchers (BeSSCR) Meeting Poster presentation: Unraveling the role of pituitary stem cells during pituitary tumorigenesis and regeneration